ENVIRONMENTAL IMPACTS OF EXHAUST GAS CLEANING SYSTEMS IN THE BALTIC SEA, NORTH SEA, AND THE MEDITERRANEAN SEA AREA

Evaluation, control and Mitigation of the EnviRonmental impacts of shippinG Emissions

This report was prepared by:
Jukka-Pekka Jalkanen, Erik Fridell, Jaakko Kukkonen, Jana Moldanova, Leonidas Ntziachristos, Achilleas Grigoriadis, Maria Moustaka, Evangelia Fragkou, George Tsegas, Androniki Maragkidou, Mikhail Sofiev, Risto Hänninen, Tiia Grönholm, Julia Palamarchuk, Elisa Majamäki, Wilfried Winiwarter, Samuel Gueret, Ranjeet S. Sokhi, Saurabh Kumar, Ummugulsum Alyuz Ozdemir, Vassilis Kolovoyiannis, Vassilis Zervakis, Aikaterini-Anna Mazioti, Evangelia Krasakopoulou, Ida-Maja Hassellöv, Anna Lunde Hermansson, Erik Ytreberg, Ian Williams, Malcolm Hudson, Lina Zapata Restrepo, Lars Robert Hole, Manuel Aghito, Oyvind Breivik, Mira Petrovic, Meritxell Gross, Sara Rodriguez-Mozaz, Maria Neophytou, Alexandra Monteiro, Michael A. Russo, Fotis Oikonomou, Andreas Gondikas, Antonio Marcomini, Elisa Giubilato, Loris Calgaro, Jouni J. K. Jaakkola, Ivy Shiue, Simo-Pekka Kiihamäki, Göran Broström, Martin Hassellöv, Joni. Kaitaranta, Maria Granberg and Kerstin Magnusson

Disclaimer

This work is part of the European Union's Horizon 2020 research and innovation programme Evaluation, control and Mitigation of the EnviRonmental impacts of shippinG Emissions (EMERGE project), grant agreement No 874990. This work reflects only the authors' view and CINEA is not responsible for any use that may be made of the information it contains.

Publisher: Finnish Meteorological Institute, Helsinki, Finland, January 2024

ISBN: 978-952-336-189-8
https://doi.org/10.35614/isbn.9789523361898

Contents

List of figures

List of tables

Abbreviations

Abbreviation	Explanation
AA-EQS	Annual average - Environmental Quality Standard
AF	Assessment Factor
AIS	Automatic Identification System
APCI	Atmospheric Pressure Chemical Ionization
AUTH	Aristotle University of Thessaloniki
BC	Black Carbon
BSD	Backscattered electron detector
CAMS	Copernicus Atmospheric Monitoring Service
CAS	Chemical Abstracts Service
CH_4	Methane
CHIMERE	Multi-scale chemistry-transport model for atmospheric composition analysis and forecast
CI	Confidence Interval
CMAQ	Community Multiscale Air Quality Model
CO	Carbon monoxide
CPC	Condensation particle counter
CRED	Criteria for reporting and evaluating ecotoxicity data
CSIC	Spanish Council for Scientific Research
CTPHT	Coal-tar pitch high temperature
DAD	Diode-array detection
DNPH	2,4-dinitrophenylhydrazine
DNVGL	Det Norske Veritas - Germanischer Lloyd
DOME	Database on the Marine Environment
DON	Dissolved organic nitrogen
DOP	Dissolved organic phosphorus
EC	Elementary Carbon
EC50	Effective Concentration 50%
ECA	Emission Control Area
ECLIPSE	Evaluating the Climate and Air Quality Impacts of Short-Lived Pollutants
ECMWF	European Centre for Medium-Range Weather Forecasts
EDS	Energy dispersive X-ray spectroscopy
ED-XRF	Energy Dispersive X-ray Fluorescence
EEA	European Environment Agency
EEDI	Energy Efficiency Design Index
EF	Emission factor
EGCS	Exhaust Gas Cleaning System
EHT	Electron high tension
ELV	Extremely low volatile
EM	Eastern Mediterranean
EMEP	The co-operative programme for monitoring and evaluation of the long-range transmission of air pollutants in Europe
EMERGE	Evaluation, control and Mitigation of the EnviRonmental impacts of shippinG Emissions

EPA	Environment Protection Agency
EQS	Environment Quality Standard
ERA	Environmental risk assessments
FID	Flame Ionisation Detector
FSC	Fuel Sulfur Content
FUGAS	Flux of Gases
GC	Gas chromatography
GES	Good Environmental Status
GHG	Greenhouse Gas
GISIS	Global Information System for International Shipping
HC	Hydrocarbon
HELCOM	The Baltic Marine Environment Protection Commission
HFO	Heavy Fuel oil
HNLC	High Nutrients, Low Chlorophyll
HOLAS	Holistic Assessment
HPLC	High-pressure Liquid Chromatography
HRMS	High-Resolution Mass Spectroscopy
HSFO	High-Sulfur Fuel Oil
ICES	International Council for the Exploration of the Seas
ICP-MS	Inductively Coupled Plasma Mass Spectrometry
IHS	Information Handling Services
IMO	International Maritime Organisation
IVL	Swedish Environment Institute
LC50	Lethal Concentration 50%
LLE	Liquid-liquid extraction
LNG	Liquid Natural Gas
LOD	Limit of Detection
LOEC	Lowest Environmental Concentration
LOQ	Limits of quantification
LPG	Liquid Petroleum Gas
LV	Low-volatile
MARPOL	The International Convention for the Prevention of Pollution from Ships
MC	Measured Concentrations
ME	Main engine
MEC	Measured Environmental Concentration
MEPC	Marine Environment Protection Committee
MERLIN	Modelling Exposure to chemicals for Risk assessment: a comprehensive Library of multimedia and PBPK models for Integration, Prediction, uNcertainty and Sensitivity analysis
MGO	Marine Gas Oil
MRV	Monitoring, Reporting and Verification
MS	Mass Spectroscopy
MSFD	Marine Strategy framework Directive
MSS	Micro Soot Sensor
NA	Not Available
NECA	Nitrogen Emission Control Area
NH_3	Ammonia
NMVOC	Non-Methane Volatile Organic hydroCarbon
NOEC	No Observed Effect Concentration

NO_x	Nitrogen Oxide
OC	Organic Carbon
OCIMF	Oil Companies International Marine Forum
OSPAR	The Convention for the Protection of the Marine Environment of the North-East Atlantic
PAC	Polycyclic aromatic compound
PAH	Polycyclic aromatic hydrocarbon
PAH16	Group of 16 polyaromatic hydrocarbons defined by the US Environment Protection Agency
PDMS	Polydimethylsiloxane
PEC	Predicted Environmental Concentrations
PLC	Pollution Load Compilation
PM	Particulate Matter
PNEC	Predicted No-Effect Concentration
$PNEC_{TGD}$	Predicted No-Effect Concentration as indicated by the EU Technical Guidance Document 27
PO4	Phosphate
PTFE	Poly-tetrafluoroethane
QSAR	Quantitative Structure-Activity Relationship
QToF	Quadrupole time-of-flight
RCR	Risk Characterization Ratio
REACH	Registration, Evaluation, Authorisation and Restriction of Chemicals
RID	Riverine input and direct discharges programme
SCIPPER	Shipping Contributions to Inland Pollution Push for the Enforcement of Regulations
SCR	Selective Catalytic Reduction
SECA	SO_X Emission Control Area
SEM	Scanning Electron Microscopy
SHYFEM	Shallow water HYdrodynamic Finite Element Mode
SILAM	System for Integrated modeLing of Atmospheric coMposition
SMPS	Scanning Mobility Particle Sizer
SO_x	Sulfur Oxide
SPE	Solid Phase Extraction
SPM	Suspended Particulate Matter
SPME	Solid phase microextraction
SSD	Species sensitivity distribution
SSS	Short Sea Shipping
STEAM	Ship Traffic Emission Assessment Model
SV	Semi volatile
SWAN	Simulating WAves Nearshore
TEM	Transfer Electron Microscopy
TGD	Technical Guidance Document
THC	Total hydrocarbons
UAV	University of Aveiro
ULSFO	Ultra-low sulfur fuel oil
US	University of Southampton
USD	US dollars
USEPA	United States Environment Protection Agency
UTC	Universal Time Coordinate
UV	University of Venice

VLSFO	Very-low sulfur fuel oil
VP	Variable pressure mode of electron microscopy
VTS	Vessel Traffic Services
WAQ	Water Quality
WET	Whole Effluent Testing
WFD	Water Framework Directive
WISE	Water Information System for Europe
WRF	Weather Research and Forecast model
WWTP	Wastewater treatment plant
XRF	X-ray Fluorescence

EXECUTIVE SUMMARY

Shipping is responsible for a range of different pressures affecting air quality, climate, and the marine environment. Most social and economic analyses of shipping have focused on air pollution assessment and how shipping may impact climate change and human health. This risks that policies may be biased towards air pollution and climate change, whilst impacts on the marine environment are not as well known. One example is the sulfur regulation introduced in January 2020, which requires shipowners to use a compliant fuel with a sulfur content of 0.5% (0.1% in SECA regions) or use alternative compliance options (Exhaust Gas Cleaning Systems, EGCS) that are effective in reducing sulfur oxide (SO_x) emissions to the atmosphere. The EGCS cleaning process results in large volumes of discharged water that includes a wide range of contaminants. Although regulations target SO_x removal, other pollutants such as polycyclic aromatic hydrocarbons (PAHs), metals and combustion particles are removed from the exhaust to the wash water and subsequently discharged to the marine environment.

Based on dilution series of the Whole Effluent Testing (WET), the impact of the EGCS effluent on marine invertebrate species and on phytoplankton was found to vary between taxonomic groups, and between different stages of the invertebrate life cycle. Invertebrates were more affected than phytoplankton, and the most sensitive endpoint detected in the present project was the fertilisation of sea urchin eggs, which were negatively affected at a sample dilution of 1 : 1,000,000. Dilutions of 1: 100,000 were harmful to early development of several of the tested species, including mussels, polychaetes, and crustaceans. The observed effects at these low concentrations of EGCS effluent were reduced egg production, and deformations and abnormal development of the larvae of the species. The ecotoxicological data produced in the EMERGE project were used to derive Predicted No Effect Concentration values.

Corresponding modelling studies revealed that the EGCS effluent can be considered as a single entity for 2-10 days from the time of discharge, depending on the environmental conditions like sea currents, winds, and temperature. Area 10-30 km outside the shipping lanes will be prone to contaminant concentrations corresponding to 1 : 1,000,000 dilution which was deemed harmful for most sensitive endpoints of WET experiments. Studies for the Saronikos Gulf (Aegean Sea) revealed that the EGCS effluent dilution rate exceeded the 1 : 1,000,000 ratio 70% of the time at a distance of about 10 km from the port. This was also observed for 15% of the time within a band of 10 km wide along the shipping lane extending 500 km away from the port of Piraeus.

When mortality of adult specimens of one of the species (copepod *Acartia tonsa*) was used as an endpoint it was found to be 3-4 orders of magnitude less sensitive to EGCS effluent than early life stage endpoints like fertilisation of eggs and larval development. Mortality of *Acartia tonsa* is commonly used in standard protocols for ecotoxicological studies, but our data hence shows that it seriously underestimates the ecologically relevant toxicity of the effluent. The same is true for two other commonly used and recommended endpoints, phytoplankton growth and inhibition of bioluminescence in marine bacteria. Significant toxic effects were reached only after addition of 20-40% effluent.

A marine environmental risk assessment was performed for the Öresund region for baseline year 2018, where Predicted Environmental Concentrations (PECs) of open loop effluent discharge water were compared to the PNEC value. The results showed modelled concentrations of open loop effluent in large areas to be two to three orders of magnitude higher than the derived PNEC value, yielding a Risk Characterisation Ratio of 500-5000, which indicates significant environmental risk. Further, it should be noted that between 2018-2022 the number of EGCS vessels more than quadrupled in the area from 178 to 781.

In this work, the EGCS discharges of the fleet in the Baltic Sea, North Sea, the English Channel, and the Mediterranean Sea area were studied in detail. The assessments of impacts described in this document were performed using a baseline year 2018 and future scenarios. These were made for the year 2050, based on different projections of transport volumes, also considering the fuel efficiency requirements and ship size developments. From the eight scenarios developed, two extremes were chosen for impact studies which illustrate the differences between a very high EGCS usage and a future without the need for EGCS while still compliant to IMO initial GHG strategy. The scenario without EGCS leads to 50% reduction of GHG emissions using low sulfur fuels, LNG, and methanol.

For the high EGCS adoption scenario in 2050, about a third of the fleet sailing the studied sea areas would use EGCS and effluent discharge volumes would be increased tenfold for the Baltic Sea and hundredfold for the Mediterranean Sea when compared to 2018 baseline discharges.

Some of the tested species, mainly the copepods, have a central position in pelagic food webs as they feed on phytoplankton and are themselves the main staple food for most fish larvae and for some species of adult fish, e.g., herring. The direct effect of the EGSE on invertebrates will therefore have an important indirect effect on the fish feeding on them. Effects are greatest in and near shipping lanes.

Many important shipping lanes run close to shore and archipelago areas, and this also puts the sensitive shallow water coastal ecosystems at risk. It should be noted that no studies on sub-lethal effects of early

life stages in fish were included in the EMERGE project, nor are there any available data on this in the scientific literature. The direct toxic effects on fish at the expected concentrations of EGCS effluent are therefore largely unknown. According to the regional modelling studies, some of the contaminants will end up in sediments along the coastlines and archipelagos.

The documentation of the complex chemical composition of EGCS effluent is in sharp contrast to the present legislation on threshold levels for content in EGCS effluent discharged from ships, which includes but a few PAHs, pH, and turbidity. Traditional assessments of PAHs in environmental and marine samples focus only on the U.S. Environmental Protection Agency (EPA) list of 16 priority PAHs, which includes only parent PAHs. Considering the complex PAHs assemblages and the importance of other related compounds, it is important to extend the EPA list to include alkyl-PAHs to obtain a representative monitoring of EGCS effluent and to assess the impact of its discharges into the marine environment.

An economic evaluation of the installation and operational costs of EGCS was conducted noting the historical fuel price differences of high and low sulfur fuels. Equipment types, installation dates and annual fuel consumption from global simulations indicated that 51% of the global EGCS fleet had already reached break-even by the end of 2022, resulting in a summarised profit of 4.7 billion $€_{2019}$. Within five years after the initial installation, more than 95% of the ships with open loop EGCS reach break-even.

The pollutant loads from shipping come both through atmospheric deposition and direct discharges. This underlines the need of minimising the release of contaminants by using fuels which reduce the air emissions of harmful components without creating new pollution loads through discharges.

Continued use of EGCS and high sulfur fossil fuels will delay the transition to more sustainable options. The investments made on EGCS enable ships to continue using fossil fuels instead of transitioning away from them as soon as possible as agreed in the 2023 Dubai Climate Change conference. Continued carriage of residual fuels also increases the risk of dire environmental consequences whenever accidental releases of oil to the sea occur.

1. INTRODUCTION

This report summarises the work done in the H2020 project Evaluation, control and Mitigation of the EnviRonmental impacts of shippinG Emissions (EMERGE) and provides information on characteristics of EGCS effluent, toxicity, air emissions from ships using an EGCS, quantities of effluents released to the sea, their dispersion and impacts to the marine environment. A global analysis of air emissions and EGCS discharges were made for the period 2014-2022, but the impact assessments included in this report have regional focus, concentrating on the Baltic Sea, North Sea, and the Mediterranean Sea areas.

There are different pathways and multiple stressors which contribute to the overall environmental performance of shipping (Figure 1). Direct discharges come from a variety of sources, and they may contain oil, metals, pharmaceuticals, and hazardous substances. Releases from EGCS, bilge water, propeller shaft lubricants, tank cleaning, greywater, sewage, cooling water and antifouling paints may include various contaminants. Further, nutrients released in sewage, greywater and food waste contribute to eutrophication. In addition to direct discharges, indirect contributions come through the atmospheric deposition of nitrogen oxides (NO_x), sulfur oxides (SO_x) and particulate matter (PM) components, like various carbon compounds and heavy metals in ash fraction of PM. Concentrations of direct discharges are highest around busy shipping lanes, which may run close to the coast and ecologically vulnerable shallow water areas, but atmospheric deposition can cover large geographical areas either on land or on water.

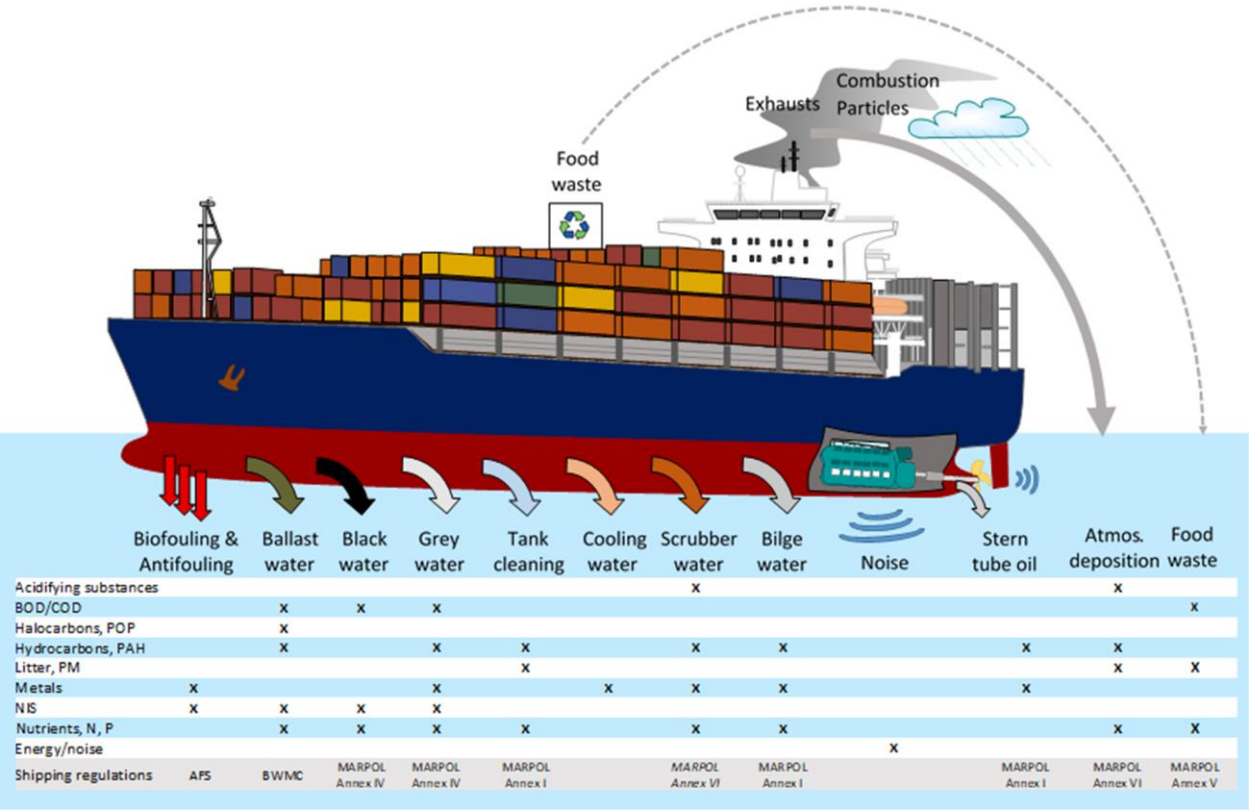

	Biofouling & Antifouling	Ballast water	Black water	Grey water	Tank cleaning	Cooling water	Scrubber water	Bilge water	Noise	Stern tube oil	Atmos. deposition	Food waste
Acidifying substances							x				x	
BOD/COD		x	x	x								x
Halocarbons, POP		x										
Hydrocarbons, PAH		x		x	x		x	x		x	x	
Litter, PM					x						x	x
Metals	x			x		x	x	x		x		
NIS	x	x	x	x								
Nutrients, N, P		x	x	x	x		x	x			x	x
Energy/noise									x			
Shipping regulations	AFS	BWMC	MARPOL Annex IV	MARPOL Annex IV	MARPOL Annex I		MARPOL Annex VI	MARPOL Annex I		MARPOL Annex I	MARPOL Annex VI	MARPOL Annex V

Figure 1 Emissions from shipping to the atmosphere and direct discharges and pressures on the marine environment.

Shipping also affects air quality and human health through emissions of PM, non-methane volatile organic compounds (NMVOC), NO_x and SO_x. Emissions to air of black carbon and greenhouse gases such as carbon dioxide (CO_2), nitrous oxide (N_2O) and methane (CH_4) are also important because of their climate impact. While scientific understanding of consequences of air pollution and climate change related to shipping have increased substantially in recent years, the knowledge base is not the same for the pressure and impacts on the marine environment and the interaction between the different contributions.

For some contaminants present in EGCS effluent there are available threshold levels that must not be exceeded in marine environments, e.g., the environmental quality standards (EQS) of the EU Water Framework Directive (2008/105/EC) for coastal water bodies, or thresholds (often the same EQS) set within Descriptor 8 of the EU Marine Strategy Framework Directive (DIR 2008/56/EC) for coastal, territorial water and open sea. Assessments of the effect of EGCS effluent once it is released to the sea are still rare, but when they have been done, they have often been based on concentrations of individual compounds and comparisons to these threshold levels. These comparisons are helpful when toxicity data based on the whole water is limited or missing. However, it is important to keep in mind that this

approach will only consider the substances that were part of the chemical analyses, while many potentially toxic compounds that are present but not analysed, will be neglected. Basing the risk assessment on threshold levels for individual compounds will also miss the effect the contaminants have when acting together in a mixture, as would be the case when EGCS effluent is discharged into the sea. It is a well-documented fact that the effect on living organisms from exposure to mixtures of many contaminating compounds can be very different from the mere sum of the effect of individual compounds (Backhaus et al. 2008). Whole effluent toxicity data on EGCS effluent discharge from ships is much needed to make sound assessments of the possible adverse effects the discharged water may have on marine ecosystems.

There is an extensive scientific literature on most of the individual groups of contaminants present in EGCS effluents which are the PAHs and other polycyclic aromatic compounds (PACs) and metals. However, scientific data on effects of the unique mix of these compounds found in the effluent are still rare. The impact on the last juvenile stage of the pelagic copepods *Calanus finmarchicus* was investigated by Thor et al. (2021), and open loop EGCS effluent at a concentration of 1% (the lowest test concentration) was found to cause a significant increase in mortality. A significant increase in mortality in adult specimens of another copepod species, *Acartia tonsa*, were detected at 10% (Koski et al. 2017). Increased mortality was found for 6 days old individuals of the crustacean *Mysidopsis bahia* and for juveniles of the fish species *Mugilogobius chulae*, after exposure to EGCS effluent at concentrations of 1.25, and 2.5%, respectively (Ji et al. 2023). Data from a few studies indicate that taxa belonging to the large and highly heterogeneous group of microplankton are less sensitive than invertebrates to the effluent. This is also supported by available literature on the effects of PAHs and other oil related compounds on these organisms. An experimental study showed that a concentration of 5 – 8% EGCS effluent affected the photosynthesis of the cyanobacteria *Nodularia spumigena* and the diatom *Melosira arctica*, where the former was inhibited, and the latter was stimulated (Ytreberg et al. 2019). A field collected community of microorganisms was found to have an altered species composition and to increase in biovolume after exposure to 3% effluent (Ytreberg et al. 2021).

Assessment of marine environmental impacts are based on data from experimental studies for ecotoxicological effects which were conducted within the project. Baseline year of 2018 was selected considering the best compromise for the availability of weather, oceanographic, air emission and water discharge data. In addition, eight future emissions and discharge scenarios were constructed to reflect potential developments of the global ship fleet, and three of these were selected for impact

assessments. The scenarios for which impact assessments were made, represent extreme cases of very high EGCS adoption, both for open and closed loop systems, as well as the situation where EGCSs are unnecessary. These selections provide guidance on the magnitude of the consequences if EGCS usage is significantly increased. It should be noted that the selection of 2018 as the baseline year reflects the situation before the significant adoption of EGCS in the global ship fleet which happened in 2019-2021 when shipowners adjusted their compliance strategy for the global 0.5% Sulfur cap in 2020.

2. Materials and methods

2.1. Onboard sampling or air emissions and discharges

EGCSs primarily work to abate air emissions of SO_2 and secondly to reduce emissions of PM. However, the legislation limits the fuel sulfur content (FSC) to 0.5% at global scale and 0.1% at specific regions, called emission control areas (ECAs). The legislative authority approves the utilisation of emission control systems, to cut SO_2 emissions, to comply with the mandatory respective FSC, as FSC equivalence. The compliance with the current regulation is demonstrated, calculating the SO_2 (ppm)/CO_2 (%) ratio, as described by the MEPC, 2015. The above ratio must be below the values of 21.7 and 4.3, when the ship is sailing worldwide and at ECA areas, respectively. Moreover, each country can enforce its own supplementary regulation in relation to the EGCS operation on their territories. Specifically, in various ports worldwide (e.g., Portugal, Singapore, Saudi-Arabia, Romania, and others) open-loop EGCS are not allowed to operate to avoid wash water discharging, while in others there is not such a restriction (e.g., Port of Piraeus in Greece).

In EMERGE, detailed emissions characterization was made, for a vessel equipped with an EGCS, and which covered both the air emissions and EGCS discharges. The selected vessel had a 2-stroke engine and was equipped with an open loop EGCS. The objective of this study was to perform an on-board sampling of effluent discharge, to assess the release of contaminants to the marine environment, and to evaluate the closure of the mass balance between air emissions and water discharges downstream of the SO_x abatement system.

Other information from ships equipped with EGCS was also gathered and analysed. The overall processing led to identification of a typical EGCS operation, as presented on Figure 2 for an assumed

trip from the North Sea to the Mediterranean Sea. EGCS operation profile is not influenced by the ship type (containers, tankers, bulk carriers, etc), but from the engine operation and the fuel sulfur regulation that a ship must comply with, according to the area of sailing. In Figure 2, the indicative ship commences its route from the port of Southampton, United Kingdom towards the Sea of Marmara. The voyage includes sailing through an ECA region (North Sea), crossing the Mediterranean Sea and finally cruising to the Turkish territory to meet the destination port. The ship needs to comply with both the global 0.5% FSC cap, as well as the stricter 0.1% FSC in ECA. Furthermore, the Turkish Ministry of Environment and Urbanization prohibits the EGCS effluent discharge from open-loop EGCS into its waters. This means that ships passing through Turkish waters must switch from open-loop EGCS operation to sulfur-compliant fuels.

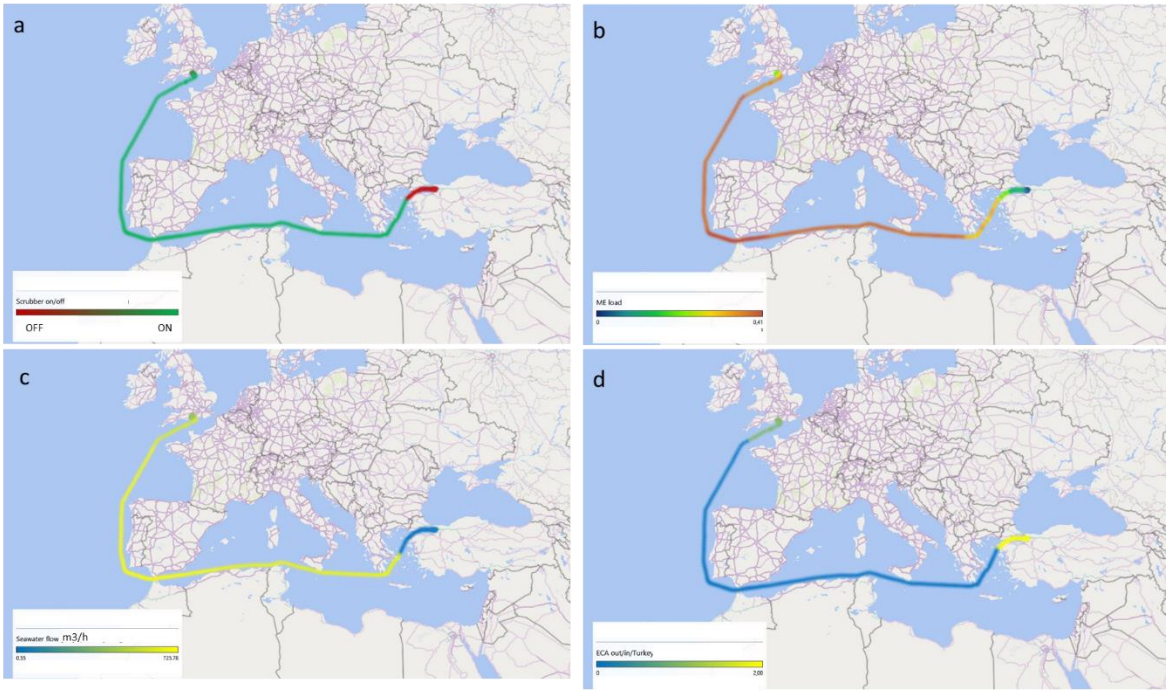

Figure 2. Vessel state during the onboard sampling campaign during 16th-24th November 2021. Top left (a) depicts the EGCS usage during the voyage, top right (b) indicates the main engine load, bottom left (c) reports the EGCS effluent discharge and bottom right (d) describes the different regulatory domains.

In Figure 2(a), the EGCS operation (On/Off) is presented, from where it is observed that the system was switched on while the ship is still berthed alongside the port of Southampton. After approximately 24 hours the ship exits the limits of the ECA and therefore, the ship needs to comply with the 21.7, SO_2/CO_2 ratio. The route of the ship in respect to local sulfur legislation is depicted in Figure 2(d).

As observed from Figure 2(b) the ship ME is assumed to be working continuously at a stable medium load throughout most of the voyage time. The engine load increases to 33%, after exiting the port of

Southampton and further increases to 38-40% when leaving the North Sea ECA. The ME load decreased to 28-30%, when the ship approached Peloponnesos, Greece. During the final stage of voyage and inside Turkish waters, the ship was slow steaming (reduced speed) at around 10% engine load, to arrive at the destination port at a certain time to minimise anchoring time (idle time).

To evaluate the closure of the mass balance between air emissions and water discharges downstream the EGCS, exhaust emissions downstream and upstream the system were analysed along with the effluent and the fuels. To assess an alternative to HFO plus EGCS operation, emissions during operation with ultra-low sulfur fuel oil (ULSFO) with EGCS deactivated were also analysed during the campaign. Figure 3 depicts the sampling and vessel operation during the campaign.

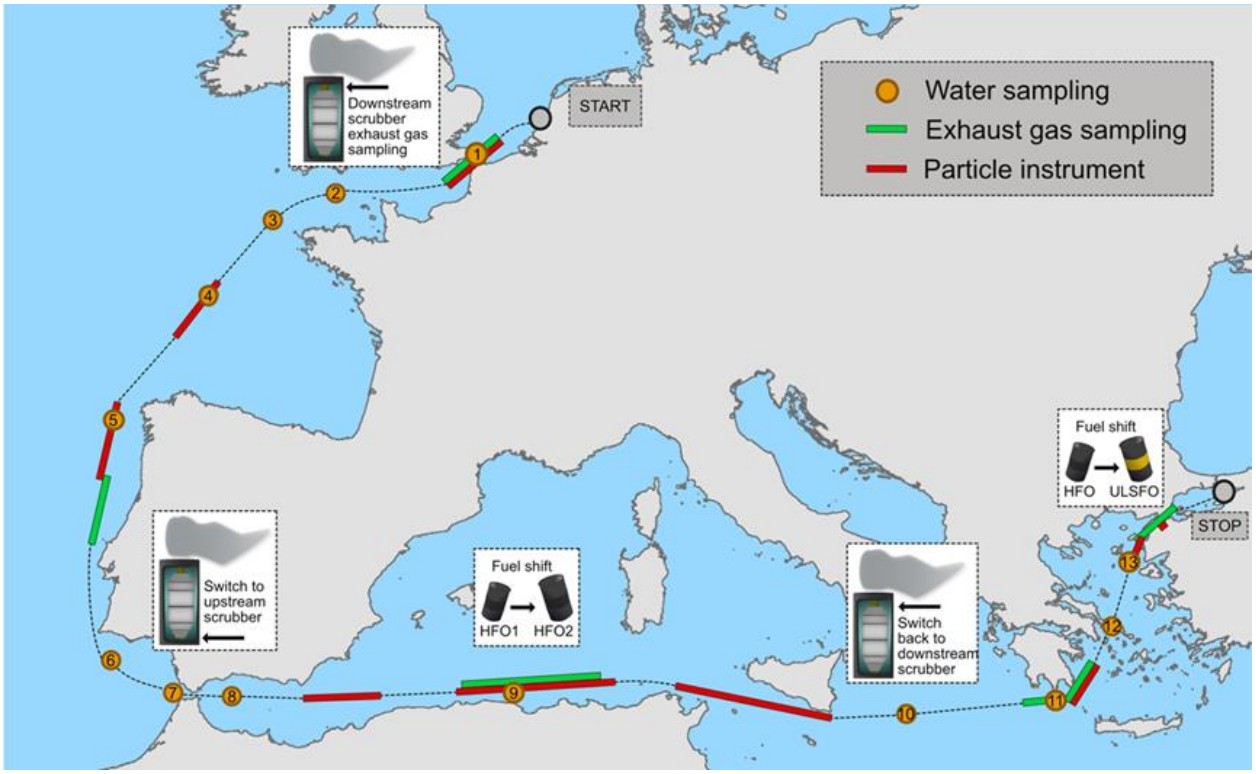

Figure 3. Map designating water, gaseous and particle sampling.

For exhaust characterisation a battery of online instruments for characterisation of gas composition and PM and its physical properties were completed with collection of pumped samples for off-line laboratory analyses. List of instruments used can be found in the Appendix (Table A- 1).

In parallel, samples of the EGCS inlet water and of the effluent were collected for laboratory analyses for PACs/PAHs and metals, for ecotoxicological tests and filtered samples of water borne particles were

collected for Transfer Electron Microscopy (TEM) and Scanning Electron Microscopy (SEM) analyses. Figure 4 shows the sampling along the sailing route.

To get a complete picture of fluxes of elements and metals in the combustion system of the vessel, samples of the fuels and engine lubricants were collected and analysed for content of heat, main elements (C, H, O, S, N), metals and PACs.

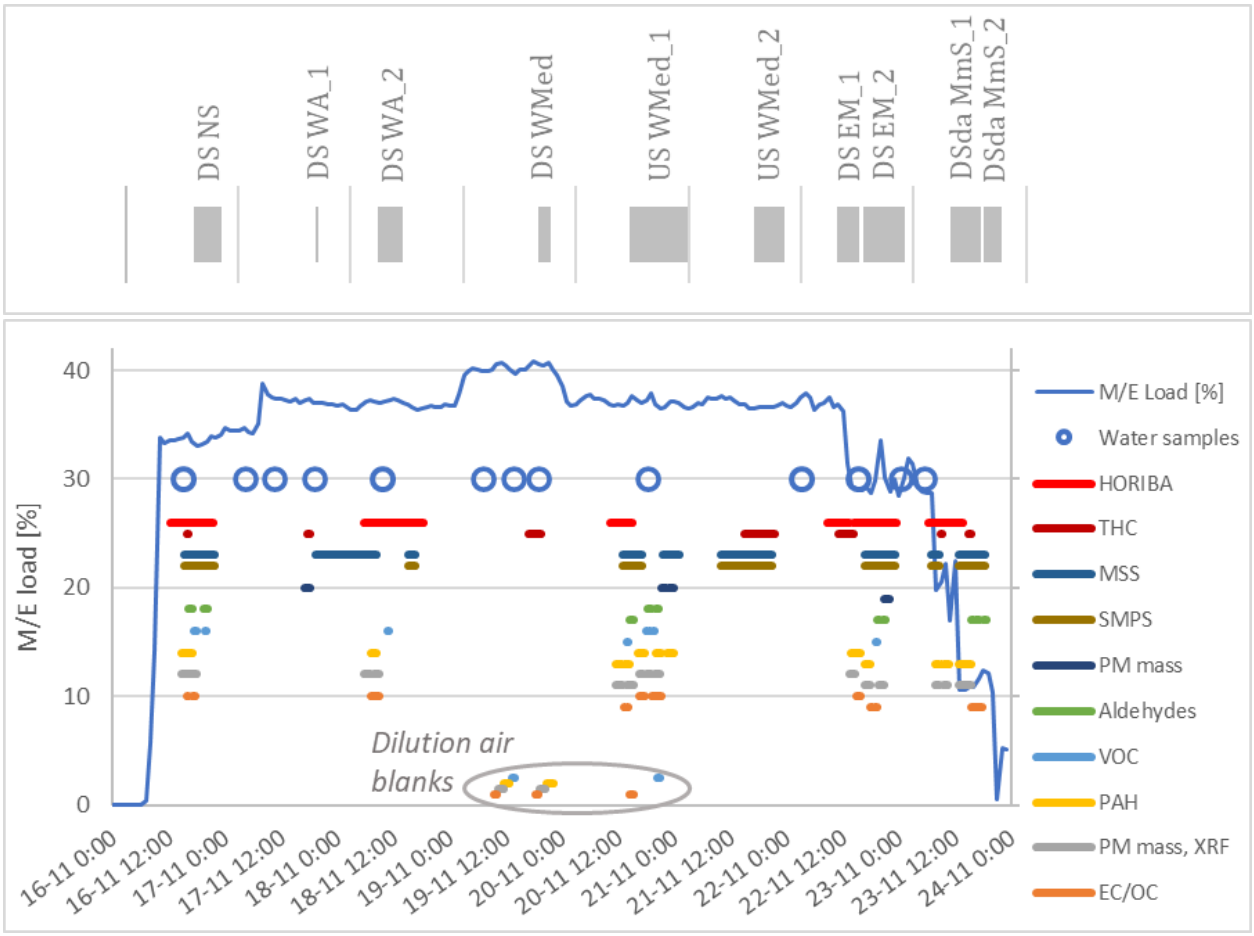

Figure 4. Engine load and sampling points along the sailing route of the campaign plotted on timeline between 16th-24th of November 2021. All times are in UTC. Abbreviations for the sampling locations: DS - Downstream EGCS, US - upstream EGCS, DSda . Downstream deactivated EGCS, NS - North Sea, WA - West-European Atlantic Coast, WMed - Western Mediterranean Sea, EM East Mediterranean Sea, MmS - Marmar Sea

2.2. Water sample analysis

The amount of hazardous particles and compounds deposited in the sea with the EGCS effluent depends on the chemical content and volumes of the discharged water. Collection of data and

calculations of emission factors from open- and closed loop EGCSs have been done within the EMERGE project but there is still limited data on the quantities of contaminants from EGCS effluents reaching different sea areas (Ytreberg et al., 2021). The input of polycyclic aromatic hydrocarbons (PAHs, an important group of oil derived pollutants), from shipping to the Baltic Sea has been estimated to derive almost entirely, 98%, from EGCS effluents (Ytreberg et al., 2022), however, data on the contribution of PAHs from shipping relative to other sources, e.g., riverine input and point sources from industrial and urban activities, in the Baltic Sea is still uncertain and suggested to be between 0.4 and 8.9%. It is also important to point out that up to date, chemical analysis on oil related compounds in EGCS effluent has mainly been restricted to include the United State Environmental Protection Agency (US EPA) 16 PAHs, whereas the true content of these compounds in water from scrubbing HFO combustion fuels most likely includes hundreds of aliphatic compounds, monoaromatics and PACs such as non-substituted-, alkylated- heterocyclic-and other PAHs (Zhao et al., 2020; and recent data from EMERGE project). The documentation of the complex chemical composition of EGCS effluent is in sharp contrast to the present legislation on threshold levels for content in EGCS effluents discharged from ships, which includes but a few PAHs, pH, and turbidity.

PAHs and alkylated PAHs collectively termed PACs (polycyclic aromatic compounds) are toxic components of petroleum oil, coal, derived products and produced water. They are also released during combustion of petroleum products and are therefore ubiquitous in the environment. The heavier PACs (three-ringed and larger) have low water solubility and high hydrophobicity and are therefore mostly adsorbed onto particulate matter, which are subsequently deposited as sediments (Geffard et al., 2003). These substances are usually present as complex mixtures of hundreds or even thousands of related compounds spanning a wide range of physical/chemical properties and toxicity to aquatic organisms. Petrogenic and pyrogenic processes produce different PAHs and alkyl-PAHs assemblages, with different proportions of parent and their alkylated derivatives (Stout et al., 2015). As a rule of thumb, in the case of petrogenic sources, alkyl-PAHs are more abundant than the parent compounds (mainly 2-3 fused aromatic rings) and among homologues those with two to four alkyl carbons are more abundant (Stout et al., 2001). Conversely, in pyrogenic PAHs assemblages, the dominant compound in each homologous series is the non-alkylated parent compound (mainly with 3 or more aromatic rings) or a homologue with only one or two alkyl substituents (Neff et al., 2005; Stout et al., 2015).

Traditional assessments of PAHs in environmental and marine samples focus only on the U.S. Environmental Protection Agency (EPA) list of 16 priority PAHs, which includes only parent PAHs (Keith, 2015). Considering the complex PAHs assemblages and the importance of other related compounds, it

is a requirement to extend the EPA list to include alkyl-PAHs to obtain a representative monitoring of EGCS effluent and to assess the impact of its discharges into the marine environment (Thor et al., 2021). Alkyl-PAHs derivatives have an enormously large number of isomers, being impossible to analyse them all. For this reason, it is necessary to select those that are the most relevant for regular monitoring and as representative to assess the contamination by EGCSs and their potential ecotoxic effects.

Most of the analytical methods used to analyse PAHs and alkyl-PAHs are based on gas chromatography coupled to mass spectrometry (GC-MS) that is a widely used technique for the identification of volatile, thermally stable, and non-polar organic pollutants. Capillary GC offers high chromatographic resolution of organic pollutants in combination with highly selective and sensitive mass spectrometric detection (de Boer and Law, 2003; Poster et al., 2006). However, the efficiency of GC-MS methods depends on the level of interferences from the sample matrix, and the achievement of lower limits of detection (LOD) require an extensive sample clean-up procedure. The use of GC coupled to triple quadrupole tandem mass spectrometry (GC-MS/MS) can overcome this limitation and provides a more selective identification of target analytes at trace levels in complex samples. However, only a limited number of studies have used GC-MS/MS for the analysis of alkyl-PAH homologues (John et al., 2014; Park et al., 2018; Sørensen et al., 2016).

On the other hand, the use of the GC coupled with the most innovative HRMS instruments, generally QTOF mass spectrometers equipped with an Atmospheric Pressure Chemical Ionization (APCI) source (GC-APCI-QToF MS), allows the identification of organic contaminants with high precision, due to the use of high resolution and mass accuracy for the molecular ions, in addition to the achievement of low LODs (Portolés et al., 2010, 2014). Furthermore, GC-HRMS can be used for wide-scope screening of previously unreported contaminants and to identify the most relevant and ubiquitous contaminants in the samples, including PAHs, alkyl-PAHs, and related contaminants (Yang et al., 2019, 2020).

Regarding the sample treatment, several extraction methods have been used, with liquid-liquid extraction (LLE) and Solid Phase Extraction (SPE) being the most common ones (Martinez et al., 2004; Qiao et al., 2013). However, LLE is time consuming, labour intensive and requires large amounts of organic solvents, while SPE requires large sample volumes and high enrichment factors to reach low LODs (from ng L-1 to pg L-1) and limits of quantification (LOQ). In addition, suspended solids and particulate matter must be filtered prior to the SPE procedure, which can result in a remarkable loss of target compounds, particularly the most hydrophobic ones (Temerdashev et al., 2021). Solid phase

microextraction (SPME) is a promising alternative to these other methods, because it is a solvent-less technique, the analytes are extracted from the liquid matrix into a non-miscible solid phase, mainly polydimethylsiloxane (PDMS), thus allowing the simultaneous concentration and purification of the samples (Piri-Moghadam et al., 2016), which can be analysed without the need of filtration, avoiding potential analyte losses. However, despite its high potential, there are only few studies that use SPME in combination with GC-MS/MS for the analysis of both parent and alkyl-PAHs (Hawthorne et al., 2005; Terzaghi et al., 2021).

In addition to the removal of sulfur, EGCSs are also efficient in removing the particle content from exhaust gas, whose composition and physical dimensions depend on the fuel used, engine characteristics, and engine load (Fridell et al., 2008). These particles will be released directly in the marine environment from open loop EGCSs. In case a settling tank is used to treat the EGCS effluent, the less buoyant fraction of the particle population will be partly retained, depending on particle properties (size and density) and tank characteristics. Particles in the water will act as vectors of transport for metals and PAHs, among other contaminants (Linders et al., 2018; Turner et al., 2017) and is thus important to determine the physical-chemical properties that regulate their transport, reactivity, and fate in the marine environment. In this work we focus on particle size distribution, number concentration, and metal content of particles isolated from EGCS effluent and attempt to use these properties to identify particles in seawater, in the vicinity of busy shipping lanes. A method based on SEM-EDS was developed to detect particles on a flat membrane and conduct elemental analysis on each particle. To avoid operator bias, an automated method was developed, based on the elemental contrast between the membrane and particles.

2.2.1. Metals analysis

Metals were analysed at the Spanish Council for Scientific Research (CSIC) (Vigo, Spain). Samples were acidified with hydrochloric acid (HCl) to a pH around 1.7, if the samples could not be previously acidified. Samples are allowed to rest at least one week to allow the recovery of any fraction of metals that may be attached onto the walls of the tubes and to release loosely bound and labile particulate metals. After that, they are centrifuged to remove the particulate matter. UV-oxidation is needed before analysis owing to organically bound metals that are not retained in the preconcentration resin. Finally, metals analysis is done by SeaFAST pre-concentration setup and Agilent 7900 Inductively Coupled Plasma Mass Spectrometry (ICP-MS). Results of the metal analysis are collected to Table 1.

Table 1. Average total[*] concentration of trace elements found in EGCS effluent (in micrograms L^{-1}), presented with a 95 % confidence interval. The ambient category represents primarily harbours and marinas where sampling of the surrounding water has been made. The pristine category represents unpolluted surface water where the concentrations have been derived from (Bruland and Lohan, 2003). N= number of studies included.

	Open loop EGCS effluent discharge		**Open loop inlet water**		**Closed loop EGCS effluent discharge**		**Pristine water**
	$\underline{X}$ ± 95% CI (microg L^{-1})	**N**	**$\underline{X}$ ± 95% CI (microg L^{-1})**	**N**	**$\underline{X}$ ± 95% CI (microg L^{-1})**	**N**	**(microg L^{-1})**
Arsenic	6.99 ± 3.58	62	5.81 ± 1.46	52	23.00 ± 10.21	22	1.9
Barium	14.69 ± 4.81	5	14.44 ± 4.98	6	-	-	15
Cadmium	0.85 ± 0.3	62	0.99 ± 0.33	54	0.58 ± 0.20	22	0.07
Chromium	14.53 ± 6.35	59	16.3 ± 18.41	52	1250 ± 2045	16	0.21
Cobalt	0.17 ± 0.14	6	0.07 ± 0.06	4	-	-	0.0018
Copper	38.75 ± 12.45	70	28 ± 14	58	519.42 ± 243.64	23	0.19
Lithium	180 ± 5.06	10	177 ± 4.9	10	-	-	179
Lead	9.20 ± 4.48	67	8.27 ± 4.95	55	8.24 ± 3.36	22	0.002
Mercury	0.08 ± 0.01	26	0.08 ± 0.02	22	0.07 ± 0.02	16	0.0002
Molybdenum	10.69 ± 0.95	7	10.72 ± 0.85	5	66	1	10
Nickel	46.86 ± 11.25	65	8.83 ± 4.5	54	2623 ± 854	22	0.47
Selenium	97.00 ± 38.12	2	-	-	-	-	0.13
Vanadium	176.59 ± 49.96	61	9.45 ± 5.29	50	1402 ± 3450	22	1.7
Zinc	110.84 ± 60.87	70	175.58 ± 147.25	56	387.71 ± 222.64	22	0.33

[*]*total concentration is the sum of particulate and dissolved, if not specified it is assumed to be the total concentration.*

2.2.2. Polycyclic aromatic hydrocarbons

Automated methods of analysis for particle analysis were developed in SEM (GeminiSEM, Zeiss) on VP mode (60 Pa), BSD detector at magnification 234 X, EHT 20 kV, and using SmartPI software. Polycarbonate membranes (10 µm pore size) were used to filter the effluent, taking care not to overload the membrane with particles, i.e., avoid stacking and filtration-induced aggregation. Brightness and contrast were adjusted to optimise contrast between carbon-containing particles and the membrane. Scanning of the membrane area was set to random, to avoid bias from flow-induced variability of particle number density in different areas on the membrane.

The wide scope screening (Table 2) applied allowed the identification of the most relevant alkyl PAHs present in EGCS effluent to be included in the target analytical method. 37 different alkyl-homologues were identified, including C1, C2, C3 and C4-naphthalenes, C1, C2 and C3-fluorenes, C1, C2, C3 and C4 phenanthrenes, C1-fluoranthene and benzo [c] phenanthrene. The on-line SPME-GC-MS/MS method developed is a reliable, sensitive, and selective tool for the determination of target PAHs and alkyl homologues. Recoveries achieved are in the acceptable range (>70%), and LODs and LOQs achieved are low enough that ensure the detection of these compounds in the EGCS effluent samples. The analysis of both unfiltered and filtered effluent is appropriate to assess the impact of particulate matter, especially for high molecular weight PAHs and alkyl derivatives.

Table 2. Alkylated PAHs analysed in the EGCS effluents from the EMERGE onboard campaign (Vessel 1), Vessel 2, and the Chalmers pilot EGCS.

	Grouping chemical analysis	**Substance name**	**CAS**
2-rings	C1-Naphthalene-1-methyl	1-Methylnaphthalene	90-12-0
	C1-Naphthalene-2-methyl	2-Methylnaphthalene	91-57-6
	C2-Naphthalene	2,6-Dimethylnaphthalene	581-42-0
		1-Ethylnaphthalene	1127-76-0
		2-Ethylnaphthalene	939-27-5
	C3-Naphthalene	2,3,5-Trimethylnaphthalene	2245-38-7
		2-Isopropylnaphthalene	2027-17-0
	C4-Naphthalene	1,4,6,7-Tetramethylnaphthalene	13764-18-6
	C1-Fluorene	1-Methylfluorene	1730-37-6
	C2-Fluorene	1,7-Dimethylfluorene	442-66-0
3-rings	C1-Phenanthrene	1-Methylphenanthrene	832-69-9
	C2-Phenanthrene	1,3-Dimethylphenanthrene	16664-45-2
		2-Ethylanthracene	52251-71-5
	C3-Phenanthrene	1,2,6-Trimethylphenanthrene	30436-55-6
	C4-Phenanthrene	1,2,6,9-Tetramethylphenanthrene	204256-39-3
		7-Isopropyl-1-methylphenanthrene (retene)	483-65-8
4-rings	C1-Fluoranthene/Pyrene	1-Methylfluoranthene	25889-60-5
		1-Methylpyrene	2381-21-7

There are several organic compounds present in the EGCS effluent, mainly originating from the fuel and the combustion of the fuel. Polycyclic aromatic hydrocarbons (PAHs) are, next to metals, the most studied constituents of the effluent. All average concentrations of PAHs, including the 95% confidence interval, for discharge water, EGCS inlet water and pristine surface seawater is presented in Table 3. The PAHs are listed based on the molecular weight, with the low molecular weight compounds at the beginning and higher molecular weights the further down in the table. The concentrations of some of the measured PAHs are higher in the EGCS effluent discharge water of both open and closed loop systems compared to the inlet water indicating that; 1) the sources of PAHs can be attributed to the abatement process and 2) that the cleaning steps of the closed loop systems are insufficient.

Table 3. Average total concentration of organic compounds found in EGCS effluent (in micrograms L^{-1}), presented with a 95 % confidence interval. The ambient category represents primarily harbours and marinas where sampling of the surrounding water has been made. The pristine category represents unpolluted surface water where the concentrations have been derived from Law et al (1997). N= number of studies included.*

	Open loop EGCS effluent discharge		Open loop inlet water		Closed loop EGCS effluent discharge		Pristine water
	$\underline{X}$ ± 95% CI (microg L^{-1})	N	$\underline{X}$ ± 95% CI (microg L^{-1})	N	$\underline{X}$ ± 95% CI (microg L^{-1})	N	(microg L^{-1})
Naphthalene	2.76 ± 0.79	55	0.11 ± 0.08	48	2.08 ± 1.13	18	< 0.010
Acenaphthylene	0.13 ± 0.07	63	0.11 ± 0.11	60	0.08 ± 0.07	11	< 0.003
Acenaphthene	0.19 ± 0.07	63	0.01 ±0.003	60	0.49 ± 0.39	11	< 0.002
Fluorene	0.46 ± 0.10	63	0.07 ± 0.06	60	1.27 ± 0.67	11	< 0.001
Phenanthrene	1.51 ± 0.30	64	0.09 ± 0.08	61	4.30 ± 1.98	12	< 0.008
Anthracene	0.08 ± 0.05	63	0.02 ± 0.02	60	0.14 ± 0.11	11	< 0.001
Fluoranthene	0.16 ± 0.05	63	0.03 ± 0.02	59	0.35 ± 0.28	11	< 0.001
Pyrene	0.32 ± 0.12	63	0.05 ± 0.04	60	0.37 ± 0.27	11	< 0.001
Benz(a)anthracene	0.13 ± 0.06	64	0.03 ± 0.02	61	0.16 ± 0.20	12	< 0.002
Chrysene	0.19 ± 0.07	63	0.05 ± 0.03	60	0.11 ± 0.08	11	< 0.002
Benzo(b)fluoranthene	0.04 ± 0.02	63	0.01 ± 0.004	60	0.04 ± 0.03	11	< 0.001
Benzo(k)fluoranthene	0.01 ± 0.01	49	0.01 ± 0.004	47	0.02 ± 0.02	11	< 0.001
Benzo(a)pyrene	0.05 ± 0.02	64	0.01 ± 0.004	61	0.04 ± 0.04	12	< 0.001
Dibenzo(a,h)anthracene	0.03 ± 0.02	63	0.02 ± 0.01	60	0.02 ± 0.02	11	< 0.001
Benzo(g,h,i)perylene	0.02 ± 0.01	63	0.009 ± 0.004	60	0.02 ± 0.02	11	< 0.001
Indeno(1,2,3-c,d)pyrene	0.07 ± 0.06	63	0.06 ± 0.06	60	0.02 ± 0.02	11	< 0.001
Sum EPA 16 PAH	2.97 ± 0.79	35	1.44 ± 2.53	18	17.8 ± 5.3	11	-
Sum PAH	7.25 ± 1.95	36	0.4 ± 0.4	28	5.12 ± 3.87	7	-

**total concentration is the sum of particulate and dissolved, if not specified it is assumed to be the total concentration.*

The methodology was successfully applied to EGCS effluent samples collected from a container ship during its journey from the North Sea to the Eastern Mediterranean. The results highlight the prevalence of naphthalene, phenanthrene, and their alkyl derivatives. In addition, the effect of sample filtration of the effluent prior to analysis was assessed, since this is a step included in some standard protocols. There was a significant loss of more hydrophobic PAHs during filtration which is a strong argument against filtration (García-Gómez et al., 2023).

2.2.3. Nutrients

Nutrients have a natural spatial and seasonal variability that will contribute to the large variability shown in Table 4. It is difficult to draw any conclusions from these data except that it is a challenge to estimate average concentrations, with small confidence intervals, of nitrogen species in the water without considering when, where and how sampling was made. This parameter should rather be considered on a case-by-case basis where the inlet concentrations can be compared to the outlet concentrations to estimate a final load emerging from the SO_x abatement process.

Specifying the forms of the nitrogen species will also indicate whether the water is reduced or oxidised. The larger the fraction of ammonium and nitrite, the more reduced the environment, i.e. less oxygen available. This will also affect the speciation of other elements and compounds.

Another potential nutrient is iron. This trace element may be the limiting factor for photosynthetic activity in High Nutrients, Low Chlorophyll (HNLC) areas, and point sources could result in local blooms in areas with otherwise low abundance of phytoplankton. Iron is not only connected to the EGCS but is widely used in anthropogenic structures such as the ship hulls and piping, which could help explain the large variety in concentration.

Table 4. Potential nutrients, nitrogen species and iron, concentrations measured in EGCS effluent from open and closed loop (in unit of milligrams L^{-1}), inlet water associated with open-loop systems. N= number of studies included.

	Open loop EGCS discharge		**Open loop inlet water**		**Closed loop EGCS discharge**	
	$\underline{X}$ ± 95% CI (millig L^{-1})	**N**	**$\underline{X}$ ± 95% CI (millig L^{-1})**	**N**	**$\underline{X}$ ± 95% CI (millig L^{-1})**	**N**
Nitrogen species						
Nitrate (NO_3^{2-})	2.83 ± 2.06	31	3.21 ± 2.23	30	110.98 ± 135.73	4
Nitrite (NO_2^-)	0.760 ± 0.68	28	0.97 ± 1.28	26	55.76 ± 130.71	4
Ammonium (NH_4^+)	0.73 ± 0.03	17	0.07 ± 0.04	14	-	-
Other						
Iron	0.24 ± 0.37	4	0.032 ± 0.08	3	-	-

2.3. Ecotoxicological experiments

Ecotoxicological experiments and tests were carried out by five research laboratories at University of Venice (UV) in Italy, University of Southampton (UoS) in Great Britain, IVL Swedish Environmental Research Institute (IVL) in Sweden, University of Aveiro (UAV) in Portugal, and Aristotle University of Thessaloniki (AUTH) in Greece (Figure 5). At all laboratories but AUTH, experiments were carried out on single species. At AUTH natural microplankton communities, with a range of different microorganisms, were collected in the field and used in experiments.

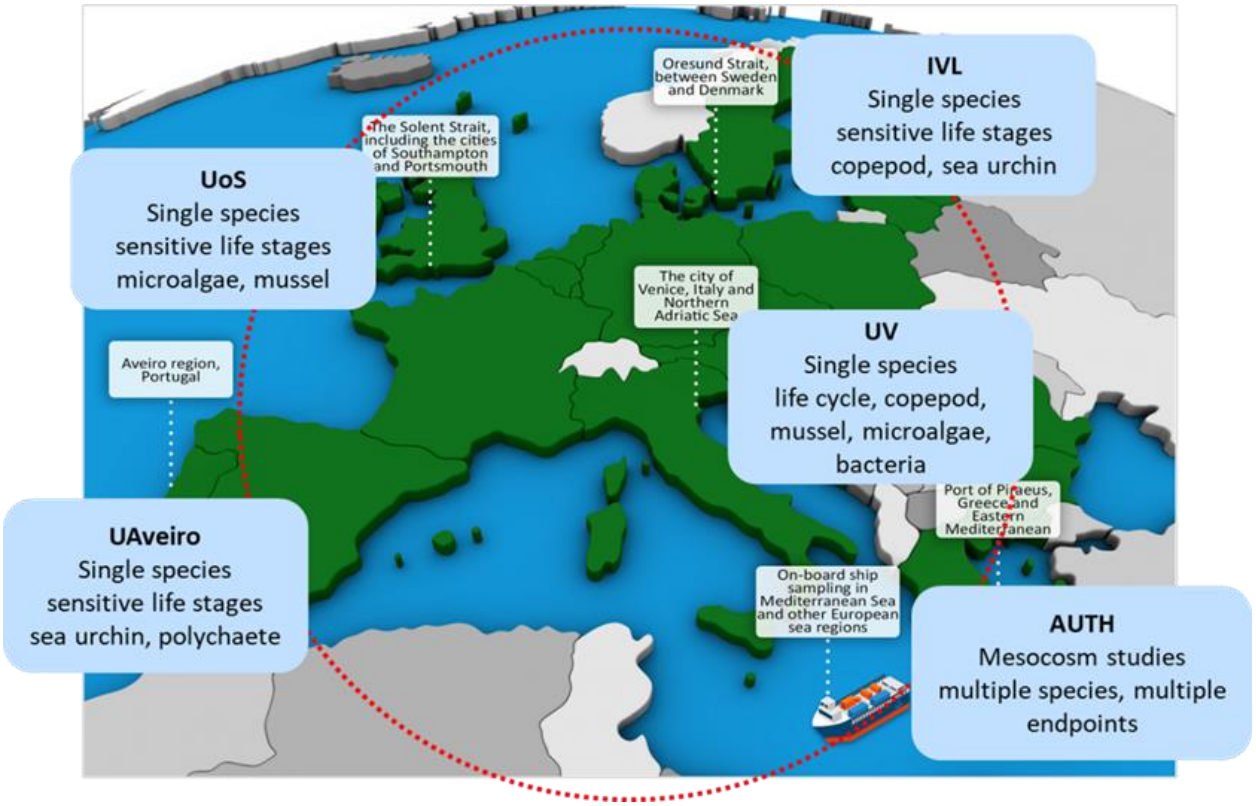

Figure 5. Ecotoxicological testing laboratories and type of analysis performed.

All testing was done on whole effluent, either from ships in operation or from a pilot laboratory scale EGCS installed at Chalmers Technical University (Santos et al., 2022). The water was collected and treated uniformly according to a protocol developed within the EMERGE project. The purpose of this was to maintain the effluents as similar as possible to the discharged effluent the marine organisms would encounter in nature. The tested waters were not identical in their chemical composition, but this reflects real life situations under which EGCS effluent is produced. Sampling on board the ship was

done as close to the discharge point to the sea as possible to obtain a water like that which the animals in the field are exposed to.

The ecotoxicological work carried out is primarily based on scientific experiments, while some of the studies follow modified standardised protocols. Modifications primarily concern the adjustment of the pH of the exposure water, which is required according to standard test protocols. Adjustments of pH were not done here since it would affect the true toxicity of the EGCS effluent and compromise the relevance of the results. Ecological relevance, i.e., the applicability of the results in real world exposure situations, is a very important aspect of ecotoxicological research and influences the utility of the generated data for risk/impact assessment.

To assure the quality and usefulness in relation to risk assessment (development of Environmental Quality Standards-EQS) of the ecotoxicological data produced within the EMERGE project, the CRED method (Moermond et al., 2016) was followed, as stated in the technical guidance document (TGD27) for deriving environmental quality standards issued by the European Commission (European Commission, 2018). The CRED method offers the ability to assess relevance of aquatic ecotoxicity data in addition to reliability criteria and is recommended to be applied for the critical studies in a dataset. The CRED method uses a set of 20 reliability and 13 relevance criteria, which support the harmonisation in the evaluation and reporting of ecotoxicological results (inherently subject to expert judgement). Each research team assessed its own ecotoxicological experiments and results against CRED criteria.

Experiments and testing

To understand the toxic impact EGCS effluent can have on marine ecosystems, it is crucial to perform tests on species that are sensitive to the hazardous compounds present in the water, and it is also important to study the animals at the most sensitive part of their life cycle. Often, animals are most sensitive during the early developmental stages (egg or larvae), so studies on individuals of a species at later developmental stages or as adults run the risk of seriously underestimating toxicity of the compound or wastewater that is being tested. To increase the chances of obtaining toxicity data that can be used to truly protect the marine ecosystems, the test organisms selected in the present project included species of invertebrates and phytoplankton from a range of different taxonomic groups, and the studies on invertebrates were mainly carried out on early life stages. In addition, experiments were done exposing natural communities of pelagic microorganisms to EGCS effluent and on a marine bacterium of the species *Aliivibrio fisheri*. Since the effluent is released into the surface of the water

column, pelagic species will encounter higher concentrations of the specific mixture of hazardous compounds present in the discharged water than bottom-dwelling species. The test species were therefore all selected to be representative of a pelagic food web. Some were species that spend their entire life in the water column, while others are pelagic during the egg and larval stages but spend the rest of their life on the seafloor or on intertidal substrates. The truly pelagic species included in the experiments were two species of the class Copepoda, *Acartia tonsa* and *Calanus helgolandicus*, and the two phytoplankton species, the diatom *Phaeodactylum tricornutum* and the green algae *Dunaliella tertiolecta*. Species with pelagic eggs and larvae were two species of the class Echinodea, the sea urchins *Strongylocentrotus droebachiensis* and *Paracentrotus lividus*, one species of the class Polychaeta, *Sabellaria alveolata*, and two species of the class Bivalvia, the blue mussels *Mytilus galloprovincialis* and *Mytilus trossulus* (Figure 6). The mesocosm experiments on natural field collected communities included organisms <200 micrometers, mainly numerous species of phyto- and bacterioplankton that were present at the time of the sampling.

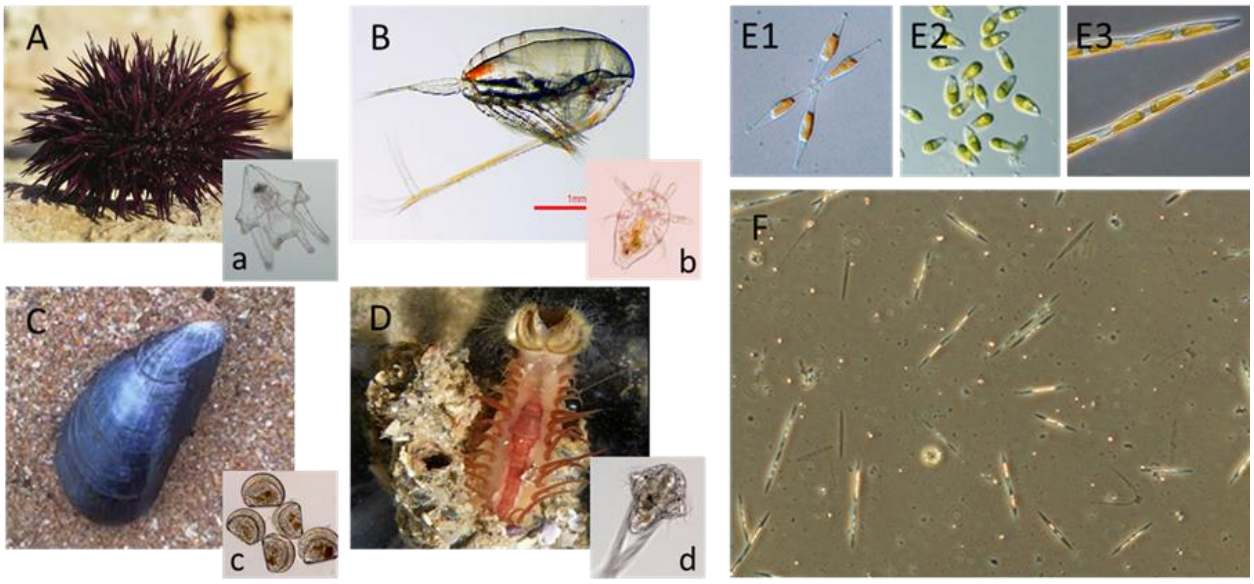

Figure 6. Images of some species, some of their larvae and planktonic communities used in the ecotoxicological experiments and tests with EGCS effluent. A,a) Sea urchins Paracentrotus lividus, with pluteus larva (Class Echinodea: Phylum Echinodermata); B,b) Copepods Calanus sp. with nauplius larva (Class Copepoda, Subphylum Crustacea); C,c) Blue mussels Mytilus sp. with veliger larva (Class Bivalvia, Phylum Mollusca); D,d) Polychaete Sabellaria alveolata with trochophore larva (Class Polychaeta, Phylum Annelida); E) Microalgae, E1 and E3: Diatoms Phaeodactylum tricornutum and Pseudo-nitzschia sp. (Class Bacillariophyceae), E2: green algae Dunaliella tertiolecta (Class Chlorophyceae); F) Phytoplankton community dominated by the microalga Pseudo-nitzschia cf. pungens (alive and dead – empty cells) in 10% EGCS effluent.

Organisms were exposed to EGCS effluent in concentrations between 0.0001 and 40%, (% of effluent diluted in natural sea water), and control animals were exposed to only seawater. Toxicity was expressed as the lowest concentration found to have an effect that was statistically different from the control (Lowest Observed Effect Concentration, LOEC), and the highest concentration with no statistically significant effect (No Observed Effect Concentration, NOEC) were calculated. In the experiments with the EGCS effluent NOEC could not be determined in all experiments since significant effects were observed already at the lowest test concentration.

The response data was also used to estimate the Effective Concentration or Lethal Concentration 10% (EC10/LC10), that is, the effluent concentration having a 10% effect on the analysed endpoint or causing the death of 10% of the exposed population of test organisms, and EC50% or LC50% (EC50/LC50), the EGCS effluent concentration having a 50% effect on the analysed endpoint or causing the death of 50% of the exposed test population. EC/LC10 and EC/LC50 were estimated from a dose-response curve based on the obtained data on effect/mortality among the organisms exposed to EGCS effluent compared to a control group exposed to sea water only. LOEC and NOEC are hence actual concentrations to which the organisms were exposed, whereas EC10 and EC50 are statistical estimates calculated from a curve fit to the obtained response data.

In the mesocosm experiments, communities of microplankton (Figure 6F) were collected in two polluted sites (a port and a marina) and two unpolluted, and the organisms were exposed to either 1 and 10%, or 1, 2 and 5% EGCS effluent. The total abundance (number of cells) was calculated for three groups of the plankton, microphytoplankton (20 - 200 micrometers), nanophytoplankton (2-20 micrometers), picophytoplankton (approximately 0.5 - 2 micrometers) and bacterioplankton. Analysis was also done on population density of a selected number of individual species.

2.4. Risk assessments

Environmental risk assessments (ERA) of chemical substances (hereafter referred to as substances) are based on the comparisons between the exposure of the ecosystem to a substance on the one hand, and the sensitivity of the ecosystem to that substance on the other. The exposure is usually estimated using chemical fate models that determine PECs in different environmental compartments. The concentration of the substance below which adverse effects in the environmental sphere of concern are not expected to occur is known as PNEC (European Union, 2007). If the PEC/PNEC ratio (also referred

to as risk characterization ratios, RCR) exceeds 1, the risk of adverse effects on the environment is denominated as unacceptable. If the RCR ratio is below 1, the risk of adverse effects on the environment is denominated as acceptable. If a product, or a waste stream, contains more than one substance, a PEC/PNEC summation approach is typically applied as a conservative first-step methodology to predict the risks for adverse effects of mixtures of contaminants (Backhaus and Faust, 2012).

The summation approach is based on the concept of concentration addition which means that all substances present in a mixture contribute to a cumulative effect.

$$RCR_{Sum} = \frac{\sum_i^n PEC_i}{\sum_i^n PNEC_i} \qquad \text{Eq 1}$$

The summation of RCRs (Eq 1, where n is the total number of substances in the mixture) is also supported by the recently approved IMO guidelines for environmental risk and impact assessments of EGCS effluent discharge water (IMO, 2022), stating that: The cumulative effects of mixtures should be taken into account and a PEC/PNEC summation approach is recommended where PEC/PNEC ratios of all mixture components (PAHs and metals) are summed up to a final Risk Quotient. The summation of toxic units (derived in a similar manner as RCRs) is justified if the mixture is well defined (European Commission, 2018). The development and Environmental Quality Standards (EQS) are important tools used for assessing the chemical and environmental status of waterbodies (European Community, 2000).

Shipping is known to emit hundreds of different substances and the liquid waste streams (Figure 1) are often chemical mixtures and the composition of each waste stream may be highly variable. Although it is possible to calculate emission factors for individual substances, it would be very time-consuming to develop and apply a chemical fate model that has the capacity to accurately predict environmental concentrations of the hundreds of substances discharged in harbours and/or ship lanes. Thus, a simplified approach is to assess the potential risk for adverse environmental effects from the cumulative RCR (hereafter referred to as RCR_{sum}) of a specific waste stream, e.g., EGCS effluent discharge, where Measured Concentrations (MC) of substances based on available data on average concentrations in the waste stream (instead of modelled PEC values) are compared with PNEC-values to derive RCR_{sum}. With this approach the different waste streams potential risks can be compared to each other.

To assess the cumulative risk of the mixture, a PNEC value is required for each substance. PNECs are

derived from ecotoxicological studies where representative species from different trophic levels (or taxonomic groups) are exposed to the specific substance. According to the TGD 27, two methods can be used to derive PNEC values, the deterministic and the probabilistic approach. For the deterministic approach, the lowest effect concentration is divided by an assessment factor (AF) whose size is dependent on the available data. The AF is used to account for the uncertainty in extrapolating between the performed tests and the field situation. The probabilistic approach requires more data, and all available ecotoxicity data (usually chronic NOEC and/or EC10 data) are ranked and a species sensitivity distribution (SSD) curve is fitted to the data. Finally, a certain percentile (usually the 5^{th} corresponding to the concentration estimated to affect 5% of all species) of the distribution is selected as threshold value (also called HC5 value). The probabilistic approach is also associated to uncertainties and requires an assessment factor, but this is often lower than for the deterministic approach due to the increased data availability and inclusion of several species. If no ecotoxicological studies have been conducted for a certain substance or the number and quality of the obtained data is not satisfactory, no PNEC can be derived, and the substance cannot be included in the RCR_{sum} assessment. To fill the data gap of these substances for which no toxicity data are available, non-testing methods, such as computational approaches with Quantitative Structure-Activity Relationship (QSAR) models, can be applied to predict the toxicity (as described by a specific ecotoxicological parameter, such as ECx or NOEC) based on the chemical structure and/or properties of the substance. However, as stated in the guidance document (European Commission, 2018) the QSAR models “should not be used to generate critical data to derive an EQS; however, predicted data can play a role in reducing uncertainty and thereby influence the size of AF chosen for extrapolation.” For more information regarding the application of QSAR and recent technological advances where QSAR has been used, see the work of Muratov et al (Muratov et al., 2020).

PNEC values were only derived for the sixty high priority substances (Table 5) as these have been detected in EGCS effluent or sludge. When deriving PNECs for each substance, three different methods were applied:

- Method 1: only experimentally measured values from the ECOTOX database (US EPA, 2023) or from literature (European Commission, 2023b; Verbruggen, 2012) are included,
- Method 2: only the QSAR model outputs (ECOSAR(Wright et al., 2022), VEGA(Benfenati et al., 2013), T.E.S.T(Martin, 2020)) are included
- Method 3: both the experimental and QSAR datasets are included.

For all methods, the PNEC was derived in accordance with the TGD No 27 where the data availability for of the trophic levels, species and endpoints determined which method to use and what assessment factor to apply.

The ecotoxicological response of whole effluent testing of EGCS effluent cannot be fully explained by the toxicity of the individual substances identified, or their synergistic effects, in the effluent. Therefore, as a complement to the conventional monitoring and modelling of individual substances (section State), we present an alternative risk assessment approach where the open loop EGCS effluent is modelled as one entity and the resulting environmental concentrations, as dilution factors, can be compared to Predicted No Effect Concentrations (as percentage EGCS effluent) from the ecotoxicological tests. The relation between the concentration of a chemical substance, expressed as either the Measured Environmental Concentration (MEC) or the Predicted Environmental Concentration (PEC) to the Predicted No Effect Concentrations (PNEC) can be expressed as a Risk Characterization Ratios (RCR).

If RCR>1, the risk of adverse effects on the environment is denominated as unacceptable. If the RCR ratio is below 1, the risk of adverse effects on the environment is denominated as acceptable. $PNEC_{TGD}$ for open loop effluent was derived from EMERGE ecotoxicological studies (Table 5) in accordance with the technical guidance (European Commission, 2018) by a deterministic approach where an assessment factor is applied to the lowest No Observed Effect Concentration (critical $value_{NOEC}$, Table 6).

Table 5. Final PNEC values (µg/L), PNECM1-3 refers to the lowest PNEC value derived from method 1, 2 or 3 described above.

		$PNEC_{M1-3}$ (microg L^{-1})	**$PNEC_{final}$ (microg L^{-1})**	**Source $PNEC_{final}$**
Alkylated PAH	**Naphthalene-2-methyl (C1)**	4.74×10^{-2}	4.74×10^{-2}	Method 1 (separate analytical report from EMERGE project)
Alkylated PAH	**Naphthalene-1-methyl (C1)**	1.23×10^{-1}	1.23×10^{-1}	Method 3
Alkylated PAH	**Naphthalene-C2**	7.80×10^{-3}	7.80×10^{-3}	Method 1
Alkylated PAH	**Naphthalene-C3**	1.46×10^{-2}	1.46×10^{-2}	Method 3
Alkylated PAH	**Naphthalene-C4**	1.70×10^{-3}	1.70×10^{-3}	Method 2
Alkylated PAH	**Phenanthrene-C1**	4.68×10^{-3}	4.68×10^{-3}	Method 3
Alkylated PAH	**Phenanthrene-C2**	9.53×10^{-4}	9.53×10^{-4}	Method 2

Alkylated PAH	**Phenanthrene-C3**	1.67×10^{-3}	1.67×10^{-3}	Method 2
Alkylated PAH	**Phenanthrene-C4**	2.04×10^{-4}	2.04×10^{-4}	Method 2
Alkylated PAH	**Fluorene-C1**	9.65×10^{-3}	9.65×10^{-3}	Method 2
Alkylated PAH	**Fluorene-C2**	7.24×10^{-3}	7.24×10^{-3}	Method 2
Alkylated PAH	**Fluoranthene-Pyrene-C1**	1.45×10^{-3}	1.45×10^{-3}	Method 2
USEPA 16 PAH	**Acenaphthene**	2.26×10^{0}	3.80×10^{-1}	EU RAR CTPHT (2008); Verbruggen (2012)
USEPA 16 PAH	**Acenaphthylene**	5.95×10^{-1}	1.30×10^{-1}	EU RAR CTPHT (2008); Verbruggen (2012)
USEPA 16 PAH	**Anthracene**	1.44×10^{-2}	1.44×10^{-2}	Method 1 (*AA-EQS=0.1 µg/L)
USEPA 16 PAH	**Benzo(a)anthracene**	1.92×10^{-3}	1.20×10^{-3}	EU RAR CTPHT (2008); Verbruggen (2012)
USEPA 16 PAH	**Benzo(a)pyrene**	7.84×10^{-3}	1.70×10^{-4}	AA-EQS marine (European Union, 2013)
USEPA 16 PAH	**Benzo(b)fluoranthene**	3.06×10^{-4}	3.06×10^{-4}	Method 3
USEPA 16 PAH	**Benzo(g,h,i)perylene**	2.60×10^{-4}	2.60×10^{-4}	Method 3
USEPA 16 PAH	**Benzo(k)fluoranthene**	1.69×10^{-2}	1.69×10^{-2}	Method 3
USEPA 16 PAH	**Chrysene**	9.00×10^{-4}	9.00×10^{-4}	Method 1
USEPA 16 PAH	**Dibenzo(a, h)anthracene**	5.66×10^{-5}	5.66×10^{-5}	Method 3
USEPA 16 PAH	**Fluoranthene**	2.40×10^{-1}	7.60×10^{-4}	Newly proposed AA-EQS marine (European Commission, 2023b)
USEPA 16 PAH	**Fluorene**	1.74×10^{0}	2.50×10^{-1}	EU RAR CTPHT (2008); Verbruggen (2012)
USEPA 16 PAH	**Indeno(1,2,3-cd) pyrene**	1.67×10^{-4}	1.67×10^{-4}	Method 3
USEPA 16 PAH	**Naphthalene**	1.53×10^{1}	2.00×10^{0}	AA-EQS marine (European Union, 2013)
USEPA 16 PAH	**Phenanthrene**	1.12×10^{0}	1.10×10^{0}	REACH (https://echa.europa.eu/regulations/reach/understanding-reach)
USEPA 16 PAH	**Pyrene**	3.60×10^{-1}	2.30×10^{-2}	EU RAR CTPHT (2008); Verbruggen (2012)
Metals	**Arsenic**		5.50×10^{-1}	(SWAM, 2019)
Metals	**Cadmium**		2.00×10^{-1}	AA-EQS marine (European Union, 2013)
Metals	**Chromium**		3.40×10^{0}	(SWAM, 2019)
Metals	**Copper**		1.45×10^{0}	(SWAM, 2019)
Metals	**Lead**		1.30×10^{0}	AA-EQS marine (European Union, 2013)
Metals	**Mercury**		6.70×10^{-2}	REACH (https://echa.europa.eu/regulations/reach/understanding-reach)
Metals	**Nickel**		8.60×10^{0}	AA-EQS marine (European Union, 2013)(Council Directive (EC), 2013)
Metals	**Vanadium**		2.50×10^{0}	REACH (https://echa.europa.eu/regulations/reach/understanding-reach)

Metals	**Zinc**		1.10×10^{0}	(SWAM, 2019)

The sum of the RCRs of the individual open loop EGCS effluent, used in the different ecotoxicological tests, were calculated according to Equation 1. The substance concentrations in the specific effluent were compared to the substance specific $PNEC_{final}$ listed in Table 5. The results from the current study indicate that the alkylated PAHs, that have previously not been included when assessing the environmental risk of EGCS effluent, could contribute to more than 85% of the cumulative risk (Figure 7). However, it must be emphasised that the QSAR models hold high uncertainties and future ecotoxicological studies should focus on testing how toxic these alkylated PAHs are for marine species (and ecosystems) to confirm the results.

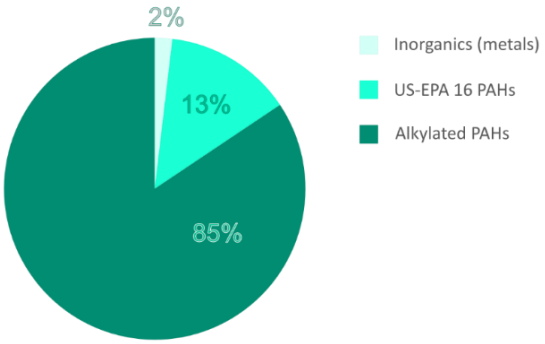

Figure 7. Relative contribution to the average cumulative risk quotient, calculated for open loop EGCS effluent from the EMERGE onboard campaign.

The predicted required dilution ratio was compared to the ecotoxicological responses in the whole effluent tests performed within EMERGE and described in a separate report. The exposure concentrations (in % effluent) from the ecotoxicological tests were recalculated to dilution ratios to enable comparison (Table 6). Although highly variable, the result suggests that by including alkylated PAHs, the prediction of toxicity of EGCS effluent can be improved (Figure 7). However, even when alkylated PAHs are included, the prediction does not manage to protect the most sensitive species (Table 6).

Table 6. Experimental ecotoxicological test results and the predicted dilution ratios required to reach RCRsum ≤ 1 based on EGCS effluent constituents. The last two columns compare the predicted dilution required if alkylated PAHs are included or not. Laboratories: University of Venice=UV, University of Aveiro=UAV, University of Southampton=US

Laboratory	**Effluent sample**	**Species**	**End-point**	**NOEC from ecotoxicological test (% effluent)**	**LOEC from ecotoxicological test**	**Dilution ratio (based on NOEC from ecotoxicological test)**	**Predicted dilution ratio (only metals and US-EPA 16 PAHs)**	**Predicted dilution ratio (metals, US-EPA 16 PAHs & alkylated PAHs)**
UV	**Chalmers**	*Acartia tonsa*	Egg production	0.001	0.01	100000	399	N/A
UV	**Chalmers**	*Acartia tonsa*	Larval development	<0.01	0.01	>10000	399	N/A
UV	**Vessel 1 (nr 10)**	*Acartia tonsa*	Egg production	0.001	0.01	100000	2193	15562
UV	**Vessel 1 (nr 10)**	*Acartia tonsa*	Larval development	0.01	0.1	10000	2193	15562
UV	**Vessel 1 (nr 10)**	*Mytilus galloprovincialis*	Larval development	0.1	1	1000	2193	15562
IVL	**Vessel 1 (nr 1)**	*Strongylocentrotus droebachiensis*	Egg fertilization	<0.0001	0.0001	>1000000	2297	13225
IVL	**Vessel 1 (nr 1)**	*Strongylocentrotus droebachiensis*	Malform. of larvae	<0.0001	0.0001	>1000000	2297	13225
IVL	**Defined in Thor et al 2018**	*Calanus helgolandicus*	Egg fertilization	0.01	0. 1	10000		
UAV	**Chalmers**	*Paracentrotus lividus*	Malform. of larvae	0.001	0.01	100000	196	599
UAV	**Chalmers**	*Paracentrotus lividus*	Egg fertilization	<0.01	0.01	>10000	196	599
UAV	**Vessel 2**	*Paracentrotus lividus*	Egg fertilization	<0.01	0.01	>10000	389	5808
UAV	**Vessel 2**	*Paracentrotus lividus*	Malform. of larvae	<0.001	0.001	>100000	389	5808
UAV	**Vessel 1 (nr 1)**	*Sabellaria alveolata*	Malform. of larvae	<0.001	0.001	>100000	2297	13225
UAV	**Vessel 2**	*Sabellaria alveolata*	Malform. of larvae	0.001	0.01	100000	389	5808
UAV	**Chalmers**	*Sabellaria alveolata*	Malform. of larvae	0.001	0.01	100000	196	599
UAV	**Vessel 1 (nr 1)**	*Paracentrotus lividus*	Fertilization success	0.01	0.1	10000	2297	13225
UAV	**Vessel 2**	*Paracentrotus lividus*	Fertilization success	1.56	3.13	64	389	5808
US	**Chalmers**	*Mytilus trossulus*	Malform. of larvae	<0.001	0.001	>100000	?	?
US	**Vessel 2**	*Mytilus trossulus*	Malform. of larvae	<0.001	0.001	>100000	?	?

The RCR_{sum} of both open and closed loop EGCS effluent discharge is substantially higher than the RCR_{sum} from the other four waste streams (Figure 8).

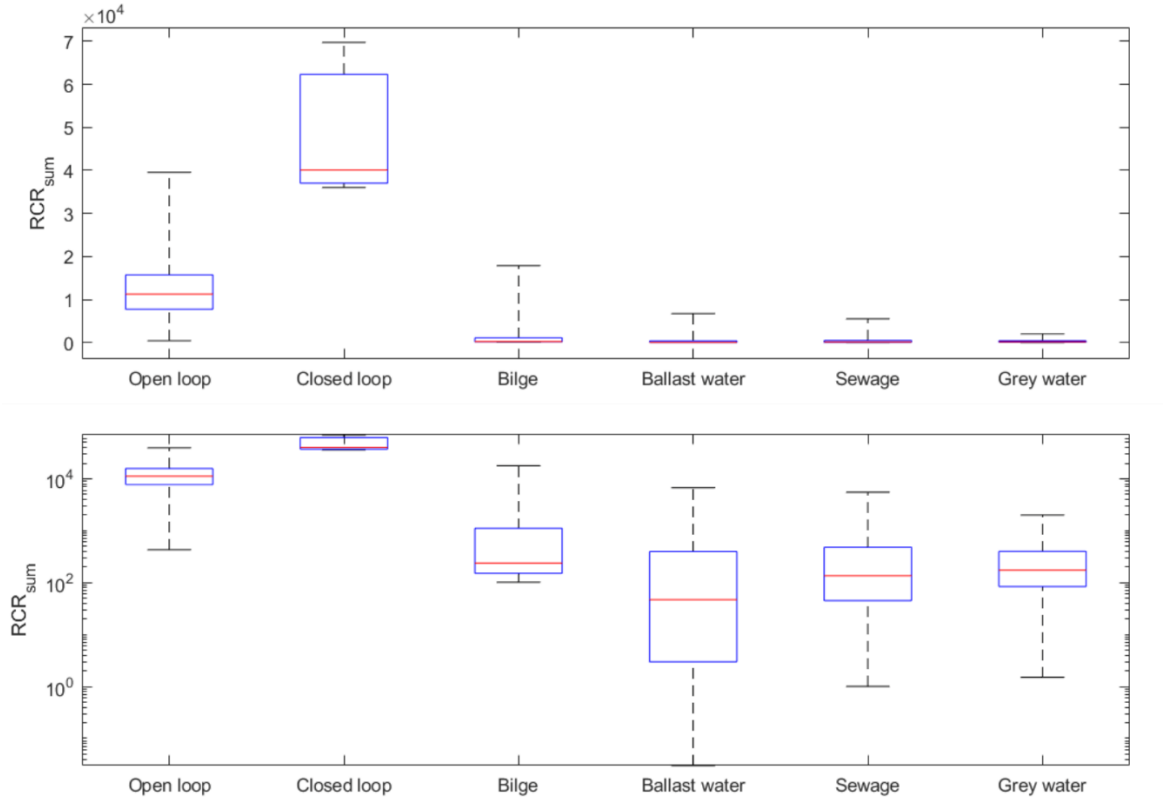

Figure 8. Comparing RCRsum of five waste streams from ships. The y-axis on the lower panel is in log10-scale for better comparison of the waste streams with lower RCRsum.

2.5. Modelling tools and input data

Several models were applied in this study, which were necessary to study the air emissions and discharges from ships, to describe the transport, transformation, and fate of pollutants in the atmosphere and oceans. A short general introduction is given below for each modelling tool applied in this work.

2.5.1. Ship Traffic Emission Assessment Model

The Ship Traffic Emission Assessment Model (STEAM) (Jalkanen et al., 2012, 2018, 2021, 2009; Johansson et al., 2013, 2017) was used to describe the environmental pressures from shipping. The STEAM model uses vessel speed and location information from Automatic Identification System (AIS) data, and technical information of individual ships from the S&P Global database, to model the power load, fuel consumption and air emissions. The modelling capability of STEAM

includes air emissions, discharges (Jalkanen et al., 2021) and underwater noise (Jalkanen et al., 2018, 2022). The working principle of the STEAM model is illustrated in Figure 3.8 for air emissions.

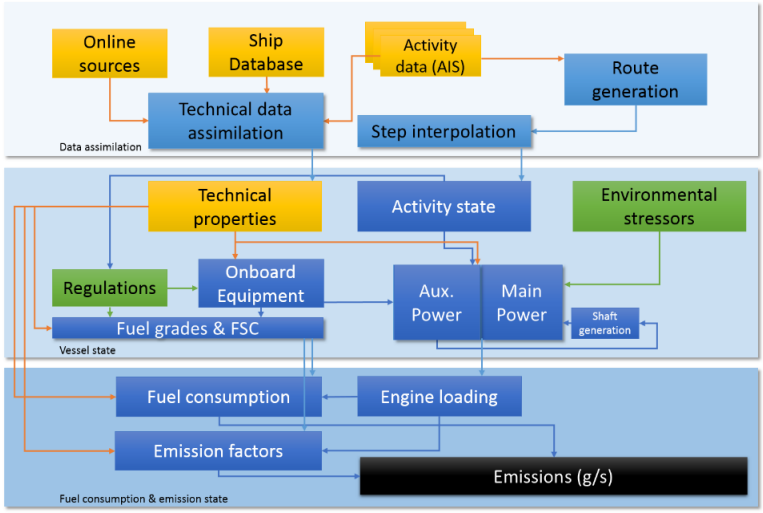

Figure 9 The working principle of the Ship Traffic Emission Assessment Model (STEAM), obtained from Johansson et al. (2017).

Accurate prediction of a ship's power output is the foundation of accurate emission modelling as the predicted emission rates are based on the estimated power output and fuel consumption of the vessel. Calm water resistance contributes to the major fraction of the total hull resistance and can be estimated based on vessel characteristics and instantaneous speed. However, a ship will also experience additional resistances due to ambient conditions. For example, Prpic-Orsic and Faltinsen (2012) modelled the annual CO_2 emissions of a container ship during a North Atlantic voyage and showed that emissions at sea increase approximately 15% due to sea and weather conditions. Resolving the impact of different factors explicitly based on AIS data, and climate and sea data, will increase the need for computational resources and this can be avoided by using a constant sea margin on top of the calm water resistance, which was the approach chosen in the Fourth IMO GHG study (Faber et al., 2020). However, describing the effect of ambient conditions by a constant scaling factor will practically neglect geographical or seasonal variations in weather and sea conditions. To reduce the uncertainty from varying operational conditions of the ship, the STEAM model was refined with a capacity to include wind, sea current, sea waves and sea ice data in the modelling and estimate the influence of ambient effects to a vessel's performance when these factors are considered. Including ambient conditions in the STEAM modelling, the inventory level uncertainty of fuel consumption modelling is less than two percent (for a fleet of

1313 vessels where commensurate activity was found) when compared to EU MRV fuel reporting data for 2022 (Jalkanen et al., 2023).

While the use of new fuels might reduce emissions of pollutants controlled by current regulations, it might introduce other issues that should be considered when evaluating the environmental performance of the ship. For example, Grönholm et al. (2021) reported that methane (CH_4) emissions from some liquified natural gas (LNG) fuelled ships were high enough to negate the GHG benefit of the reduction of carbon dioxide emissions (CO_2) when using LNG instead of conventional marine fuels. To estimate the impact of new fuels on air quality and GHG emissions from shipping, reliable emission inventories are needed. Therefore, the STEAM model has been updated with a capacity to model emissions from vessels using methanol or ammonia as a fuel.

To evaluate more accurately the amount of EGCS effluents and pollutants discharged into the environment, the list of vessels with a EGCS installation and areas with EGCS use limitations were updated in the STEAM model to include details of equipment type and installation date. This includes information from S&P Global and Global Information System for International Shipping (IMO GISIS).

In accordance with the review of Teuchies et al (2020), the EGCS effluent discharge rate was set to 90 m^3 MWh^{-1} and 0.45 m^3 MWh^{-1} for open and closed loop systems, respectively. Adoption of real discharge rates instead of normalised values (open loop 45 m^3 MWh^{-1}, closed loop 0.15 m^3 MWh^{-1}) also requires that the consecutive laboratory analysis of EGCS effluent samples need to use the actual concentrations instead of normalised numbers to maintain consistency of mass fluxes of contaminants. This is considered in all analysis carried out in the project.

2.5.2. Atmospheric chemical transport models

The atmospheric component of the EMERGE consortium involves 4 atmospheric models: the System for Integrated Modelling of Atmospheric Composition (SILAM), the Multi-scale chemistry-transport model for atmospheric composition analysis and forecast (CHIMERE), Community Multiscale Air Quality Model (CMAQ) modelling system and European Monitoring and Evaluation Programme (EMEP) model. In addition, the Weather Research and Forecast (WRF) model has been used to create the meteorological inputs for all three models. Meteorological data created by the European Centre for Medium-Range Weather Forecasts (ECMWF) were also used by the SILAM model. The data were for the year 2018. All models used the ship emission inventories obtained from the STEAM ship emission model.

The simulations conducted by each modelling group involved running several scenarios: a set of simulations with different shipping emission scenarios and one simulation without shipping emissions, all with the same land-based emissions. The STEAM emissions and CAMS (Copernicus Atmospheric Monitoring Services) emission inventory were used as the emission sources for shipping and land-based emissions, respectively, in the air quality models. All models simulated shipping emissions for year 2018 and for year 2050 in the S3 and S8 scenarios in combination with CAMS land-based emissions for year 2018. The 2050 shipping scenarios were simulated also with land-based 2050 emissions (ECLIPSE Maximum Feasible Reduction) with the EMEP model.

The simulations of shipping 2050 scenarios with two different scenarios for land emissions provided a sensitivity test of impact of the land emissions on the shipping signal simulated with the models. This sensitivity study showed low sensitivity of the shipping signal in terms of deposition of N, S, and metals, on changes in land-based emissions. Therefore, we have concluded that the shipping contributions for scenario S3 and S8 calculated with the model ensemble using the year 2018 land-based simulations represent well the shipping deposition signal in the year 2050.

Fate of atmospheric emissions of metals from shipping were calculated as part of ash particles resulting from the combustion of HFO. Emission factors for metals relative to emissions of ash are based on literature review performed in EMERGE (Table A- 2, in Appendix). Two models, EMEP and SILAM, have calculated the deposition of metals associated with shipping. Since emission inventories for other sources than shipping are only available for some of the relevant components, lead (Pb) and cadmium (Cd) in particular, only these 2 metals were calculated explicitly in the SILAM model, and the deposition of all other metals were calculated from the ash deposition data. In the case of EMEP, deposition of all metals was calculated from the ash data.

No significant difference between the SILAM and EMEP results were found considering the two different approaches used. Also, intercomparison with EMEP simulations of deposition of Pb and Cd (as well as S and N) on the Baltic Sea (Gauss et al., 2020) shows good agreement between the models.

In this work, emission factors relative to species calculated by the STEAM model have also been developed for PAHs (Table A- 3 in Appendix). The association with the STEAM species has been done about their volatility classes (semi volatile, SV, low volatile, LV, and extremely low volatile, ELV): The SV and LV PAH species were associated with STEAM HC emissions, the ELV species with OC emissions. To simulate fate of PAHs is complex as they undergo gas-to-particle

partitioning and atmospheric degradation in both phases, there is generally rather low understanding of these processes and only few chemistry transport models include chemistry of PAHs, typically only BaP. Since none of the models involved includes PAH chemistry, atmospheric deposition of PAHs could not be modelled within the project.

Concentrations of air pollutants simulated with the models are used to calculate deposition fluxes of the shipping-related air pollutants (metals, N and S) to the sea as well to calculate human exposures to evaluate the associated negative health impacts.

2.5.3. ChemicalDrift

Our approach for waterborne stressors includes nesting of several models. These use as inputs various discharge streams from STEAM and atmospheric deposition from chemical transport models. The case studies of this work rely on description of regional dispersion using the ChemicalDrift model to provide local boundaries for high resolution local scale modelling. Figure 10 depicts a general framework for water transport modelling (all steps), whereas regional scale modelling using ChemicalDrift includes steps 1-3 in Figure 10.

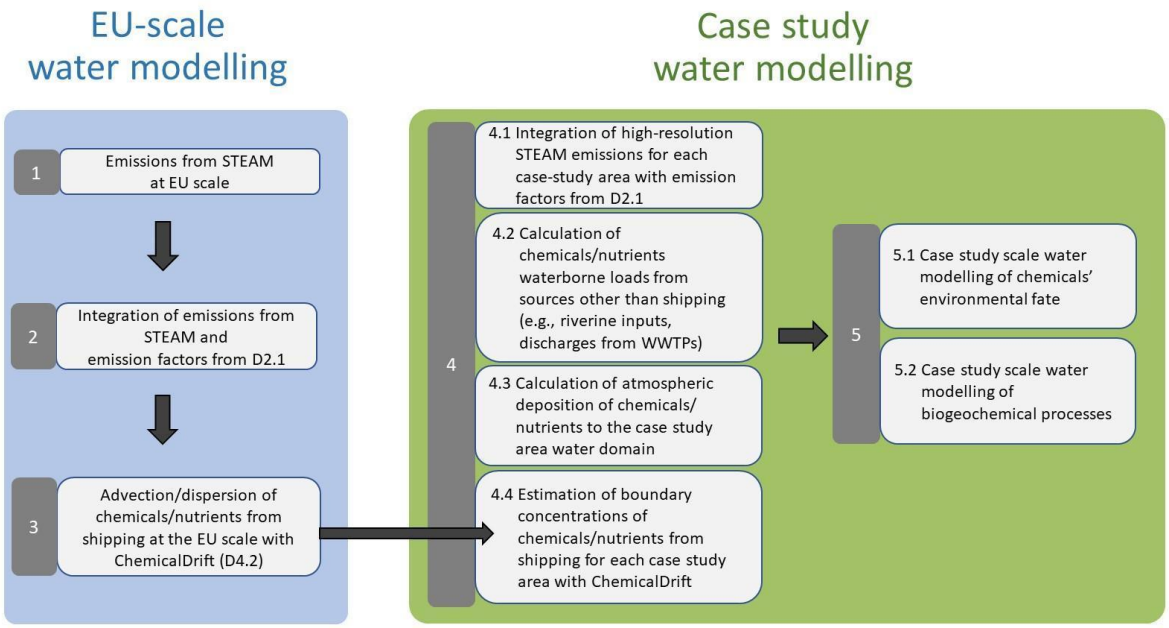

Figure 10. The concept for water modelling framework; WWTPs indicates Wastewater Treatment Plants.

ChemicalDrift model has been developed for this project by Aghito et al. (2023). It is integrated in the open-source Lagrangian framework OpenDrift, and the first version was developed for organic compounds and heavy metals.

The supported chemical processes of ChemicalDrift include degradation, volatilization and partitioning between the different phases that a target chemical can be associated to in the aquatic environment, e.g., dissolved, bound to suspended particles, or deposited to the seabed sediments, as shown in Figure 11. The dependencies of the chemical processes on changes of temperature, salinity, and particle concentration, are formulated and implemented. The chemical fate modelling is combined with wide support for hydrodynamics by the integration within the Lagrangian framework which provides, e.g., advection by ocean currents, diffusion, wind induced turbulent mixing, and Stokes drift generated by waves.

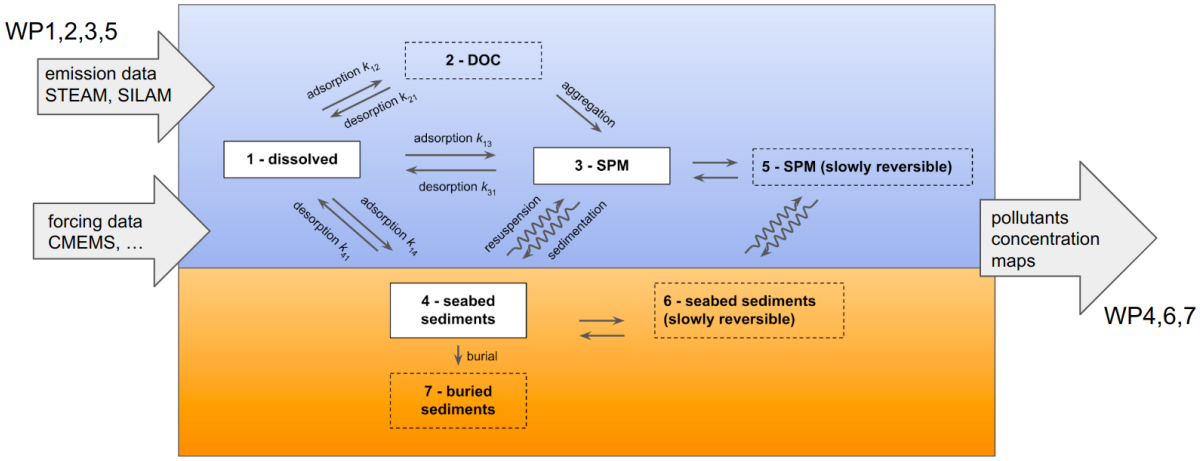

Figure 11. The model compartments implemented in ChemicalDrift and the corresponding exchange processes and transfer rates. The default (dissolved, adsorbed to SPM and sediments) compartments are indicated with solid contours. Optional compartments are depicted with dashed contours.

A flexible interface compatible with a wide range of available metocean data is made accessible by the integration, making the tool easily adaptable to different spatio-temporal scales, and fit for modelling of complex coastal regions. Further inherent capabilities of the Lagrangian approach include the seamless tracking and separation of multiple sources as, e.g., pollutants emitted from ships or from rivers or water treatment plants. The model includes a database of chemical parameters for a set of polyaromatic hydrocarbons, and a database of emission factors for different chemicals found in discharged waters from sulfur emission abatement systems in marine vessels. A post-processing tool for generating mean concentrations of a target chemical, over customizable spatio-temporal grids, is provided. ChemicalDrift is a flexible, freely available, and open-source tool for chemical fate and transport, that can be applied to assessment of the risks of contamination by organic pollutants in the aquatic environment.

While the atmospheric component of the impact studies has achieved a high degree of homogeneity in terms of the atmospheric circulation and dispersion models being used, this is not the case for the marine component. The diversity of the model suites used is dictated by the specific marine conditions that require numerical models of different characteristics and computing requirements for study scales. For example, while the Eastern Mediterranean case study includes a relatively deep basin with moderate stratification, the Northern Adriatic case study focuses on a semi-enclosed basin whose circulation dynamics are mainly determined by its low bathymetry, atmospheric forcing, and by freshwater discharges from the main rivers along the Italian coast. The Öresund case study describes a strait with extremely high stratification and

very strong currents.

2.5.4. Delft3D

Two case-studies were selected in the Eastern Mediterranean: The Saronikos Gulf in the Aegean Sea and the Venice lagoon in the Northern Adriatic. The former is a relatively deep coastal basin with moderately stratified waters, consisting of the southern boundary of the major metropolitan area of Athens and under the influence of the maritime traffic from and to the port of Piraeus. Contrary to Saronikos, the Venice lagoon is a shallow, well mixed most of the time coastal embayment, separated from the open sea by a series of islets, influenced by riverine waters and by mostly cruise-line traffic. The different geographic and oceanographic characteristics of the two basins imposed different modelling approaches for the marine environment.

In Saronikos Gulf, a full three-dimensional numerical simulation was selected, both for the physical (ocean circulation) and the water quality modelling. To that aim, the model-suite Delft3D was selected, of which the Delft3D-FLOW model was used for simulating the circulation of the Gulf, and the Delft3D-WAQ (WAter Quality) biogeochemical model was used to simulate the fate of the various pollutants introduced to the marine environment. A very similar approach, using the Delft3D model suite, has also been adopted in the Aveiro case study.

Delft3D-FLOW: This numerical model, used to simulate the state and circulation of a coastal region is a primitive-equation model solving the Navier-Stokes equations of water flow using the finite differences approach (Deltares Systems, 2023a). The model was adopted to cover the Saronikos Gulf, with a horizontal resolution ranging from 300 to 1400 m in the horizontal, and a vertical resolution determined by 20 sigma-layers (Kolovoyiannis et al., 2023). The Copernicus circulation hindcast, along with two locally developed regional-scale models (Mamoutos et al., 2021; Petalas et al., 2022) were used to provide the most suitable lateral boundary conditions that would lead to the most faithful simulation to 2018 observations. Atmospheric forcing was provided by the Aristoteles University of Thessaloniki in the framework of their contribution to this project.

Delft3D-WAQ: The Water Quality module of the Delft3D model suite, covers the basic marine biogeochemical processes of the, while being able to simulate the fate of a range of pollutants in the coastal environment (Deltares Systems, 2023b). Nutrients (NO3, NH4, DON, PO4, DOP, Si), and phytoplankton (diatoms, non-diatoms) have been simulated by the geochemical component

of Delft3D-WAQ, while the background concentrations of five trace elements (Cadmium, Nickel, Copper, Zinc, Lead) and four PAHs (Benzo(a)pyrene, Fluoranthene, Pyrene, Anthracene) have been reproduced by the model. To improve the assessment of gas exchanges through the air-sea interface, the model SWAN (The Swan team, 2013-2023) was used to simulate wind waves (Booij et al., 1999; Ris et al., 1999) and the model FUGAS (Vieira et al., 2013, 2018) to assess the fluxes of NO_x and SO_x through the air-water interface.

The Venice case study uses the SHYFEM model for water circulation and the Chemical Drift to assess the impact of the pollutants on the marine environment.

SHYFEM is a finite element, unstructured hydrodynamic model (Bellafiore and Umgiesser, 2010) covering the whole of the Adriatic Sea and its main coastal lagoons (Marano-Grado, Venice, and the Po River delta). To adequately resolve the river–sea continuum, the unstructured grid also includes the lower part of the major rivers flowing into the Adriatic Sea. The numerical grid consists of approximately 110,000 triangular elements with a resolution that varies from 5 km in the open sea to a few hundred metres along the coast and to tens of metres in the inner lagoon channels (Ferrarin et al., 2019).

Dilution approach.

Modelling of the fate of shipping discharges in the marine environment in the regional scale focused on simulating the environmental fate of single chemicals (benzo-a-pyrene, fluoranthene, cadmium, and lead), thus investigating shipping contribution to the long-term overall exposure of the coastal environment to these contaminants.

On the other hand, the results of an ecotoxicological test showed evidence of adverse effects on several marine organisms of EGCS effluent tested as a whole-effluent and based on these results a Predicted No Effect Concentration (PNEC) has been derived. Thus, the impact of the EGCS effluent on marine organisms has been determined at various dilution ratios based on these controlled ecotoxicological laboratory experiments. The assessment of the impact of EGCS effluent on the various case studies based on these ecotoxicological results requires a novel analytical approach that would enable us to assess the level of EGCS effluent dilution based on the results of the biochemical / water quality models (such as Delft3D-WAQ or Chemical Drift). Therefore, a synthetical approach to estimate persistence of the effluent as a homogeneous mixture in the environment is necessary, to derive a Predicted Environmental Concentration

(PEC) of the whole effluent (expressed as dilution rate) comparable to the available PNEC.

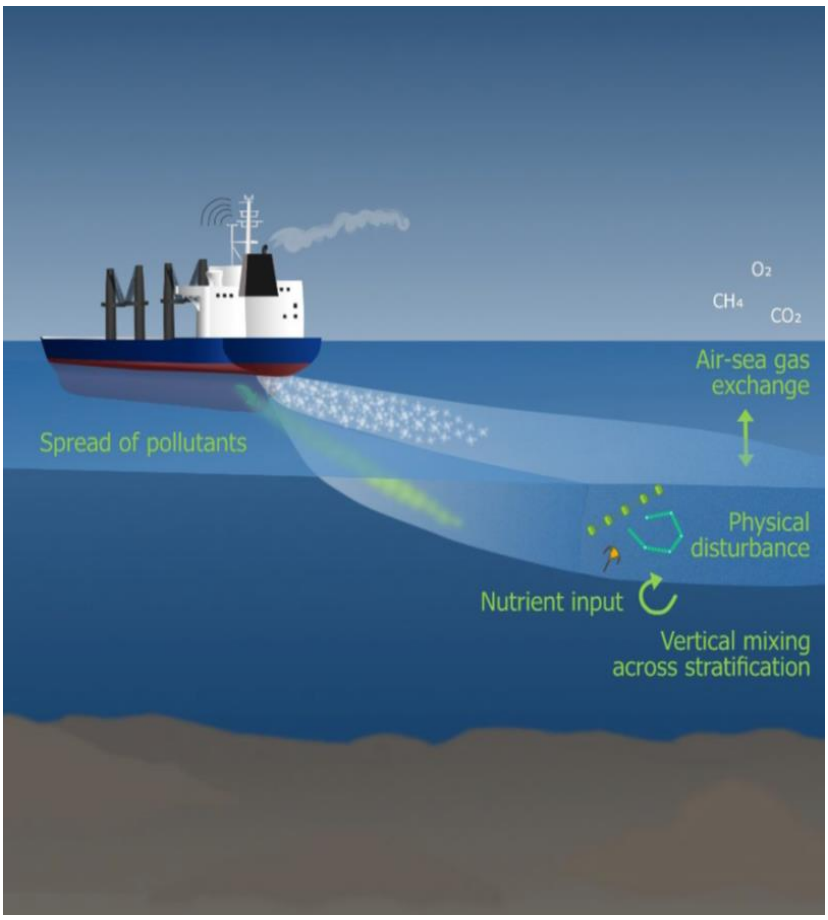

Figure 12. Dilution of discharges in ship wake, image from Nylund (2021)

The dominant process in reducing the concentration of EGCS effluent as soon as it is released in the marine environment is turbulent mixing (Figure 12). Then, as time passes, the intensity of mixing is gradually reduced in the wake of each vessel and biogeochemical processes (e.g., partitioning between water and suspended particles, sinking of particle-bound chemical, degradation, volatilization, biochemical processes) take over in determining different rates of concentration decay for each pollutant.

At the initial, “turbulent” stage of the presence of the effluent in the sea, violent mixing of EGCS effluent with ambient seawater causes a rapid decay of the concentrations of all elements of the initial mixture, however the relative concentrations (between each-other) in the mixture remain the same. On the contrary, at later stages, when different biogeochemical processes take over

for each element, the relative concentrations will start to diverge.

Thus, if we quantify the relative decay ratio of the i-th element of the effluent mixture as ((Eq *2*)

$$I_d^i = \frac{C^i(x,y,z,t)}{C_{ship}^i} \qquad \text{(Eq 2)}$$

where C_{ship}^i the concentration of the element in the EGCS effluent aboard the ship prior to its introduction to the marine environment, and $C^i(x,y,z,t)$ the concentration of the same element at the position x,y,z and time t in the wake (or, out of the wake) of the ship(s), then the degree of "consistency similarity" of the water at that position and time to the initial effluent can be quantified by the variance of the normalized decay ratios of all the elements comprising the effluent mixture ((Eq 3)

$$\sigma^2(I_d)(x,y,z,t) = \frac{1}{N-1}\sum_i^N \left(\frac{I_d^i(x,y,z,t)}{I_d(x,y,z,t)} - 1\right)^2, \qquad \text{(Eq 3)}$$

where N the number of effluent mixture compounds examined and $I_d(x,y,z,t)$ the "best" estimate of the dilution of the mixture. We have chosen to use the decay ratio of Cadmium as the best estimate of I_d due to its minimal biogeochemical activity relative to the other compounds. The above measure of consistency similarity is expected to exhibit very low values during the turbulent mixing stage of the EGCS effluent presence in the marine environment, and to continuously rise when the dilution ratios start to diverge due to different biogeochemical processes acting on the different compounds. Examples of the clarity of the use of this measure are shown in Figure 13, where the transition from turbulence to biogeochemical processes (and, consequently, from a homogeneous effluent mixture to an inhomogeneous mixture of pollutant compounds) is reflected by the abrupt start of rising values of the variance.

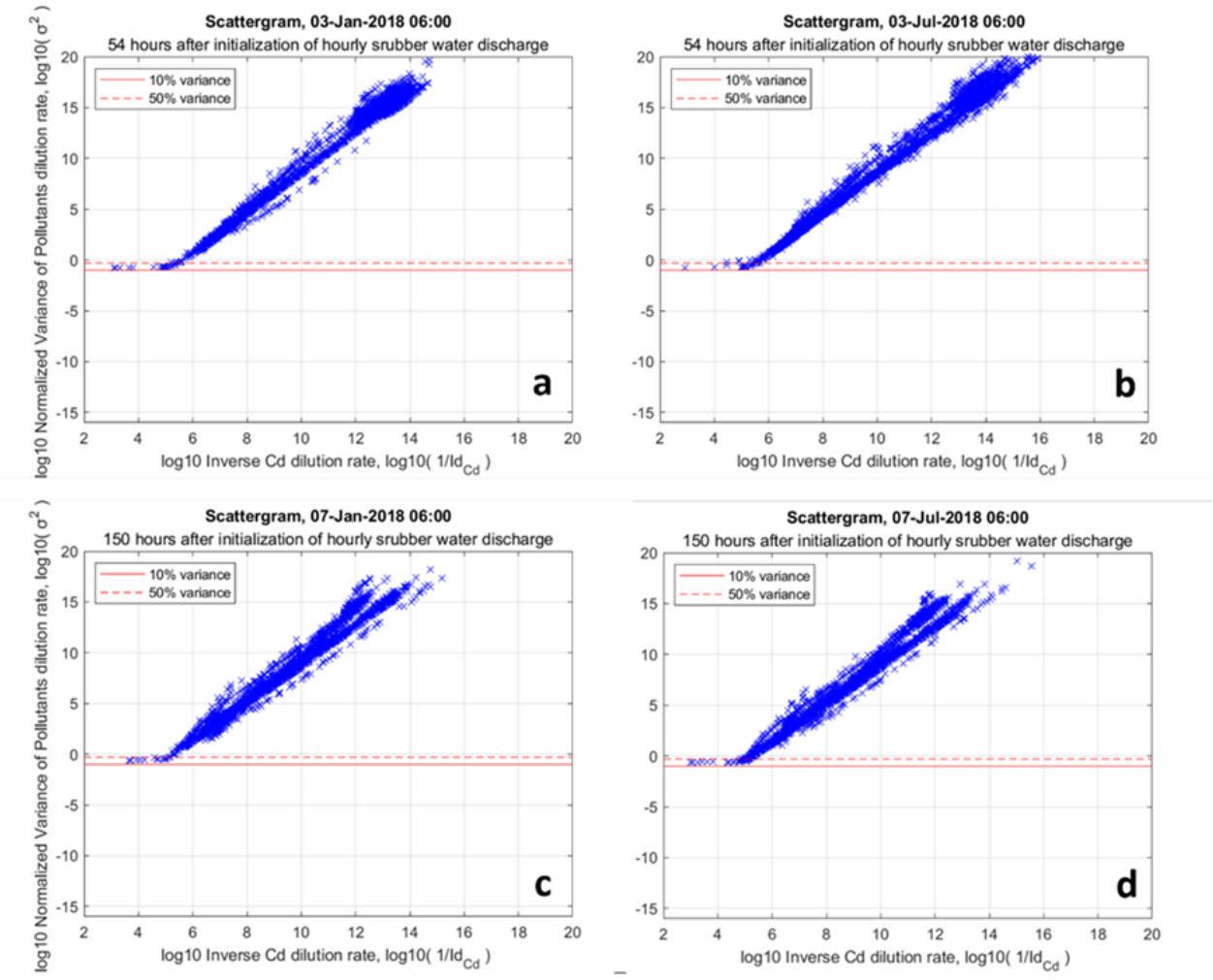

Figure 13. Scattergrams of normalised variance of pollutants dilution indices vs Inverse Cd dilution index, in log_{10} scale for the Saronikos Gulf case study: snapshots during 10-days experiments for Jan 2018 (a and c) and Jul 2018 (b and d).

Having developed this measure of homogeneity of the effluent mixture, we can estimate both the spatiotemporal variability of dilution rates and exposure of marine organisms to different levels of dilution, providing a direct link to the results of ecotoxicological experiments.

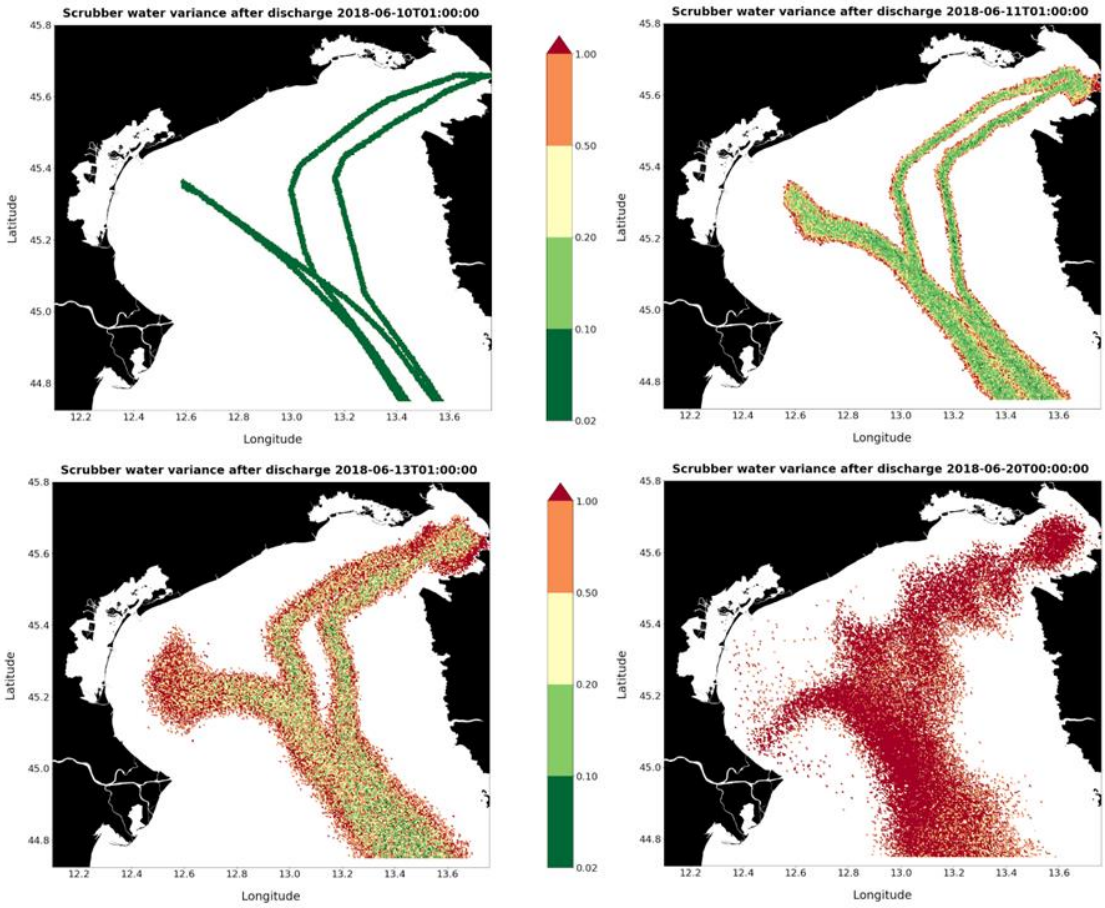

Figure 14. Variance of EGCS effluent after 1 (a), 24 (b), 72 (c), and 240 (d) hours after discharge into the water column on June 10th, 2018.

As an example, Figure 14 shows the variance maps obtained for the discharge of EGCS effluent in the Northern Adriatic case study for June 10th, 2018. Similar simulations were carried out also for the other EGCS effluent discharges simulated during the rest of the year show similar results (Figure 15). The simulations showed how, given the water currents and meteorological conditions of the case study area, the effluent forms a shipping lane about 2.5 km wide one hour after discharge, then reaching about 20-30 km before transforming into its separate components.

If a variance threshold of 0.1 is used, most of the EGCS effluent could be considered as degraded within four days. The period when EGCS effluent dispersion is mainly controlled by mechanical mixing (time_mix) varied between 2 and 20 hours, then first order degradation phenomena became prevalent with an estimated half-life of 8-16 hours.

However, these estimations are dependent on the variance threshold considered, thus we present also the results obtained by changing the value of the variance threshold between 0.02 and 0.5 (Table 7), leading to the presence of EGCS effluent lasting up to 6-9 days.

Table 7. The time when EGCS effluent dispersion is mainly controlled by mechanical mixing (time_mix) and effluent half-life calculated using a variance threshold ranging between 0.02 and 0.5.

	Variance threshold				
	0.02	0.05	0.1	0.2	0.5
time_mix (hours)	2-10	2-17	2-20	7-50	10-58
half-life (hours)	2-6	5-10	8-16	13-30	32-94

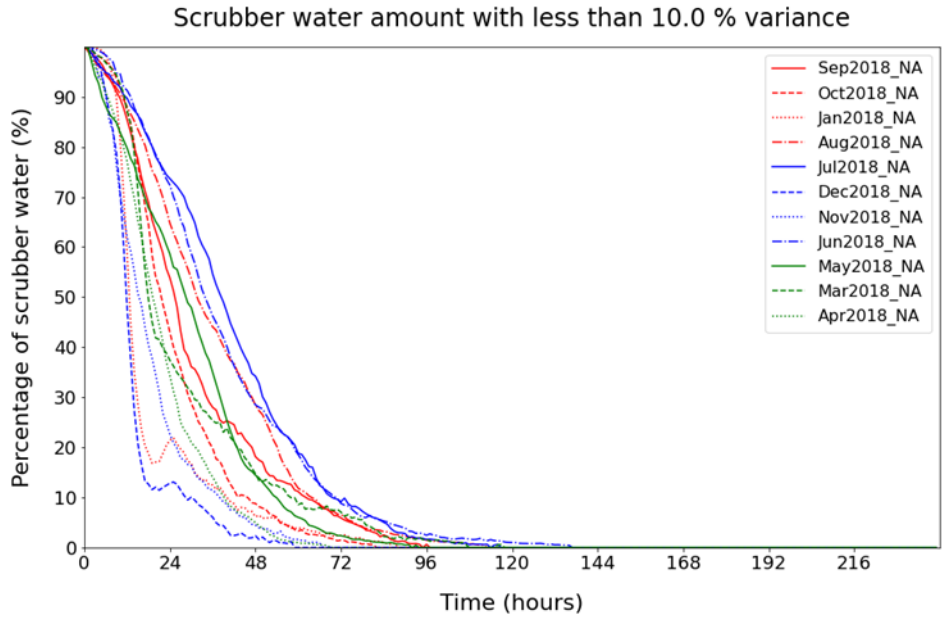

Figure 15. Percentage of residual EGCS effluent after a single discharge modelled for the highest EGCS effluent discharge occurring each month in the Northern Adriatic case study for 2018 (variance threshold of 0.1.)

These results show how this approach can be used to estimate the environmental fate of complex mixtures after their discharge into the water column, thus providing a direct link between

environmental exposure estimation and ecotoxicological information based on whole effluent testing procedures.

2.5.5. Merlin-EXPO

To explore the possible effects of changes in marine contamination on the potential bioaccumulation by aquatic organisms, bioaccumulation modelling has been performed to simulate the change in tissue concentrations of mussels considering the 2050 future scenarios. For this purpose, the MERLIN-Expo software toolbox (Ciffroy et al., 2016) has been used, as it provides the user with a library of flexible and freely combinable models to simulate environmental fate and biota exposure to different classes of chemicals (including both organic contaminants and metals) over time. The models for aquatic bioaccumulation implemented in MERLIN-Expo (generic models for “phytoplankton”, “aquatic invertebrate” and “fish”) account separately for bioaccumulation from the dissolved phase and from food (Giubilato et al., 2016) and can be used to describe the time-course of the internal concentration dynamics in different organisms. For the EMERGE work, the simplified trophic chain reported in Figure 16 has been used to simulate the internal concentration of benzo[a]pyrene, fluoranthene, cadmium and lead of mussels feeding on phyto- and zoo-planktonic species. Several parameters need to be set according to the target species and chemicals: general physiological parameters (e.g., allometric exponent, fraction of assimilated food), specific physiological and ecological parameters of modelled biota species (e.g., weight, length, diet preferences), chemical-specific parameters (e.g., K_{ow}, bioconcentration factor). Model parameterisation were as in Giubilato and Radomyski et al. (Giubilato et al., 2016; Radomyski et al., 2018). The selected model configuration has been calibrated using daily water concentration data provided by ChemicalDrift model for the baseline scenario 2018 and measured concentrations in mussels in coastal areas, monitored according to the Italian decree n.152/2006 (Italian parlament, 2006).

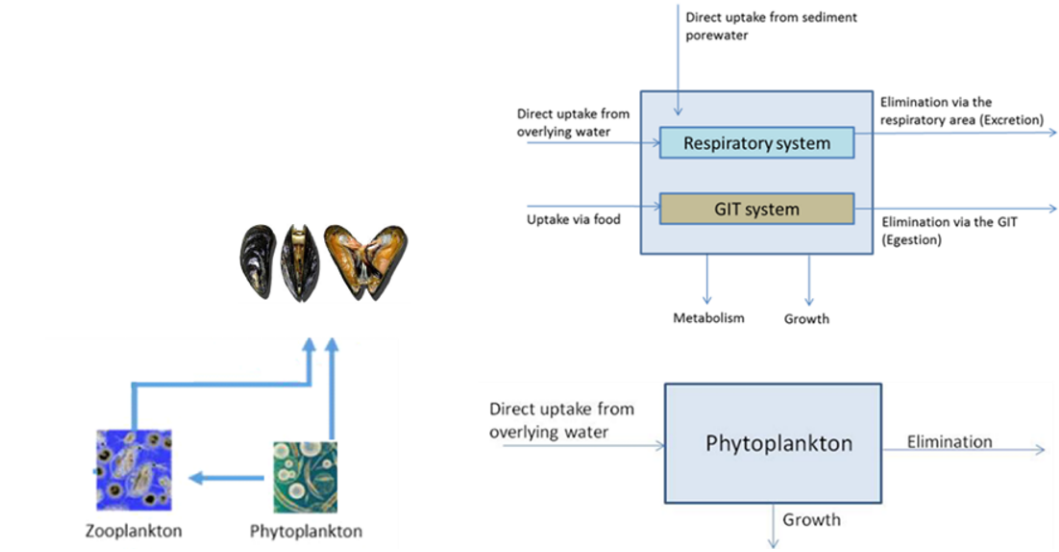

Figure 16. Simplified trophic chain used for bioaccumulation modelling (left); Conceptual models of "Phtyoplankton" and "Invertebrate" models in MERLIN-Expo (right).

2.6. Emission and discharge scenarios

For the impact analysis, the year 2018 was chosen as the baseline, because this represented the best compromise considering the availability of weather, oceanographic, air emission and water discharge data. However, it should be noted that the selection of 2018 as the baseline year reflects the situation before the significant increase of EGCSs in the global ship fleet which happened in 2019-2021 when ship owners adjusted their compliance strategy for the global 0.5% Sulfur cap. The number of ships equipped with EGCS and sailing the regional seas increased significantly over the last few years. In 2018, which is the baseline study year of EMERGE, only 178 vessels with an EGCS were identified (Figure 17, top left) in the Baltic Sea area. Based on these numbers, it can be concluded that the Baltic Sea EGCS fleet has more than quadrupled in size since 2018. A similar increase was observed for the North Sea fleet (Figure 17, top right), and for the Mediterranean Sea the increase of EGCS vessels was the largest of the studied regions (Figure 17, bottom).

The global EGCS fleet is over 4800 vessels. Any cost calculation of economic viability of EGCS should be done at global level and include all routes, regardless of location. Usually, the incentive to install and use an EGCS is the cost saving, which can be achieved by using

cheaper high-sulfur HFO instead of switching to more expensive low-sulfur distillate fuels. The price difference between the 0.1% distillate fuel and the high sulfur residual fuel oil was about 300 USD/tonne in October 2023 (Ship & Bunker, 2023).

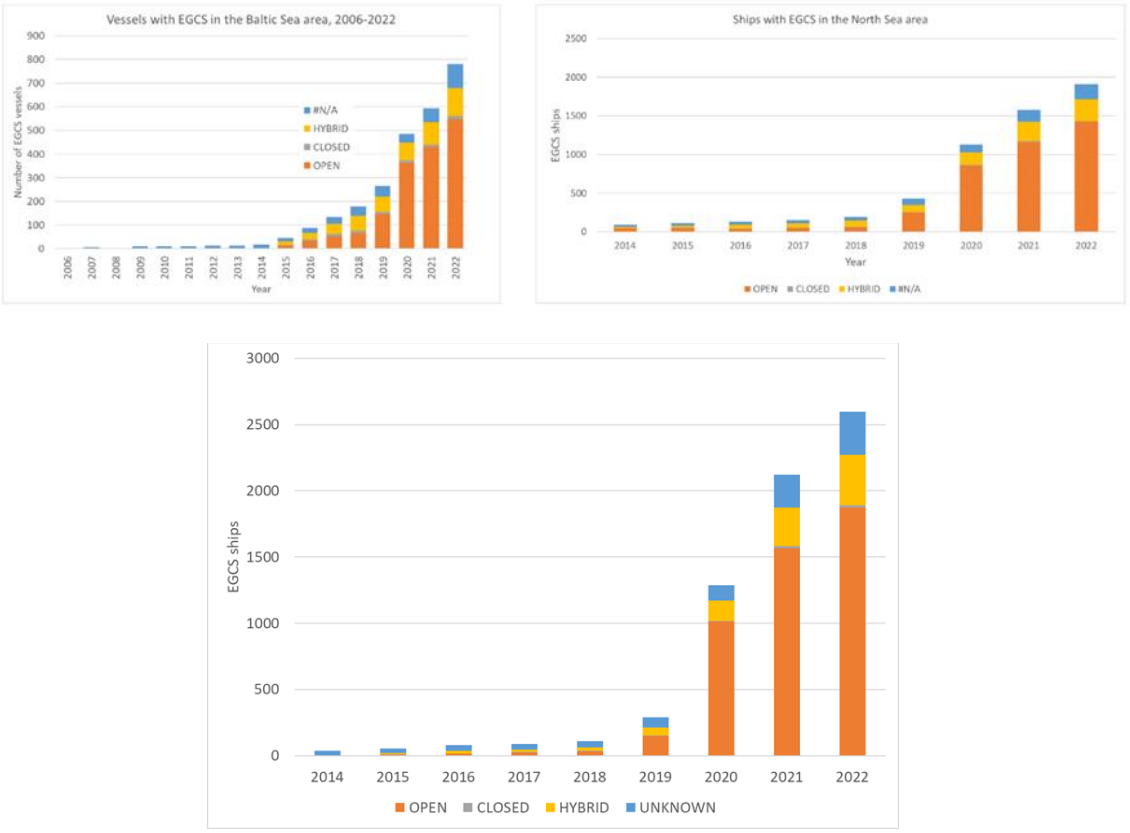

Figure 17. EGCS installations in the Baltic Sea (top left), North Sea/English Channel (top right) and the Mediterranean Sea (bottom) fleet by equipment type. For an unknown equipment type, an open loop system is assumed, because this is the most common option.

The scenarios developed for this work consist of eight potential future developments using the DNVGL report (Endresen et al., 2019) for traffic growth rates and transport work definitions (Table 8). In this work, scenarios from one to four vary with the assumptions of SCR and EGCS usage and in ship traffic growth. These four scenarios are not compliant with the initial IMO GHG strategy of 50% reduction of GHG emissions from ships, whereas scenarios five through eight are in line with it. Scenarios 3a, 3b and 8 were selected for impact assessment work, because they represent the highest and the lowest environmental pressures from EGCS perspective.

Additionally, Scenario 3 assumes A European Emission Control Area for NO_x and SO_x to be established within the Exclusive Economic Zone borders.

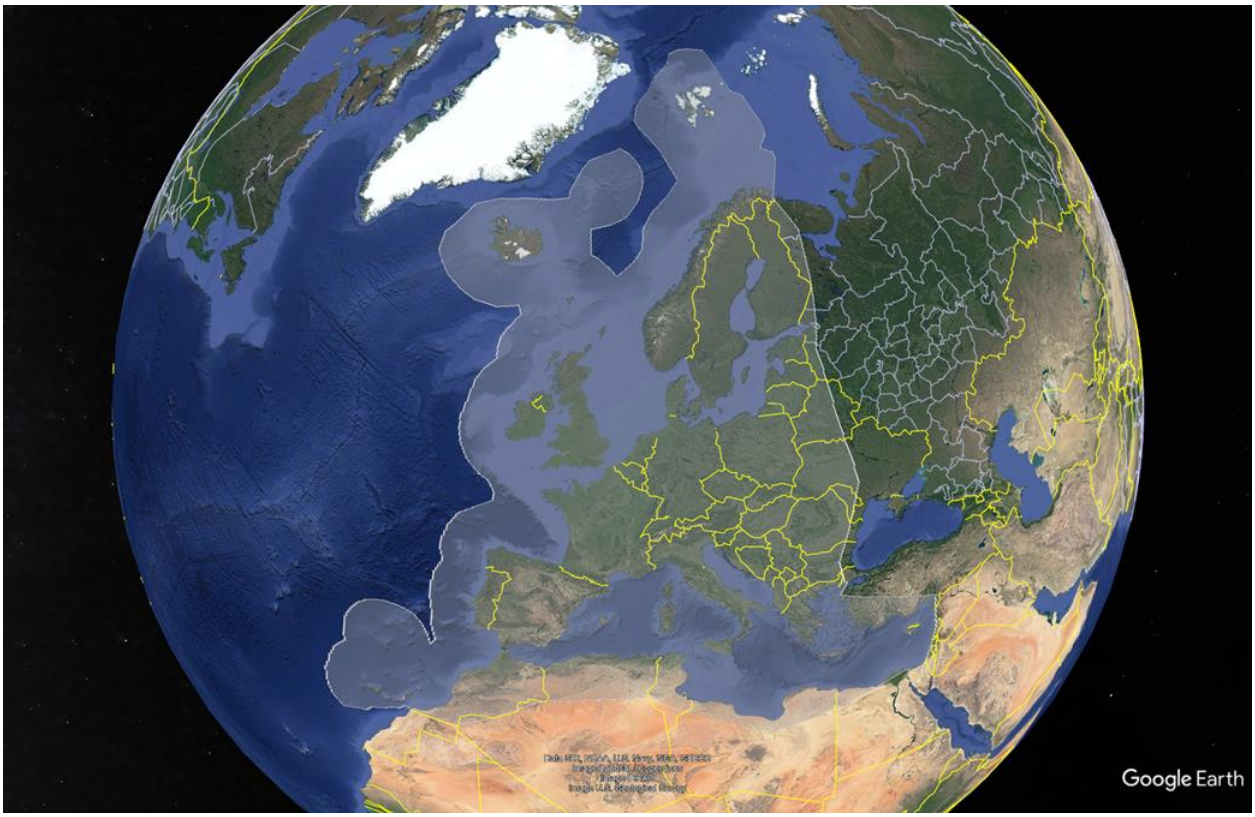

Figure 18. The European ECA assumed by Scenario 3.

Scenario 1 (S1) is a high-pressure scenario. The maritime transport development is high, there are no further measures to reduce the use of fossil fuels in shipping other than those already decided today, there is significant use of open-loop EGCS and high use of SCR in existing NECA areas (Baltic/North Sea).

Scenario 2 (S2) is the same as S1 but instead of open-loop EGCS the same ships are assumed to have EGCS which operate in closed-loop mode.

In **Scenario 3** (S3) we use the same assumptions as in S1 and that sulfur and nitrogen oxide emission control zones are introduced in all European sea areas. Scenario 3a uses open loop and Scenario 3b the closed loop EGCS as the default compliance option. Scenario 3 was selected for future impact assessment studies, because it includes the most EGCS installations and thus represents a high-pressure scenario.

In **Scenario 4** (S4) there is low development of ship traffic and more use of natural gas for short-sea shipping but otherwise identical to S1

Scenario 5 (S5) is a low-pressure scenario. There is low development of ship traffic, measures

are assumed to be in place for shipping to reach the IMO objective of a 50% reduction in the emissions of green-house gases by 2050, there is no use of EGCS and low use of SCR.

For **Scenario 6** (S6) we assume high development in ship traffic, measures in place to reach the IMO 50% goal, high use of EGCS operating in open loop mode, and high use of SCR.

Scenario 7 (S7) is like S6 but with low use of both EGCS (operating in open loop mode) and SCR.

Scenario 8 (S8) is an LNG scenario. It has the same assumptions as S7 but with an extensive use of LNG in Europe. In this scenario, there is no need for EGCS since the use of low-sulfur liquid fuels, LNG and methanol obviates the need of SO_x abatement.

Table 8. Overview of EMERGE scenarios. Those with grey background were selected for future assessment of impacts.

Scenario number	DNVGL scenario	EGCS scenario	SCR	Low sulfur	GHG origin	Alternative fuel
1	High growth	High	NECA	SECA	Fossil fuel	
2	High growth	High	NECA	SECA	Fossil fuel	
3	High growth	High	All of Europe	All of Europe	Fossil fuel	
4	Low growth	High	NECA	SECA	Fossil fuel	LNG (SSS)
5	Low growth	No HFO	None	SECA	50% renewable	Methanol
6	High growth	High	NECA	SECA	50% renewable	Methanol
7	High growth	Low	None	SECA	50% renewable	Methanol
8	High growth	No HFO	None	SECA	50% renewable	LNG & Methanol

SSS=Short-Sea Shipping; High growth and Low growth refer to DNVGL definitions for different ship types.

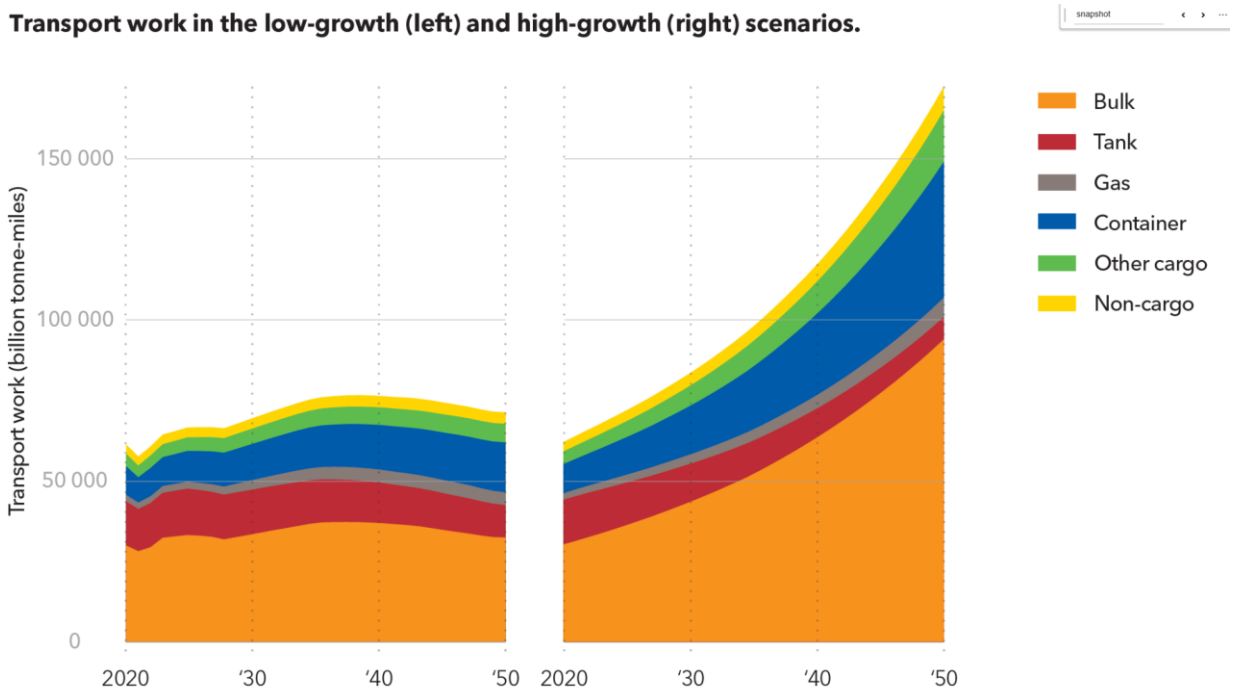

Figure 19. Transport work development in low- and high-growth scenarios, according to DNV GL (Endresen et al., 2019)*. Traffic growth rates defined for each ship type separately in STEAM were made to match the definitions of DNVGL for different decades. Image from DNVGL Maritime Forecast to 2050 report.*

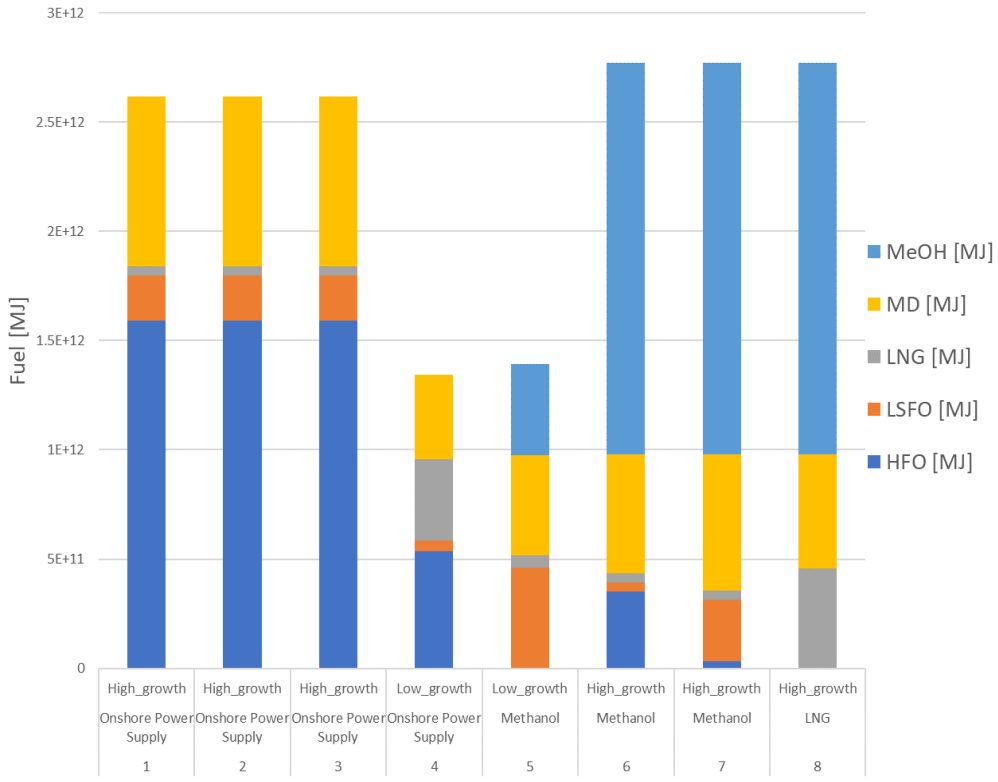

Figure 20. Fuel mix in 2050 (as fuel heat content in MJ) in different scenarios.

Our focus is on emission abatement equipment and consequences of secondary emissions. Thus, we have focused the scenario work on these parameters together with the development of marine fuels and propulsion systems. Therefore, we have chosen to adopt the scenarios describing the development of transport demand and development of ship size and energy efficiency. The scenarios were developed according to the DNVGL Energy Transition Outlook - Maritime Forecast report (Endresen et al., 2019).

3. Pressures

3.1. Baseline 2018

Before the introduction of the global 2020 sulfur cap of 0.5%, most of the EGCS discharges were concentrated on SO_x ECAs and European sea regions where additional sulfur regulation was in effect for passenger traffic on a regular schedule (European Parliament, 2016). In Figure 21, spatial distribution of the discharges from open loop EGCS is presented. After the decision taken in MEPC70 to lower the global sulfur limit to 0.5% (by weight), significant increase in the ships equipped with EGCS was observed and the spatial distribution of EGCS discharges became global. In 2018, which is the baseline year of this study, represents the time before the significant increase of EGCS effluent discharge from vessels (Figure 22).

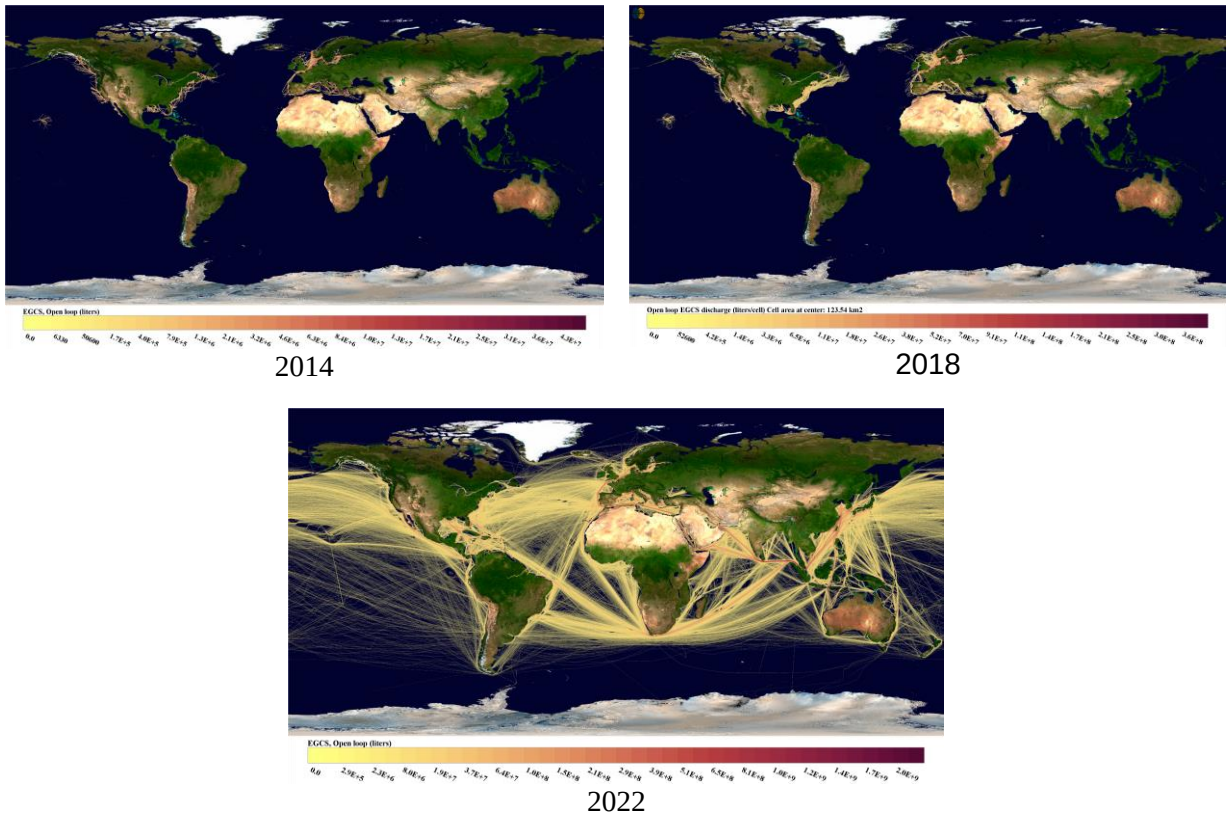

Figure 21. Discharge of open loop EGCS effluent from the global fleet in 2014 (top left), 2018 (top right) and 2022 (below). All values are given in litres of effluent discharged per map grid cell. In 2014, EGCS effluents were mostly discharged in Baltic Sea/North Sea area. After the introduction of the North American ECA, EGCS effluent discharges were increased in that area. In 2022, EGCS effluents are discharged globally.

In 2022, the global EGCS effluent discharge volumes exceeded 18 gigatonnes, of which 99.99%

was from open loop systems. It should be noted that these volumes were calculated using a higher discharge rate, 90 m^3 MWh^{-1} for open loop and 0.45 m^3 MWh^{-1} for closed loop, than the normalised rates (45 and 0.3 m^3 MWh^{-1}). According to the review made by Teuchies et al (2020), higher discharge rates are justified. For the baseline 2018 studies reported in this work, and the impact studies, global discharges were about 718 million tonnes of which two thirds occurred in European sea areas.

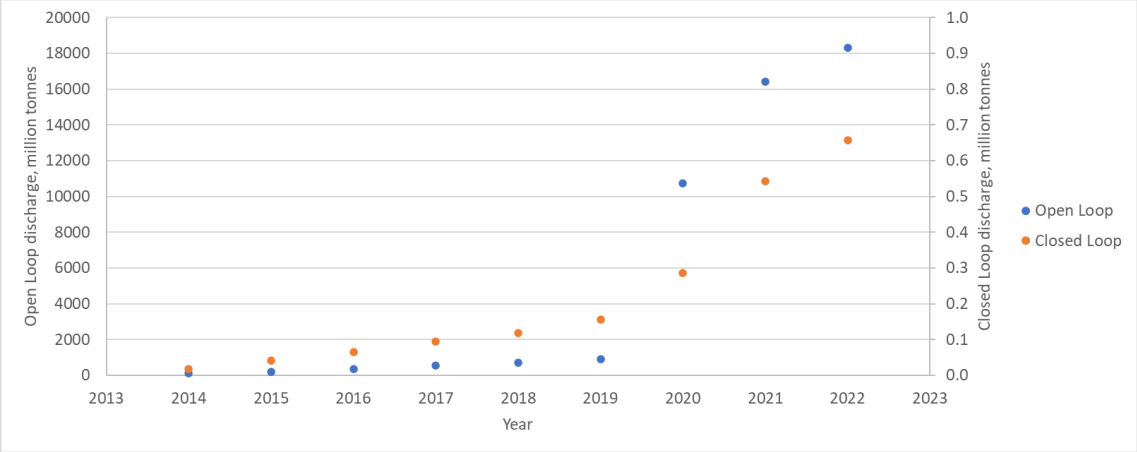

Figure 22. Global discharges from EGCS during 2014-2022. The adoption of the global Sulfur cap of 2020 motivated a significant increase in EGCS usage.

3.1.1. Regional

3.1.1.1. Baltic and the North Sea area

Volume of EGCS discharges were estimated using the STEAM model, and discharge rate of 90 m^3 MWh^{-1} from open loop and 0.45 m^3 MWh^{-1} from closed loop systems were used in the modelling. For 2018, the estimated volumes of effluent discharge by sea region are given in Table 9 and the spatial distributions of effluent discharge from open loop systems are depicted in Figure 23 and Figure 24.

In Figure 23, for the Bothnian Bay, the northernmost part of the Baltic Sea area, use of open loop EGCS is not predicted. The low alkalinity of seawater in the Bothnian bay area (Müller et al., 2016) would require significant increase in effluent volume (OCIMF, 2016) and vessels are thought to switch to low sulfur fuels or use closed loop mode of EGCS in this area. In the modelling of

discharges, we have attempted to include relevant area definitions for open loop EGCS discharge ban areas. However, the requirement for such an area in the model requires that there is an existing, well documented decree from a relevant maritime authority which includes a definition of the area and a starting date. Also, for these areas, ban of open loop discharge is required to be compulsory. There are several examples of local recommendations not to discharge EGCS effluent from open loop systems, but since these are not compulsory open loop effluent discharge is allowed in STEAM.

Table 9. Discharges of EGCS effluents in the Baltic Sea and the North Sea areas in 2018

Area	**Open loop (million tonnes)**	**Closed loop (million tonnes)**
Baltic Sea	192	0.2
North Sea and the English Channel	170	0.02

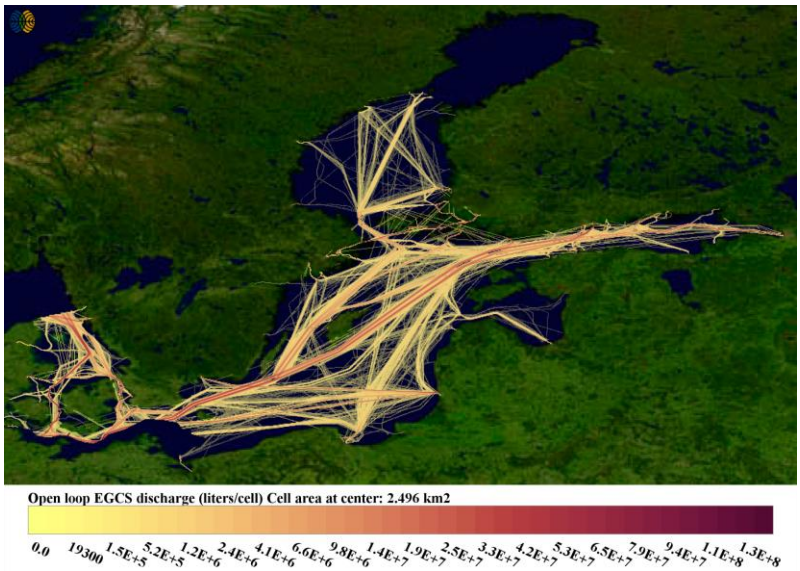

Figure 23. Spatial distribution of EGCS effluent discharges from open loop systems in 2018 in the Baltic Sea area. The unit of discharge is litres per map grid cell.

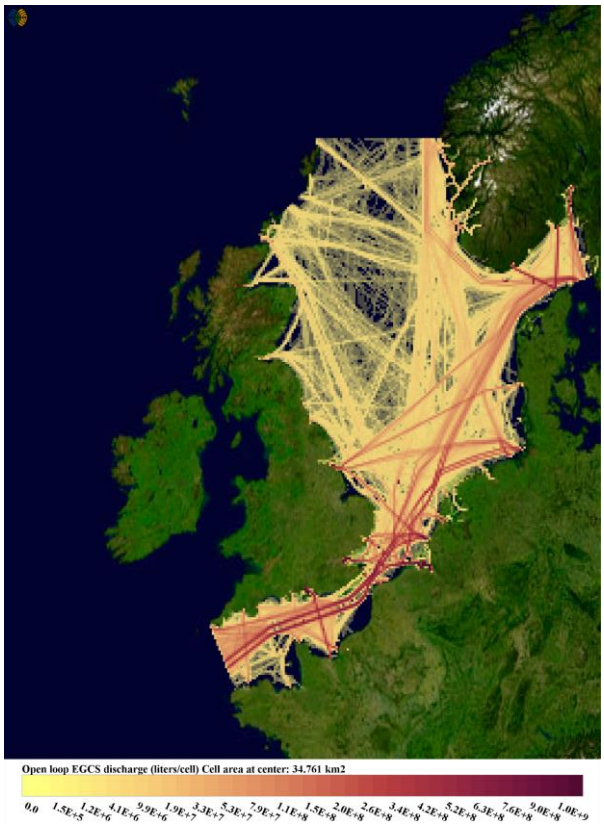

Figure 24. Spatial distribution of EGCS effluent discharges from open loop systems in 2018 in the North Sea and the English Channel. The unit of discharge is litres per map grid cell.

The discharge volumes modelled were combined with the water analysis from earlier work, and onboard sampling of this project. It should be noted that the discharge rates were not modelled as normalised values, which requires that determined contaminant concentrations of laboratory analysis are used, not normalised concentrations. This approach ensures that the mass fluxes of the total effluent discharge are correctly represented.

Considering environmental pollution from shipping, both direct discharge from ships to the sea and indirect contribution through atmospheric deposition need to be considered. However, the description of the contribution of atmospheric deposition in case of contaminants is challenging because the compounds relevant for water pollution are not routinely reported as part of atmospheric emission inventories. This means that emissions from other sources than shipping for PAH16 or various metals may not be readily available, even if they can be estimated for ships. Air emission inventories from other sectors than shipping are available for less than half of the compounds listed in Table 10. This is a good reminder that for air quality impact assessments, a very different set of compounds may be relevant than for water pollution impacts (Table 11). Consecutive impact studies must include all relevant contaminants, otherwise they will not be representative of the full effect from relevant substances.

Table 10. Total mass of contaminants emitted to the air in different sea regions in 2018.

Contaminant	**Baltic Sea area, tonnes**	**North Sea and the English Channel, tonnes**
Arsenic	0.3	0.7
Cadmium	0.1	0.2
Chromium	0.6	1.2
Copper	0.7	1.4
Iron	4.6	8.2
Mercury	0.0	0.0
Nickel	1.8	2.1
Lead	0.4	0.8
Vanadium	3.4	3.9

Zinc	6.2	12.1
Naphthalene	6.8	8.1
Acenaphthene	0.1	0.1
Acenaphthylene	0.1	0.2
Fluorene	0.1	0.2
Phenanthrene	0.6	0.9
Anthracene	0.0	0.0
Fluoranthene	0.1	0.3
Pyrene	0.1	0.2
Benzo[a]anthracene	0.0	0.1
Chrysene	0.2	0.3
Benzo[b]fluoranthene	0.0	0.1
Benzo[k]fluoranthene	0.0	0.1
Benzo[a]pyrene	0.0	0.1
Dibenzo[a,h]anthracene	0.0	0.0
Benzo[g,h,i]perylene	0.0	0.1
Indeno[1,2,3-cd]pyrene	0.0	0.1

Table 11. Total mass of contaminants discharged to the sea in different sea regions in 2018.

Contaminant	**Baltic Sea area, tonnes**	**North Sea and the English Channel, tonnes**
Arsenic	1.3	1.2
Cadmium	0.16	0.15
Chromium	3.0	2.5
Copper	7.5	6.6
Iron	46	41
Mercury	0.015	0.014

Nickel	9.4	8.1
Lead	1.8	1.6
Vanadium	34	30
Zinc	21	19
Naphthalene	0.53	0.47
Acenaphthene	0.036	0.032
Acenaphthylene	0.025	0.022
Fluorene	0.088	0.078
Phenanthrene	0.29	0.26
Anthracene	0.015	0.014
Fluoranthene	0.031	0.027
Pyrene	0.061	0.055
Benzo(a)anthracene	0.025	0.022
Chrysene	0.036	0.032
Benzo(b)fluoranthene	0.008	0.010
Benzo(k)fluoranthene	0.002	0.002
Benzo(a)pyrene	0.010	0.01
Dibenzo(a,h)anthracene	0.006	0.005
Benzo(g,h,i)perylene	0.004	0.003
Indeno[1,2,3-cd]pyrene	0.013	0.012

Input of metals and nutrients from atmospheric deposition

In Table 12 and Table 13 the input of metals to the Baltic Sea, North Sea, and English Channel, simulated with atmospheric chemistry transport models is presented. It should be noted that these deposition data represent total shipping contribution, and not just the ship emissions from ships sailing the Baltic Sea or the North Sea areas. Emissions from ships sailing the Norwegian Sea, or further, can be carried to the Baltic Sea/North Sea areas through atmospheric transport. In Table 12, deposition of Pb and Cd from shipping in 2018 is presented together with the total

atmospheric deposition of these metals in 2018. The table shows that shipping-related part of the total deposition is negligible, but this analysis can only be made for some metals because emission data from other sources than shipping is not available. Low contribution from ship emitted metals is due to the shift to low sulfur fuels and the use of EGCS in the SECA sea regions. This is also clearly visible on the deposition map for 2018 in Figure 25, with a distinct difference of high deposition of metals at the western entrance to the English Channel. Metals and PAHs are partly washed to the sea with the EGCS effluent instead of being emitted to the air.

*Table 12. Annual mean deposition of Pb and Cd (tonnes year^{-1}) during 2018 baseline in the Baltic Sea, North Sea, and English Channel. Mean values of EMEP and SILAM model simulations, * shows results from the SILAM model only.*

Sea	Total deposition* (tonnes/year)	Shipping contribution	
		Absolute (tonnes/year)	Relative (%)
Annual lead deposition			
Baltic Sea	60	7.21E-03	0.01%
North Sea	72	1.85E-02	0.03%
English Channel	8	7.71E-03	0.09%
Annual cadmium deposition			
Baltic Sea	3.4	3.85E-04	0.01%
North Sea	3.9	9.88E-04	0.03%
English Channel	0.4	4.12E-04	0.11%

Table 13. Annual deposition of metals from shipping (tonnes year^{-1}) in the Baltic Sea, North Sea, and English Channel for 2018, mean values of EMEP and SILAM model simulations (column 2-4).

Metal	Atmospheric deposition from shipping (tonnes/year)		
	Baltic Sea area	North Sea	English Channel
Arsenic	4.94E-03	1.27E-02	5.29E-03
Cadmium	3.85E-04	9.88E-04	4.12E-04
Chromium	1.28E-02	3.29E-02	1.37E-02
Copper	1.54E-02	3.95E-02	1.65E-02
Iron	1.5	4.0	1.6
Mercury	3.85E-04	9.88E-04	4.12E-04

Metal	Atmospheric deposition from shipping (tonnes/year)		
	Baltic Sea area	**North Sea**	**English Channel**
Nickel	2.5	6.4	2.7
Lead	7.09E-03	1.82E-02	7.58E-03
Vanadium	5.1	13.0	5.4
Zinc	0.15	0.38	0.16

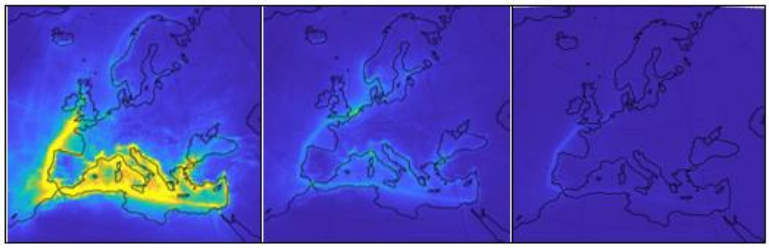

Deposition [mg/m²]

Ash	As	Cd	Cr	Cu	Fe	Hg	Ni	Pb	V	Zn
1.4	1.1E-4	8.8E-6	2.9E-4	3.5E-4	3.5E-2	8.8E-6	5.7E-2	1.6E-4	1.2E-1	3.4E-3
1.2	9.7E-5	7.6E-6	2.5E-4	3.0E-4	3.0E-2	7.6E-6	4.9E-2	1.4E-4	1.0E-1	2.9E-3
1	8.1E-5	6.3E-6	2.1E-4	2.5E-4	2.5E-2	6.3E-6	4.1E-2	1.2E-4	8.3E-2	2.4E-3
0.8	6.5E-5	5.0E-6	1.7E-4	2.0E-4	2.0E-2	5.0E-6	3.3E-2	9.3E-5	6.6E-2	1.9E-3
0.6	4.9E-5	3.8E-6	1.3E-4	1.5E-4	1.5E-2	3.8E-6	2.5E-2	7.0E-5	5.0E-2	1.5E-3
0.4	3.2E-5	2.5E-6	8.4E-5	1.0E-4	1.0E-2	2.5E-6	1.6E-2	4.6E-5	3.3E-2	9.7E-4
0.2	1.6E-5	1.3E-6	4.2E-5	5.0E-5	5.0E-3	1.3E-6	8.2E-3	2.3E-5	1.7E-2	4.8E-4
0	0	0	0	0	0	0	0	0	0	0

Figure 25. Contribution of shipping to the atmospheric deposition of ash particles and metals (in milligrams m^2) in Europe in 2018, 2050 S3 and 2050 S8 scenarios simulated with the EMEP model.

Table 14 shows input of nitrogen and sulfur to the sea as a model mean of SILAM, EMEP and CMAQ models deployed in EMERGE. Contribution of shipping to the total N deposition in the region is 13-16%. In 2050 scenarios the relative shipping contribution decreases to 6-7% in S3 and 7-12% in S8. Contribution from the atmospheric deposition is dominating the contribution of N from shipping to the sea in 2018, the contribution is 99%. In 2050 scenario S3 the relative significance of input of N from the EGCS effluent increases to 13-14%. In the S8 scenario no releases of EGCS effluent are predicted. Other important shipping-related sources of nitrogen are discharges of sewage and food waste, these are, however, much lower than atmospheric deposition. Regarding the sulfur deposition, in 2018 both the absolute and the relative

contributions of shipping are increasing from the Baltic Sea to the North Sea and the English Channel with decreasing distance to the sea regions without SECA limit on fuel sulfur content. In 2050 the shipping contribution to sulfur deposition decreases by 40 - 70% compared to year 2018, however, the relative contribution increases as the land-based sulfur emissions decrease even more. In the S8 scenario the decrease in absolute shipping contribution is almost 90% and the relative contribution to S deposition decreases.

Table 14. Annual deposition of total nitrogen (oxidised + reduced, Ntot) and sulfur (S) on the Baltic Sea, North Sea, and English Channel in kt/year in 2018. Mean values of EMEP, SILAM and CMAQ model simulations.

Sea	**Total deposition (1000 tonnes y^{-1})**	**Shipping contribution (kt/year)**		**Atmospheric deposition from shipping rel. shipping deposition plus EGCS effluent discharges**
		Absolute (1000 tonnes y^{-1})	**Relative Total**	
Annual Ntot deposition				
Baltic Sea	171.5	22.9	13.4%	98.8%
North Sea	284.3	42.1	14.8%	99.5%
English Channel	46.9	8.3	17.7%	
Annual S deposition				
Baltic Sea	70.4	2.9	4.2%	
North Sea	85.3	7.6	8.9%	
English Channel	14.7	4.1	28.1%	

Loads of metals and PAHs to the Baltic Sea from shipping relative to other sources The load of PAHs (16 US EPA priority PAHs) and metals (As, Cd, Cr, Cu, Pb, Hg, Ni, V and Zn) from atmospheric deposition, riverine inputs, point sources (coastal industries and wastewater treatment plants), maritime shipping and leisure boating to the Baltic Sea were calculated based on data from various sources (see Figure 26 and Ytreberg et al., 2022) for a thorough description on data sources used and methodology applied). A simplified extrapolation method was used to estimate loads of atmospheric emissions and deposition fluxes since only Cd, Cu, Hg, Pb and benzo[*a*]pyrene are included in EMEP chemistry transport model on the Baltic Sea scale (Gauss et al., 2020). Hence, annual atmospheric loadings of metals and PAHs to the surface water of the Baltic Sea were calculated by extrapolating the deposition fluxes of 9 metals (including Pb, Cd, V and Ni) and 12 PAHs (including fluoranthene and benzo[a]pyrene) at Swedish background stations to the surface area of the Baltic Sea subbasins (see Ytreberg et al. 2022). National data

of annual riverine input of metals reported by the HELCOM contracting parties were collected for the period 2015–2017 (HELCOM, 2022).

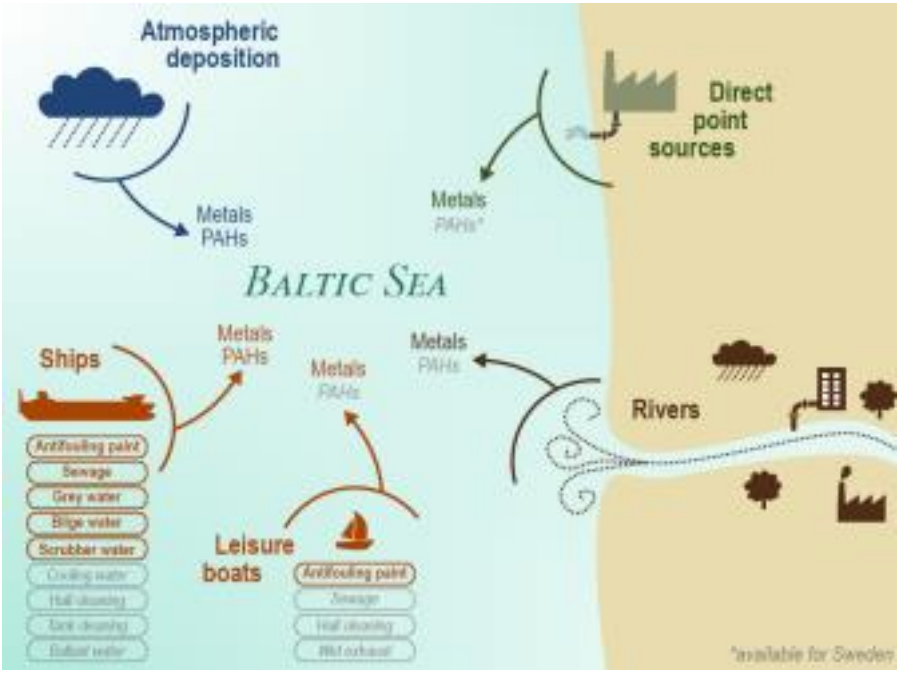

Figure 26. Direct discharges and atmospheric deposition of metals and PAHs to the Baltic Sea. Grey text in italic indicates substances and sources where data is lacking and thus not included. (From Ytreberg et al., 2022)

The loads of metals from point sources with outlets directly to the coast were compiled from HELCOM PLC7 (HELCOM, 2022). The data includes loads from industrial point sources and larger coastal municipal wastewater treatment plants (WWTPs) during the period 2016–2018. In the load compilation, all inputs from atmospheric deposition, rivers and point sources are expressed as annual inputs and represent the period between 2015 and 2018. This implies that in all future EMERGE scenarios for 2050, the loads the atmospheric deposition, rivers and point sources will remain the same as in 2015–2018 while the emissions from shipping will change due to different policy measures and assumptions in shipping development.

The total annual load of Ni to the Baltic Sea region in 2018 was 700 tonnes (Figure 27A), of which direct discharges from open loop EGCS accounted for 11.4 tonnes (1.7%). The input from EGCS is considerably higher in scenario 3 (2050), accounting for 84 tonnes of Ni (or 10.5% of the total input). For Cd (Figure 27B), the total annual load to the Baltic Sea region in 2018 was estimated

to be 26 tonnes and the contribution from EGCS effluent was 0.2 tonnes (0.7%). Similarly to Ni, the share of Cd from EGCS compared to the total input increased significantly in Scenario 3 from 0.7% to 5.2%. For Pb (Figure 27C), less than 1% of the total input originated from EGCSs in 2018. The share from EGCSs increased to 5.3% in scenario 3 (2050).

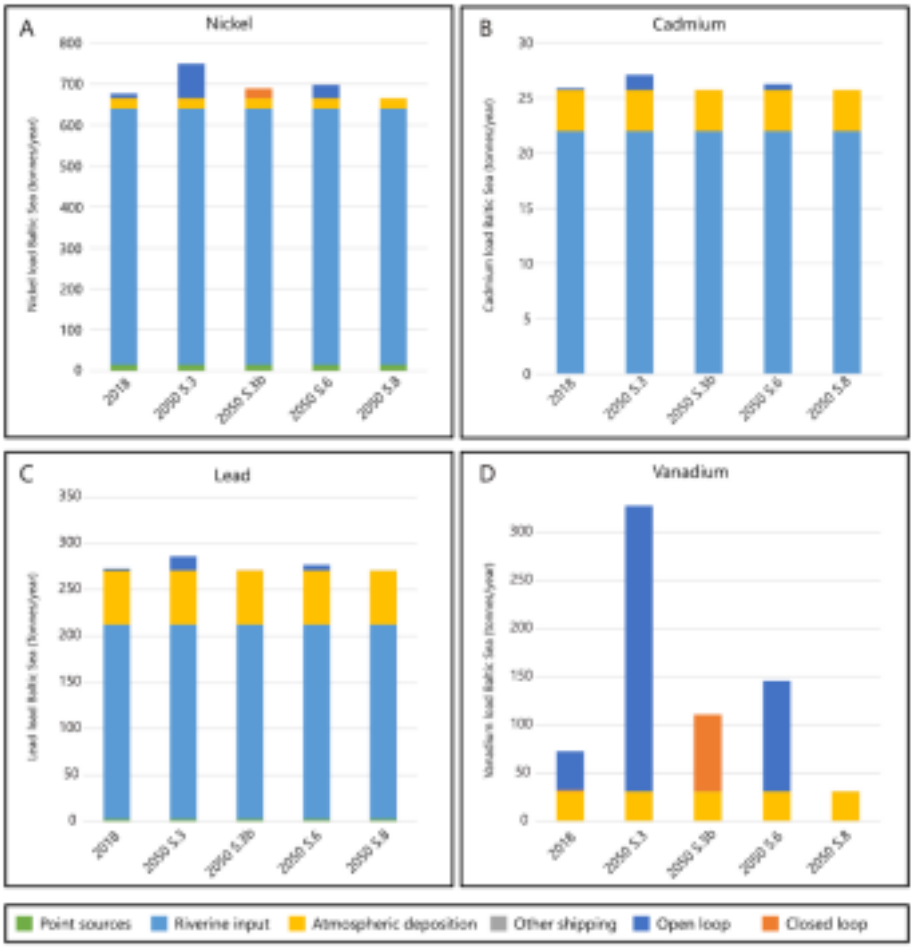

Figure 27. Comparison of loads (tonnes/ year) of Ni (A), Cd (B), Pb (C) and V (D) from rivers, atmospheric deposition, direct point sources, open loop EGCS, closed loop EGCS and other sources of shipping (bilge water, sewage, and greywater) to the Baltic Sea region in 2018 and different shipping scenarios for 2050. For V, riverine input and point sources were excluded due to insufficient data coverage (only Sweden).

For V (Figure 27D), riverine input is only available from Swedish rivers and no country reported inputs from coastal point sources. Thus, a thorough load compilation was not possible to perform since the assessment is limited to inputs from shipping and atmospheric deposition. Nonetheless, open loop EGCSs were found to discharge 41 tonnes of V in 2018, which is higher compared to the atmospheric deposition (31 tonnes) and like the riverine input from Swedish rivers (47 tonnes).

The load in 2050, according to scenario 3 from open loop EGCSs, is as high as 297 tonnes of V, while the closed loop mode scenario (scenario 3b) showed lower inputs (80 tonnes).

Loads of metals and PAHs to the North Sea from shipping relative to other sources

Inputs of metals and PAHs from shipping to the North Sea were estimated using STEAM. Load of metals and PAHs in riverine input and direct discharges from industries and WWTPs to the North Sea was compiled from the Riverine input and direct discharges programme (RID) from OSPAR (https://www.ospar.org/work areas/hasec/hazardous-substances/rid). RID aims to monitor and assess all inputs and discharges of selected contaminants to the OSPAR maritime area and its regions that are carried via rivers into tidal waters or are discharged directly into the sea. Monitoring and reporting of the concentrations and load of relevant metals such as Cd, Cu, Pb, Hg and Zn is mandatory for OSPAR member states. However, no country reports inputs of V or PAHs. Here, we used the average yearly load of riverine input during a three-year period (2018 - 2020). The annual load of Pb and Cd to the North Sea is shown in Figure 28, and similarly to the Baltic Sea an increase of open loop EGCS related load is estimated in scenario S3, while the environmental pressure from EGCSs in Scenario S3b is very low (<0.1 tonnes/year).

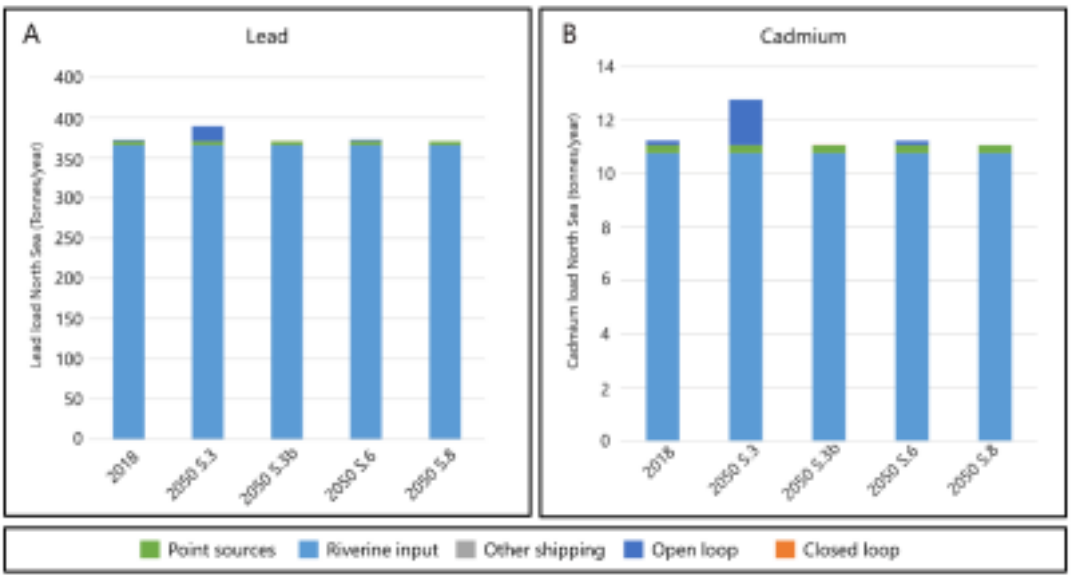

Figure 28. Comparison of loads (tonnes/ year) of Pb (A) and Cd (B) from rivers, direct point sources, open loop EGCSs, closed loop EGCS and other sources of shipping (bilge water, sewage and greywater) to the North Sea (OSPAR region) in 2018 and different shipping scenarios for 2050.

3.1.1.2. Mediterranean Sea

All estimations of emissions and discharges from shipping were produced using the Ship Traffic Emission Assessment Model (STEAM). Figure 29 shows the spatial distribution of total emissions of particulate matter (PM2.5), methane (CH_4), nitrogen oxides (NO_x), and sulfur oxides (SO_x) from shipping in the EMERGE baseline year 2018. Air emissions of heavy metals and PAHs from shipping in the Mediterranean Sea area are collected to Table 15 and for discharges to Table 16.

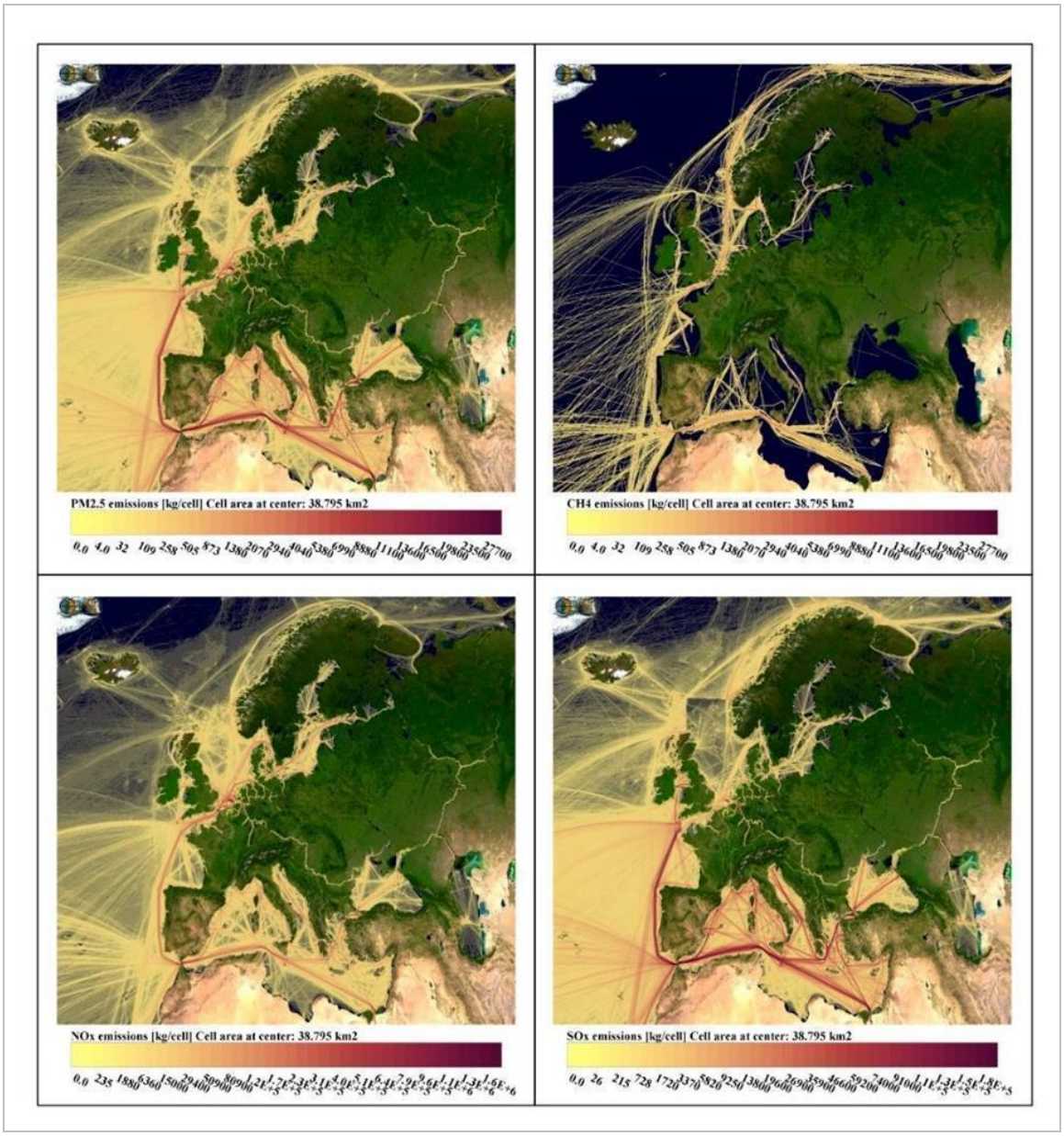

Figure 29. Emissions of $PM_{2.5}$(top left), CH_4 (top right), NO_X (bottom left) and SO_X (bottom right) from shipping in 2018 (EMERGE baseline year). Data from STEAM. Note: different colour scales.

Table 15. Air emissions of contaminants from ships sailing the Mediterranean Sea during 2018. The unit of emissions is tonnes.

Contaminant	Mass, tonnes	Contaminant	Mass, tonnes
Arsenic	3.6	**Fluorene**	1.4
Cadmium	0.8	**Phenanthrene**	6.8
Chromium	6.9	**Anthracene**	0.2
Copper	8	**Fluoranthene**	0.8
Iron	178.1	**Pyrene**	0.8
Mercury	0	**Benzo[a]anthracene**	0.7
Nickel	236.2	**Chrysene**	5.2
Lead	4.4	**Benzo[b]fluoranthene**	0.5
Vanadium	476.3	**Benzo[k]fluoranthene**	0.4
Zinc	71	**Benzo[a]pyrene**	0.5
		Dibenzo[a,h]anthracene	0.4
Naphthalene	96.3	**Benzo[g,h,i]perylene**	0.6
Acenaphthene	1.9	**Indeno[1,2,3-cd]pyrene**	0.4
Acenaphthylene	0.6		

Table 16. Discharges of contaminants from ships sailing the Mediterranean Sea during 2018. The unit of emissions is tonnes.

Contaminant	Mass, tonnes	Contaminant	Mass, tonnes
Arsenic	0.58	**Fluorene**	0.038
Cadmium	0.07	**Phenanthrene**	0.13
Chromium	1.2	**Anthracene**	0.007
Copper	3.2	**Fluoranthene**	0.013
Iron	20	**Pyrene**	0.027
Mercury	0.07	**Benzo[a]anthracene**	0.011

Nickel	3.9	**Chrysene**	0.016
Lead	0.76	**Benzo[b]fluoranthene**	0.003
Vanadium	15	**Benzo[k]fluoranthene**	0.001
Zinc	9.2	**Benzo[a]pyrene**	0.004
		Dibenzo[a,h]anthracene	0.002
Naphthalene	0.23	**Benzo[g,h,i]perylene**	0.002
Acenaphthene	0.016	**Indeno[1,2,3-cd]pyrene**	0.006
Acenaphthylene	0.011		

As can be seen from Table 15 and Table 16, which describe the air emissions and discharges of various contaminants from shipping, most of the contaminants are emitted to the air. For example, in 2018 the amount of Nickel emitted to the air because of combustion of HFO was 236 tonnes, whereas the corresponding amount in discharges was less than four tonnes. In 2018, EGCS effluent discharge volumes were low because mainly passenger vessels on a regular schedule were using EGCS in the area. However, in 2022, the balance of contaminants from air emissions and discharges was shifted towards the discharges, because a lot more ships were using EGCS to remove sulfur from ship exhaust. In 2022, Nickel emissions to the air were about 27 tonnes from low sulfur fuels, whereas Nickel in EGCS effluent discharges was 70 tonnes.

Total EGCS effluent discharge volumes in the Mediterranean Sea are shown in Figure 30. In EMERGE baseline year 2018, most of the EGCS effluent were released by passenger vessels (Cruise, RoPax). After implementation of the global sulfur cap in 2020, most of the effluent was released by container vessels (Figure 31) and the discharges were spatially distributed along the economic exclusive zones of Spain, France, Italy and Greece (Figure 32).

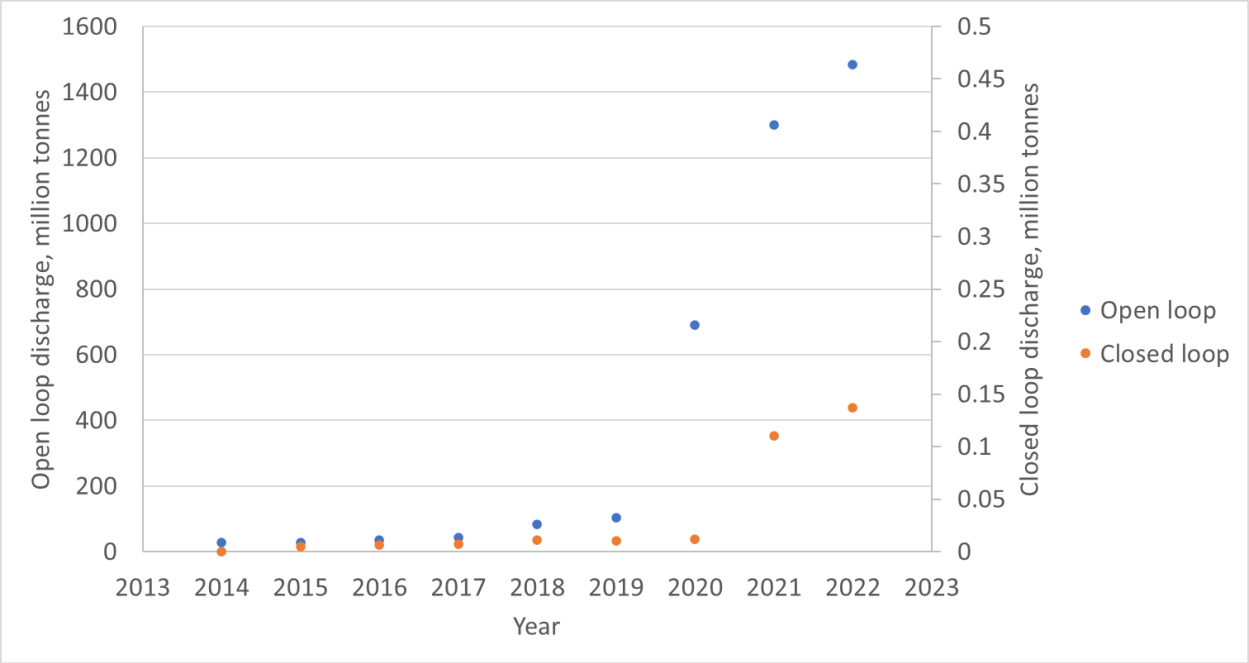

Figure 30. Discharges from EGCS in the Mediterranean Sea area during 2014-2022. In 2018, over 83 million tonnes of EGCS effluents (83 million tonnes from open loop, 0.01 tonnes from closed loop) were discharged to the Mediterranean Sea.

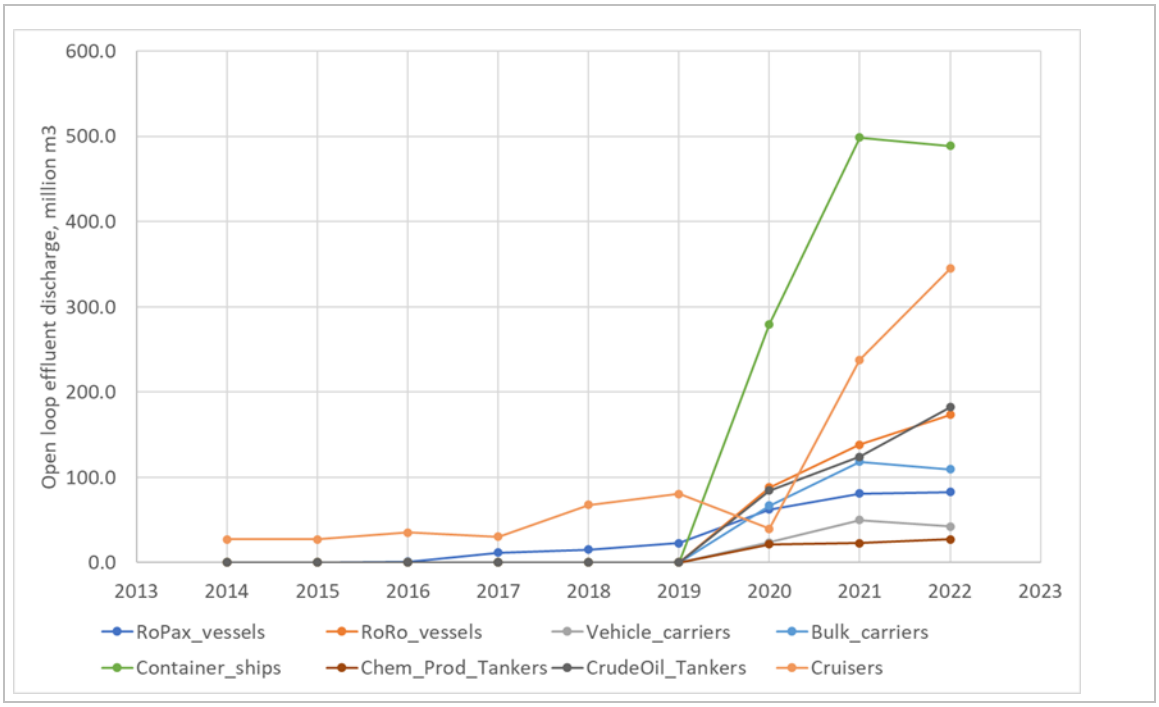

Figure 31. EGCS effluent discharge from ships of various types sailing the Mediterranean Sea during 2014-2022

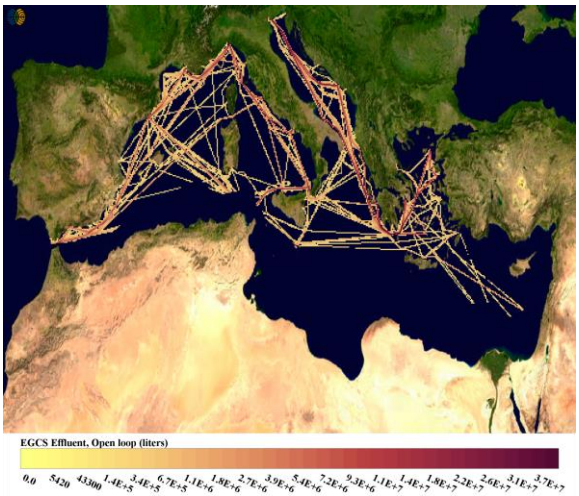

2014 (Scale maximum: 37,000,000 litres)

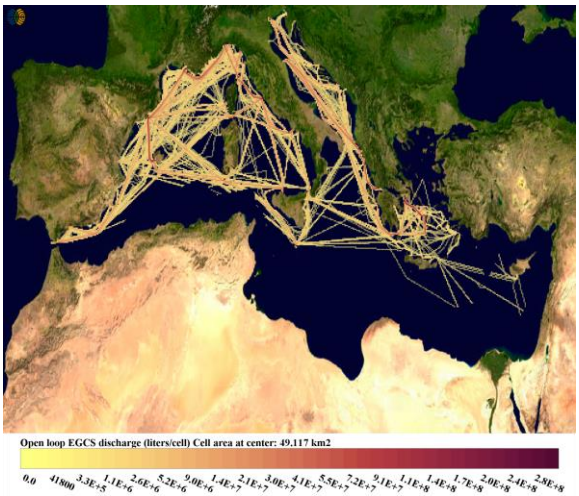

2018 (Scale maximum 280,000,000 litres)

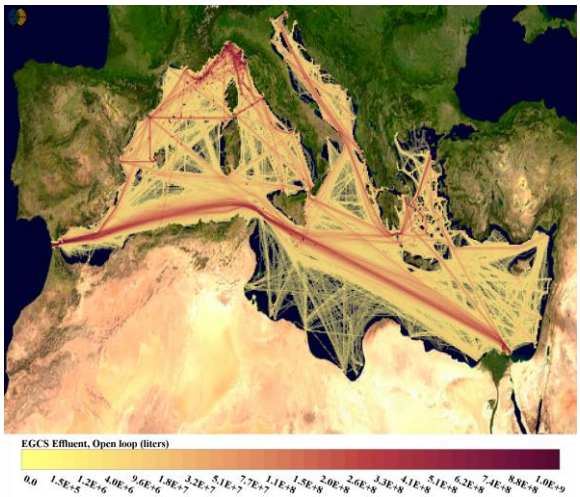

2022 (Scale maximum 1,000,000,000 litres)

Figure 32. The geographical distribution of open-loop EGCS water discharges in 2014, 2018 and 2022. Note the change of scale maximum in each case.

Input of metals and nutrients from atmospheric deposition

In Table 17 and Table 18 the input of metals to the Mediterranean Sea, simulated with atmospheric chemistry transport models, is presented. In Table 17 deposition of lead of cadmium from shipping is presented together with the total atmospheric deposition of these metals. Table 18 shows deposition of all investigated metals from shipping, but only Pb and Cd can be given in relation to other emission sources. Table 19 reports the shipping share of nutrients from total airborne nutrient loading in European sea areas.

*Table 17. Annual mean deposition fluxes to the Mediterranean Sea of lead and cadmium in t/year. Mean values of EMEP and SILAM model simulations, * shows results from the SILAM model only.*

Metal	Total deposition* (tonne y^{-1})	Shipping contribution	
		Absolute (tonne y-1)	Relative (%)
Lead	328	3.14E-01	0.10%
Cadmium	10.2	1.67E-02	0.16%

Table 18. Annual mean deposition fluxes of metals from shipping in tonnes $year^{-1}$ on the Mediterranean Sea for 2018, mean values of EMEP and SILAM model simulations are shown.

Metal	Atmospheric deposition from shipping (tonne y^{-1})
Arsenic	0.22
Cadmium	0.017
Chromium	0.56
Copper	0.67
Iron	67
Mercury	0.017
Nickel	109
Lead	0.31
Vanadium	221
Zinc	6.4

Contribution of shipping to the total N deposition in the region is 24%. Also, in the Mediterranean Sea the contribution from atmospheric deposition is dominating the contribution of N from shipping to the sea in 2018. Regarding the sulfur deposition, in 2018 the shipping to the total deposition is 34%.

Table 19. Annual deposition of total nitrogen (oxidised + reduced) and sulfur (S) on European seas in kt/year in 2018. Mean values of EMEP, SILAM and CMAQ model simulations.

Deposition 2018	Total deposition (1000 tonne y^{-1})	Shipping contribution	
		Absolute (1000 tonne y^{-1})	Relative total
Total N	652	154	24%
Total S	633	213	34%

3.1.2. Case studies

In addition to regional studies of ship sourced pollution, several case studies were included in this work. The onboard case study to collect and analyse samples of air emissions and discharges represents one of the case studies. Further, there were five other studies (Öresund (Sweden/Denmark), Solent (United Kingdom), Venice (Italy), Piraeus (Greece), Aveiro (Portugal)) which were conducted to understand the local impacts of EGCS effluent discharges. Four case studies were in the Baltic, North Sea, and the Mediterranean Sea study areas and three (Öresund, Venice, Piraeus) included impact analyses for air emission and discharges which are reported in this document.

3.1.2.1. Öresund Strait

The Öresund strait is one of two connections between the North Sea and the Baltic Sea and has one of the busiest shipping lanes in the world (Figure 33). The case study provides analysis of impacts of baseline 2018 and abatement scenario shipping in the strait on water and air quality. The area is a transit fairway for all traffic entering or exiting the Baltic Sea, with several medium-size ports located in a high densely populated area but also integrated in a high ecological valuable area (both Natura 2000 and nature reserves). A detailed description of Öresund hydrodynamics can be found in a separate report of this project.

Atmospheric emissions and discharges from STEAM were used as input to consecutive modelling using both regional and local scale models for the transport of air (EMEP model) and water pollutants (ChemicalDrift and MITgcm).

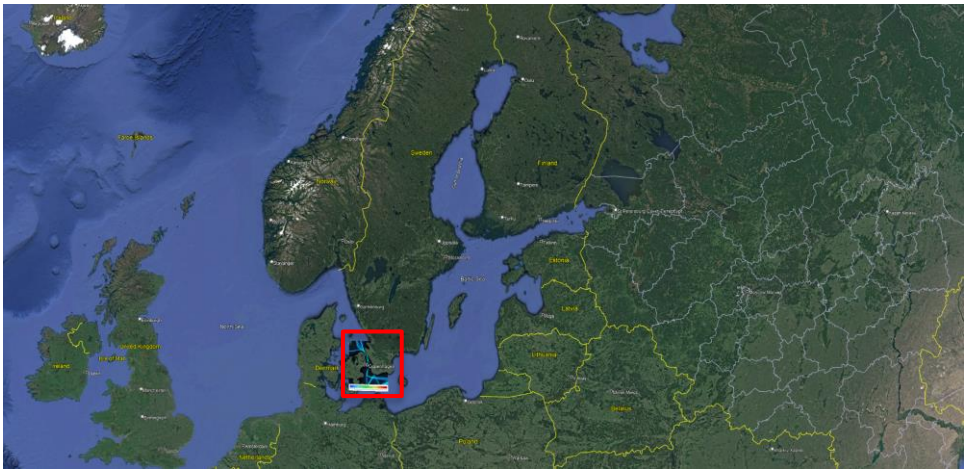

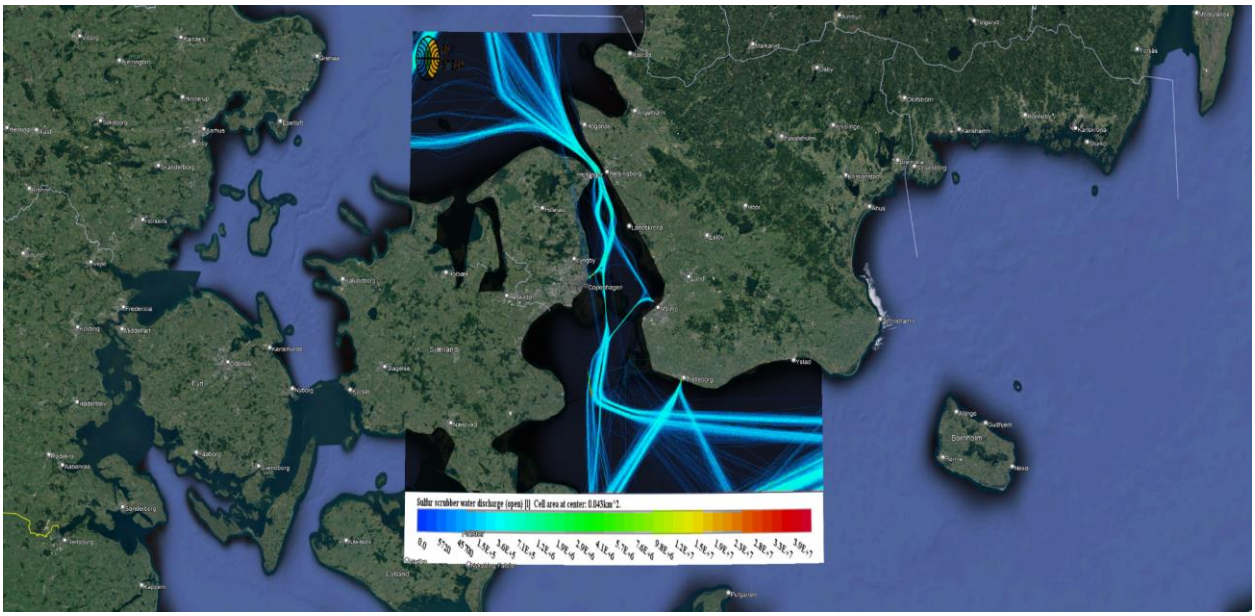

Figure 33. Baltic Sea area (top) and the spatial distribution of EGCS effluent discharges from open loop systems in the Öresund case study area during 2018

3.1.2.2. Eastern Mediterranean

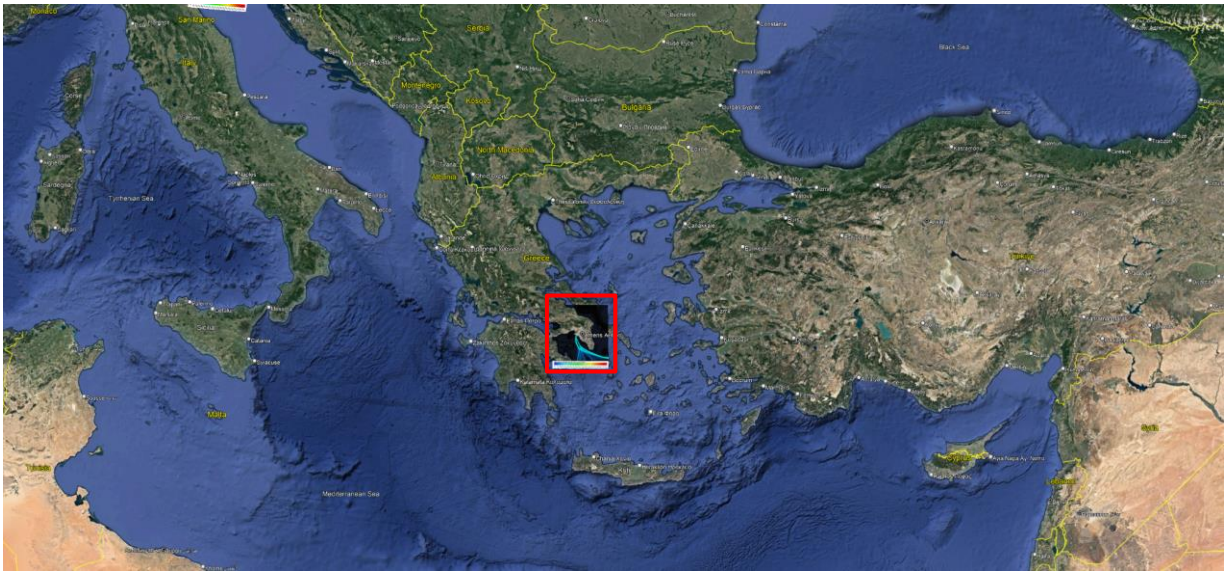

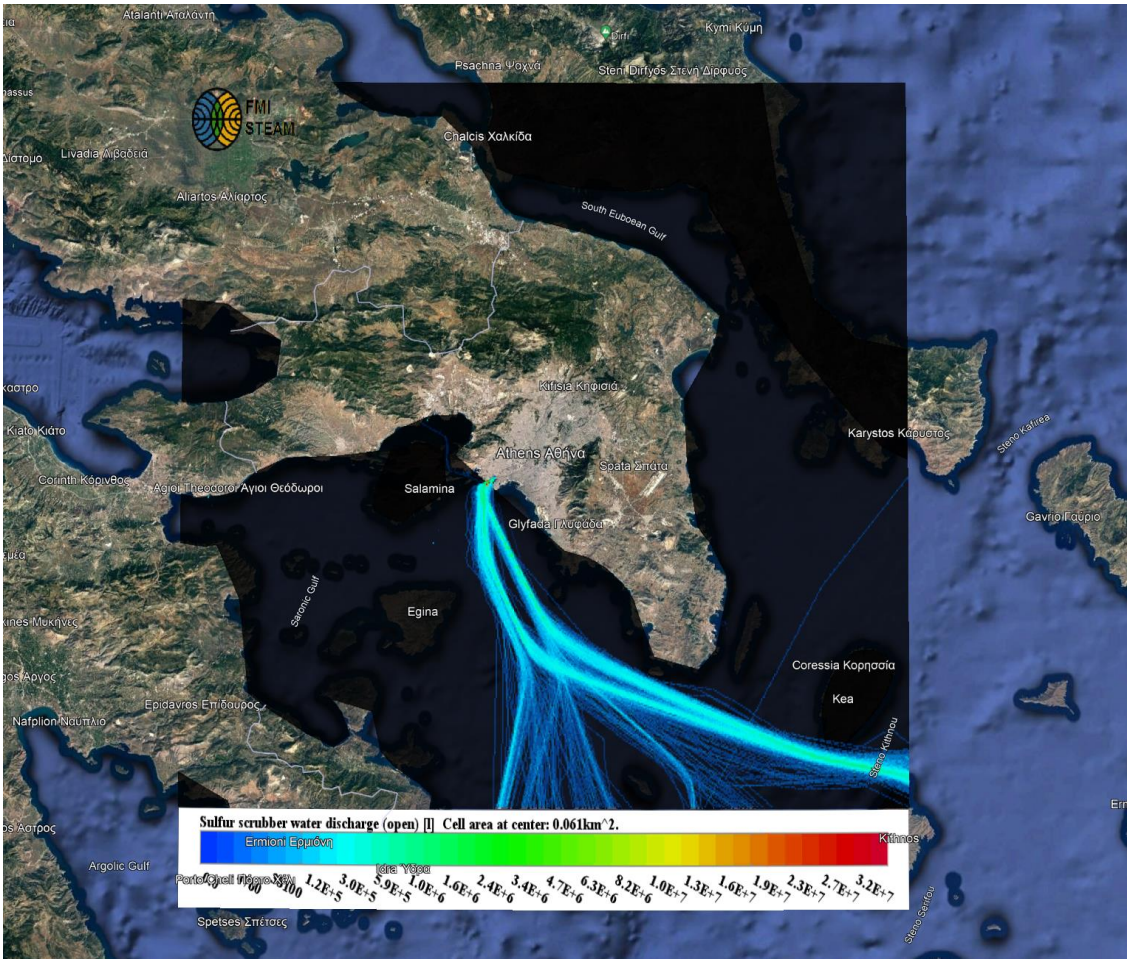

Figure 34. Location of the Eastern Mediterranean case study area (top) and the spatial distribution of EGCS effluent discharge from the open loop systems in the Eastern Mediterranean case study area during 2018 (bottom).

The loads of selected pollutants in the Saronikos Gulf/Piraeus case study area for shipping were based on the data from STEAM, in combination with the chemical characterisation data from Section 2.2. Loads are differentiated to those from sources other than shipping directly discharged in the sea (industrial activity, wastewater treatment plants, river runoff, etc.) as described in Deliverable 4.3 and to those from shipping, whether through direct discharge or through atmospheric deposition to sea surface (from SILAM atmospheric model output). Table 20 summarises these data as total annual mass loads for the trace metals Cadmium and Lead (in tons/year) and the PAH species Benzo(a)pyrene and Fluoranthene (in kg/year) for the three.

Table 20. Total annual mass loads for trace metals Cadmium and Lead (in tons/year) and PAHs Benzo(a)pyrene and Fluoranthene (in kg year^{-1}) introduced in the Saronikos Gulf domain from both shipping and all other sources for the baseline year 2018 and 2050 under the assumptions of Scenarios 3 and 8. For 2018, loads are differentiated into contribution from shipping through direct discharges to sea surface (STEAM model output) and through atmospheric deposition to sea surface (SILAM atmospheric model output).

	Cadmium (tonnes y^{-1})	**Lead (tonnes y^{-1})**	**Benzo(a)pyrene (kg y^{-1})**	**Fluoranthene (kg y^{-1})**
Sources other than shipping	**1.1**	**7.4**	**1002**	**1002.2**
2018 STEAM discharges	**0.0018**	**0.0197**	**0.1084**	**0.356**
2018 Atmospheric deposition	**0.0216**	**0.36**	**-**	**-**
2018 STEAM + Atmospheric deposition	**0.0234**	**0.3797**	**0.1084**	**0.356**
2050 SCEN3 STEAM + Atmospheric deposition	**0.0672**	**0.8572**	**2.676**	**8.576**
2050 SCEN8 STEAM + Atmospheric deposition	**0.0218**	**0.3656**	**0.0044**	**0.026**

Several conclusions can be drawn from Table 20. Firstly, it becomes apparent that the contribution of all other-than-shipping sources to total pollution loading is quite significant, as it is calculated to be orders of magnitude larger than the contribution of shipping. However, it is important to consider that sources other than shipping are located along the coastline and their discharges take place at certain geographic locations. While shipping discharges/emissions take place generally offshore, they are located along shipping lanes and can be quite diffused in the case of atmospheric deposition. Secondly, atmospheric deposition of pollutants is calculated to be an order of magnitude larger than direct shipping discharges to the sea for 2018.

3.1.2.3. Northern Adriatic

The Adriatic Sea comprises three regional basins differing in latitude, bathymetry, physiographic properties, and physical, chemical, and biological features. This EMERGE case study concerns the Northern Adriatic Sea, a semi-enclosed basin whose boundary is conventionally defined at the 100 m isobath. The case-study domain is illustrated in Figure 35.

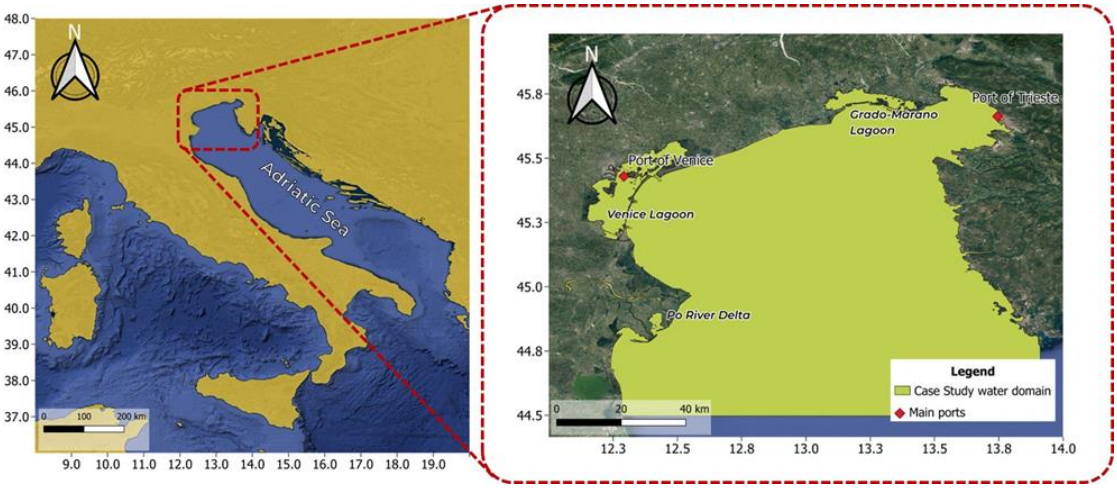

Figure 35. Area considered for the EMERGE Northern Adriatic Sea case-study.

The basin is narrow and shallow (average depth of 29 m), with a very short residence time (less than 3.3 months on average)(Artioli et al., 2008). The hydrodynamic scheme is dominated by a cyclonic circulation influenced by the Dalmatian current, ascending/rising along the Eastern coast of the basin, and by the descending current along the Western coast. Physical properties and circulation dynamics of the Northern Adriatic Sea are mainly determined by its low bathymetry, atmospheric forcing, such as wind stress and heat fluxes, and by freshwater discharges from the main rivers along the Italian coast. Tidal currents vary between 2 and 10 cm s^{-1} and are amplified up to 10–20 cm s^{-1} by wind action (Bellafiore and Umgiesser, 2010; Scroccaro et al., 2010).

The main freshwater inputs are on the western coast (due to important rivers such as Po, Adige, Brenta, Piave, Isonzo, and Tagliamento), where slopes are gentler and muddy–sandy, while the eastern coasts are steeper, rocky and reach greater depths, with the coastline characterised by bays and deep fjords. In addition, temperature and salinity patterns are different between the Eastern and Western coast (Russo and Artegiani, 1996). Consequently, the two sides of the Northern Adriatic generally present different habitats for marine species.

Table 21. Comparison of annual loads of chemical pollutants (kg) to the Northern Adriatic Sea basin from riverine input and from shipping discharges in 2018. NA= Not Available.

		Riverine load (kg)	Shipping load (kg)	Shipping contribution to total (%)
METALS	**As**	1.30E+05	6.61E+01	0.05%
	Cd	3.39E+03	1.41E+01	0.42%
	Cr	8.15E+04	1.28E+02	0.16%
	Cu	1.88E+05	1.14E+04	5.68%
	Pb	6.03E+04	8.76E+01	0.15%
	Hg	3.30E+03	4.53E-01	0.01%
	Ni	1.65E+05	1.68E+03	1.01%
	Zn	7.72E+05	9.00E+03	1.15%
	Fe	NA	1.86E+03	-
	V	NA	3.46E+03	-
PAHs	**Naphthalene**	3.88E+03	8.69E+02	18.29%
	Anthracene	3.72E+02	1.95E+00	0.52%
	Fluoranthene	3.74E+02	8.46E+00	2.21%
	Benzo(b)fluoranthene	3.72E+02	4.26E+00	1.13%
	Benzo(k)fluoranthene	3.69E+02	2.96E+00	0.80%
	Benzo(a)pyrene	3.69E+02	4.11E+00	1.10%
	Benzo(g,h,i)perylene	2.48E+02	5.08E+00	2.01%
	Indeno(1,2,3,cd)pyrene	2.48E+02	3.52E+00	1.40%
	Dibenzo(a,h)anthracene	NA	3.17E+00	-
	Pyrene	NA	8.66E+00	-
	Benzo(a)anthracene	NA	5.98E+00	-
	Chrysene	NA	3.99E+01	-
	Acenaphthylene	NA	6.18E+00	-
	Acenaphthene	NA	1.71E+01	-

	Fluorene	NA	1.40E+01	-
	Phenanthrene	NA	6.57E+01	-

River discharges have a major impact also on the trophic network due to the high nutrients loads (200,000 t y^{-1} of total nitrogen, 7,500 t y^{-1} of total phosphorus (Volf et al., 2013), particularly from the Po River, responsible for half of the total runoff (about 3000 m^3 s^{-1}) into the Northern Adriatic Sea.

The Northern Adriatic Sea is under significant pollution pressure because it is surrounded by densely inhabited and highly urbanised areas, especially in the Italian Po River valley. The main sources of pollutants (nutrients and toxic chemicals) entering the Northern Adriatic coastal waters are related to urban/domestic and industrial effluents (treated and untreated), agricultural activities, and in general a diversity of anthropic activities (such as tourism, transport of freights and people, mining, aquaculture) leading to the release of various types of pollutants (Table 21). It is worth noting that the Northern Adriatic Sea represents an important maritime transport route used by merchant ships (in national and international trade), cruise ships, fishing boats, leisure boats and military ships. The main ports in the area are those of Venice and Trieste (on the Italian coast), and Koper (Slovenia). The case-study area is characterised by the presence of many valuable habitats and includes several protected areas (in transitional, coastal, and marine environments). The spatial distribution of EGCS effluent discharge from open loop systems is given in Figure 36. In the Venice VTS area, open loop effluent release is forbidden.

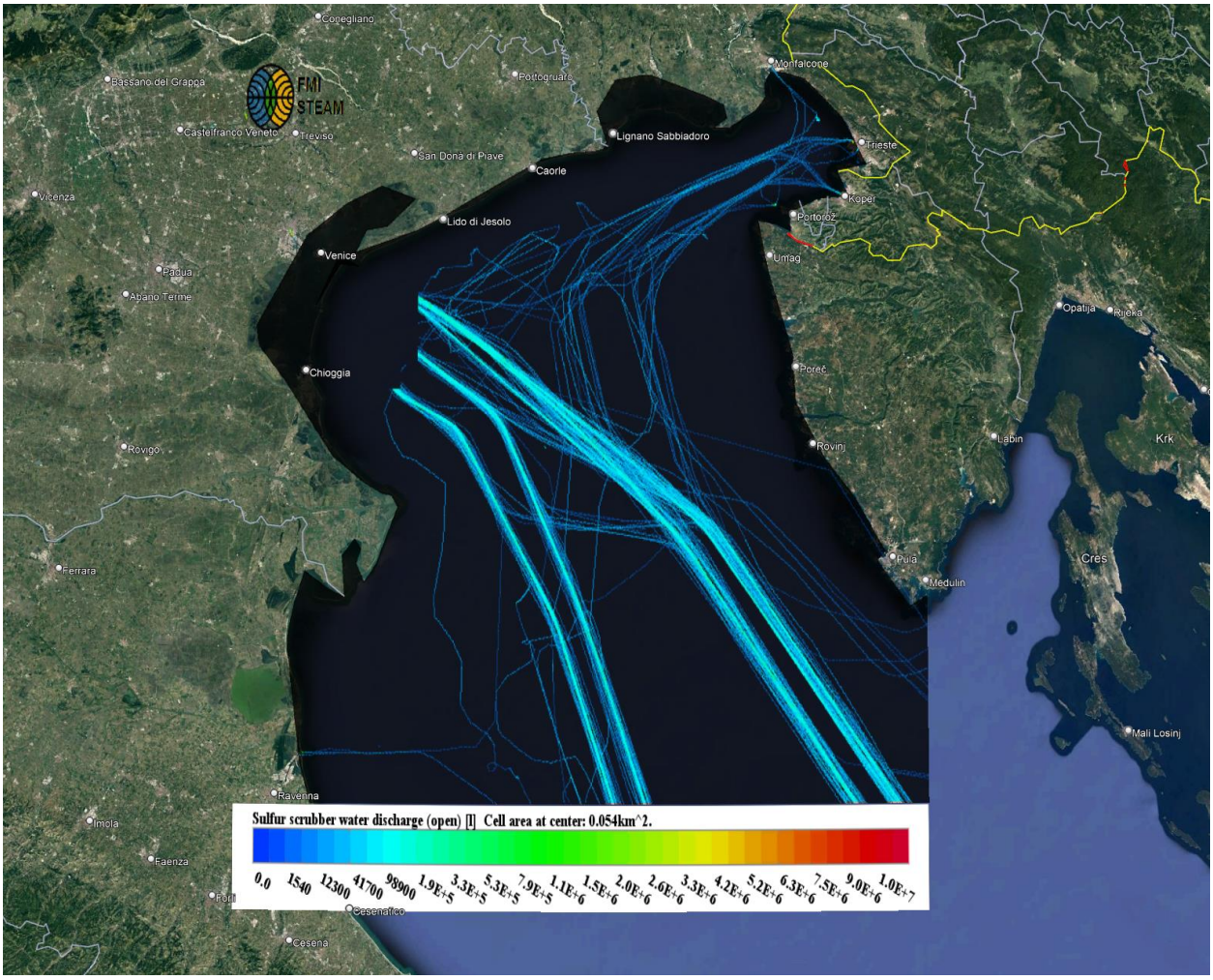

Figure 36. Spatial distribution of EGCS effluent discharges from open loop systems in the Northern Adriatic case study area in 2018. Release of open loop effluent is prohibited in the Venice VTS area (Ministero delle infrastrutture e dei trasporti, 2019)

The estimate of the loads of chemical pollutants and nutrients to the Northern Adriatic Sea from both land-based sources and shipping has been performed by integrating different data sources (river flow measurements, water quality data, STEAM output, SILAM air modelling results), and the results obtained for benzo-a-pyrene, fluoranthene, cadmium, and lead are reported in Figure 37.

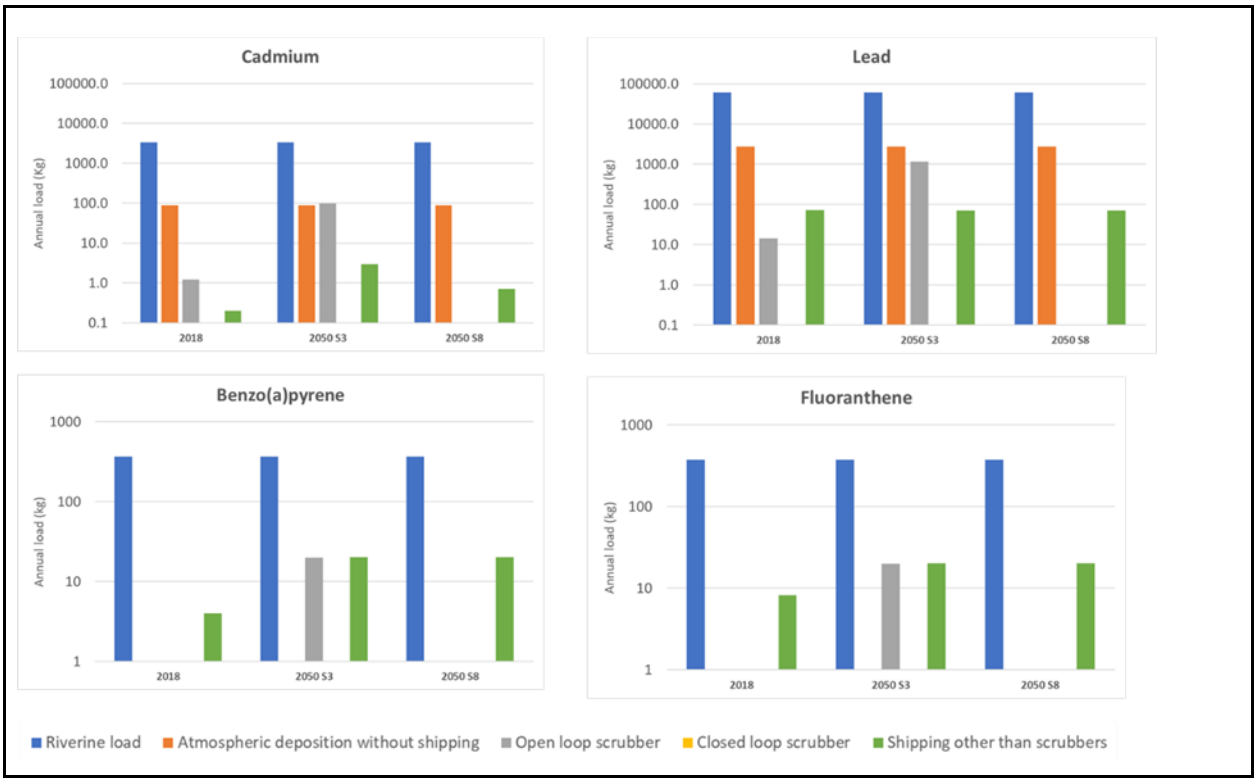

Figure 37. Annual loads (kg) of Cd, Pb, BaP and Fl from rivers, open loop EGCSs, closed loop EGCSs and other shipping sources (bilge water, sewage, and greywater) to the Northern Adriatic Sea basin in 2018 and under S3 and S8 scenarios in 2050. Log-scale is used on the vertical axis. "Atmospheric deposition without shipping" data not available for PAHs.

3.2. Scenarios for 2050

The emissions are modelled with the STEAM model and for the scenarios the emission factors have been updated to include new fuels such as methanol and ammonia as well as more detailed emission factors for ships using abatement equipment. Scenario results are calculated for the years 2018, 2030 and 2050. The results consist of total emissions to air and discharges to the sea.

To evaluate the fuel consumption for future years, we have included assumptions for the following parameters:

- Transport development
- Ship size change

- Energy efficiency improvements
- Improved utilization

These developments are assumed to be different for different ship segments. Development of transport work and utilization improvement are applied linearly on all ships in a certain segment, while the other parameters are applied only on new-built ships.

For ship development we assume a size development following DNV GL (Endresen et al., 2019) meaning that container ships increase in size by 30% up to 2050, gas tankers with 40%, bulk ships with 10% while other ship types remain with the same average size. We also assume that all ship types show an increased fuel efficiency following the EEDI regulation which sets a standard for new ships (MEPC, 2022). In the modelling, old ships are replaced by new ones through an assumed average ship lifetime of 25 years for all ship types. Further, improvements in cargo utilization are assumed and taken from DNV GL (Endresen et al., 2019) to be 10% in 2030 and 25 % in 2050.

We have used three different scenarios for open-loop EGCS use in 2050. One is that no EGCSs are needed (Scenario 8). This is to get a baseline with no discharges of EGCS effluent. For the two other assumed levels of EGCS use we apply a model based on cost efficiency. The reason for ships to use EGCSs is that the cost for HFO can be significantly lower than for VLSFO, MGO or other low-sulfur fuels. Thus, if the price difference for the annual fuel consumption between these fuels is larger than the annual capital and operational costs for a EGCS it will be beneficial for a ship to install it. There may be other factors such as the age of the ship that influence the decision. The capital costs we have used are taken from Winnes et al. (2020) and we have assumed two different fuel price differences:

- High EGCS use: based on a high price difference between VLSFO and HFO, 200 €/ton fuel.
- Low EGCS use: based on a low-price difference between VLSFO and HFO, 60 €/ton fuel.

The price difference between HFO and VLSFO during 2019-2021 averaged on about 120 €/ton (Ship & Bunker 2022). The price different between HFO and MGO is larger, thus there may be an even higher incentive for the use of EGCS within SECAs. However, for the purpose of this study the chosen assumptions of the use of EGCSs will give a large variation between scenarios suitable for the further analysis. The costs are applied on the global STEAM-data for 2018 and

visualized in Figure 38. The assumption applied in the scenario analysis is that the fractions of ships for the different ship categories that have a cost saving (i.e., ships above 0 €/ton fuel in the figure) will use EGCS. These fractions are presented in Table 22. The interest rate in this calculation is assumed to be 10 % and the depreciation period 10 years.

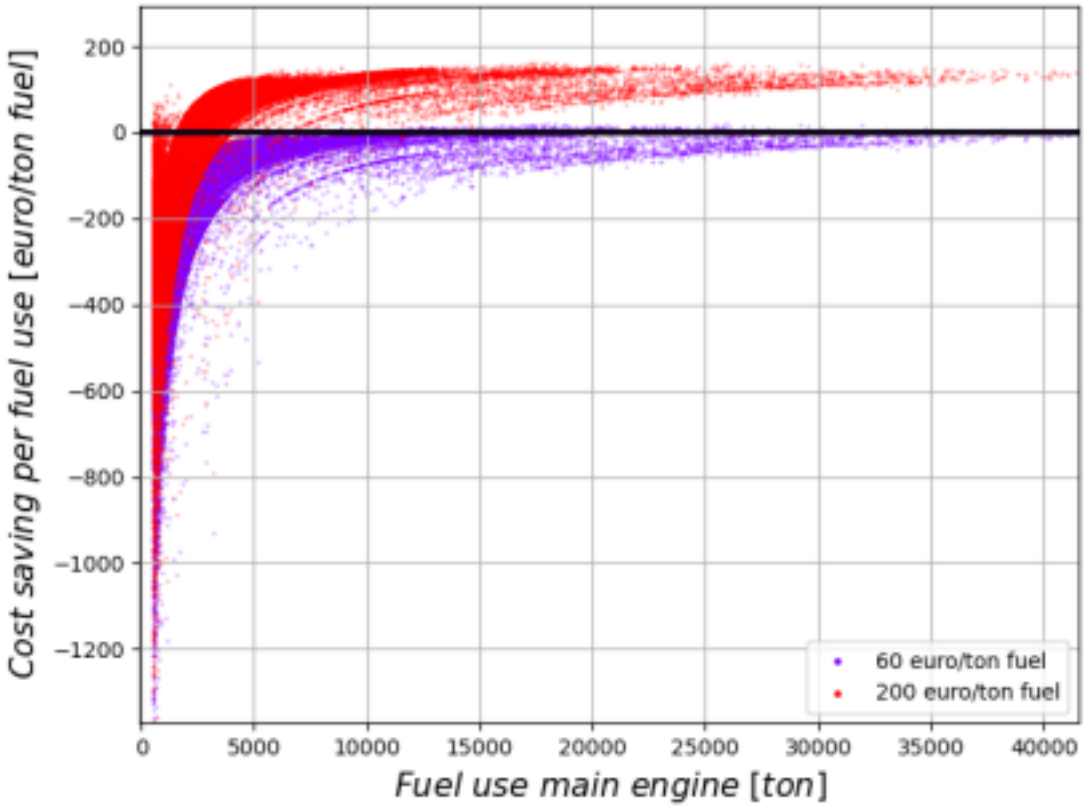

Figure 38. Cost savings vs fuel use for all ships in Europe when using open-loop EGCSs rather than VLSFO, i.e., the assumed price difference between VLSFO and HFO. 60 and 200 €/ton fuel refer to the high and low-price difference between VLSFO and HFO.

In one scenario we have assumed that the ships use closed rather than open-loop EGCS (see Winnes et al., 2020 for description) and that the same fraction of ships as in the high use scenario for open-loop EGCSs then use closed loop EGCS. This results in significantly lower volumes of bleed-off water compared with the effluent from open loops EGCSs, but with a higher concentration of contaminants. This scenario is constructed to illustrate the difference in emissions between open-loop and closed loop EGCSs and it should be noted that the higher capital costs for closed loop systems would make it costly for many ships to invest in this technology with a difference in fuel prices between HFO and VLSFO of €200.

Table 22. Fraction of engine work and fraction of ships using open loop EGCS in the High and Low EGCS model, respectively.

Ship type	**Number of ships (%)**		**Engine work (%)**	
	60 euro (Low)	**200 euro (High)**	**60 euro (Low)**	**200 euro (High)**
Bulk Cargo ships	2.9%	72%	1.1%	91.3%
Containerships	2.9%	73%	0.3%	95.2%
General cargo ships	0.0%	4%	0.0001%	34.7%
Cruise ships	7.2%	56%	2.6%	97.8%
Refrigerated cargo ships	3.5%	25%	5.2%	74.1%
RoRo/Passenger ships	4.6%	29%	5.0%	84.0%
RoRo cargo ships	4.7%	33%	11.5%	85.7%
Chemical tankers	0.1%	20%		68.3%
Crude Oil tankers	13.4%	68%	2.2%	96.7%
LNG tankers*	0%	100%	0%	100%
LPG tankers	4.7%	32%	0.0001%	78.7%
Product tankers	0.2%	22%		76.1%
Vehicle carriers	2.9%	72%	1.2%	98.0%

***LNG carriers are special cases and are excluded from the analysis in Figure 38. Instead, they are assumed to have 0% in low EGCS case and 100 % in high EGCS cases.

EMERGE scenarios 3, 3b, and 8 all assume that ship traffic will grow significantly in the coming decades. Following the high-growth pathway of ship traffic up to 2050 (Endresen et al., 2019), the transport work is tripled. Same traffic development assumptions are used in all three scenarios and therefore, the number of ships operating in the regional sea areas remains constant for these three scenarios. In scenarios 3 and 3b, it is assumed that the price difference between HFO and low sulfur fuels is high, and that it is profitable to install an EGCS on all vessels that consume more than 2,500 tonnes of fuel annually. The use of EGCS is also at a high level as it is assumed that a new SECA is implemented in Europe within 200 nautical miles from the coastline starting in 2030. In scenario 8, it is assumed that HFO is no longer used in shipping and therefore, there are no EGCSs in use. The number of ships operating in the Baltic Sea and the North Sea, and the respective number of EGCSs in use for the baseline year and the selected scenarios are shown in Table 23, Table 24 and Table 25.

Table 23. The total number of ships (including ships with open-loop and closed-loop EGCS) operating in the Baltic Sea, the North Sea, and the Mediterranean Sea in EMERGE baseline year (2018) and future scenarios (2050).

	2018	**Scenario 3**	**Scenario 3b**	**Scenario 8**
Baltic Sea				
Ships Total	8 931	31 833	31 833	31 833
Open loop or hybrid EGCS	178	9460	0	0
Closed loop EGCS	10	0	9460	0

Table 24. The total number of ships (including ships with open-loop and closed-loop EGCS) operating in the North Sea and the Mediterranean Sea in EMERGE baseline year (2018) and future scenarios (2050).

North Sea	**2018**	**Scenario 3**	**Scenario 3b**	**Scenario 8**
Ships Total	17 151	75 000	75 000	75 000
Open loop or hybrid EGCS	190	22 710	0	0
Closed loop EGCS	6	0	22 710	0

Table 25. The total number of ships (including ships with open-loop and closed-loop EGCS) operating in the Mediterranean Sea in EMERGE baseline year (2018) and future scenarios (2050).

Mediterranean Sea	**2018**	**Scenario 3**	**Scenario 3b**	**Scenario 8**
Ships Total	19 717	77 833	77 833	77 833
Open loop or hybrid EGCS	103	23 556		
Closed loop EGCS	5		23 556	

Considering the significant increase in projected transport work by shipping segment in high-growth scenarios, the size of the fleet will increase significantly. According to the DNVGL scenario, a significant increase in the transport work of bulk cargo and containership sectors were predicted, whereas the liquid bulk cargo share decreased (Table B.4 in DNVGL report).

Scenario 3a (all open loop EGCS) and 3b (all closed loop EGCS) were developed to investigate the maximum environmental pressure from EGCS. Considering the price difference of various fuels, and global shipping activity and fuel consumed by each ship in the fleet, roughly a third of the fleet in the Baltic Sea, North Sea and the Mediterranean Sea were considered fit for EGCS installation.

4. Environmental state in the baseline and scenarios

4.1. Regional

4.1.1. Europe

The aggregated assessment for the European seas, including all descriptors, show that almost all water basins fail to achieve GES. Especially northern Europe waters fail to reach GES with respect to descriptor D8, Contaminants (Figure 39 Right). On a European scale, out of the 21 indicators included in the high-resolution evaluation of D8, only six had no detected failures to reach GES. This means that >70% of the indicators have at least one basin where the status is assigned “not good” by one or more contaminants.

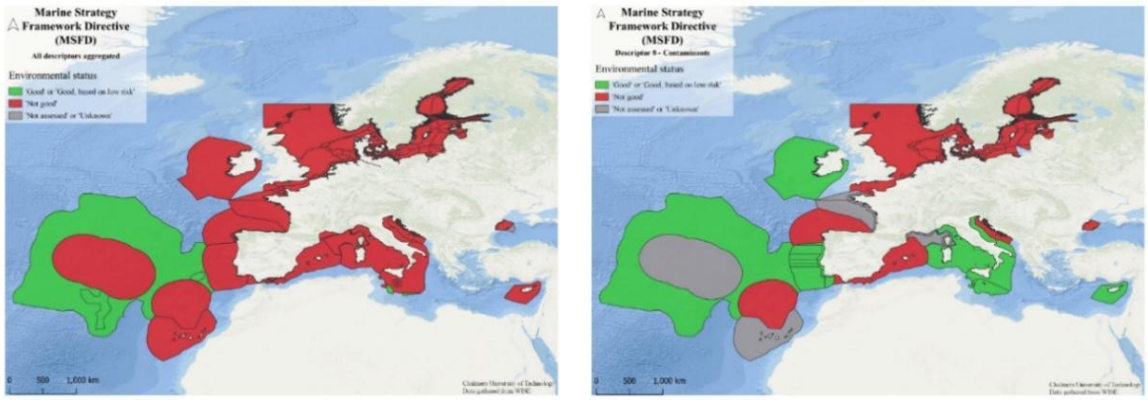

Figure 39. Environmental status of European sea areas as reported by EU Member States in 2018 according to the Marine Strategy Framework Directive (2008/56/EC). Left panel shows the overall environmental status considering all descriptors and the right panel shows the result for D.8 (contaminants).

As shown in Figure 39, most European coastal areas have an unacceptable ecological status, and a contributing factor to this is the high concentrations of certain PAHs and metals which are present in EGCS effluent. The status assessment was done in 2018, just three years after installations of EGCSs on ships began and was hence based on a situation when only a few ships were using EGCSs. Since then, the number of ships with EGCS has increased dramatically and

it is inevitable the continuous discharge of EGCS effluent into shipping lanes along the European coasts will result in even higher concentrations of these PAHs and heavy metals.

Figure 40 illustrates the changes of spatial distribution of Naphthalene in EU sea areas, starting from the 2018 baseline (top image), and extending to the maximum pressure scenario (S3) in 2050 (bottom image). As can be seen from these two examples, EGCS effluent discharges are no longer restricted to just ECAs, but extend all regional seas. The snapshot of surface concentrations given in the bottom image (Figure 40) highlights almost all the coastal areas and the archipelago areas of the Aegean Sea. It should be noted that the assessment done in Figure 39 does not consider the increase of EGCS effluent discharges, which add to the environmental burden of sea areas which are already have a poor environmental status.

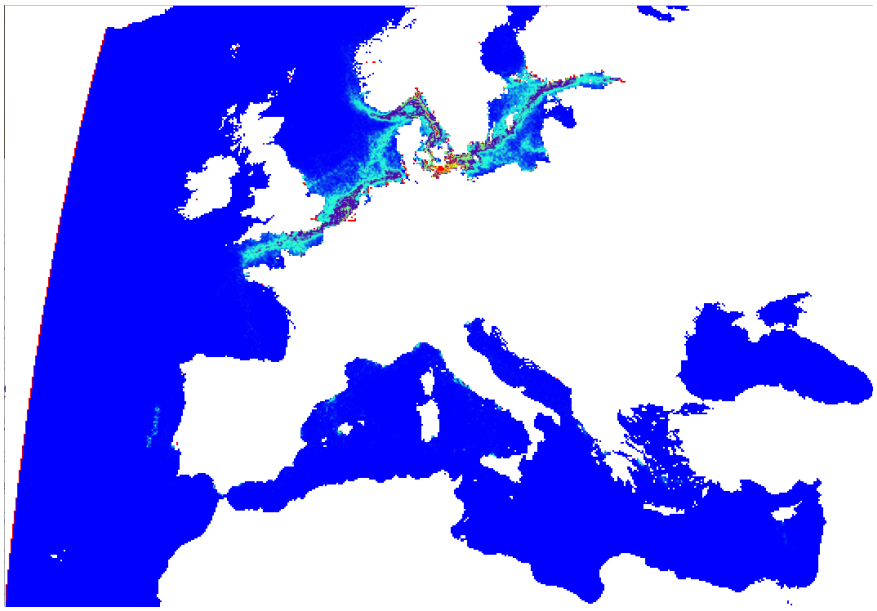

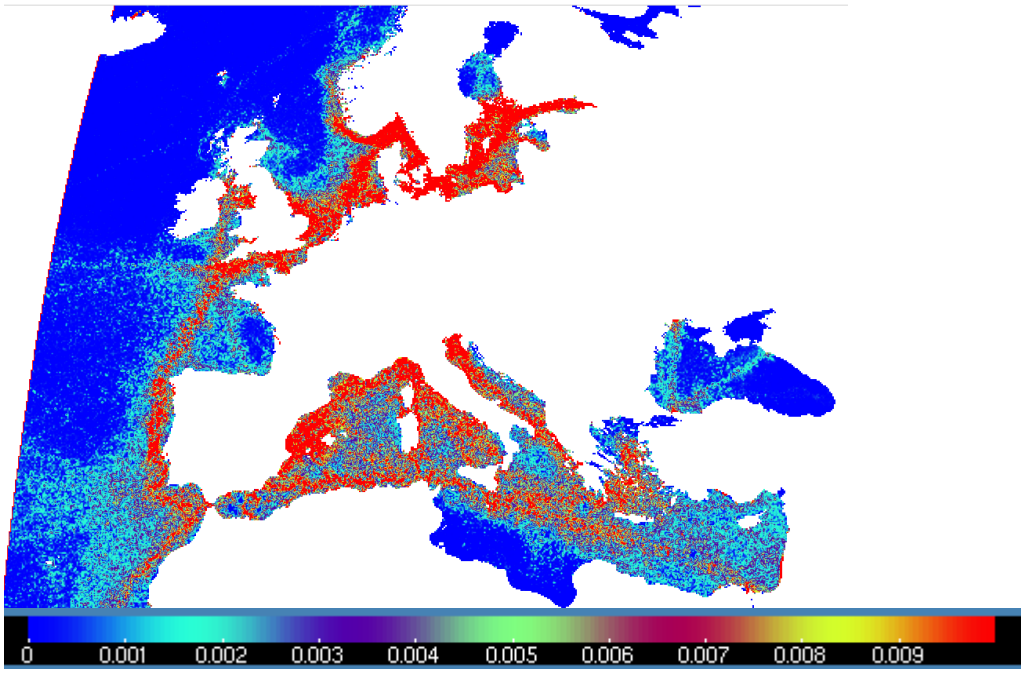

Figure 40. Surface concentrations of the PAH Naphthalene from open loop EGCSs at the end of baseline year 2018 (in micrograms per m^3) (top image). Surface concentrations of the PAH Naphthalene from open loop EGCS at the end of year 2050, for scenario 3 (in micrograms per m^3) (bottom image). The simulations are carried out with ChemicalDrift with STEAM data as input and ocean forcing from Mercator Ocean / Copernicus.

4.1.1.1. Baltic and the North Sea area

The assessment of environmental status of European sea areas is based on Member State reporting on MSFD indicators and descriptors. In Figure 39, the results from Member States' 2018 reporting on their progress to achieve GES were collected from WISE Marine (https://water.europa.eu/marine). WISE Marine is an EU platform hosted by the European Commission and the European Environmental Agency (EEA) that offers access to information and data on the state of Europe's Sea. The aggregated assessment (Figure 39 Left) includes all the reported data and was organised per indicator, per descriptor, and considering all descriptors using the One Out All Out–Principle.

The aggregated assessment, including all descriptors, showed almost all water basins to fail to achieve GES. Especially northern Europe waters fail to reach GES with respect to descriptor 8, Contaminants (Figure 39 Right). Out of the 21 indicators included in the high-resolution evaluation of D8, only six had no detected failures to reach GES, meaning that >70% of the

indicators have at least one basin where the status is assigned “not good” by one or more contaminants.

Since the status assessment reported by EU Member States does not include information on actual water concentrations (all data is reported in the format GES achieved or GES failed) additional monitoring data for Ni, Cd, Pb, V, B*a*P and, fluoranthene was gathered from ICES DOME (https://www.ices.dk/data/data-portals/Pages/DOME.aspx) (Figure 41). In this figure, the WFD limit values are also shown.

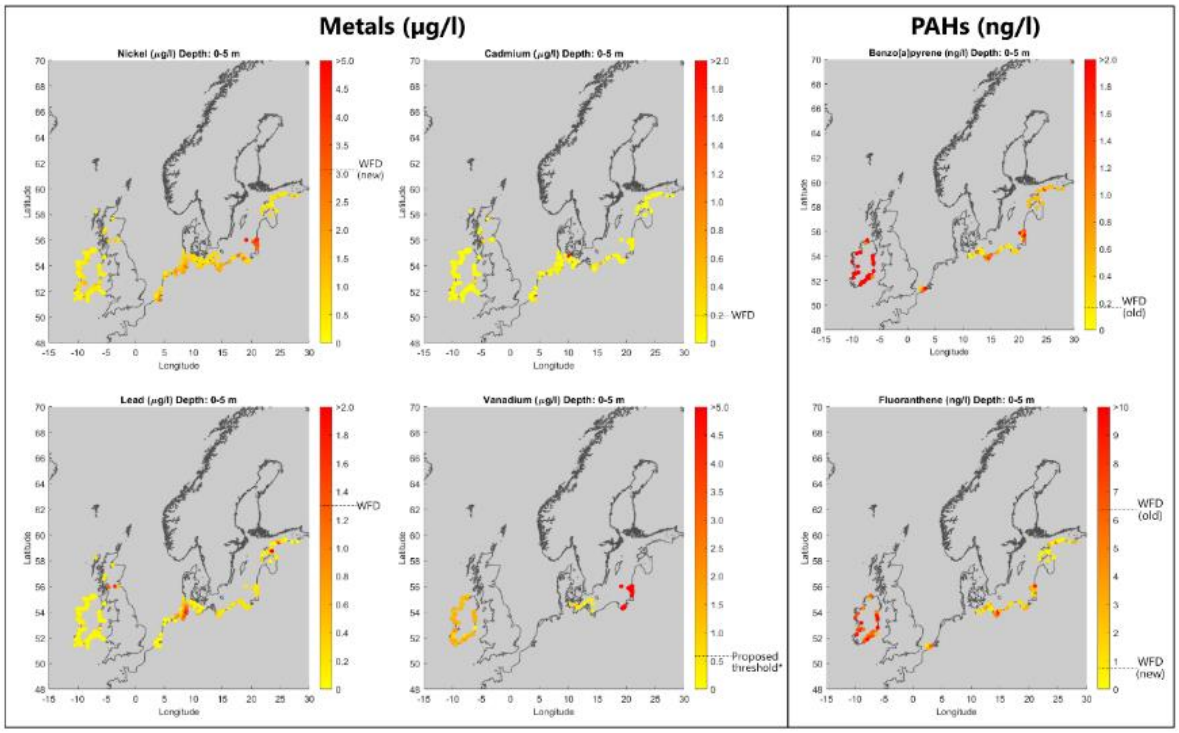

Figure 41. Environmental concentrations from monitoring data of 4 metals (Ni, Cd, Pb and V) and 2 PAHs (fluoranthene and benzo[a]pyrene) from surface water (0-5 m) in Baltic and North Sea region collected between 2015-2022 (https://www.ices.dk/data/data-portals/Pages/DOME.aspx)

The results indicate 1% of the stations to exceed the AA-EQS (Table 26) with respect to Ni (n_{tot}=1319) (newly proposed AA-EQS) and Cd (n_{tot} =1255). For Pb (n_{tot} =1149) and V (n_{tot} =482), the corresponding percentage of stations that exceeded the AA-EQS (Pb) and proposed PNEC (V) was 2% and 90%, respectively. For benzo[*a*]pyrene (n_{tot} =185) none of the stations exceeded the new proposed AA-EQS but >90% exceeded the current AA-EQS. For fluoranthene (n_{tot} =160), almost 40% of the stations exceeded the current AA-EQS and 84% exceeded the newly proposed AA-EQS.

Table 26. Current and proposed threshold values (e.g., Annual Average Environmental Quality Standard (AA-EQS) for 4 metals and 2 PAHs. Proposed AA-EQS collected from dossiers published here: https://circabc.europa.eu/ui/group/9ab5926d-bed4-4322-9aa7-9964bbe8312d/library/69579412-bcc1-4740-b14b-88980756e6c3?p=1&n=10&sort=modified_DESC

Substance	Current AA-EQS	Proposed AA-EQS	Reference**
Nickel	8.6 µg/l	3.1 µg/l	(European Union, 2008)
Cadmium	0.2 µg/l	N/A	(European Union, 2008)
Lead	1.3 µg/l	N/A	(European Union, 2008)
Vanadium*	N/A	0.57 µg/l	(Tulcan et al., 2021)
Fluoranthene	6.3 ng/l	0.76 ng/l	(European Union, 2008)
Benzo[a]pyrene	0.17 ng/l	22 ng/l	(European Union, 2008)

*vanadium threshold value is obtained from Tulcan et al., 2021 who derived a predicted no-effect concentration (PNEC) value based on a chronic species sensitivity distribution curve.

** proposed EQS values from dossiers: https://circabc.europa.eu/ui/group/9ab5926d-bed4-4322-9aa7-9964bbe8312d/library/69579412-bcc1-4740-b14b-88980756e6c3?p=1&n=10&sort=modified_DESC

A more detailed analysis for the status of the Baltic Sea at sub-basin level was recently released by the Baltic Marine Environment Protection commission (HELCOM, 2023). This 3rd Holistic Marine Assessment for the Baltic Sea also included that all sub-basins do not reach the good environmental status Figure 42.

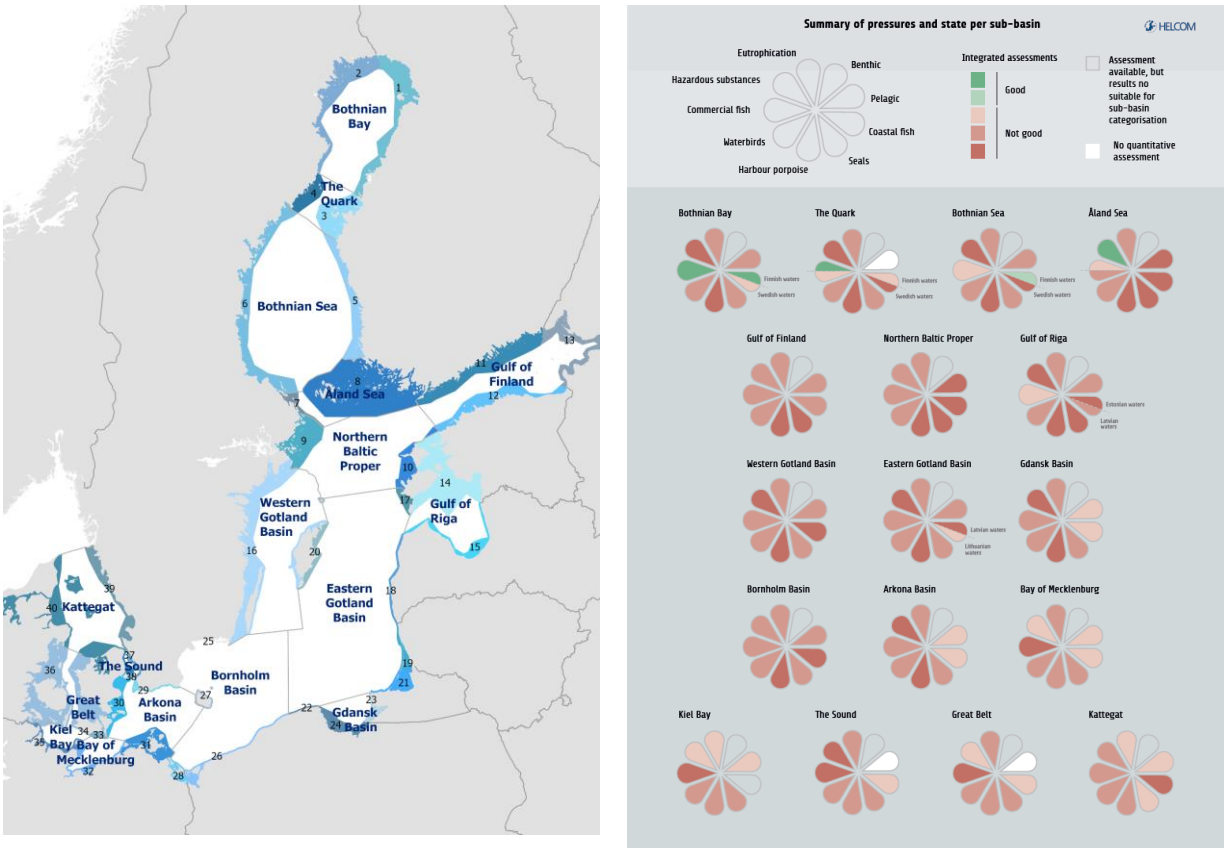

Figure 42. Sub basins of the Baltic Sea (left). Assessment of the environmental status of the Baltic Sea sub-basins (right). Images from HELCOM HOLAS3 report (HELCOM, 2023)

Modelling of contaminant concentration as a result of ship emissions and atmospheric deposition is conducted on a regional scale using ChemicalDrift model (Aghito et al., 2023) and on Öresund case study level with the MITgcm model (Marotzke et al., 1999). At regional level, the modelled predicted environmental concentrations in the upper 5 m of Ni, Cd, Pb, V, BaP, Fluoranthene due to open loop EGCS effluent discharge in 2018 and in S3 (2050) are presented in Figure 43.

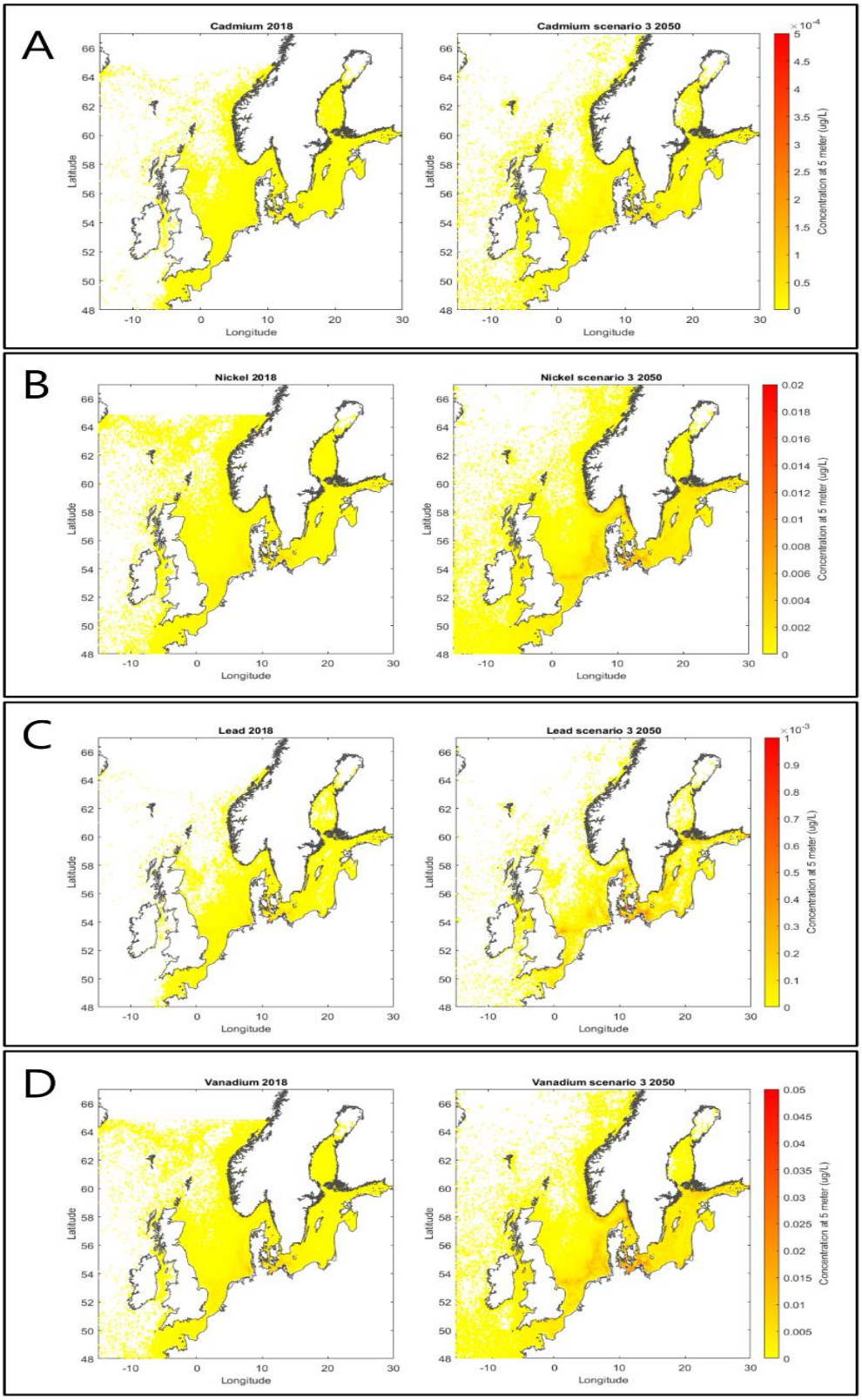

Figure 43. Predicted concentrations of Cd, Ni, Pb and V for baseline year 2018 and 2050 (scenario 3). Values of contaminant concentrations in the upper layer (<5m) of the water column are shown.

ChemicalDrift delivers predicted environmental concentrations from single sources and the concentrations should be interpreted as added concentrations in the environment due to a certain activity. The concentrations for metals (Figure 43) are expressed in dissolved fraction while the concentrations of PAHs (not shown) are based on the sum of dissolved fraction and fraction adsorbed to suspended particulate matter (SPM). The results obtained using ChemicalDrift show, for most substances, highest concentrations in the Southern Baltic Sea region (Bornholm basin and Arkona basin). As expected, the modelled concentrations are higher in S3 (2050) as compared to the baseline scenario of 2018. The highest detected concentrations in S3 (2050) of Cd and Ni was 0.0005 micrograms L^{-1} and 0.02 micrograms L^{-1}, respectively. For Pb and V the corresponding maximum concentrations were 0.001 micrograms L^{-1} and 0.05 micrograms L^{-1}, respectively.

4.1.1.2. Mediterranean Sea

Predicted concentrations of the selected PAHs and metals (i.e. benzo-a-pyrene, fluoranthene, cadmium, and lead) in the water column and in the sediments have been obtained for the whole European domain by applying the ChemicalDrift model for the transport and the fate of pollutants. This was achieved by considering inputs of chemicals from several sources related to shipping activity. In detail, chemicals' loads from open loop EGCSs were estimated by integrating wastewater discharge volume fluxes from the STEAM model with the emission factors reported by Lunde Hermansson and co-workers (Lunde Hermansson et al., 2021). Atmospheric deposition of the selected metals to the sea surface was computed for both shipping and land-based sources using the SILAM model (Sofiev et al., 2006). In some detail, Scenario 3 predicts a high growth of shipping transport, with a high use of EGCSs, with SECA and NECA introduced in all European sea areas, while Scenario 8 predicts a high growth of shipping transport with extensive use of LNG and methanol and no use of EGCSs.

Concentrations in the water column and in the sediments for benzo-a-pyrene (BaP), fluoranthene (Flu), cadmium (Cd), and lead (Pb) were estimated with 1-year simulations, and an example of the obtained maps is shown in Figure 44, Figure 45 and Figure 46 for BaP and Cd.

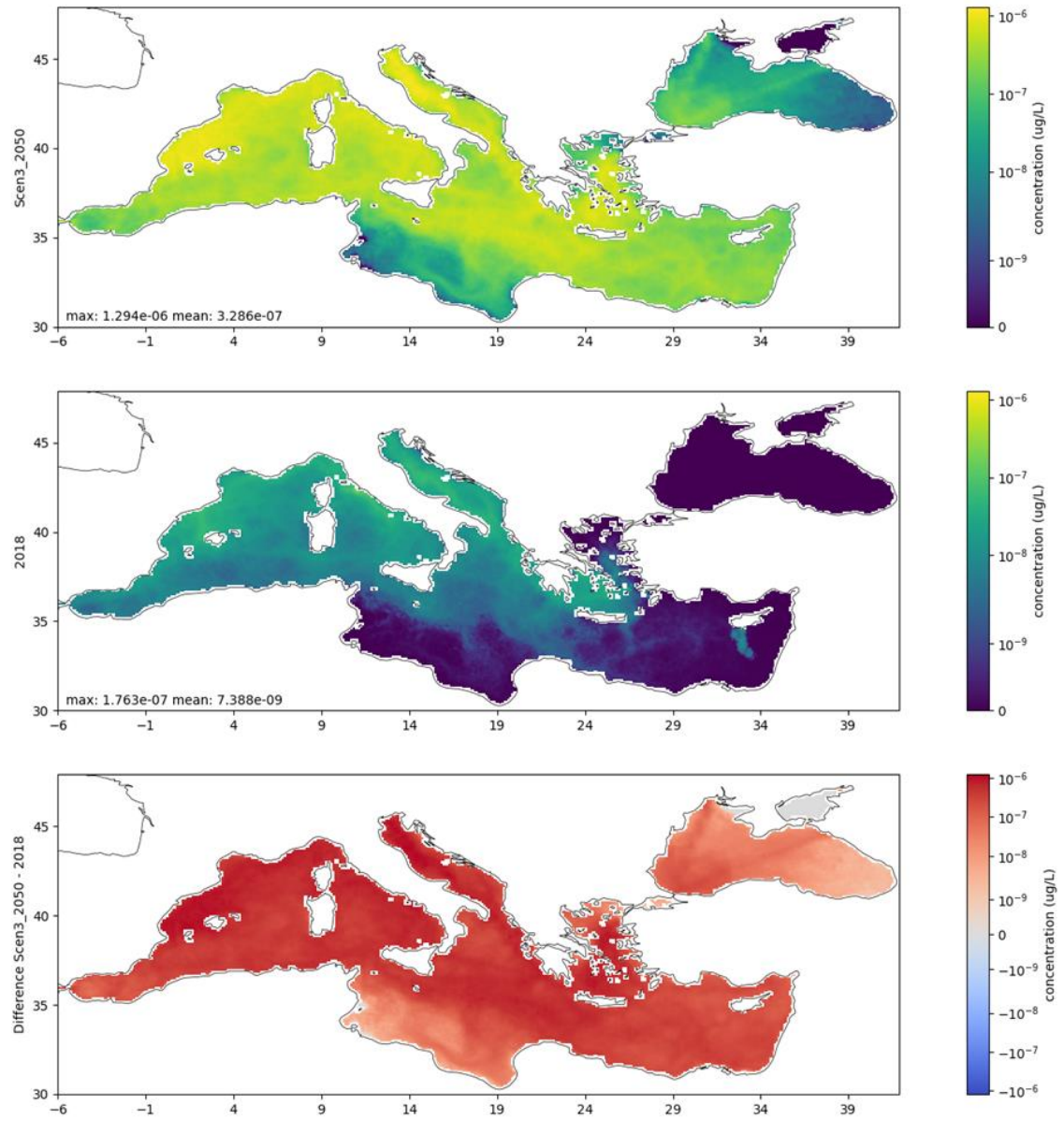

Figure 44. Predicted mean annual concentration of Benzo-a-pyrene in Mediterranean Sea from discharges by open loop EGCSs in Scenario 3 (top panel), compared to 2018 (middle panel). Concentrations are reported for the surface layer (0 to 5 meter). Mean and maximum values over the 10x10km grid cells are indicated in each panel. Units are micrograms L^{-1}. The change from 2018 to 2050 is shown in the bottom panel.

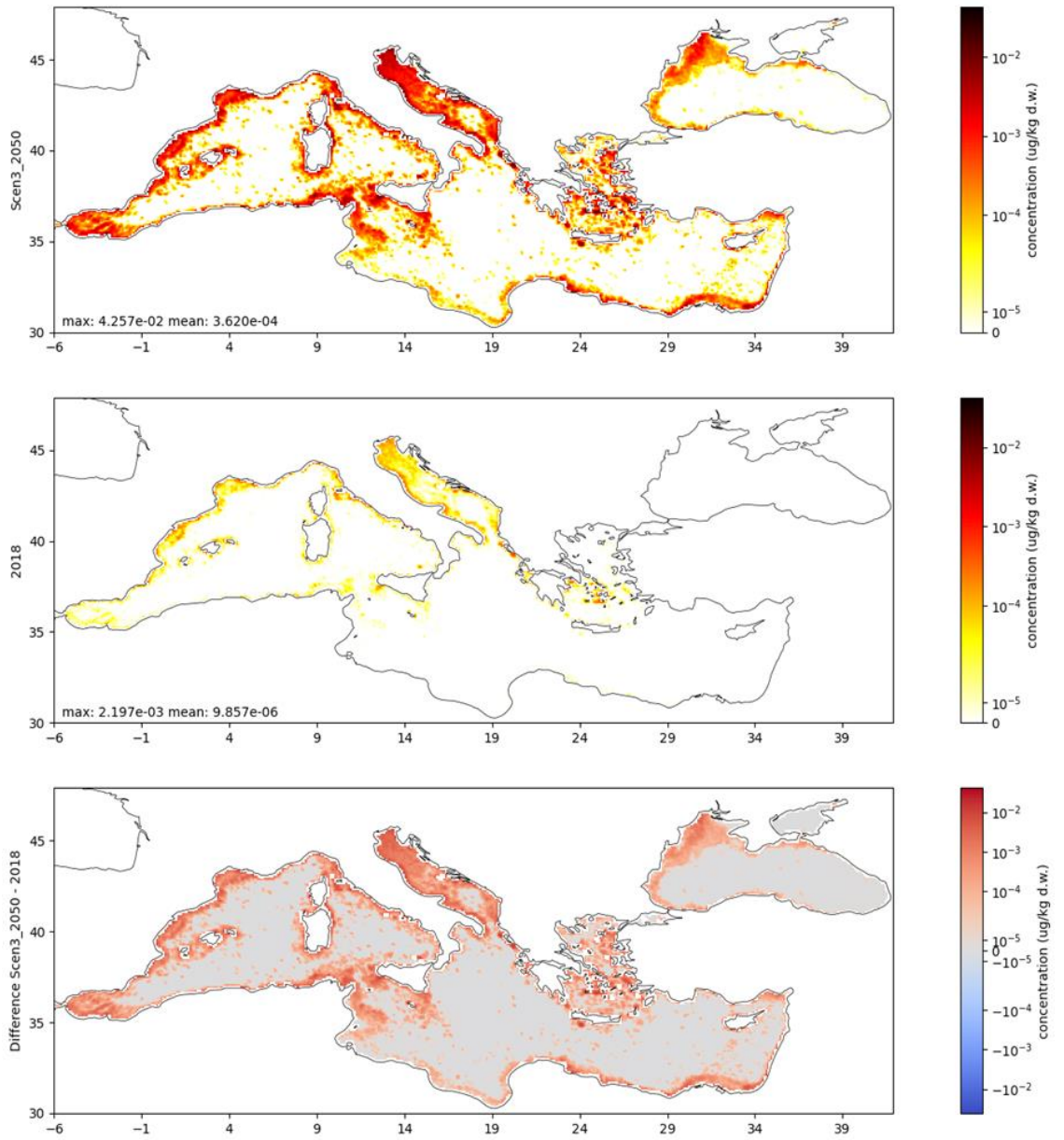

Figure 45. Predicted accumulated concentration of Benzo-a-pyrene in sediment layer after one year of discharges by open loop EGCSs in Scenario 3 (top panel), compared to 2018 (middle panel). Mean and maximum values over the Mediterranean Sea are indicated in each panel. Units are micrograms kg^{-1} d.w. The change from 2018 to 2050 is shown in the bottom panel.

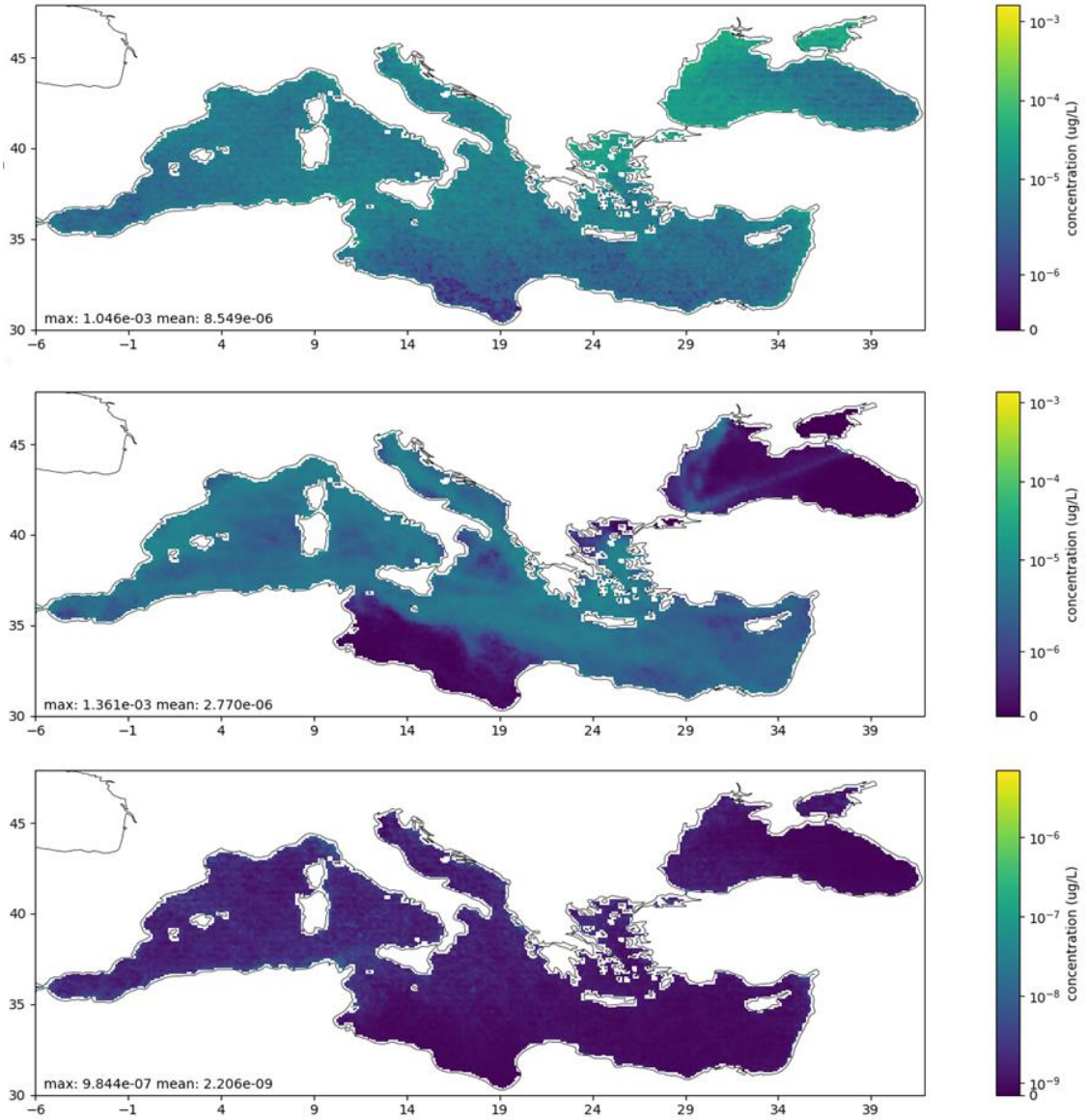

Figure 46. Predicted mean annual concentrations of Cadmium in the Mediterranean Sea in 2050, Scenario 3. The contributions from the modelled input sources are shown: atmospheric emission from other sources than shipping (top panel), open loop EGCSs (middle panel), atmospheric emissions from shipping (bottom panel). Concentrations are reported for the surface layer (0 to 5 metre). Mean and maximum values over the 10x10km grid cells are indicated in each panel. Units are micrograms L^{-1}.

The overall results obtained for the selected chemicals are summarised in Table 27 and Table 28, indicating mean annual concentration in water, mean sediment concentrations accumulated at the end of the year, and the changes between the baseline situation in 2018 and the 2050 scenarios. The provided mean values are calculated over all modelled grid cells (10km x 10km) in the Mediterranean Sea. In detail, the reported examples show the predicted concentrations in

Scenario 3 in the water column and in the sediments due to the emissions of BaP from open-loop EGCSs (Figure 44 and Figure 45), while the predicted concentrations of Cd in the water column due the considered sources are compared in Figure 46. Similar maps are available for all the emissions listed in the tables, but these are not shown here.

Table 27 below indicates that the load of contaminants to the sea through atmospheric deposition are reduced in 2050 but are increased in seawater by the EGCS effluent discharges.

Table 27. Contributions to predicted concentration levels in water column (top 5m) for each modelled emissions source and scenario. Mean values are calculated over the whole Mediterranean. Significant increments and reductions from baseline year are marked in red and blue. Important sources for each compound are written in bold.

Chemical	Scenario	Source	Annual mean 2050 (micrograms L^{-1})	Mean change from 2018 (micrograms L^{-1})
Benzo[a]pyrene	**Scen3_2050**	**open loop EGCSs**	**3.29E-07**	**3.21E-07**
Fluoranthene	**Scen3_2050**	**open loop EGCS**	**9.74E-07**	**9.52E-07**
Cadmium	Scen3_2050	atm. dep. shipping	2.21E-09	-8.00E-09
Cadmium	**Scen3_2050**	**atm. dep. other sources**	**8.55E-06**	**-**
Cadmium	**Scen3_2050**	**open loop EGCS**	**2.77E-06**	**2.71E-06**
Lead	Scen3_2050	atm. dep. shipping	2.23E-08	-8.25E-08
Lead	**Scen3_2050**	**atm. dep. other sources**	**1.32E-04**	**-**
Lead	**Scen3_2050**	**open loop EGCS**	**1.57E-05**	**1.54E-05**
Cadmium	Scen8_2050	atm. dep. shipping	2.56E-10	-9.95E-09
Cadmium	**Scen8_2050**	**atm. dep. other sources**	**8.61E-06**	**-**

Lead	Scen8_2050	atm. dep. shipping	2.67E-09	-1.02E-07
Lead	**Scen8_2050**	**atm. dep. other sources**	**1.34E-04**	**-**

Table 28. Contributions to predicted concentration levels in sediment layer for each modelled emissions source and scenario. Mean values are calculated over the whole Mediterranean. Significant increments and reductions from baseline year are marked in red and blue. Important sources for each compound are written in bold.

Chemical	**Scenario**	**Source**	**Week 52 mean, 2050 (micrograms kg^{-1} d.w.)**	**Mean change from 2018 (micrograms kg^{-1} d.w.)**
Benzo-a-pyrene	**Scen3_2050**	**open loop EGCS**	**3.62E-04**	**3.52E-04**
Fluoranthene	**Scen3_2050**	**open loop EGCS**	**7.75E-04**	**7.53E-04**
Cadmium	Scen3_2050	atm. dep. shipping	6.53E-06	-2.28E-05
Cadmium	**Scen3_2050**	**atm. dep. other sources**	**3.10E-02**	**-**
Cadmium	**Scen3_2050**	**open loop EGCS**	**7.05E-03**	**6.83E-03**
Lead	Scen3_2050	atm. dep. shipping	1.39E-04	-4.89E-04
Lead	**Scen3_2050**	**atm. dep. other sources**	**9.11E-01**	**-**
Lead	**Scen3_2050**	**open loop EGCS**	**8.85E-02**	**8.57E-02**
Cadmium	Scen8_2050	atm. dep. shipping	6.99E-07	-2.86E-05
Cadmium	**Scen8_2050**	**atm. dep. other sources**	**3.09E-02**	**-**
Lead	Scen8_2050	atm. dep. shipping	1.47E-05	-6.14E-04

Lead	**Scen8_2050**	**atm. dep. other sources**	**9.09E-01**	**-**

These results can be used to assess the contribution of the selected sources and the effects of different emission scenarios. It is also important to consider that the data provided is not a complete representation of the total environmental concentration, which is expected to be significantly higher. This is due to, for multiple various reasons: i) emissions from rivers and other land-based sources (e.g., wastewater treatment plants) were not available for the regional modelling from all relevant locations, and ii) the data used lacked information on atmospheric deposition of PAHs, since most PAHs and metals are not reported by air emission inventories and would be available for this study only for ships. Without a complete description of emissions from all sources, covering airborne and waterborne sources, the analysis will be incomplete. Ytreberg and colleagues have shown that other sources than shipping also contribute to a significant percentage of the pollution loads in the Baltic Sea (Ytreberg et al., 2022). Further, regional scale simulations results are provided for 10km x 10 km grid cells, therefore local maxima in proximity of major point sources and narrow regions with high traffic are not represented accurately. In addition, the water quality simulations cover only one year of emissions and background levels are not utilised, so the accumulation effect of multiple years of continuous emissions cannot be considered.

Figure 44 (middle panel) shows the annual mean concentration of BaP in the Mediterranean Sea, highlighting higher levels of pollution near the southern coasts of Europe, while the concentration near Africa, the Eastern Mediterranean, and in the Black Sea is about 2-3 orders of magnitude lower, due to the lower traffic of ships equipped with EGCS. Moreover, Figure 44 (top and bottom panels), shows that the increase of BaP concentration in the surface waters of the Mediterranean and the Black Sea due the extensive use of EGCS in the high-pressure Scenario 3 is notable.

The 2050 estimated mean annual concentrations indicate that this increase will be more prominent at the European Seas - the NW Mediterranean and particularly the Balearic and Tyrrhenian Seas, the coasts of France, the Adriatic Sea, and the Ionian and Aegean Seas - further burdening the marine areas that are currently affected (as shown in Figure 44 - mid panel) by shipping discharges. The Eastern Mediterranean and the Black Sea, which appear relatively unaffected in 2018, show an increase in surface BaP as well. The coasts of Libya and Tunisia (North Africa) seem to be affected to a lesser extent by the general increase in EGCS effluent

discharge. Mean BaP surface concentration over the whole domain increases by about two orders of magnitude (from 7.388e-09 micrograms L^{-1} in 2018 to 3.286e-07 micrograms L^{-1} for Scenario 3), while maximum BaP surface concentration increases by an order of magnitude (from 1.763e-07 micrograms L^{-1} in 2018 to 1.294e-06 micrograms L^{-1} for Scenario 3, that is, more than 600%).

The shown increase can be ascribed to the higher shipping traffic estimated, but also to the introduction of a Sulfur Emission Control Area (SECA), which is expected to cause a drastic increase of the number of EGCSs present in the modelling domain.

Figure 45 indicates that during the annual simulation period, the accumulation of BaP at the top sediment layer occurs mainly at the shallower parts of the European seas, along the coastline, following the increased water concentrations as shown in Figure 44. Top panel of Figure 45 top panel presents the impact of Scenario 3, a rather substantial increase in the accumulation of BaP at the top sediment layer, extending spatially at all shallower parts of the Mediterranean basin along the coastline and the west part of the Black Sea. Mean BaP sediment concentration over the whole domain increases by about two orders of magnitude (from 9.857e-06 micrograms kg^{-1} d.w in 2018 to 3.620e-04 micrograms kg^{-1} d.w for Scenario 3), while maximum BaP sediment concentration increases by about an order of magnitude (from 2.197e-03 micrograms kg^{-1} d.w in 2018 to 4.257e-02 micrograms kg^{-1} d.w for Scenario 3). This characteristic accumulation spatial pattern can be attributed to factors such as the extent of the simulation period (1 year) combined with the sinking velocity of particles used in simulations as they do not reach the deeper parts of the basins within the annual simulation period).

Similar results were also obtained after modelling the environmental fate of Flu shipping emissions, as can be seen from the concentrations reported in Table 27 and Table 28.

In both scenarios, a significant reduction of concentrations of Cadmium and Lead from deposition of atmospheric emissions from shipping is observed, with respect to baseline year 2018. These reductions are negligible compared to the overall concentrations, since atmospheric depositions from shipping represent a very small fraction of the total contribution (0.1 to 0.2%).

Model results, as shown in Figure 46, highlight that, for Scenario 3, among the considered Cd emission sources, the contributions from open loop EGCSs (middle panel) that was negligible in 2018 will reach a contribution similar to the one given by atmospheric emission from sources other than shipping (top panel) and lead generally to comparable surface Cd concentrations (the same order of magnitude for mean and maximum values). Conversely, the effect of atmospheric emissions from shipping on the determination of surface cadmium concentration in the

Mediterranean Sea in 2050 appears 3-4 orders of magnitude lower, thus limited (bottom panel). In detail, the effect of EGCS effluent discharge was lower in the Black Sea and the coastal area north of Libya (middle panel).

Figure 46 also highlights that atmospheric deposition of pollutants (top and bottom panels) is diffused quite evenly over the whole region, while loads from EGCS effluent discharges (middle panel) are concentrated along shipping routes.

Similar results were also obtained after modelling the environmental fate of Pb emissions, as can be seen from the concentrations reported in Table 27 and Table 28.

4.1.2. Case study areas

4.1.2.1. Öresund Strait

At the Öresund case study, the difference between scenario 3 (2050) and the baseline (2018) shows a similar trend where the marine surface water concentration of the selected metals (Cd and Pb) and PAHs (fluoranthene and benzo[a]pyrene) increase (Figure 47). For scenario 8, where no EGCSs are in operation, the concentrations are expected to decrease. The model outputs on regional and case study level from 2018 simulations are compared in Table 29 where the concentrations are estimated in orders of magnitude level in the Öresund area.

The MITgcm model includes several waste streams from ships and atmospheric deposition while the ChemicalDrift model output only predicts environmental concentrations due to open loop EGCS effluent discharge. Therefore, any comparison of the model simulations should be treated as indicative. The dilution approach (second column, Table 29), described in Section 2.5.4, is based on a modelling exercise where the distribution and dilution of open loop EGCS effluents are modelled using MITgcm, and the final concentrations of Cd, Pb, Fla and B[*a*]P are estimated from initial EGCS effluent concentrations.

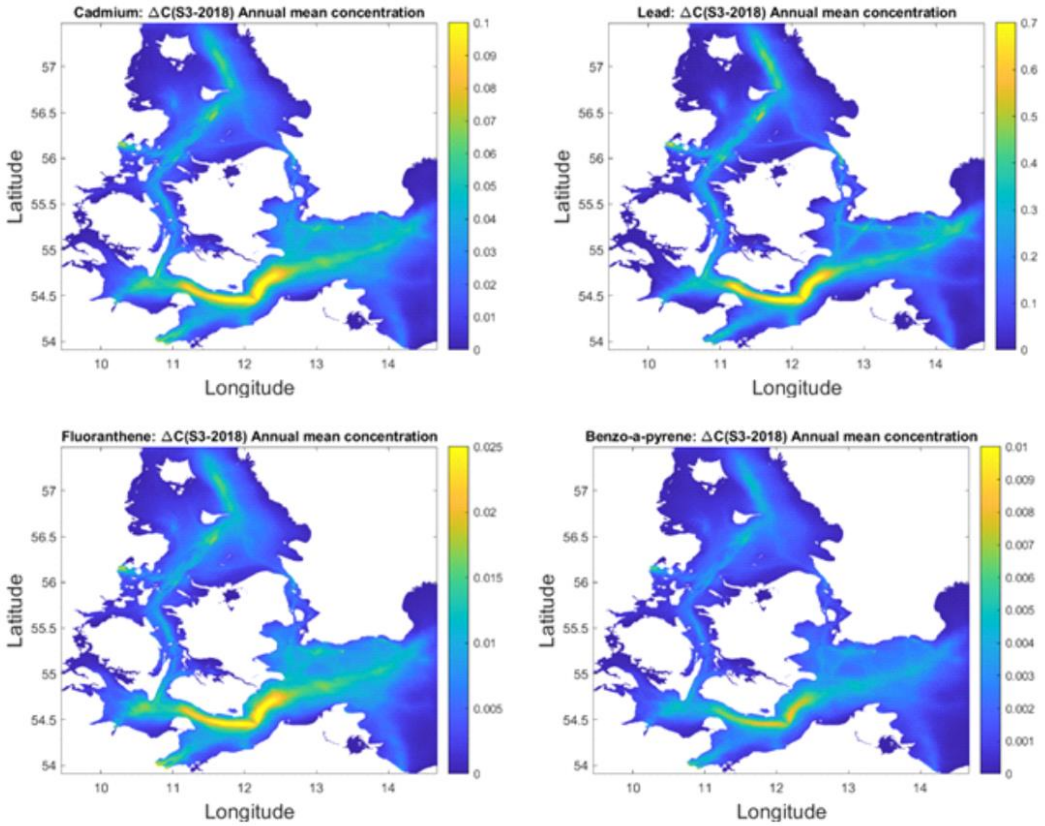

Figure 47. The difference between Scenario 3 and baseline year 2018 for Cd, Pb, BaP, Fluoranthene at 5 m depth. Concentrations are in micrograms L^{-1}.

Table 29. Comparison between regional scale and local scale modelling results and monitoring data from ICES Dome. All units are micrograms L^{-1}. Comparison limited to Öresund Case study. The dilution approach is based on modelling described in Section 2.5.4 and the distribution of open loop EGCS effluent is modelled using MITgcm. Final concentrations estimated from initial effluent concentrations reported in Section 2.2. NOTE: different approaches are included in the model simulations and any comparison should be treated as indicative.

	ChemDrift2018 (only open loop EGCS discharge)	**Dilution approach (only open loop EGCS discharge)**	**MITgcm 2018 (annual average from shipping and atmospheric deposition)**	**ICES DOME (monitoring data, selection Figure 41)**
Cadmium	2×10^{-5}	0.9×10^{-5}	0.03	0.02-28
Lead	2×10^{-4}	9.2×10^{-5}	0.1	0.02-8.3
Fluoranthene	1.5×10^{-6}	0.2×10^{-5}	1.5×10^{-3}	0.002-0.0085
Benzo[*a*]pyrene	2×10^{-7}	5×10^{-7}	0.2×10^{-3}	0.0022-0.002

The modelled PECs within the Öresund case study surface water (1.5 m) and full depth profiles of five locations from the 2018 baseline data (Figure 48, Figure 49) are compared to $PNEC_{TGD}$, critical $value_{NOEC}$ and Lowest Observed Effect Concentration (LOEC) based on the

ecotoxicological tests of open loop EGCS effluent exposures. The surface water concentrations in Figure 48 show the results from a simulation running from January to July 2018, but due to the pre-defined sinking velocity, can also be interpreted as the resulting PEC from near-time shipping (<2 days). Initial results suggest that after two days from discharge in the Öresund area, the EGCS effluent should not be considered an entity, because it will be diluted close to background concentrations by the sea currents in the area. The vertical profiles in Figure 49 show the daily concentration profiles that will vary depending on the discharge rate and the daily conditions, e.g., wind, currents, etc.

From the modelling results, discharge of open loop EGCS effluent will result in environmental exceedance of the derived $PNEC_{TGD}$ which would correspond to unacceptable environmental risks. When comparing PEC with the lowest detected LOEC (0.0001%) and the critical $value_{NOEC}$ (0.001%), there exists a risk of adverse effects in several parts of the Öresund surface water as well as in large parts of the water column for the various locations.

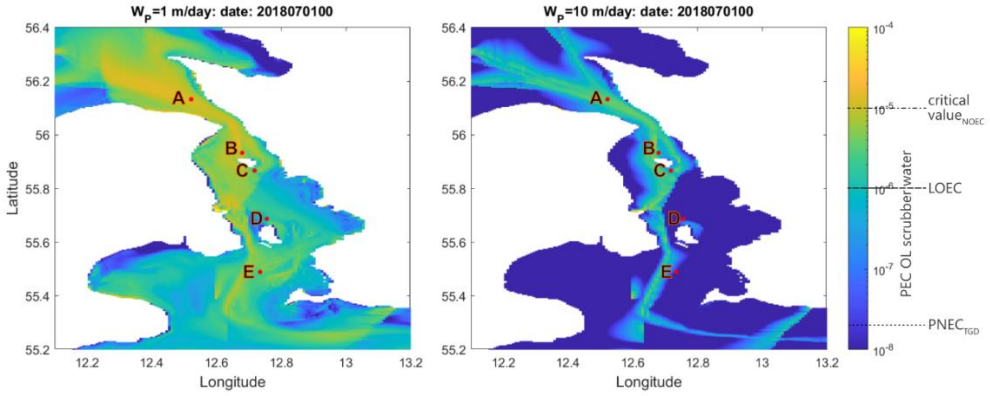

Figure 48. Simulations estimating the dilution of EGCS effluents in the Öresund area at 1.5 meters depth, simulations run from 1st January to 1st of July 2018 with STEAM input of open loop EGCS effluent discharge. Concentrations are expressed as mass of effluent per mass seawater where the left figure show PEC based on sinking velocity of 1 m day-1 and the right figure show sinking velocity of 10 m day-1. Letters indicate the position of the 5 locations in Figure 49. Dotted line shows $PNEC_{TGD}$, dashed line is the lowest LOEC and dotted-dashed line represent the critical $value_{NOEC}$.

The selected locations A-E (Figure 48) represent areas of high shipping intensity in potential conflict with marine protected areas (MPAs) and Natura 2000 areas (A, D and E) as well as important fishing grounds (A-C) where discharge of EGCS effluents may have adverse effects.

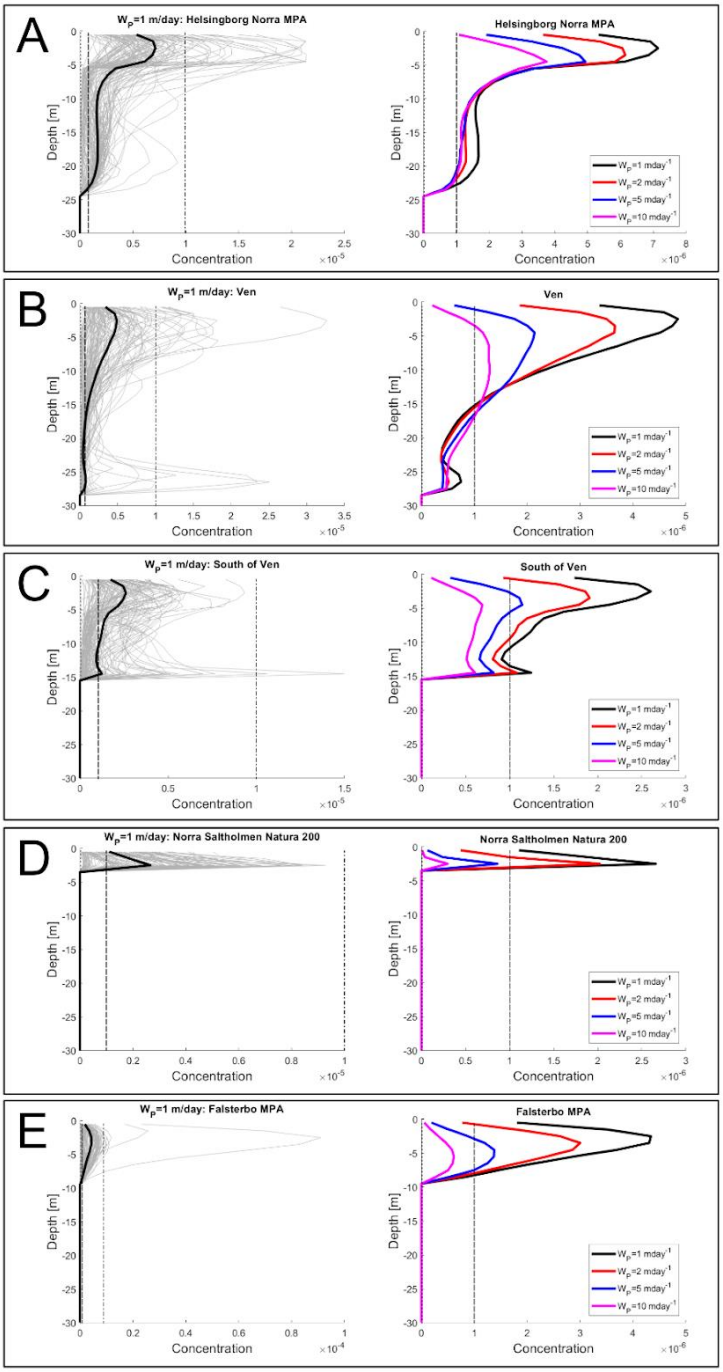

Figure 49. Daily snap-shot concentration profiles over depth at five selected positions (Figure 48) from May to August (average is bold line) at sinking velocity W_P=1 m day^{-1} (left) and average at different W_P (right). Dotted line shows $PNEC_{TGD}$, dashed line is the lowest LOEC and dotted-dashed line represents the critical value$_{NOEC}$.

The results from the modelling of open loop effluent distribution represent the ship traffic intensity of 2018 where the number of ships in the Baltic Sea Area were less than two hundred. The number

of vessels equipped with EGCS has increased substantially since and therefore the 2018 results should be interpreted as a lower estimate of risk. The modelling efforts of ChemicalDrift and MITgcm also suggest that a substantial fraction of the contaminants will accumulate at the seafloor, in the sediment.

4.1.2.2. Eastern Mediterranean

The assessment of the environmental impact of shipping in the case of Eastern Mediterranean - Saronikos Gulf, the combination of Delft3D-FLOW (for circulation) and Delft3D_WAQ (for water quality) models were used, while lateral fluxes (as boundary conditions) were provided by regional-scale simulations (locally generated in the University of the Aegean for circulation, and Chemical Drift from the EMERGE group. After successful reproduction of the year 2009 conditions (when a wealth of oceanographic data for Saronikos Gulf provided the necessary validation basis), the baseline year 2018 was simulated, along with two future scenarios (3 and 8) for the year 2050.

Since in the greater Athens Metropolitan Area a wide spectrum of human activities (urban wastewater treatment plant, oil refineries, shipyards, etc), introduce coastal pollution, a significant amount of work was dedicated in identifying and quantifying each coastal or land source of coastal pollution to reproduce the observed fields of the various pollutants. The highest concentrations of pollutants were found in the semi-enclosed bay of Elefsis (the bay area between the northernmost island and the mainland in Figure 50), a site of intense industrial activity and high residence times of the water due to weak water circulation. The fate of selected trace metals (Cd and Pb) and PAHs (Benzo(a)pyrene and Fluoranthene) was simulated, and the changes between the baseline year conditions and the predicted conditions based on the two selected scenarios were recorded.

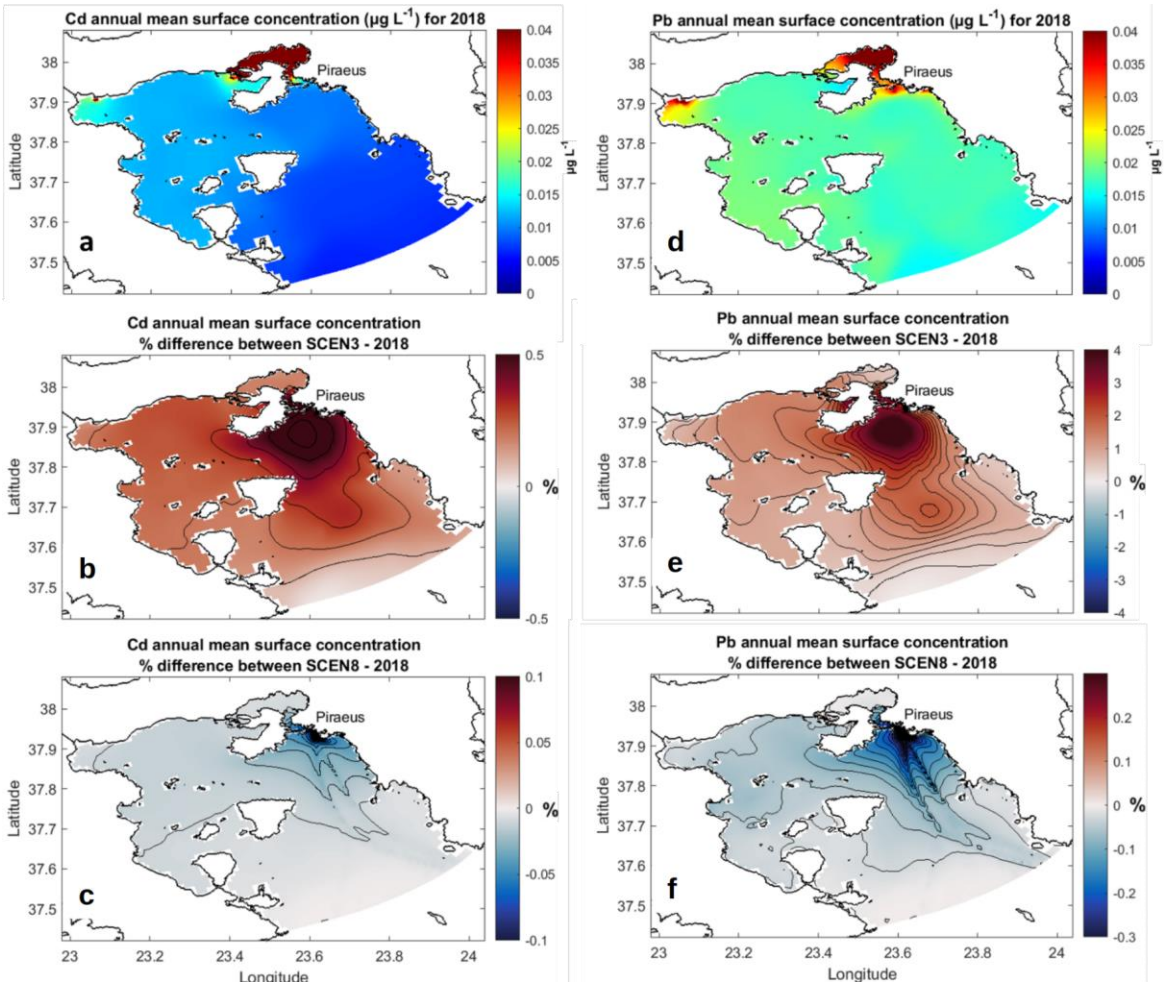

Figure 50. Annual Mean surface concentrations of Cd (a) and Pb (d) for the baseline year 2018. For comparison, the same concentrations for 2050 are presented for Scenario 3 (b and e respectively) and Scenario 8 (c and f respectively).

As depicted in Figure 50, the land-based Cd and Pb pollution sources are dominant in the baseline year, thus the pollution is mainly located in the Elefsis Bay, site of oil refineries, shipyards, and additional industrial activity. However, under scenario 3 in 2050 a small increase (0,5% in the case of Cd, 4% in the case of Pb) in surface concentrations is projected along the maritime traffic lane leaving the port of Piraeus. Accordingly, a small decrease (less than 1%) in have metal concentrations is expected under the “no EGCSs” scenario 8 for 2050 (Figure 50 c and f).

Regarding the Polyaromatic Hydrocarbons’ pollution of Saronikos Gulf, the results are like the heavy metals’ analysis. As revealed by Figure 51, the marine pollution at the surface layer is

mostly located in Elefsis bay, as well as the coastal region near the oil refinery of Aghioi Theodoroi, a fact suggesting domination of the land sources when compared to shipping.

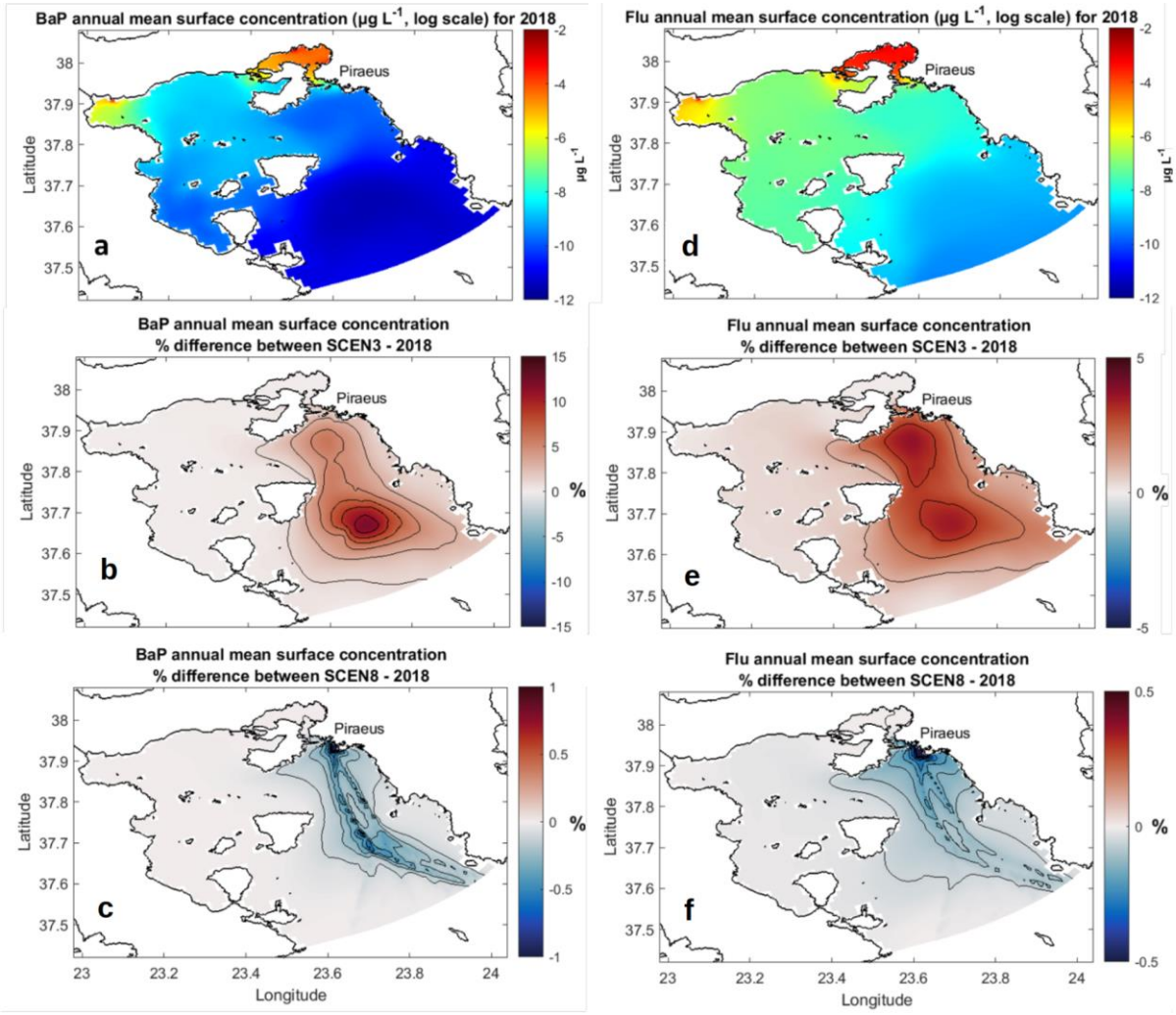

Figure 51. Annual Mean surface concentrations of benzo-a-pyrene (a) and fluoranthene (d) for the baseline year 2018. For comparison, the same concentrations for 2050 are presented for Scenario 3 (b and e respectively) and Scenario 8 (c and f respectively).

In addition of the simulations for individual contaminants, the dilution methodology described in Section 2.5.4 was also applied in the Saronikos Gulf case study to investigate the spatiotemporal characteristics and thresholds. Initially, two 10-day-long experiments were conducted, for the first 1-10 January 2018 and the 1–10 July 2018 periods respectively, with hourly time steps. The idea was to simulate a winter-well mixed water column period of lower shipping activity and a summer-stratified water column period with higher shipping activity. Hourly EGCS effluent discharges from STEAM were used to continuously force the model with pollutant release at the sea surface.

Considering the findings of the WET experiments using various animals, and their response to EGCS effluents, geographical areas of Saronikos gulf impacted by EGCS effluents in quantities larger than 1:100,000 and 1:1,000,000 were identified. These are depicted in Figure 52.

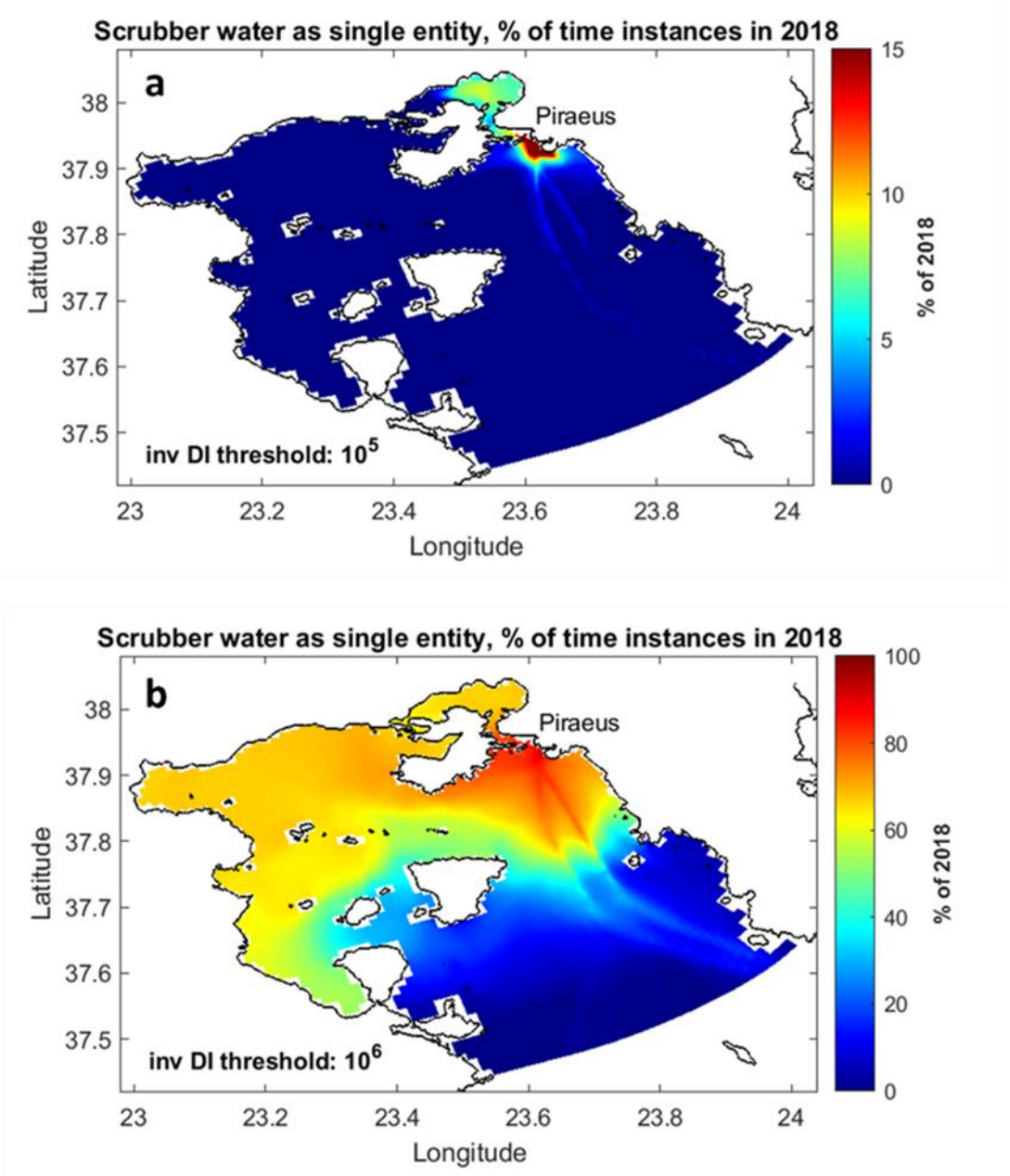

Figure 52. Percentage of time instances in 2018 that EGCS effluent was present as 'single entity' at the surface waters of Saronikos Gulf based on 6-hourly model output and inverse Cd dilution index (inv DI) threshold values of (a) 10^5 and (b) 10^6 (i.e., dilution of EGCS effluent 10^5 and 10^6 times respectively). Note the different values reported for the colour scale of each panel.

Concerning Figure 52, the method is sensitive to the inverse dilution value chosen to determine the threshold above which EGCS effluent ceases to be considered a single entity. In Figure 52(a), where the lower dilution value of 10^5 is used, lower percentages of time (or duration) when 'EGCS effluent' is present are calculated, in fewer areas of the Saronikos domain as well. The areas around the port of Piraeus and along the shipping lanes are shown as the ones most affected, with time percentages up to 15% of 2018. Interestingly, the enclosed gulf of Salamina also appears affected, due to the advection of surface water masses from the innermost part of Saronikos Gulf.

Following the 2050 EGCS use scenarios, an increase of up to 15% for the mean surface concentrations of benzo-a-pyrene and up to 5% for fluoranthene is expected for Scenario 3 in the open sea (as the coastal signal is dominated by the land sources). In the case of Scenario 8, small reductions (reaching up to -1%) of PAHs concentrations are expected along the shipping lanes.

4.1.2.3. Northern Adriatic

To assess the water quality of the Northern Adriatic case study area the ChemicalDrift model was applied, simulating the fate and transport of Cd, Pb, BaP and Flu in the marine environment for both the baseline scenario (year 2018) and two future scenarios for the year 2050. The results showed that, for the 2018 simulations, the highest concentrations of the selected pollutants in the water column were reached in some parts of Venice Lagoon and along the coast, especially at the delta of the Po River (Cd) and in the Gulf of Trieste (BaP, Flu, and Pb; Figure 53).

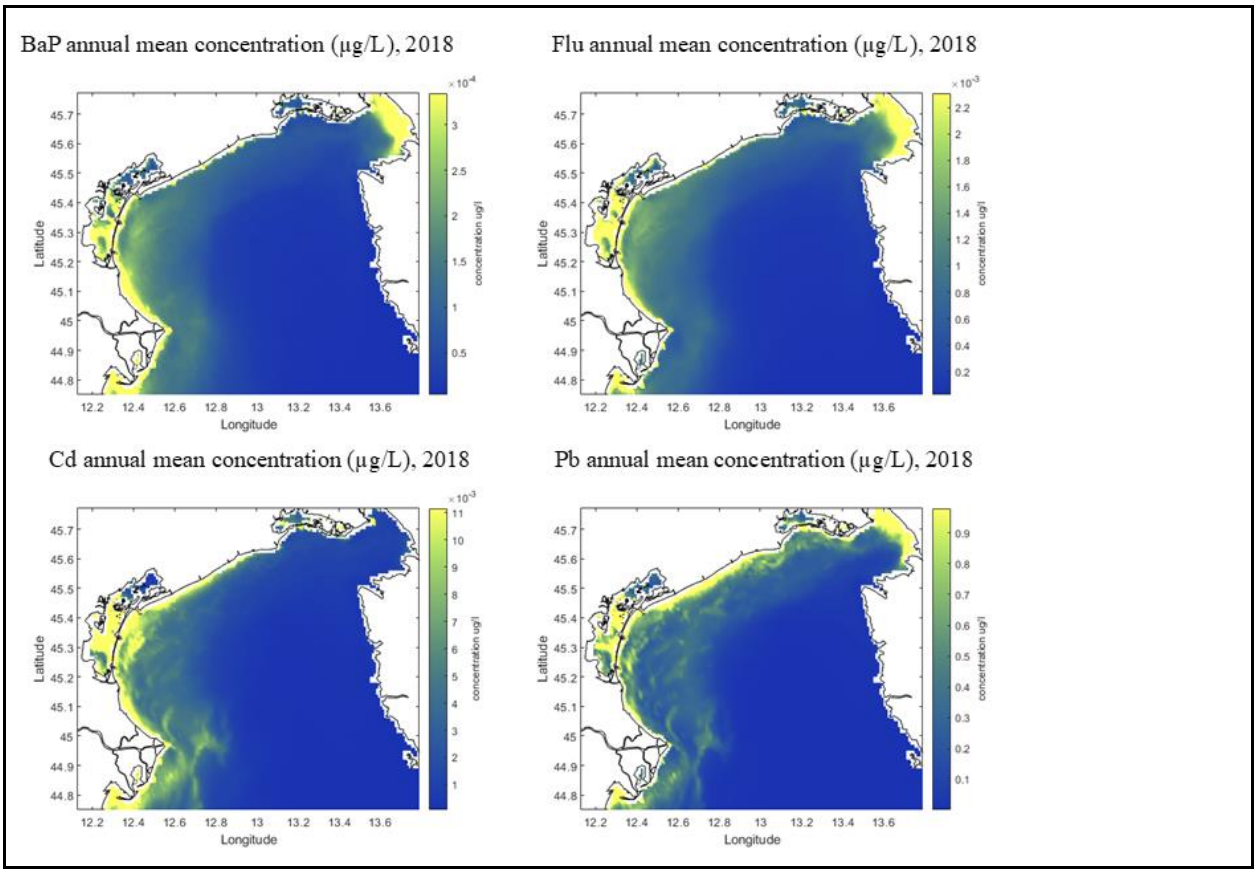

Figure 53. Benzo-a-pyrene (BaP), fluoranthene (Flu), cadmium (Cd), and lead (Pb) annual mean concentrations in the Northern Adriatic Sea for the baseline year 2018. Units are in micrograms L^{-1}.

As for 2050 simulations, while the concentration of the selected pollutants in the water column remained strongly dependant on land-based inputs (land-based emissions at their 2018 levels) and background contamination of sediments, the increase in shipping activity and EGCS use assumed for Scenario 3 caused a minor increase in water concentration, especially in the area near the Port of Trieste. Conversely, Scenario 8 showed a very slight decrease (about 0.01%) of the concentration of studied chemicals thanks to the use of cleaner fuels as an alternative to EGCSs.

Table 30 reports the average concentrations of the target chemicals within the case study transitional and coastal (until 12 miles from the coast) waters, as well the contribution of shipping to these concentrations for the baseline year and for both 2050 scenarios. Modelling results show a limited contribution of shipping to coastal pollution, but they also highlight that this contribution is much more relevant in the open sea (up to 9% for Cd, 12% for Pb, 40% for BaP and 25% for Flu).

Table 30. Average concentrations of the benzo-a-pyrene (BaP), fluoranthene (Flu), cadmium (Cd), and lead (Pb) within transitional and Italian territorial waters considering all pollution sources, as well the contribution of shipping to these concentrations for the baseline year and for both scenarios in 2050.

	2018 All sources	**Shipping contr. (2018)**	**2050 S3 All sources**	**Shipping contr. (2050 S3)**	**2050 S8 All sources**	**Shipping contr. (2050 S8)**	**Current AA-EQS**
	µg/L	%	µg/L	%	µg/L	%	µg/L
BaP	1.00E-04	5.88E-03	1.00E-04	2.89E-01	1.00E-04	1.65E-04	1.7E-04
Flu	3.37E-04	1.05E-02	3.39E-04	5.08E-01	3.37E-04	5.81E-04	6.3E-03
Cd	1.08E-02	1.57E-03	1.08E-02	8.47E-02	1.08E-02	1.80E-03	2.0E-01
Pb	3.21E-01	4.01E-04	3.21E-01	1.89E-02	3.21E-01	4.68E-04	1.3E+00

Bioaccumulation modelling for the Northern Adriatic case study

The MERLIN-Expo tool was applied to simulate the concentrations (annual mean) in mussels under Scenario 3 in 2050, using as input the daily concentrations of target contaminants in the mussel farm area as provided by ChemicalDrift run for the selected scenario (considering loads from land-based and shipping sources, as described in Deliverable 4.3).

Results of bioaccumulation modelling are reported in Table 31 and show that simulated concentrations in molluscs are below the maximum levels acceptable in seafood (bivalve molluscs) by the EU Regulation (European Commission, 2023a).

The water concentration of the selected pollutants in the mussel farms is almost completely controlled by the River Po discharge, and it is difficult to detect contributions from shipping. However, it is worth noting that this approach could also be used to estimate the influence of shipping activities to bioaccumulation in areas where this contribution is more pronounced.

Table 31. Annual mean concentrations of target chemicals in water (in mussel farms area) simulated by ChemicalDrift for 2050 S3 (considering loads from land-based and shipping sources), and concentrations in mussels modelled with MERLIN-Expo compared against food safety thresholds for bivalve molluscs established in Reg.EU 915/2023.

	Water conc 2050 S3 (annual mean)	Concentration modelled in mussel (annual mean)		Maximum levels in bivalve molluscs (Reg.EU 915/2023)	
Chemical	micrograms L^{-1}				
Cd	1.39E-02	0.009	millig/kg $_{fw}$	1	millig/kg $_{fw}$
Pb	3.17E-01	0.087	millig/kg $_{fw}$	1.5	millig/kg $_{fw}$
BaP	4.64E-04	2.21	microg/kg$_{fw}$	10	microg/kg$_{fw}$
Fl	6.18E-04	3.98	microg/kg$_{fw}$	//	

5. Impacts

In this work, impacts assessments are divided in two parts which include the environmental and economic aspects. Further, environmental impacts are considered per species studied and by the spatial distribution in relation to the shipping lanes. To answer the needs to understand the extent of the EGCS investment payback periods, an economic assessment was made as a part of this study. These are described in the following sections.

5.1. Environmental impacts

5.1.1. Results from ecotoxicological experiments

Significant effects on early life stages of invertebrate species of different taxa were detected after exposure to concentrations below 1% EGCS effluent (Table 32). The most sensitive endpoint analysed in the present project was fertilisation of eggs of the green sea urchin *Strongylocentrotus droebachiensis*, where the LOEC, i.e. the lowest concentration causing a significant reduction of the fertilisation success of the eggs, was found at 0.0001% EGCS effluent (1 millilitre effluent water in m^3 seawater). This was the lowest tested concentration, and, in this experiment, it was therefore not possible to determine a NOEC. The second most sensitive endpoints were malformation of the larvae of the sea urchin *Paracentrotus lividu*s, the polychaete *Sabella alveolata* and the blue mussel *Mytilus trossulus* with LOECs of 0.001% EGCS effluent. Even in these tests LOEC was equal to the lowest tested EGCS effluent concentration. Figure 54 shows a series of photos of malformed sea urchin larvae of the species *Strongylocentrotus droebachiensis*, exposed to 0 - 10% EGCS effluent. In this species significant effects (LOEC) were detected at 0.1%. At 0.01% EGCS effluent the egg production and larval development of the copepod *Acartia tonsa* were significantly reduced. The LOEC was 1000 times higher, 10%, when testing adult specimens of *Acartia tonsa* and using mortality as an endpoint. This was the same LOEC as found in another study with EGCS effluent and *Acartia tonsa* (Koski et al., 2017). The two phytoplankton species and the marine bacteria were much less sensitive to the effluent than the invertebrates with NOECs between 10 and 20% effluent, and LOECs between 20 and 40% (Table 6). The results show how important it is to use a sensitive endpoint in order not to underestimate the toxicity. A graphic overview of results from the experimental studies with individual species of invertebrates divided into taxonomic groups, phytoplankton and bacteria is shown in Figure 55.

In addition to ecotoxicological experiments on single species, studies were also made on microplankton communities (<200 micrometres) retrieved from a relatively pristine (Plagia, Greece) and a polluted (Thessaloniki, Greece) site in the Eastern Mediterranean. Results show that the algal species were more resilient to EGCS effluent exposure while the bacterial community composition changed differently depending on whether they had been pre-exposed to shipping effluents in their natural environment or not (Figure 56). The bacterial communities from Plagia (pristine) showed a strong response to EGCS effluent changing into strains capable of using PAHs as substrate (Genitsaris et al., 2023). This indicates a higher resilience in more healthy ecosystems. How this microbial community change will affect other functional properties of the micropelagic ecosystem, such as carbon and nitrogen cycling, are yet unknown.

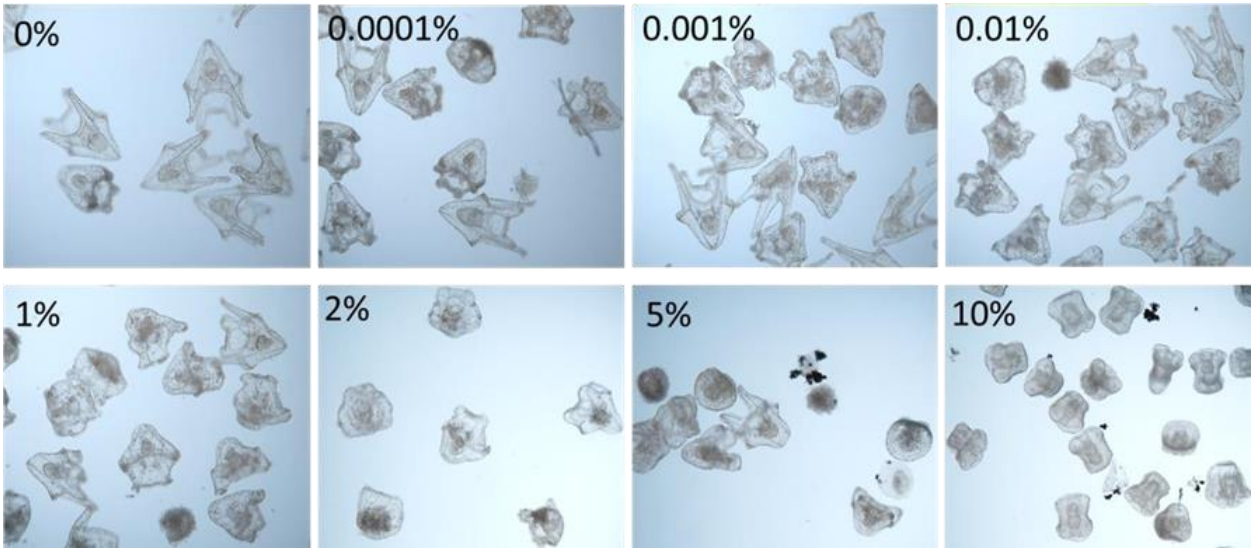

Figure 54. Microscope images of sea urchin larvae (Strongylocentratus droebachiensis) exposed to EGCS effluent dilution series. At 0.0001% dilution, 23% of the larvae had malformations. At 10% dilution, 97% of the larvae were malformed.

Table 32. Summary of a selection of endpoints and the concentrations of EGCS effluent causing a toxic response. LOEC (Lowest Observed Effect Concentration) = the lowest tested concentration of EGCS effluent having a significant effect, NOEC (No Observed Effect Concentration) = the highest tested concentration of EGCS effluent with no significant effect. Note that for several endpoints significant effects were detected at the lowest test concentration and no NOEC could be presented. Concentrations are expressed as the percentage of EGCS effluent (ScrW) in the exposure water.

Species	End point	NOEC (% ScrW)	LOEC (% ScrW)

Sea urchin, *Strongylocentrotus droebachiensis*	Reduced fertilisation success	<0.0001	0.0001
Sea urchin, *Strongylocentrotus droebachiensis*	Malformation of larvae	0.01	0.1
Sea urchin, *Paracentrotus lividus*	Reduced fertilisation success	<0.01	0.01
Sea urchin, *Paracentrotus lividus*	Malformation of larvae	<0.001	0.001
Copepod, *Acartia tonsa*	Reduced egg production in females	0.001	0.01
Copepod, *Acartia tonsa*	Impaired larval development	<0.01	0.01
Copepod, Acartia tonsa	Mortality of adults	5	10
Polychaete, *Sabellaria alveolata*	Malformation of larvae	<0.001	0.001
Blue mussel, *Mytilus trossulus*	Malformation of larvae	<0.001	0.001
Blue mussel, *Mytilus galloprovincialis*	Impaired larval development	0.1	1.0
Phytoplankton, *Phaeodactylum tricornutum*	Growth rate	20	40
Phytoplankton, *Dunaliella tertiolecta*	Growth rate	10	20
Bacteria, *Aliivibrio fisheri*	Bioluminescence, inhibition	10	20

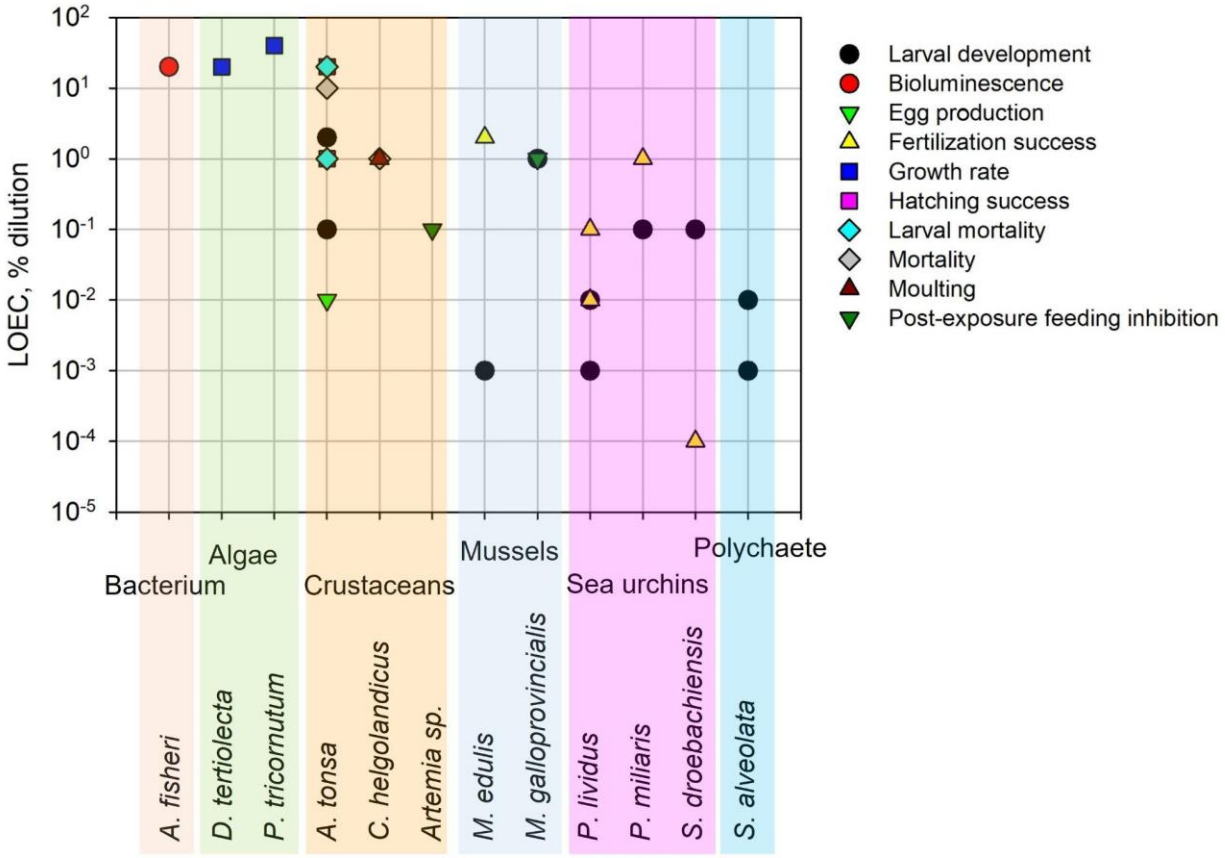

Figure 55. Lowest Effect Concentration (LOEC) of EGCS effluents (% dilution) detected for organisms of different taxonomic groups, and for different endpoints. Several of the LOECs were also the lowest test concentration applied in the experiment, including the LOEC for the sea urchin S. droebachiesis. See Table 6 for more detailed information.

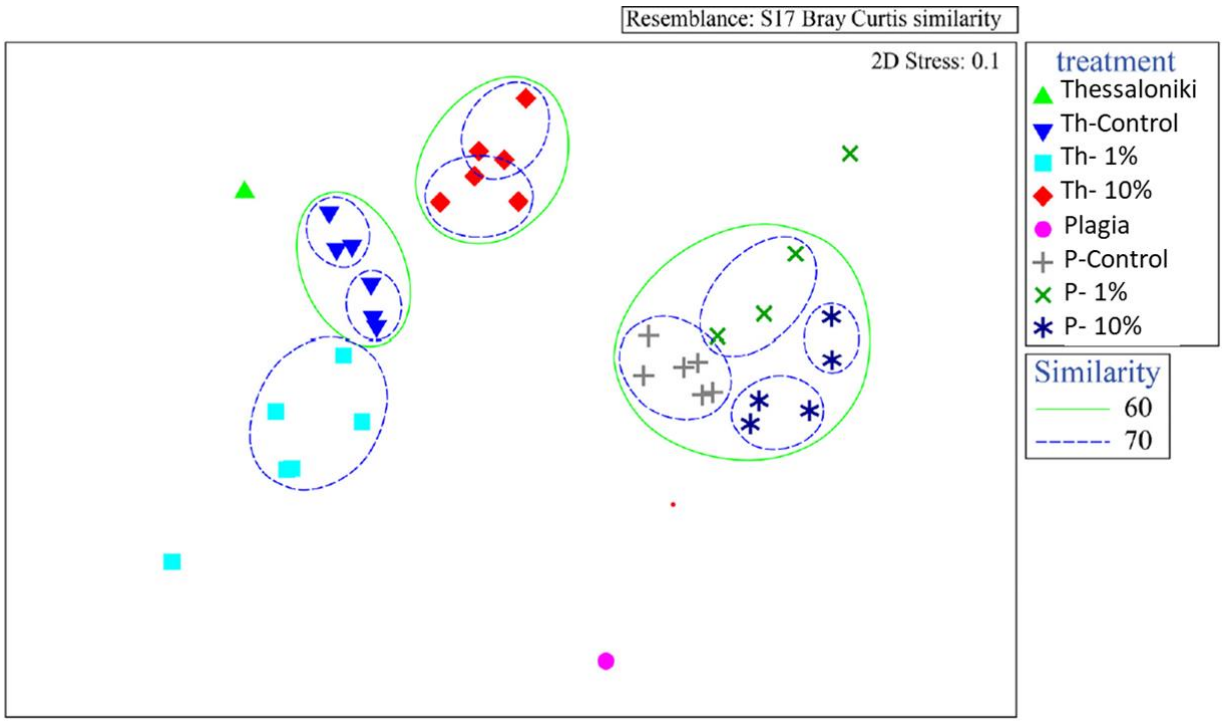

Figure 56. Multidimensional scaling projection of bacterial community composition data based on Bray Curtis similarities. Microbial communities were collected from marine sites outside Thessaloniki, Greece (polluted site) and Plagia, Greece (Pristine site) and were then exposed to either 1 or 10% EGCS effluent. Groupings show 60 (green) and 70 (blue %) similarities among replicate analyses of bacterial community composition (Genitsaris et al., 2023).

The experimental toxicity tests in the project were conducted on twelve species from several of the most important taxonomic groups of marine organisms, and invertebrates during their early life stages were found to be the most sensitive endpoints. The EGCS effluent caused harm to basic processes like fertilisation success of eggs and skeletal development larvae. The same kind of effects were detected in invertebrates from different taxonomic groups, suggesting that they are of a more general character. It is therefore likely that the same toxic effects would occur also on other invertebrate species than those tested within the project. Data on EGCS effluent toxicity are still lacking for many important groups of marine organisms. There is practically no available information on the impact of EGCS effluents on early life stages of fish.

5.1.2. EGCS effluent - a complex mixture

It is a well-documented fact that the effect on living organisms from exposure to mixtures of hazardous compounds can be very different from the mere sum of the effect of individual compounds (Backhaus and Faust, 2012). The work performed in EMERGE is a striking example of this. Assessment of EGCS effluent based on how the concentrations of individual chemical

compounds relate to existing threshold values indicates a toxicity that is many orders of magnitude lower than what is found to be the case when living organisms are exposed to whole effluent. It is not known which contaminants were responsible for the toxicological effects observed in the many ecotoxicological experiments carried out within the EMERGE project. Some information can be obtained by investigating what the concentrations of some of the potentially most toxic chemicals in the effluent were when statistically significant effects were detected. A significant effect on fertilisation of sea urchin (*Strongylocentrotus droebachiensis*) eggs occurred when the concentration of 16 PAH was 0.02 nanograms L^{-1} of exposure water, alkylated PAHs 0.04 nanograms L^{-1}, vanadium 0.4 nanograms L^{-1}, zinc 0.05 nanograms L^{-1} and copper 0.01 nanograms L^{-1}. Malformation of larvae of sea urchin, polychaete and blue mussels occurred at EGCS effluent concentrations of 0.001%, which corresponded to approximately 0.08 nanograms of 16 PAH L^{-1}, 0.13 nanograms alkylated PAH L^{-1} and 1.0, 0.4 and 0.07 nanograms L^{-1} for vanadium, zinc, and copper. These concentrations are far below the threshold levels set by national and international agencies. It is thus clear that toxic effects of complex mixtures such as EGCS effluents cannot be determined based on chemical analysis alone, but experimental testing of relevant species and sensitive endpoints is necessary.

Factors other than contaminants can also contribute to effluent toxicity, and reduced pH caused by the acidic EGCS effluent is one of them. However, at the lowest concentrations with a significant toxic effect, 0.0001 – 0.001% effluent in the exposure water, the change in pH from natural seawater was negligible. The various kinds of combustion particles present in the effluent can also be expected to have contributed to the toxicity. Many of these particles have high concentrations of PACs and metals adsorbed to the surface, but it is still not clear how available these contaminants are for uptake in living organisms. Combustion particles were observed both in the stomachs of exposed sea urchin larvae and adsorbed to larval carcasses (Figure 54 in photos from 5% and 10% effluent).

5.1.3. Shipping lanes - destruction zones for key species

Pelagic larvae and species in areas around shipping lanes will encounter the highest concentrations and the most complex mixture of the components in EGCS effluent. Model simulations of effluent fate in the Öresund, carried out within the EMERGE project, also show that diluted effluent concentrations will, in the whole recipient, exceed those causing toxic effect on

early life stages of invertebrate larvae. Of vital ecological importance is the high sensitivity found in marine invertebrate larvae and some of the early life stages of the pelagic copepods *Acartia tonsa* and *Calanus helgolandicus.* Especially, the copepods are important grazers on microalgae and are themselves essential prey for pelagic fish, such as cod (Beaugrand et al., 2003). The Öresund shipping lanes in the Baltic Sea area pass right through important spawning areas for cod, and in the Baltic Proper cod larvae are obliged to cross busy shipping lanes when passing from the most important spawning areas located at the open sea to the near shore nursery grounds (Bagge et al., 1994). The cod populations around the world have declined drastically over the past decades, and although overfishing is an important reason for this, there is convincing evidence in the scientific literature that the reduction in cod also is caused by a reduction in populations of pelagic copepods (Beaugrand and Kirby, 2010; Heath and Lough, 2007). In addition, the three ringed PAHs occurring at the high concentrations in EGCS effluents, particularly phenanthrene, are known to have direct toxic effects on early life stages of fish, including cardiotoxicity and malformations of cranium and spine of the larvae (Incardona and Scholz, 2016). Although effects of EGCS effluents were not tested on fish or fish larvae within the EMERGE project, direct effects on fish larvae as well as indirect effects of reduced prey abundance, foremost copepods, on fish are likely and important negative consequences of EGCS effluent discharge which will affect both ecosystems and commercial fish species.

The observed effects on the free-swimming larvae of bottom dwelling organisms at very low concentrations can have a serious impact on both soft bottom and hard bottom marine ecosystems. There has been a dramatic decline in some bottom-living species over the past year, perhaps one of the more noticeable is the blue mussel in the North Atlantic where the populations have gone from very abundant to rare in just over a decade (Baden et al., 2021). Again, there are most likely several reasons for this decline, but pollution is likely part of the explanation. Exposure to EGCS effluent that causes increased mortality of invertebrate larvae will directly affect populations and ecosystems due to reduced recruitment. This, in turn, can lead to negative consequences for relevant economic activities, such as mussel farming, which in the North Adriatic area relies almost exclusively on harvesting wild larvae.

The ecotoxicological results from EMERGE further underline the need to monitor the use of open-loop EGCS in the North Adriatic, also in consideration of the expected introduction of a SECA in the Mediterranean Sea from 1 July 2025, which is envisaged to increase the use of EGCS in the area. An increase in the number of ships equipped with open-loop EGCS will inevitably lead to

increased exposure for the plankton communities along the main shipping lanes to all hazardous components present in the EGCS effluent. Under these conditions (described by Scenario 3), coastal waters will be particularly vulnerable to EGCS effluent discharges since they are heavily trafficked and at the same time harbour a high biodiversity. Furthermore, despite the dilution of the EGCS effluent once discharged, surface waters along the main shipping lanes will be frequently supplied of contaminants in EGCS effluents, increasing the risk that adverse effect concentration is exceeded. In fact, simulations carried out following the “diluted EGCS effluent discharge approach” with emission data from 2018 showed how a continued release of EGCS effluents over several days could lead to concentrations shown to have significant negative effects on organisms tested within EMERGE. This impact will be even more pronounced with the increase in EGCS effluent discharge by almost two orders of magnitude as is projected by 2050.

5.2. Economic impacts

The use of EGCSs as an appropriate means of compliance (i.e., Equivalents) has been questioned, but also concerns have been raised regarding the fate of the EGCS investments already made. As the wide-scale use of EGCSs will also imply costs related to the degradation of the marine environment, the cost of not restricting EGCSs has been raised as an important aspect that should be considered. Therefore, the study by Lunde Hermansson et al (2023), in review) i) estimates the extent of global EGCS fleet has reached economic break-even on their EGCS installations, and the potential monetary gain of using HFO as compared to the more expensive MGO or VLSFO, and ii) evaluates the external costs of not restricting EGCS effluent discharge by determining societal damage costs connected to marine ecotoxicity, i.e. deterioration of the marine environment, resulting from discharge of EGCS effluents. The main findings of the Lunde Hermansson et al. are outlined below.

The study was compiled based on the real-world simulations of the global EGCS-vessel activity from STEAM, applying actual fuel costs from each past year (Ship & Bunker) and the expenses related to EGCS installation and operation. Results indicate that 51% of the global EGCS-fitted fleet reached economic break-even by the end of 2022, with a surplus of 4.7 billion €$_{2019}$, and the forecast, based on historical fuel consumption and fuel prices at the first half of 2023, show that many more vessels (63-86% in total) would have reached their point of break-even in 2023. Within five years after installation, more than 95% of the ships with open loop EGCS systems reach break-even.

The cumulative societal damage cost (represented by the marine ecotoxicity damage cost), by not restricting EGCS effluent discharges in the Baltic Sea Area since the implementation of SECA in 2015, amounts to 680 million €$_{2019}$. From the private perspective, the shipowners have saved more than 1.7 billion €$_{2019}$, by not switching to the more expensive but less polluting MGO when operating in the Baltic Sea Area.

Continued use of EGCS and high sulfur fossil fuels will delay the transition to more sustainable options. The investments made on EGCS enable ships to continue using fossil fuels instead of transitioning away from them as soon as possible as agreed in the 2023 Dubai Climate Change conference. Continued carriage of residual fuels also increases the risk of dire environmental consequences whenever accidental releases of oil to the sea occur.

6. Conclusions

This document summarises four years of research work carried out to understand the environmental impacts of EGCS. Based on the experimental characterisation of EGCS effluents, it is evident that the complexity of the effluent composition should be considered in more detail. Most of the ecotoxicological effects were connected to alkylated PAH compounds, which may be more toxic than their parent compounds. Thus, the current limits for pH, PAH content and turbidity are unable to capture the toxicologically most significant compounds. According to the experiments done in this work, it is possible to comply with the current requirements for EGCS effluents and at the same time do significant harm to the marine environment. Exclusion of alkylated PAH compounds from the EGCS effluent discharge criteria is unfortunate because these are responsible for a major part of toxicological effects of the effluent.

The sensitivity of the biological response to very low concentration of EGCS effluent indicates that especially the early life stages of various organisms are prone to detrimental effects. These organisms are at various levels of the trophic chains of marine food webs, and the indirect effects of reducing the food sources of other animals should be acknowledged. Commercially relevant fish species are impacted through this mechanism globally.

Based on the whole effluent testing, the EGCS effluent remains at harmful levels at very low concentrations. This, together with the marine modelling dilution experiments indicate that each EGCS discharge remained harmful for 2-10 days in the Northern Adriatic Sea environment and dispersed to 10-30 km from the shipping lanes. Additional ship passages and EGCS effluent releases exacerbate the effect and enlarge the impact area.

Modelled transport of contaminants indicates sedimentation in coastal zones and archipelago areas. These have high biodiversity and represent significant spawning areas for many marine species. Considering the existence of densely trafficked shipping lanes in regional seas, most of the European coastline, and marine life on those areas, will be impacted by EGCS effluents.

Based on the economic studies of EGCS investment payback periods, the majority of the global EGCS fleet has already amortised the costs of their investments. Within a period of five years,

about two thirds of the global EGCS fleet makes profit with the continued use of high sulfur fuels when compared to switching to low sulfur fuels. The continued use of EGCS encourages the continued use of fossil high sulfur fuels slowing down the shift to more sustainable options.

It is evident that the additional burden of contaminants from EGSC effluent discharges worsen the state of regional sea areas which are already in poor condition.

References

Aghito, M., Calgaro, L., Dagestad, K. F., Ferrarin, C., Marcomini, A., Breivik, Ø. and Hole, L. R.: ChemicalDrift 1.0: an open-source Lagrangian chemical-fate and transport model for organic aquatic pollutants, Geosci. Model Dev., 16(9), 2477–2494, doi:10.5194/gmd-16-2477-2023, 2023.

Artioli, Y., Friedrich, J., Gilbert, A. J., McQuatters-Gollop, A., Mee, L. D., Vermaat, J. E., Wulff, F., Humborg, C., Palmeri, L. and Pollehne, F.: Nutrient budgets for European seas: A measure of the effectiveness of nutrient reduction policies, Mar. Pollut. Bull., 56(9), 1609–1617, doi:10.1016/j.marpolbul.2008.05.027, 2008.

Backhaus, T. and Faust, M.: Predictive environmental risk assessment of chemical mixtures: A conceptual framework, Environ. Sci. Technol., 46(5), 2564–2573, doi:10.1021/es2034125, 2012.

Baden, S., Hernroth, B. and Lindahl, O.: Declining populations of mytilus spp. In north atlantic coastal waters-A swedish perspective, J. Shellfish Res., 40(2), 269–296, doi:10.2983/035.040.0207, 2021.

Bagge, O., Thurow, F., Steffensen, E. and Bay, J.: The Baltic cod, Dana, 10(Figure 2), 1–28 [online] Available from: http://agris.fao.org/agris-search/search/display.do?f=1995/DK/DK95002.xml;DK9521335, 1994.

Beaugrand, G. and Kirby, R. R.: Climate, plankton and cod, Glob. Chang. Biol., 16(4), 1268–1280, doi:10.1111/j.1365-2486.2009.02063.x, 2010.

Beaugrand, G., Brander, K. M., Lindley, J. A., Souissi, S. and Reid, P. C.: Plankton effect on cod recruitment in the North Sea, Nature, 426(6967), 661–664, doi:10.1038/nature02164, 2003.

Bellafiore, D. and Umgiesser, G.: Hydrodynamic coastal processes in the North Adriatic investigated with a 3D finite element model, Ocean Dyn., 60(2), 255–273, doi:10.1007/s10236-009-0254-x, 2010.

Benfenati, E., Manganaro, A. and Gini, G.: VEGA-QSAR: AI inside a platform for predictive toxicology, in PAI2013 Popularize Artificial Intelligence, pp. 21–28, Turin, Italy. [online] Available from: https://ceur-ws.org/Vol-1107/PAI2013.pdf, 2013.

de Boer, J. and Law, R. J.: Developments in the use of chromatographic techniques in marine laboratories for the determination of halogenated contaminants and polycyclic aromatic hydrocarbons, J. Chromatogr. A, 1000(1–2), 223–251, doi:https://doi.org/10.1016/S0021-9673(03)00309-1, 2003.

Booij, N., Ris, R. C. and Holthuijsen, L. H.: A third-generation wave model for coastal regions 1. Model description and validation, J. Geophys. Res. Ocean., 104(C4), 7649–7666, doi:10.1029/98JC02622, 1999.

Bruland, K. W. and Lohan, M. C.: 6.02 - Controls of Trace Metals in Seawater, Treatise on Geochemistry, 6, 23–47, doi:https://doi.org/10.1016/B0-08-043751-6/06105-3, 2003.

Ciffroy, P., Alfonso, B., Altenpohl, A., Banjac, Z., Bierkens, J., Brochot, C., Critto, A., De Wilde, T., Fait, G., Fierens, T., Garratt, J., Giubilato, E., Grange, E., Johansson, E., Radomyski, A., Reschwann, K., Suciu, N., Tanaka, T., Tediosi, A., Van Holderbeke, M. and Verdonck, F.: Modelling the exposure to chemicals for risk assessment: a comprehensive library of multimedia and PBPK models for integration, prediction, uncertainty and sensitivity analysis – the MERLIN-Expo tool, Sci. Total Environ., 568(March), 770–784, doi:10.1016/j.scitotenv.2016.03.191, 2016.

Deltares Systems: Delft3D-FLOW: Simulation of multi-dimensional hydrodynamic flows and transport phenaomena, including sediments (v4.05 rev 78731), delft., 2023a.

Deltares Systems: Delft3D FM Suite 2D3D - Part D: Water Quality (v1.1 rev 78845), Delft, the Netherlands., 2023b.

Endresen, O., Eide, M., Longva, T., Mjelde, A., Frimann-Dahl, J., Rivedal, N., Wold, M., Hustad, H., Haugom, G., Langli, A., Kvålsvold, J., Chryssakis, C., Helgesen, H., Vedeler, J., Martinsen, K., MjOs, N., Gravir, G., Sverud, T., Hermunsgard, H., Walenkiewicz, J., Adams, S., Schäfer, J., Alvik, S., Özgun, O., Bakken, B. and Vartdal, B.: Maritime Forecast To 2050 - Energy transition outlook 2019., 2019.

European Commission: Technical Guidance For Deriving EQS (Guidance Document No. 27), updated 2018, Eur. Community Rep., 11-12 June(27), 210 pp [online] Available from: https://rvs.rivm.nl/sites/default/files/2019-04/Guidance No 27 - Deriving Environmental Quality Standards - version 2018.pdf, 2018.

European Commission: COMMISSION REGULATION (EU) 2023/915 on maximum levels for certain contaminants in food., 2023a.

European Commission: WFD CIRCA, WFD CIRCA [online] Available from: https://circabc.europa.eu/ui/group/9ab5926d-bed4-%0A4322-9aa7-9964bbe8312d/library/cfbf7cb2-b8cc-463d-b541-%0A7a34e3ab52df?p=1&n=10&sort=modified_DESC (Accessed 29 December 2023b), 2023.

European Community: Directive 2000/60/EC of the European Parliament and of the Council of 23 October 2000 establishing a framework for Community action in the field of water policy, Off. J. Eur. Parliam., L327(September 1996), 1–82, doi:10.1039/ap9842100196, 2000.

European Parliament: DIRECTIVE (EU) 2016/802 reduction in the sulphur content of certain liquid fuels, European Commission, Europe., 2016.

European Union: Concerning the Registration, Evaluation, Authorisation and Restriction of Chemicals (REACH), establishing a European Chemicals Agency, Official Journal of the European Union, 29.5.2007, European Union., 2007.

European Union: DIRECTIVE 2008/105/EC OF THE EUROPEAN PARLIAMENT AND OF THE COUNCIL on environmental quality standards in the field of water policy. [online] Available from: https://eur-lex.europa.eu/legal-content/EN/TXT/PDF/?uri=CELEX:32008L0105, 2008.

European Union: DIRECTIVE 2013/39/EU OF THE EUROPEAN PARLIAMENT AND OF THE COUNCIL as regards priority substances in the field of water policy, European Commission., 2013.

Faber, J., Hanayama, S., Zhang, S., Pereda, P., Comer, B., Hauerhof, E., Schim van der Loeff, W., Smith, T., Zhang, Y., Kosaka, H., Adachi, M., Bonello, J., Galbraith, C., Gong, Z., Hirata, K., Hummels, D., Kleijn, A., Lee, D., Liu, Y., Lucchesi, A., Mao, X., Muraoka, E., Osipova, L., Qian, H., Rutherford, D., Suárez de la Fuente, S., Yuan, H., Velandia Perico, C., Wu, L., Sun, D., Yoo, D. and Xing, H.: The Fourth IMO GHG Study, London, UK., 2020.

Ferrarin, C., Davolio, S., Bellafiore, D., Ghezzo, M., Maicu, F., Mc Kiver, W., Drofa, O., Umgiesser, G., Bajo, M., De Pascalis, F., Malguzzi, P., Zaggia, L., Lorenzetti, G. and Manfè, G.: Cross-scale operational oceanography in the Adriatic Sea, J. Oper. Oceanogr., 12(2), 86–103, doi:10.1080/1755876X.2019.1576275, 2019.

Fridell, E., Steen, E. and Peterson, K.: Primary particles in ship emissions, Atmos. Environ., 42(5), 1160–1168, doi:10.1016/j.atmosenv.2007.10.042, 2008.

García-Gómez, E., Insa, S., Gros, M. and Petrović, M.: Rapid and sensitive method for the simultaneous determination of PAHs and alkyl-PAHs in scrubber water samples using HS-SPME-GC-MS/MS, Methods X, in review, 2023.

Gauss, M., Gusev, A., Aas, W., Hjellbrekke, A.-G., Ilyin, I., Klein, H., Heiko, A., Rozovskaya, O., Shatalov, V., Strijkina, I. and Travnikov, O.: Atmospheric Supply of Nitrogen, Cadmium, Lead, Mercury, PCDD/Fs, PCB-153, and B(a)P to the Baltic Sea EMEP/MSC-W Report for HELCOM. [online] Available from: https://emep.int/publ/helcom/2020/EMEP_TechnicalReport_3_2020.pdf, 2020.

Geffard, O., Geffard, A., His, E. and Budzinski, H.: Assessment of the bioavailability and toxicity of sediment-associated polycyclic aromatic hydrocarbons and heavy metals applied to Crassostrea gigas embryos and larvae, Mar. Pollut. Bull., 46(4), 481–490, doi:10.1016/S0025-326X(02)00451-4, 2003.

Genitsaris, S., Kourkoutmani, P., Stefanidou, N., Michaloudi, E., Gros, M., García-Gómez, E., Petrović, M., Ntziachristos, L. and Moustaka-Gouni, M.: Effects from maritime scrubber effluent on phytoplankton and bacterioplankton communities of a coastal area, Eastern Mediterranean Sea, Ecol. Inform., 77(June), doi:10.1016/j.ecoinf.2023.102154, 2023.

Giubilato, E., Radomyski, A., Critto, A., Ciffroy, P., Brochot, C., Pizzol, L. and Marcomini, A.: Modelling ecological and human exposure to POPs in Venice lagoon. Part I — Application of MERLIN-Expo tool for integrated exposure assessment, Sci. Total Environ., 565, 961–976, doi:10.1016/j.scitotenv.2016.04.146, 2016.

Grönholm, T., Mäkelä, T., Hatakka, J., Jalkanen, J.-P., Kuula, J., Laurila, T., Laakso, L. and Kukkonen, J.: Evaluation of Methane Emissions Originating from LNG Ships Based on the Measurements at a Remote Marine Station, Environ. Sci. Technol., 55, 13577–13686, doi:10.1021/acs.est.1c03293, 2021.

Hawthorne, S. B., Grabanski, C. B., Miller, D. J. and Kreitinger, J. P.: Solid-phase microextraction measurement of parent and alkyl polycyclic aromatic hydrocarbons in milliliter sediment pore water samples and determination of KDOC values, Environ. Sci. Technol., 39(8), 2795–2803, doi:10.1021/es0405171, 2005.

Heath, M. R. and Lough, R. G.: A synthesis of large-scale patterns in the planktonic prey of larval and juvenile cod (Gadus morhua), Fish. Oceanogr., 16(2), 169–185, doi:10.1111/j.1365-2419.2006.00423.x, 2007.

HELCOM: Pollution load on the Baltic Sea - Summary of the HELCOM Seventh Pollution Load Compilation (PLC-7), Helsinki, Finland. [online] Available from: www.helcom.fi, 2022.

HELCOM: State of the Baltic Sea. Third HELCOM holistic assessment 2016-2021, Balt. Sea Environ. Proc., n°194, 1–133 [online] Available from: www.helcom.fiavailableat:https://helcom.fi/post_type_publ/holas3_sobsStateoftheBalticSeawebsite:https://stateofthebalticsea.helcom.fi, 2023.

IMO: Guidelines for risk and impact assessments of the discharge water from exhaust gas cleaning systems , , MEPC.1/Cir(0), 0–26, 2022.

Incardona, J. P. and Scholz, N. L.: The influence of heart developmental anatomy on cardiotoxicity-based adverse outcome pathways in fish, Aquat. Toxicol., 177(February 2018), 515–525, doi:10.1016/j.aquatox.2016.06.016, 2016.

Italian parlament: Norme in materia ambientale, Italy. [online] Available from: https://www.normattiva.it/esporta/attoCompleto?atto.dataPubblicazioneGazzetta=2006-04-14&atto.codiceRedazionale=006G0171, 2006.

Jalkanen, J.-P., Johansson, L., Kukkonen, J., Brink, A., Kalli, J. and Stipa, T.: Extension of an assessment model of ship traffic exhaust emissions for particulate matter and carbon monoxide, Atmos. Chem. Phys., 12(5), 2641–2659, doi:10.5194/acp-12-2641-2012, 2012.

Jalkanen, J.-P., Johansson, L., Liefvendahl, M., Bensow, R., Sigray, P., Östberg, M., Karasalo, I., Andersson, M., Peltonen, H. and Pajala, J.: Modelling of ships as a source of underwater noise, Ocean Sci., 14(6), 1373–1383, doi:10.5194/os-14-1373-2018, 2018.

Jalkanen, J.-P., Johansson, L., Wilewska-Bien, M., Granhag, L., Ytreberg, E., Eriksson, K. M., Yngsell, D., Hassellöv, I.-M., Magnusson, K., Raudsepp, U., Maljutenko, I., Winnes, H. and Moldanova, J.: Modelling of discharges from Baltic Sea shipping, Ocean Sci., 17(3), 699–728, doi:10.5194/os-17-699-2021, 2021.

Jalkanen, J.-P., Majamäki, E., Heikkilä, M. and Johansson, L.: Emissions from Baltic Sea shipping in 2022, HELCOM Balt. Sea Environ. Fact Sheets 2023, 1–36 [online] Available from: https://helcom.fi/wp-content/uploads/2023/12/BSEFS-Emissions-from-Baltic-Sea-Shipping-in-2022-2023-1.pdf (Accessed 29 December 2023), 2023.

Jalkanen, J. P., Brink, A., Kalli, J., Pettersson, H., Kukkonen, J. and Stipa, T.: A modelling system for the exhaust emissions of marine traffic and its application in the Baltic Sea area, Atmos. Chem. Phys., 9(23), 9209–9223, doi:10.5194/acp-9-9209-2009, 2009.

Jalkanen, J. P., Johansson, L., Andersson, M. H., Majamäki, E. and Sigray, P.: Underwater noise emissions from ships during 2014–2020, Environ. Pollut., 311, 119766, doi:10.1016/j.envpol.2022.119766, 2022.

Johansson, L., Jalkanen, J.-P. P., Kalli, J. and Kukkonen, J.: The evolution of shipping emissions and the costs of regulation changes in the northern EU area, Atmos. Chem. Phys., 13(22), 11375–11389, doi:10.5194/acp-13-11375-2013, 2013.

Johansson, L., Jalkanen, J.-P. J.-P. and Kukkonen, J.: Global assessment of shipping emissions in 2015 on a high spatial and temporal resolution, Atmos. Environ., 167(Fig 1), 403–415, doi:10.1016/j.atmosenv.2017.08.042, 2017.

John, G. F., Yin, F., Mulabagal, V., Hayworth, J. S. and Clement, T. P.: Development and application of an analytical method using gas chromatography/triple quadrupole mass spectrometry for characterizing alkylated chrysenes in crude oil samples, Rapid Commun. Mass Spectrom., 28(8), 948–956, doi:10.1002/rcm.6868, 2014.

Keith, L. H.: The Source of U.S. EPA's Sixteen PAH Priority Pollutants, Polycycl. Aromat. Compd., 35(2–4), 147–160, doi:10.1080/10406638.2014.892886, 2015.

Kolovoyiannis, V., Mazioti, A. A., Krasakopoulou, E., Zervakis, V., Tragou, E. A., Mamoutos, I., Potiris, E., Petalas, S., Chatzilaou, C., Mosiou, K., Kontoyiannis, H., Paraskevopoulou, V. and Athiniotis, A.: Implementation of a modelling system for the investigation of the Saronikos Gulf marine ecosystem (Eastern Mediterranean), EGU Gen. Assem. 2023, 24–28 April 2023, 2023.

Koski, M., Stedmon, C. and Trapp, S.: Ecological effects of scrubber water discharge on coastal plankton: Potential synergistic effects of contaminants reduce survival and feeding of the copepod Acartia tonsa, Mar. Environ. Res., 129, 374–385, doi:https://doi.org/10.1016/j.marenvres.2017.06.006, 2017.

Linders, T., Infantes, E., Joyce, A., Karlsson, T., Ploug, H., Hassellöv, M., Sköld, M. and

Zetsche, E. M.: Particle sources and transport in stratified Nordic coastal seas in the Anthropocene, Elementa, 6, doi:10.1525/elementa.149, 2018.

Lunde Hermansson, A., Hassellöv, I. M., Moldanová, J. and Ytreberg, E.: Comparing emissions of polyaromatic hydrocarbons and metals from marine fuels and scrubbers, Transp. Res. Part D Transp. Environ., 97(June), doi:10.1016/j.trd.2021.102912, 2021.

Lunde Hermansson, A., Hassellöv, I.-M., Grönholm, T., Jalkanen, J.-P., Fridell, E., Parsmo, R., Hassellöv, J. and Ytreberg, E.: Ship pollution promotion – the strong economic incentives of scrubbers, Nat. Sustain., in review, doi:https://doi.org/10.21203/rs.3.rs-3534127/v1, 2023.

Mamoutos, I. G., Potiris, E., Tragou, E., Zervakis, V. and Petalas, S.: A high-resolution numerical model of the north aegean sea aimed at climatological studies, J. Mar. Sci. Eng., 9(12), doi:10.3390/jmse9121463, 2021.

Marotzke, J., Giering, R., Zhang, K. Q., Stammer, D., Hill, C. and Lee, T.: Construction of the adjoint MIT ocean general circulation model and application to Atlantic heat transport sensitivity, J. Geophys. Res. Ocean., 104(C12), 29529–29547, doi:10.1029/1999jc900236, 1999.

Martin, T. M.: User's Guide for T. E. S. T. (Toxicity Estimation Software Tool) Version 5.1, , 163 [online] Available from: https://www.epa.gov/sites/default/files/2016-05/documents/600r16058.pdf, 2020.

Martinez, E., Gros, M., Lacorte, S. and Barceló, D.: Simplified procedures for the analysis of polycyclic aromatic hydrocarbons in water, sediments and mussels, J. Chromatogr. A, 1047(2), 181–188, doi:10.1016/j.chroma.2004.07.003, 2004.

MEPC: 2022 GUIDELINES ON THE METHOD OF CALCULATION OF THE ATTAINED ENERGY EFFICIENCY DESIGN INDEX (EEDI) FOR NEW SHIPS., 2022.

Moermond, C. T. A., Kase, R., Korkaric, M. and Ågerstrand, M.: CRED: Criteria for reporting and evaluating ecotoxicity data, Environ. Toxicol. Chem., 35(5), 1297–1309, doi:10.1002/etc.3259, 2016.

Müller, J. D., Schneider, B. and Rehder, G.: Long-term alkalinity trends in the Baltic Sea and their implications for CO2-induced acidification, Limnol. Oceanogr., 61(6), 1984–2002, doi:10.1002/lno.10349, 2016.

Muratov, E. N., Bajorath, J., Sheridan, R. P., Tetko, I. V., Filimonov, D., Poroikov, V., Oprea, T. I., Baskin, I. I., Varnek, A., Roitberg, A., Isayev, O., Curtalolo, S., Fourches, D., Cohen, Y., Aspuru-Guzik, A., Winkler, D. A., Agrafiotis, D., Cherkasov, A. and Tropsha, A.: QSAR without borders, Chem. Soc. Rev., 49(11), 3525–3564, doi:10.1039/d0cs00098a, 2020.

Neff, J. M., Stout, S. A. and Gunster, D. G.: Ecological risk assessment of polycyclic aromatic

hydrocarbons in sediments: identifying sources and ecological hazard., Integr. Environ. Assess. Manag., 1(1), 22–33, doi:10.1897/IEAM_2004a-016.1, 2005.

Nylund, A. T.: Turbulent ship wakes and their spatiotemporal extent, Chalmers University of Technology., 2021.

OCIMF: Guide for Implementation of Sulphur Oxide Exhaust Gas Cleaning Systems (First Edition 2016). [online] Available from: https://www.ocimf.org/media/60654/Guide-for-Implementation-of-Sulphur-Oxide-Exhaust-Gas-Cleaning-Systems-030816.pdf, 2016.

Park, G., Brunswick, P., Kwok, H., Haberl, M., Yan, J., Macinnis, C., Kim, M., Helbing, C., Van Aggelen, G. and Shang, D.: A rapid gas chromatography tandem mass spectrometry method for the determination of 50 PAHs for application in a marine environment, Anal. Methods, 10(46), 5559–5570, doi:10.1039/c8ay02258e, 2018.

Petalas, S., Tragou, E., Mamoutos, I. G. and Zervakis, V.: Simulating the Interconnected Eastern Mediterranean–Black Sea System on Climatic Timescales: A 30-Year Realistic Hindcast, J. Mar. Sci. Eng., 10(11), doi:10.3390/jmse10111786, 2022.

Piri-Moghadam, H., Ahmadi, F. and Pawliszyn, J.: A critical review of solid phase microextraction for analysis of water samples, TrAC - Trends Anal. Chem., 85, 133–143, doi:10.1016/j.trac.2016.05.029, 2016.

Portolés, T., Sancho, J. V., Hernández, F., Newton, A. and Hancock, P.: Potential of atmospheric pressure chemical ionization source in GC-QTOF MS for pesticide residue analysis, J. Mass Spectrom., 45(8), 926–936, doi:10.1002/jms.1784, 2010.

Portolés, T., Mol, J. G. J., Sancho, J. V. and Hernández, F.: Use of electron ionization and atmospheric pressure chemical ionization in gas chromatography coupled to time-of-flight mass spectrometry for screening and identification of organic pollutants in waters, J. Chromatogr. A, 1339, 145–153, doi:10.1016/j.chroma.2014.03.001, 2014.

Poster, D. L., Schantz, M. M., Sander, L. C. and Wise, S. A.: Analysis of polycyclic aromatic hydrocarbons (PAHs) in environmental samples: A critical review of gas chromatographic (GC) methods, Anal. Bioanal. Chem., 386(4), 859–881, doi:10.1007/s00216-006-0771-0, 2006.

Prpić-Oršić, J. and Faltinsen, O. M.: Estimation of ship speed loss and associated CO 2 emissions in a seaway, Ocean Eng., 44, 1–10, doi:10.1016/j.oceaneng.2012.01.028, 2012.

Qiao, M., Qi, W., Liu, H. and Qu, J.: Simultaneous determination of typical substituted and parent polycyclic aromatic hydrocarbons in water and solid matrix by gas chromatography-mass spectrometry, J. Chromatogr. A, 1291, 129–136, doi:10.1016/j.chroma.2013.03.044, 2013.

Radomyski, A., Giubilato, E., Suciu, N. A., Critto, A. and Ciffroy, P.: Modelling Bioaccumulation

in Aquatic Organisms and in Mammals, in The Handbook of Environmental Chemistry, edited by P. Ciffroy, A. Tediosi, and E. Capri, pp. 191–210, Springer International Publishing AG, Cham, Switzerland., 2018.

Ris, R. C., Holthuijsen, L. H. and Booij, N.: A third-generation wave model for coastal regions - 2. Verification, J. Geophys. Res., 104(C4), 7667–7681, doi:http://dx.doi.org/10.1029/1998JC900123, 1999.

Russo, A. and Artegiani, A.: Adriatic Sea hydrography, Sci. Mar., 60(SUPPL. 2), 33–43, 1996.

Santos, L. F. E. d., Salo, K. and Thomson, E. S.: Quantification and physical analysis of nanoparticle emissions from a marine engine using different fuels and a laboratory wet scrubber, Environ. Sci. Process. Impacts, 24(10), 1769–1781, doi:10.1039/d2em00054g, 2022.

Scroccaro, I., Ostoich, M., Umgiesser, G., De Pascalis, F., Colugnati, L., Mattassi, G., Vazzoler, M. and Cuomo, M.: Submarine wastewater discharges: Dispersion modelling in the Northern Adriatic Sea, Environ. Sci. Pollut. Res., 17(4), 844–855, doi:10.1007/s11356-009-0273-7, 2010.

Ship & Bunker: Ship & Bunker, [online] Available from: https://shipandbunker.com/ (Accessed 5 October 2023), 2023.

Sofiev, M., Siljamo, P., Valkama, I., Ilvonen, M. and Kukkonen, J.: A dispersion modelling system SILAM and its evaluation against ETEX data, Atmos. Environ., 40(4), 674–685, doi:10.1016/j.atmosenv.2005.09.069, 2006.

Sørensen, L., Meier, S. and Mjøs, S. A.: Application of gas chromatography/tandem mass spectrometry to determine a wide range of petrogenic alkylated polycyclic aromatic hydrocarbons in biotic samples, Rapid Commun. Mass Spectrom., 30(18), 2052–2058, doi:10.1002/rcm.7688, 2016.

Stout, S. A., Magar, V. S., Uhler, R. M., Ickes, J., Abbott, J. and Brenner, R.: Characterization of naturally-occurring and anthropogenic PAHs in urban sediments—Wycoff/Eagle Harbor Superfund site, Environ. Forensics, 2(4), 287–300, doi:https://doi.org/10.1006/enfo.2001.0057, 2001.

Stout, S. A., Emsbo-Mattingly, S. D., Douglas, G. S., Uhler, A. D. and McCarthy, K. J.: Beyond 16 Priority Pollutant PAHs: A Review of PACs used in Environmental Forensic Chemistry, Polycycl. Aromat. Compd., 35(2–4), 285–315, doi:10.1080/10406638.2014.891144, 2015.

SWAM: Havs- och vattenmyndighetens föreskrifter om klassificering och miljökvalitetsnormer avseende ytvatten; 2019:25, Swedish Agency for Marine and Water Management, Sweden. [online] Available from: https://www.havochvatten.se/download/18.4705beb516f0bcf57ce1c145/1576576601249/HVMFS 2019-25-ev.pdf, 2019.

Temerdashev, Z. A., Musorina, T. N., Chervonnaya, T. A. and Arutyunyan, Z. V.: Possibilities and Limitations of Solid-Phase and Liquid Extraction for the Determination of Polycyclic Aromatic Hydrocarbons in Environmental Samples, J. Anal. Chem., 76(12), 1357–1370, doi:10.1134/S1061934821120133, 2021.

Terzaghi, E., Falakdin, P., Fattore, E. and Di Guardo, A.: Estimating temporal and spatial levels of PAHs in air using rain samples and SPME analysis: Feasibility evaluation in an urban scenario, Sci. Total Environ., 762, 144184, doi:10.1016/j.scitotenv.2020.144184, 2021.

Teuchies, J., Cox, T. J. S., Van Itterbeeck, K., Meysman, F. J. R. and Blust, R.: The impact of scrubber discharge on the water quality in estuaries and ports, Environ. Sci. Eur., 32(1), doi:10.1186/s12302-020-00380-z, 2020.

Thor, P., Granberg, M. E., Winnes, H. and Magnusson, K.: Severe Toxic Effects on Pelagic Copepods from Maritime Exhaust Gas Scrubber Effluents, Environ. Sci. Technol., 55(9), 5826–5835, doi:10.1021/acs.est.0c07805, 2021.

Tulcan, R. X. S., Ouyang, W., Lin, C., He, M. and Wang, B.: Vanadium pollution and health risks in marine ecosystems: Anthropogenic sources over natural contributions, Water Res., 207, 117838, 2021.

Turner, D. R., Hassellöv, I. M., Ytreberg, E. and Rutgersson, A.: Shipping and the environment: Smokestack emissions, scrubbers and unregulated oceanic consequences, Elem. Sci. Anthr., 5, 1–10, doi:10.1525/elementa.167, 2017.

US EPA: US EPA - Ecotox knowledgebase, US EPA - Ecotox knowledgebase [online] Available from: https://cfpub.epa.gov/ecotox/ (Accessed 29 December 2023), 2023.

Verbruggen, E. M. J.: Environmental risk limits for polycyclic aromatic hydrocarbons (PAHs): For direct aquatic, benthic, and terrestrial toxicity. [online] Available from: https://www.rivm.nl/bibliotheek/rapporten/607711007.pdf, 2012.

Vieira, V. M. N. C. S., Martins, F., Silva, J. and Santos, R.: Numerical tools to estimate the flux of a gas across the air-water interface and assess the heterogeneity of its forcing functions, Ocean Sci., 9(2), 355–375, doi:10.5194/os-9-355-2013, 2013.

Vieira, V. M. N. C. S., Jurus, P., Clementi, E. and Mateus, M.: The fugas 2.3 framework for atmosphere-ocean coupling: Comparing algorithms for the estimation of solubilities and gas fluxes, Atmosphere (Basel)., 9(8), 5–11, doi:10.3390/atmos9080310, 2018.

Volf, G., Atanasova, N., Kompare, B. and Ožanić, N.: Modeling nutrient loads to the northern adriatic, J. Hydrol., 504, 182–193, doi:10.1016/j.jhydrol.2013.09.044, 2013.

Winnes, H., Fridell, E. and Moldanová, J.: Effects of marine exhaust gas scrubbers on gas and

particle emissions, J. Mar. Sci. Eng., 8(4), doi:10.3390/JMSE8040299, 2020.

Wright, R. T., Fay, K., Kennedy, A., Mayo-Bean, K., Meylan, W., Ranslow, P., Lock, M., Nabholz, J. V., von Runnen, J., Cassidy, L. M. and Tunkel, J.: Operation Manual for the ECOlogical Structure-Activity Relationship Model (ECOSAR) Class Program. Estimating toxicity of industrial chemicals to aquatic organisms using the ECOSAR (ECOlogical Structure-Activity Relationship) class program., v2.2., Office of Pollution Prevention and Toxics, U.S. Environmental Protection Agency, Washington DC. [online] Available from: https://www.epa.gov/system/files/documents/2022-03/operation-manual-v.2.2_1.pdf, 2022.

Yang, C., Brown, C. E., Lai, J., Yang, Z., Hollebone, B. and Lambert, P.: Determination of polycyclic aromatic sulfur heterocycles (PASHs) in petroleum and environmental samples using gas chromatography-quadrupole time-of-flight (GC-QTOF) mass spectrometry, in 42nd AMOP Technical Seminar on Environmental Contamination and Response, pp. 26–46, Environment and Climate Change Canada, Halifax, Canada., 2019.

Yang, C., Lambert, P., Nguyen, M., Yang, Z., Hollebone, B. P., Fieldhouse, B. and Brown, C. E.: Application of gas chromatography-high resolution quadrupole time-of-flight mass spectrometry in fingerprinting analysis of polycyclic aromatic sulfur heterocycles, J. Chromatogr. A, 1630, 461577, doi:10.1016/j.chroma.2020.461577, 2020.

Ytreberg, E., Karlberg, M., Hassellöv, I.-M., Hedblom, M., Nylund, A. T., Salo, K., Imberg, H., Turner, D., Tripp, L., Yong, J. and Wulff, A.: Effects of seawater scrubbing on a microplanktonic community during a summer-bloom in the Baltic Sea, Environ. Pollut., 291(April), 118251, doi:10.1016/j.envpol.2021.118251, 2021.

Ytreberg, E., Hansson, K., Hermansson, A. L., Parsmo, R., Lagerström, M., Jalkanen, J. P. and Hassellöv, I. M.: Metal and PAH loads from ships and boats, relative other sources, in the Baltic Sea, Mar. Pollut. Bull., 182(June), doi:10.1016/j.marpolbul.2022.113904, 2022.

Zhao, J., Zhang, Y., Chang, J., Peng, S., Hong, N., Hu, J., Lv, J., Wang, T. and Mao, H.: Emission characteristics and temporal variation of PAHs and their derivatives from an ocean-going cargo vessel, Chemosphere, 249, 126194, doi:10.1016/j.chemosphere.2020.126194, 2020.

Appendix

Table A- 1. The following parameters and methods were deployed in the exhaust emissions investigation.

CO_2, NO_x, NO, SO_2, CO, O_2	measured with Horiba instrument
Total Hydrocarbons	measured with FID instrument
Particle number, size	measured with Condensation Particle Counter (CPC), Scanning Mobility Particle Sizer SMPS
Volatility of PM fractions	conditioning of the samples with thermodenuder and catalytic stripper removing the volatile part of PM, followed by CPC and SMPS
BC	measured with optoacoustic Micro Soot Sensor, MSS
NMVOC	gas chromatography with a flame ionisation detector (GC-FID) and mass selective detector (GC–MS) of samples collected on Tenax TA - Carbopax X adsorbent tubes
Aldehydes	high-performance liquid chromatography with diode-array detection (HPLC-DAD) of samples collected on 2,4-dinitrophenylhydrazine (DNPH) cartridges),
Polyaromatic Compounds, PAHs, alkyl-PAH, nitro-PAH, oxy-PAH	analysed with GC-MS from samples collected on sampler composed of PTFE filter followed by XAD-2 adsorbent tubes
PM mass, metal content	analysed with Gravimetry and Energy Dispersive X-ray Fluorescence (ED-XRF) of PM samples collected on PTFE filters
EC/OC	analysed with thermo-optical analysis of PM samples collected on quartz filters
Micro-physical and micro-chemical properties of particles	analysed with Transfer- and Scanning Electron Microscopy (TEM and SEM) of PM samples collected on Pt-coated carbon filters

Table A- 2. Emission Factors for metals relative to associated STEAM compounds for HFO combustion.

Compound	Related STEAM compound	Rel. EF HFO combustion
Arsenic	Ash	8.09E-05
Cadmium	Ash	6.30E-06
Chromium	Ash	2.10E-04
Copper	Ash	2.52E-04
Iron	Ash	2.52E-02
Mercury	Ash	6.30E-06
Nickel	Ash	4.10E-02
Lead	Ash	1.16E-04
Vanadium	Ash	8.30E-02
Zinc	Ash	2.42E-03

Table A- 3. Emission Factors for PAHs relative to associated SCIPPER compounds. Rows 2-3 present emission factors (in g/kWh) of the STEAM compounds for the studied fuel-aftertreatment combinations.

Compound	Related compound	Volatility class	HFO combustion	HFO+ EGCS	MGO	HFO+ SCR	MGO+ SCR
HC (g/kWh)			0.44	0.29	0.44	0.13	0.09
OC (g/kWh)			0.25	0.13	0.14	0.18	0.06
	Relative Emission Factors (g/g)						
Ace	HC	SV	1.91E-04	2.48E-04	1.34E-05	3.18E-05	3.35E-06
Acy	HC	SV	5.45E-05	7.34E-05	2.73E-05	9.09E-06	6.82E-06
Ant	HC	SV	1.86E-05	2.24E-05	5.00E-06	3.11E-06	1.25E-06
BaA	OC	ELV	3.75E-05	6.05E-05	6.52E-06	2.52E-05	8.15E-06
BaP	OC	ELV	2.46E-05	4.26E-05	7.25E-06	1.65E-05	9.06E-06
BbF	OC	ELV	2.58E-05	4.41E-05	7.25E-06	1.73E-05	9.06E-06
BghiP	OC	ELV	3.06E-05	5.38E-05	9.42E-06	2.06E-05	1.18E-05
BkF	OC	ELV	1.73E-05	2.99E-05	6.52E-06	1.16E-05	8.15E-06
Chr	OC	ELV	2.70E-04	4.78E-04	2.17E-05	1.81E-04	2.72E-05
DahA	OC	ELV	1.98E-05	3.43E-05	4.35E-06	1.33E-05	5.43E-06
Fla	HC	LV	7.27E-05	9.44E-05	4.09E-05	4.85E-05	4.09E-05
Flo	HC	SV	1.39E-04	6.99E-05	2.95E-05	2.31E-05	7.39E-06
InP	OC	ELV	1.73E-05	2.91E-05	1.23E-05	1.16E-05	1.54E-05
Nap	HC	SV	9.77E-03	1.43E-02	7.73E-04	1.63E-03	1.93E-04
Phe	HC	SV	6.82E-04	6.29E-04	1.14E-04	1.14E-04	2.84E-05
Pyr	HC	LV	7.73E-05	9.79E-05	3.18E-05	5.15E-05	3.18E-05

Table A- 4. Data of emissions for all scenarios for 2030 and 2050 split on ship type and sea area.

Scenario	year	Ship_Type_DNVGL	Ocean_zone	EGCS effluent (L)	CO_2 (kg)	SO_X (kg)	NO_X (kg)	$PM_{2.5}$ (kg)	NH_3 (kg)
1	2030	Bulk	Atlantic Ocean	6.3E+11	6.5E+09	1.6E+07	1.1E+08	8.2E+06	0.0E+00
1	2030	Other-cargo	Atlantic Ocean	7.8E+11	8.4E+09	2.0E+07	1.5E+08	1.0E+07	0.0E+00
1	2030	Container	Atlantic Ocean	1.5E+12	1.4E+10	3.7E+07	2.6E+08	1.9E+07	0.0E+00
1	2030	Non-cargo	Atlantic Ocean	4.1E+11	4.2E+09	1.0E+07	6.3E+07	5.3E+06	0.0E+00
1	2030	Tank	Atlantic Ocean	3.2E+11	3.3E+09	8.1E+06	6.1E+07	4.2E+06	0.0E+00
1	2030	Gas	Atlantic Ocean	1.4E+11	2.2E+09	3.4E+06	2.5E+07	1.9E+06	0.0E+00
1	2030	Bulk	Black Sea	1.1E+11	1.4E+09	2.9E+06	2.8E+07	1.5E+06	0.0E+00
1	2030	Other-cargo	Black Sea	1.1E+11	1.5E+09	2.9E+06	2.4E+07	1.5E+06	0.0E+00
1	2030	Container	Black Sea	5.1E+10	5.6E+08	1.3E+06	1.1E+07	6.8E+05	0.0E+00
1	2030	Non-cargo	Black Sea	1.5E+10	1.7E+08	3.8E+05	2.3E+06	2.0E+05	0.0E+00
1	2030	Tank	Black Sea	5.7E+10	7.8E+08	1.5E+06	1.4E+07	8.1E+05	0.0E+00
1	2030	Gas	Black Sea	6.8E+09	8.1E+07	1.8E+05	1.5E+06	9.3E+04	0.0E+00
1	2030	Bulk	Mediterranean Sea	9.6E+11	1.1E+10	2.5E+07	2.2E+08	1.3E+07	0.0E+00
1	2030	Other-cargo	Mediterranean Sea	1.2E+12	1.4E+10	3.1E+07	2.3E+08	1.6E+07	0.0E+00
1	2030	Container	Mediterranean Sea	2.9E+12	2.9E+10	7.3E+07	5.6E+08	3.8E+07	0.0E+00

1	2030	Non-cargo	Mediterranean Sea	1.5E+12	1.5E+10	3.7E+07	2.2E+08	1.9E+07	0.0E+00
1	2030	Tank	Mediterranean Sea	5.2E+11	6.3E+09	1.4E+07	1.2E+08	7.1E+06	0.0E+00
1	2030	Gas	Mediterranean Sea	2.3E+11	3.2E+09	6.0E+06	4.7E+07	3.2E+06	0.0E+00
1	2030	Bulk	Baltic Sea	1.3E+10	1.6E+09	8.5E+05	2.4E+07	6.1E+05	6.2E+04
1	2030	Other-cargo	Baltic Sea	1.5E+11	4.4E+09	2.3E+06	5.3E+07	2.6E+06	1.8E+05
1	2030	Container	Baltic Sea	6.1E+10	2.5E+09	1.3E+06	3.0E+07	1.3E+06	1.4E+05
1	2030	Non-cargo	Baltic Sea	3.0E+11	6.0E+09	3.2E+06	7.7E+07	4.3E+06	1.9E+05
1	2030	Tank	Baltic Sea	9.7E+09	1.3E+09	7.0E+05	1.8E+07	4.9E+05	6.0E+04
1	2030	Gas	Baltic Sea	2.2E+09	2.3E+08	1.2E+05	3.2E+06	8.9E+04	1.0E+04
1	2030	Bulk	North Sea	9.0E+10	4.8E+09	2.6E+06	8.4E+07	2.3E+06	1.2E+05
1	2030	Other-cargo	North Sea	1.6E+11	9.4E+09	5.0E+06	1.4E+08	4.3E+06	2.6E+05
1	2030	Container	North Sea	5.6E+11	1.5E+10	8.2E+06	2.7E+08	9.4E+06	3.0E+05
1	2030	Non-cargo	North Sea	2.1E+11	4.6E+09	2.3E+06	6.0E+07	3.1E+06	1.3E+05
1	2030	Tank	North Sea	4.5E+10	3.6E+09	2.0E+06	5.8E+07	1.5E+06	1.2E+05
1	2030	Gas	North Sea	1.4E+10	1.4E+09	5.4E+05	1.8E+07	4.7E+05	5.0E+04
1	2050	Bulk	Atlantic Ocean	9.2E+11	1.0E+10	2.5E+07	1.7E+08	1.3E+07	0.0E+00
1	2050	Other-cargo	Atlantic Ocean	7.9E+11	1.2E+10	3.1E+07	1.9E+08	1.6E+07	0.0E+00

1	2050	Container	Atlantic Ocean	2.3E+12	2.2E+10	5.9E+07	3.7E+08	3.0E+07	0.0E+00
1	2050	Non-cargo	Atlantic Ocean	5.0E+11	5.4E+09	1.4E+07	6.7E+07	7.2E+06	0.0E+00
1	2050	Tank	Atlantic Ocean	1.4E+11	1.7E+09	4.2E+06	2.7E+07	2.2E+06	0.0E+00
1	2050	Gas	Atlantic Ocean	1.7E+11	2.7E+09	4.6E+06	3.0E+07	2.5E+06	0.0E+00
1	2050	Bulk	Black Sea	1.5E+11	1.7E+09	4.1E+06	2.9E+07	2.1E+06	0.0E+00
1	2050	Other-cargo	Black Sea	6.9E+10	1.9E+09	4.4E+06	2.6E+07	2.3E+06	0.0E+00
1	2050	Container	Black Sea	8.6E+10	9.3E+08	2.3E+06	1.5E+07	1.2E+06	0.0E+00
1	2050	Non-cargo	Black Sea	2.0E+10	2.4E+08	6.1E+05	3.0E+06	3.1E+05	0.0E+00
1	2050	Tank	Black Sea	2.4E+10	3.4E+08	7.5E+05	5.5E+06	3.9E+05	0.0E+00
1	2050	Gas	Black Sea	7.6E+09	9.8E+07	2.4E+05	1.6E+06	1.3E+05	0.0E+00
1	2050	Bulk	Mediterranean Sea	1.3E+12	1.4E+10	3.5E+07	2.4E+08	1.8E+07	0.0E+00
1	2050	Other-cargo	Mediterranean Sea	1.3E+12	1.9E+10	4.6E+07	2.8E+08	2.4E+07	0.0E+00
1	2050	Container	Mediterranean Sea	4.1E+12	4.1E+10	1.1E+08	6.9E+08	5.6E+07	0.0E+00
1	2050	Non-cargo	Mediterranean Sea	1.8E+12	1.9E+10	5.0E+07	2.3E+08	2.6E+07	0.0E+00
1	2050	Tank	Mediterranean Sea	2.2E+11	2.8E+09	6.7E+06	4.7E+07	3.5E+06	0.0E+00
1	2050	Gas	Mediterranean Sea	3.0E+11	4.1E+09	8.4E+06	5.5E+07	4.4E+06	0.0E+00

1	2050	Bulk	Baltic Sea	1.7E+10	2.1E+09	1.1E+06	6.3E+06	8.0E+05	2.8E+05
1	2050	Other-cargo	Baltic Sea	1.9E+11	6.4E+09	3.3E+06	1.3E+07	3.6E+06	8.2E+05
1	2050	Container	Baltic Sea	8.7E+10	3.8E+09	2.1E+06	1.0E+07	1.9E+06	5.1E+05
1	2050	Non-cargo	Baltic Sea	3.3E+11	7.6E+09	4.1E+06	1.4E+07	5.1E+06	9.9E+05
1	2050	Tank	Baltic Sea	4.7E+09	6.0E+08	3.2E+05	1.6E+06	2.3E+05	8.0E+04
1	2050	Gas	Baltic Sea	2.2E+09	2.9E+08	1.5E+05	8.3E+05	1.1E+05	3.7E+04
1	2050	Bulk	North Sea	1.1E+11	5.5E+09	3.0E+06	1.7E+07	2.7E+06	7.4E+05
1	2050	Other-cargo	North Sea	1.9E+11	1.2E+10	6.6E+06	2.9E+07	5.4E+06	1.6E+06
1	2050	Container	North Sea	7.2E+11	1.8E+10	1.0E+07	5.4E+07	1.2E+07	2.5E+06
1	2050	Non-cargo	North Sea	2.4E+11	5.8E+09	2.9E+06	1.1E+07	3.7E+06	7.1E+05
1	2050	Tank	North Sea	1.9E+10	1.4E+09	7.4E+05	3.9E+06	5.9E+05	1.8E+05
1	2050	Gas	North Sea	1.4E+10	1.6E+09	6.0E+05	4.0E+06	5.2E+05	1.5E+05
2	2030	Bulk	Atlantic Ocean	3.6E+09	6.5E+09	1.6E+07	1.1E+08	8.2E+06	0.0E+00
2	2030	Other-cargo	Atlantic Ocean	4.5E+09	8.4E+09	2.0E+07	1.5E+08	1.0E+07	0.0E+00
2	2030	Container	Atlantic Ocean	8.6E+09	1.4E+10	3.7E+07	2.6E+08	1.9E+07	0.0E+00
2	2030	Non-cargo	Atlantic Ocean	2.4E+09	4.2E+09	1.0E+07	6.3E+07	5.3E+06	0.0E+00
2	2030	Tank	Atlantic Ocean	1.9E+09	3.3E+09	8.1E+06	6.1E+07	4.2E+06	0.0E+00
2	2030	Gas	Atlantic Ocean	7.9E+08	2.2E+09	3.4E+06	2.5E+07	1.9E+06	0.0E+00

2	2030	Bulk	Black Sea	6.5E+08	1.4E+09	2.9E+06	2.8E+07	1.5E+06	0.0E+00
2	2030	Other-cargo	Black Sea	6.2E+08	1.5E+09	2.9E+06	2.4E+07	1.5E+06	0.0E+00
2	2030	Container	Black Sea	3.0E+08	5.6E+08	1.3E+06	1.1E+07	6.8E+05	0.0E+00
2	2030	Non-cargo	Black Sea	8.5E+07	1.7E+08	3.8E+05	2.3E+06	2.0E+05	0.0E+00
2	2030	Tank	Black Sea	3.3E+08	7.8E+08	1.5E+06	1.4E+07	8.1E+05	0.0E+00
2	2030	Gas	Black Sea	4.0E+07	8.1E+07	1.8E+05	1.5E+06	9.3E+04	0.0E+00
2	2030	Bulk	Mediterranean Sea	5.6E+09	1.1E+10	2.5E+07	2.2E+08	1.3E+07	0.0E+00
2	2030	Other-cargo	Mediterranean Sea	6.9E+09	1.4E+10	3.1E+07	2.3E+08	1.6E+07	0.0E+00
2	2030	Container	Mediterranean Sea	1.7E+10	2.9E+10	7.3E+07	5.6E+08	3.8E+07	0.0E+00
2	2030	Non-cargo	Mediterranean Sea	8.7E+09	1.5E+10	3.7E+07	2.2E+08	1.9E+07	0.0E+00
2	2030	Tank	Mediterranean Sea	3.0E+09	6.3E+09	1.4E+07	1.2E+08	7.1E+06	0.0E+00
2	2030	Gas	Mediterranean Sea	1.4E+09	3.2E+09	6.0E+06	4.7E+07	3.2E+06	0.0E+00
2	2030	Bulk	Baltic Sea	6.5E+07	1.6E+09	8.5E+05	2.4E+07	6.1E+05	6.2E+04
2	2030	Other-cargo	Baltic Sea	7.4E+08	4.4E+09	2.3E+06	5.3E+07	2.6E+06	1.8E+05
2	2030	Container	Baltic Sea	3.0E+08	2.5E+09	1.3E+06	3.0E+07	1.3E+06	1.4E+05
2	2030	Non-cargo	Baltic Sea	1.4E+09	6.0E+09	3.2E+06	7.7E+07	4.3E+06	1.9E+05

2	2030	Tank	Baltic Sea	4.8E+07	1.3E+09	7.0E+05	1.8E+07	4.9E+05	6.0E+04
2	2030	Gas	Baltic Sea	1.1E+07	2.3E+08	1.2E+05	3.2E+06	8.9E+04	1.0E+04
2	2030	Bulk	North Sea	4.4E+08	4.8E+09	2.6E+06	8.4E+07	2.3E+06	1.2E+05
2	2030	Other-cargo	North Sea	7.9E+08	9.4E+09	5.0E+06	1.4E+08	4.3E+06	2.6E+05
2	2030	Container	North Sea	2.7E+09	1.5E+10	8.2E+06	2.7E+08	9.4E+06	3.0E+05
2	2030	Non-cargo	North Sea	1.0E+09	4.6E+09	2.3E+06	6.0E+07	3.1E+06	1.3E+05
2	2030	Tank	North Sea	2.2E+08	3.6E+09	2.0E+06	5.8E+07	1.5E+06	1.2E+05
2	2030	Gas	North Sea	6.8E+07	1.4E+09	5.4E+05	1.8E+07	4.7E+05	5.0E+04
2	2050	Bulk	Atlantic Ocean	5.4E+09	1.0E+10	2.5E+07	1.7E+08	1.3E+07	0.0E+00
2	2050	Other-cargo	Atlantic Ocean	4.6E+09	1.2E+10	3.1E+07	1.9E+08	1.6E+07	0.0E+00
2	2050	Container	Atlantic Ocean	1.3E+10	2.2E+10	5.9E+07	3.7E+08	3.0E+07	0.0E+00
2	2050	Non-cargo	Atlantic Ocean	2.9E+09	5.4E+09	1.4E+07	6.7E+07	7.2E+06	0.0E+00
2	2050	Tank	Atlantic Ocean	8.0E+08	1.7E+09	4.2E+06	2.7E+07	2.2E+06	0.0E+00
2	2050	Gas	Atlantic Ocean	9.7E+08	2.7E+09	4.6E+06	3.0E+07	2.5E+06	0.0E+00
2	2050	Bulk	Black Sea	8.6E+08	1.7E+09	4.1E+06	2.9E+07	2.1E+06	0.0E+00
2	2050	Other-cargo	Black Sea	4.0E+08	1.9E+09	4.4E+06	2.6E+07	2.3E+06	0.0E+00
2	2050	Container	Black Sea	5.0E+08	9.3E+08	2.3E+06	1.5E+07	1.2E+06	0.0E+00
2	2050	Non-cargo	Black Sea	1.2E+08	2.4E+08	6.1E+05	3.0E+06	3.1E+05	0.0E+00

2	2050	Tank	Black Sea	1.4E+08	3.4E+08	7.5E+05	5.5E+06	3.9E+05	0.0E+00
2	2050	Gas	Black Sea	4.4E+07	9.8E+07	2.4E+05	1.6E+06	1.3E+05	0.0E+00
2	2050	Bulk	Mediterranean Sea	7.3E+09	1.4E+10	3.5E+07	2.4E+08	1.8E+07	0.0E+00
2	2050	Other-cargo	Mediterranean Sea	7.3E+09	1.9E+10	4.6E+07	2.8E+08	2.4E+07	0.0E+00
2	2050	Container	Mediterranean Sea	2.4E+10	4.1E+10	1.1E+08	6.9E+08	5.6E+07	0.0E+00
2	2050	Non-cargo	Mediterranean Sea	1.0E+10	1.9E+10	5.0E+07	2.3E+08	2.6E+07	0.0E+00
2	2050	Tank	Mediterranean Sea	1.3E+09	2.8E+09	6.7E+06	4.7E+07	3.5E+06	0.0E+00
2	2050	Gas	Mediterranean Sea	1.7E+09	4.1E+09	8.4E+06	5.5E+07	4.4E+06	0.0E+00
2	2050	Bulk	Baltic Sea	8.4E+07	2.1E+09	1.1E+06	6.3E+06	8.0E+05	2.8E+05
2	2050	Other-cargo	Baltic Sea	9.5E+08	6.4E+09	3.3E+06	1.3E+07	3.6E+06	8.2E+05
2	2050	Container	Baltic Sea	4.2E+08	3.8E+09	2.1E+06	1.0E+07	1.9E+06	5.1E+05
2	2050	Non-cargo	Baltic Sea	1.6E+09	7.6E+09	4.1E+06	1.4E+07	5.1E+06	9.9E+05
2	2050	Tank	Baltic Sea	2.3E+07	6.0E+08	3.2E+05	1.6E+06	2.3E+05	8.0E+04
2	2050	Gas	Baltic Sea	1.1E+07	2.9E+08	1.5E+05	8.3E+05	1.1E+05	3.7E+04
2	2050	Bulk	North Sea	5.6E+08	5.5E+09	3.0E+06	1.7E+07	2.7E+06	7.4E+05
2	2050	Other-cargo	North Sea	9.5E+08	1.2E+10	6.6E+06	2.9E+07	5.4E+06	1.6E+06

2	2050	Container	North Sea	3.5E+09	1.8E+10	1.0E+07	5.4E+07	1.2E+07	2.5E+06
2	2050	Non-cargo	North Sea	1.2E+09	5.8E+09	2.9E+06	1.1E+07	3.7E+06	7.1E+05
2	2050	Tank	North Sea	9.3E+07	1.4E+09	7.4E+05	3.9E+06	5.9E+05	1.8E+05
2	2050	Gas	North Sea	6.9E+07	1.6E+09	6.0E+05	4.0E+06	5.2E+05	1.5E+05
3	2030	Bulk	Atlantic Ocean	7.5E+11	6.5E+09	3.6E+06	5.6E+07	8.2E+06	5.5E+05
3	2030	Other-cargo	Atlantic Ocean	9.3E+11	8.4E+09	4.6E+06	1.2E+08	1.0E+07	3.2E+05
3	2030	Container	Atlantic Ocean	1.8E+12	1.4E+10	7.7E+06	1.9E+08	1.9E+07	6.7E+05
3	2030	Non-cargo	Atlantic Ocean	4.8E+11	4.2E+09	2.3E+06	5.3E+07	5.3E+06	1.2E+05
3	2030	Tank	Atlantic Ocean	3.8E+11	3.3E+09	1.9E+06	4.2E+07	4.2E+06	1.8E+05
3	2030	Gas	Atlantic Ocean	1.6E+11	2.2E+09	7.4E+05	2.8E+07	1.9E+06	7.4E+04
3	2030	Bulk	Baltic Sea	1.3E+10	1.6E+09	8.5E+05	2.4E+07	6.1E+05	6.2E+04
3	2030	Other-cargo	Baltic Sea	1.5E+11	4.4E+09	2.3E+06	5.3E+07	2.6E+06	1.8E+05
3	2030	Container	Baltic Sea	6.1E+10	2.5E+09	1.3E+06	3.0E+07	1.3E+06	1.4E+05
3	2030	Non-cargo	Baltic Sea	3.0E+11	6.0E+09	3.2E+06	7.7E+07	4.3E+06	1.9E+05
3	2030	Tank	Baltic Sea	9.7E+09	1.3E+09	7.0E+05	1.8E+07	4.9E+05	6.0E+04
3	2030	Gas	Baltic Sea	2.2E+09	2.3E+08	1.2E+05	3.2E+06	8.9E+04	1.0E+04
3	2030	Bulk	Black Sea	1.3E+11	1.4E+09	7.5E+05	2.3E+07	1.5E+06	4.6E+04
3	2030	Other-cargo	Black Sea	1.3E+11	1.5E+09	8.2E+05	1.9E+07	1.5E+06	6.1E+04

3	2030	Container	Black Sea	6.0E+10	5.6E+08	3.1E+05	6.5E+06	6.8E+05	4.1E+04
3	2030	Non-cargo	Black Sea	1.7E+10	1.7E+08	9.6E+04	7.9E+05	2.0E+05	1.9E+04
3	2030	Tank	Black Sea	6.8E+10	7.8E+08	4.3E+05	1.1E+07	8.1E+05	3.3E+04
3	2030	Gas	Black Sea	8.1E+09	8.1E+07	4.5E+04	1.2E+06	9.3E+04	3.3E+03
3	2030	Bulk	Mediterranean Sea	1.1E+12	1.1E+10	6.0E+06	1.8E+08	1.3E+07	3.2E+05
3	2030	Other-cargo	Mediterranean Sea	1.4E+12	1.4E+10	7.5E+06	1.8E+08	1.6E+07	5.3E+05
3	2030	Container	Mediterranean Sea	3.5E+12	2.9E+10	1.6E+07	4.6E+08	3.8E+07	9.8E+05
3	2030	Non-cargo	Mediterranean Sea	1.8E+12	1.5E+10	8.3E+06	1.9E+08	1.9E+07	4.4E+05
3	2030	Tank	Mediterranean Sea	6.2E+11	6.3E+09	3.5E+06	8.8E+07	7.1E+06	2.9E+05
3	2030	Gas	Mediterranean Sea	2.8E+11	3.2E+09	1.4E+06	4.0E+07	3.2E+06	1.6E+05
3	2030	Bulk	North Sea	9.0E+10	4.8E+09	2.6E+06	8.4E+07	2.3E+06	1.2E+05
3	2030	Other-cargo	North Sea	1.6E+11	9.4E+09	5.0E+06	1.4E+08	4.3E+06	2.6E+05
3	2030	Container	North Sea	5.6E+11	1.5E+10	8.2E+06	2.7E+08	9.4E+06	3.0E+05
3	2030	Non-cargo	North Sea	2.1E+11	4.6E+09	2.3E+06	6.0E+07	3.1E+06	1.3E+05
3	2030	Tank	North Sea	4.5E+10	3.6E+09	2.0E+06	5.8E+07	1.5E+06	1.2E+05
3	2030	Gas	North Sea	1.4E+10	1.4E+09	5.4E+05	1.8E+07	4.7E+05	5.0E+04

3	2050	Bulk	Atlantic Ocean	1.1E+12	1.0E+10	5.6E+06	3.0E+07	1.3E+07	1.3E+06
3	2050	Other-cargo	Atlantic Ocean	9.4E+11	1.2E+10	6.9E+06	3.1E+07	1.6E+07	1.6E+06
3	2050	Container	Atlantic Ocean	2.7E+12	2.2E+10	1.2E+07	6.4E+07	3.0E+07	2.9E+06
3	2050	Non-cargo	Atlantic Ocean	5.9E+11	5.4E+09	3.0E+06	1.0E+07	7.2E+06	7.1E+05
3	2050	Tank	Atlantic Ocean	1.6E+11	1.7E+09	9.2E+05	4.7E+06	2.2E+06	2.2E+05
3	2050	Gas	Atlantic Ocean	2.0E+11	2.7E+09	9.8E+05	6.9E+06	2.5E+06	2.3E+05
3	2050	Bulk	Baltic Sea	1.7E+10	2.1E+09	1.1E+06	6.3E+06	8.0E+05	2.8E+05
3	2050	Other-cargo	Baltic Sea	1.9E+11	6.4E+09	3.3E+06	1.3E+07	3.6E+06	8.2E+05
3	2050	Container	Baltic Sea	8.7E+10	3.8E+09	2.1E+06	1.0E+07	1.9E+06	5.1E+05
3	2050	Non-cargo	Baltic Sea	3.3E+11	7.6E+09	4.1E+06	1.4E+07	5.1E+06	9.9E+05
3	2050	Tank	Baltic Sea	4.7E+09	6.0E+08	3.2E+05	1.6E+06	2.3E+05	8.0E+04
3	2050	Gas	Baltic Sea	2.2E+09	2.9E+08	1.5E+05	8.3E+05	1.1E+05	3.7E+04
3	2050	Bulk	Black Sea	1.8E+11	1.7E+09	9.6E+05	5.1E+06	2.1E+06	2.3E+05
3	2050	Other-cargo	Black Sea	8.2E+10	1.9E+09	1.1E+06	3.9E+06	2.3E+06	2.6E+05
3	2050	Container	Black Sea	1.0E+11	9.3E+08	5.2E+05	2.7E+06	1.2E+06	1.2E+05
3	2050	Non-cargo	Black Sea	2.4E+10	2.4E+08	1.3E+05	4.3E+05	3.1E+05	3.2E+04
3	2050	Tank	Black Sea	2.9E+10	3.4E+08	1.8E+05	9.4E+05	3.9E+05	4.4E+04
3	2050	Gas	Black Sea	9.0E+09	9.8E+07	5.4E+04	2.8E+05	1.3E+05	1.3E+04

3	2050	Bulk	Mediterranean Sea	1.5E+12	1.4E+10	7.9E+06	4.3E+07	1.8E+07	1.9E+06
3	2050	Other-cargo	Mediterranean Sea	1.5E+12	1.9E+10	1.1E+07	4.5E+07	2.4E+07	2.5E+06
3	2050	Container	Mediterranean Sea	4.9E+12	4.1E+10	2.3E+07	1.2E+08	5.6E+07	5.4E+06
3	2050	Non-cargo	Mediterranean Sea	2.1E+12	1.9E+10	1.0E+07	3.4E+07	2.6E+07	2.5E+06
3	2050	Tank	Mediterranean Sea	2.6E+11	2.8E+09	1.6E+06	8.2E+06	3.5E+06	3.7E+05
3	2050	Gas	Mediterranean Sea	3.5E+11	4.1E+09	1.9E+06	1.1E+07	4.4E+06	4.5E+05
3	2050	Bulk	North Sea	1.1E+11	5.5E+09	3.0E+06	1.7E+07	2.7E+06	7.4E+05
3	2050	Other-cargo	North Sea	1.9E+11	1.2E+10	6.6E+06	2.9E+07	5.4E+06	1.6E+06
3	2050	Container	North Sea	7.2E+11	1.8E+10	1.0E+07	5.4E+07	1.2E+07	2.5E+06
3	2050	Non-cargo	North Sea	2.4E+11	5.8E+09	2.9E+06	1.1E+07	3.7E+06	7.1E+05
3	2050	Tank	North Sea	1.9E+10	1.4E+09	7.4E+05	3.9E+06	5.9E+05	1.8E+05
3	2050	Gas	North Sea	1.4E+10	1.6E+09	6.0E+05	4.0E+06	5.2E+05	1.5E+05
4	2030	Bulk	Atlantic Ocean	4.7E+11	4.8E+09	1.2E+07	8.5E+07	6.2E+06	0.0E+00
4	2030	Other-cargo	Atlantic Ocean	5.6E+11	6.0E+09	1.4E+07	1.1E+08	7.4E+06	0.0E+00
4	2030	Container	Atlantic Ocean	1.1E+12	1.0E+10	2.7E+07	1.9E+08	1.4E+07	0.0E+00
4	2030	Non-cargo	Atlantic Ocean	3.6E+11	3.8E+09	9.2E+06	5.6E+07	4.8E+06	0.0E+00

4	2030	Tank	Atlantic Ocean	4.6E+11	4.9E+09	1.2E+07	8.9E+07	6.1E+06	0.0E+00
4	2030	Gas	Atlantic Ocean	2.1E+11	3.3E+09	5.3E+06	3.9E+07	2.9E+06	0.0E+00
4	2030	Bulk	Black Sea	8.7E+10	1.1E+09	2.3E+06	2.2E+07	1.2E+06	0.0E+00
4	2030	Other-cargo	Black Sea	7.6E+10	1.1E+09	2.1E+06	1.7E+07	1.1E+06	0.0E+00
4	2030	Container	Black Sea	3.8E+10	4.2E+08	9.7E+05	7.9E+06	5.0E+05	0.0E+00
4	2030	Non-cargo	Black Sea	1.3E+10	1.5E+08	3.4E+05	2.0E+06	1.8E+05	0.0E+00
4	2030	Tank	Black Sea	8.3E+10	1.1E+09	2.2E+06	2.1E+07	1.2E+06	0.0E+00
4	2030	Gas	Black Sea	1.1E+10	1.3E+08	2.8E+05	2.4E+06	1.5E+05	0.0E+00
4	2030	Bulk	Mediterranean Sea	7.5E+11	8.5E+09	1.9E+07	1.7E+08	1.0E+07	0.0E+00
4	2030	Other-cargo	Mediterranean Sea	8.4E+11	9.6E+09	2.2E+07	1.7E+08	1.1E+07	0.0E+00
4	2030	Container	Mediterranean Sea	2.2E+12	2.2E+10	5.4E+07	4.2E+08	2.8E+07	0.0E+00
4	2030	Non-cargo	Mediterranean Sea	1.3E+12	1.3E+10	3.3E+07	2.0E+08	1.7E+07	0.0E+00
4	2030	Tank	Mediterranean Sea	7.5E+11	9.1E+09	2.0E+07	1.7E+08	1.0E+07	0.0E+00
4	2030	Gas	Mediterranean Sea	3.6E+11	5.0E+09	9.4E+06	7.4E+07	5.0E+06	0.0E+00
4	2030	Bulk	Baltic Sea	1.0E+10	1.2E+09	6.4E+05	1.8E+07	4.5E+05	4.4E+04
4	2030	Other-cargo	Baltic Sea	1.1E+11	3.1E+09	1.6E+06	3.8E+07	1.9E+06	1.3E+05

4	2030	Container	Baltic Sea	4.5E+10	1.8E+09	9.8E+05	2.3E+07	9.5E+05	1.1E+05
4	2030	Non-cargo	Baltic Sea	2.6E+11	5.3E+09	2.9E+06	6.8E+07	3.9E+06	1.7E+05
4	2030	Tank	Baltic Sea	1.4E+10	1.9E+09	1.0E+06	2.6E+07	7.1E+05	8.7E+04
4	2030	Gas	Baltic Sea	3.4E+09	3.6E+08	1.9E+05	5.0E+06	1.4E+05	1.6E+04
4	2030	Bulk	North Sea	6.9E+10	3.7E+09	2.0E+06	6.4E+07	1.7E+06	9.5E+04
4	2030	Other-cargo	North Sea	1.2E+11	6.7E+09	3.6E+06	1.0E+08	3.1E+06	1.9E+05
4	2030	Container	North Sea	4.1E+11	1.1E+10	6.1E+06	2.0E+08	7.0E+06	2.2E+05
4	2030	Non-cargo	North Sea	1.8E+11	4.1E+09	2.1E+06	5.3E+07	2.8E+06	1.2E+05
4	2030	Tank	North Sea	6.5E+10	5.2E+09	2.8E+06	8.2E+07	2.2E+06	1.8E+05
4	2030	Gas	North Sea	2.2E+10	2.2E+09	8.4E+05	2.9E+07	7.4E+05	8.0E+04
4	2050	Bulk	Atlantic Ocean	2.9E+11	3.5E+09	8.2E+06	5.6E+07	4.2E+06	0.0E+00
4	2050	Other-cargo	Atlantic Ocean	1.6E+11	4.2E+09	5.9E+06	4.4E+07	3.2E+06	0.0E+00
4	2050	Container	Atlantic Ocean	7.2E+11	8.2E+09	1.9E+07	1.2E+08	9.8E+06	0.0E+00
4	2050	Non-cargo	Atlantic Ocean	1.6E+11	3.5E+09	4.3E+06	2.7E+07	2.4E+06	0.0E+00
4	2050	Tank	Atlantic Ocean	1.7E+11	2.6E+09	5.2E+06	3.6E+07	2.7E+06	0.0E+00
4	2050	Gas	Atlantic Ocean	2.3E+11	4.5E+09	6.3E+06	4.3E+07	3.5E+06	0.0E+00
4	2050	Bulk	Black Sea	4.7E+10	5.9E+08	1.3E+06	9.5E+06	6.9E+05	0.0E+00
4	2050	Other-cargo	Black Sea	9.8E+09	6.5E+08	7.1E+05	5.6E+06	4.0E+05	0.0E+00

4	2050	Container	Black Sea	2.7E+10	3.5E+08	7.3E+05	5.1E+06	3.8E+05	0.0E+00
4	2050	Non-cargo	Black Sea	9.0E+08	1.4E+08	3.6E+04	5.9E+05	3.2E+04	0.0E+00
4	2050	Tank	Black Sea	3.0E+10	5.3E+08	9.4E+05	7.4E+06	5.0E+05	0.0E+00
4	2050	Gas	Black Sea	7.9E+09	1.6E+08	2.6E+05	1.9E+06	1.4E+05	0.0E+00
4	2050	Bulk	Mediterranean Sea	4.0E+11	4.9E+09	1.1E+07	7.9E+07	5.8E+06	0.0E+00
4	2050	Other-cargo	Mediterranean Sea	1.8E+11	6.2E+09	7.0E+06	5.7E+07	4.0E+06	0.0E+00
4	2050	Container	Mediterranean Sea	1.3E+12	1.5E+10	3.5E+07	2.3E+08	1.8E+07	0.0E+00
4	2050	Non-cargo	Mediterranean Sea	3.7E+11	1.2E+10	9.8E+06	6.6E+07	5.9E+06	0.0E+00
4	2050	Tank	Mediterranean Sea	2.8E+11	4.4E+09	8.4E+06	6.3E+07	4.5E+06	0.0E+00
4	2050	Gas	Mediterranean Sea	4.1E+11	6.8E+09	1.1E+07	7.9E+07	6.1E+06	0.0E+00
4	2050	Bulk	Baltic Sea	5.5E+09	7.2E+08	3.8E+05	2.2E+06	2.7E+05	9.5E+04
4	2050	Other-cargo	Baltic Sea	1.4E+10	2.2E+09	9.2E+05	4.6E+06	7.1E+05	2.3E+05
4	2050	Container	Baltic Sea	2.8E+10	1.5E+09	7.7E+05	3.9E+06	6.8E+05	1.9E+05
4	2050	Non-cargo	Baltic Sea	6.9E+10	5.1E+09	2.1E+06	1.0E+07	1.9E+06	5.1E+05
4	2050	Tank	Baltic Sea	6.4E+09	9.7E+08	5.1E+05	2.6E+06	3.5E+05	1.3E+05
4	2050	Gas	Baltic Sea	2.2E+09	4.9E+08	2.5E+05	1.4E+06	1.7E+05	6.1E+04

4	2050	Bulk	North Sea	3.7E+10	1.9E+09	1.0E+06	5.7E+06	9.0E+05	2.5E+05
4	2050	Other-cargo	North Sea	2.0E+10	4.3E+09	2.1E+06	1.0E+07	1.4E+06	5.2E+05
4	2050	Container	North Sea	2.3E+11	7.0E+09	3.6E+06	2.1E+07	4.0E+06	8.9E+05
4	2050	Non-cargo	North Sea	8.7E+10	3.9E+09	1.6E+06	7.5E+06	1.8E+06	4.0E+05
4	2050	Tank	North Sea	2.5E+10	2.2E+09	1.2E+06	6.3E+06	9.0E+05	2.9E+05
4	2050	Gas	North Sea	1.5E+10	2.7E+09	1.0E+06	7.0E+06	8.0E+05	2.5E+05
5	2030	Bulk	Atlantic Ocean	4.7E+11	4.8E+09	1.2E+07	8.5E+07	6.2E+06	0.0E+00
5	2030	Other-cargo	Atlantic Ocean	5.6E+11	6.0E+09	1.4E+07	1.1E+08	7.4E+06	0.0E+00
5	2030	Container	Atlantic Ocean	1.1E+12	1.0E+10	2.7E+07	1.9E+08	1.4E+07	0.0E+00
5	2030	Non-cargo	Atlantic Ocean	3.6E+11	3.8E+09	9.2E+06	5.6E+07	4.8E+06	0.0E+00
5	2030	Tank	Atlantic Ocean	4.6E+11	4.9E+09	1.2E+07	8.9E+07	6.1E+06	0.0E+00
5	2030	Gas	Atlantic Ocean	2.1E+11	3.3E+09	5.3E+06	3.9E+07	2.9E+06	0.0E+00
5	2030	Bulk	Black Sea	8.7E+10	1.1E+09	2.3E+06	2.2E+07	1.2E+06	0.0E+00
5	2030	Other-cargo	Black Sea	7.6E+10	1.1E+09	2.1E+06	1.7E+07	1.1E+06	0.0E+00
5	2030	Container	Black Sea	3.8E+10	4.2E+08	9.7E+05	7.9E+06	5.0E+05	0.0E+00
5	2030	Non-cargo	Black Sea	1.3E+10	1.5E+08	3.4E+05	2.0E+06	1.8E+05	0.0E+00
5	2030	Tank	Black Sea	8.3E+10	1.1E+09	2.2E+06	2.1E+07	1.2E+06	0.0E+00
5	2030	Gas	Black Sea	1.1E+10	1.3E+08	2.8E+05	2.4E+06	1.5E+05	0.0E+00

5	2030	Bulk	Mediterranean Sea	7.5E+11	8.5E+09	1.9E+07	1.7E+08	1.0E+07	0.0E+00
5	2030	Other-cargo	Mediterranean Sea	8.4E+11	9.6E+09	2.2E+07	1.7E+08	1.1E+07	0.0E+00
5	2030	Container	Mediterranean Sea	2.2E+12	2.2E+10	5.4E+07	4.2E+08	2.8E+07	0.0E+00
5	2030	Non-cargo	Mediterranean Sea	1.3E+12	1.3E+10	3.3E+07	2.0E+08	1.7E+07	0.0E+00
5	2030	Tank	Mediterranean Sea	7.5E+11	9.1E+09	2.0E+07	1.7E+08	1.0E+07	0.0E+00
5	2030	Gas	Mediterranean Sea	3.6E+11	5.0E+09	9.4E+06	7.4E+07	5.0E+06	0.0E+00
5	2030	Bulk	Baltic Sea	1.0E+10	1.2E+09	6.4E+05	1.8E+07	4.5E+05	0.0E+00
5	2030	Other-cargo	Baltic Sea	1.1E+11	3.1E+09	1.6E+06	3.8E+07	1.9E+06	0.0E+00
5	2030	Container	Baltic Sea	4.5E+10	1.8E+09	9.8E+05	2.3E+07	9.5E+05	0.0E+00
5	2030	Non-cargo	Baltic Sea	2.6E+11	5.3E+09	2.9E+06	6.8E+07	3.9E+06	0.0E+00
5	2030	Tank	Baltic Sea	1.4E+10	1.9E+09	1.0E+06	2.6E+07	7.1E+05	0.0E+00
5	2030	Gas	Baltic Sea	3.4E+09	3.6E+08	1.9E+05	5.0E+06	1.4E+05	0.0E+00
5	2030	Bulk	North Sea	6.9E+10	3.7E+09	2.0E+06	6.4E+07	1.7E+06	0.0E+00
5	2030	Other-cargo	North Sea	1.2E+11	6.7E+09	3.6E+06	1.0E+08	3.1E+06	0.0E+00
5	2030	Container	North Sea	4.1E+11	1.1E+10	6.1E+06	2.0E+08	7.0E+06	0.0E+00
5	2030	Non-cargo	North Sea	1.8E+11	4.1E+09	2.1E+06	5.3E+07	2.8E+06	0.0E+00

5	2030	Tank	North Sea	6.5E+10	5.2E+09	2.8E+06	8.2E+07	2.2E+06	0.0E+00
5	2030	Gas	North Sea	2.2E+10	2.2E+09	8.4E+05	2.9E+07	7.4E+05	0.0E+00
5	2050	Bulk	Atlantic Ocean	0.0E+00	2.6E+09	5.5E+06	4.9E+07	3.0E+06	0.0E+00
5	2050	Other-cargo	Atlantic Ocean	0.0E+00	3.4E+09	7.0E+06	5.7E+07	3.8E+06	0.0E+00
5	2050	Container	Atlantic Ocean	0.0E+00	6.2E+09	1.3E+07	1.1E+08	7.1E+06	0.0E+00
5	2050	Non-cargo	Atlantic Ocean	0.0E+00	2.9E+09	6.1E+06	4.2E+07	3.3E+06	0.0E+00
5	2050	Tank	Atlantic Ocean	0.0E+00	2.1E+09	4.2E+06	3.7E+07	2.3E+06	0.0E+00
5	2050	Gas	Atlantic Ocean	0.0E+00	2.9E+09	2.9E+06	2.6E+07	1.7E+06	0.0E+00
5	2050	Bulk	Black Sea	0.0E+00	5.9E+08	1.2E+06	1.0E+07	6.1E+05	0.0E+00
5	2050	Other-cargo	Black Sea	0.0E+00	7.6E+08	1.3E+06	1.1E+07	7.1E+05	0.0E+00
5	2050	Container	Black Sea	0.0E+00	3.3E+08	6.6E+05	5.7E+06	3.5E+05	0.0E+00
5	2050	Non-cargo	Black Sea	0.0E+00	1.7E+08	3.5E+05	2.3E+06	1.8E+05	0.0E+00
5	2050	Tank	Black Sea	0.0E+00	5.6E+08	9.7E+05	9.4E+06	5.2E+05	0.0E+00
5	2050	Gas	Black Sea	0.0E+00	1.7E+08	3.4E+05	2.9E+06	1.8E+05	0.0E+00
5	2050	Bulk	Mediterranean Sea	0.0E+00	3.8E+09	7.5E+06	7.2E+07	4.1E+06	0.0E+00
5	2050	Other-cargo	Mediterranean Sea	0.0E+00	5.5E+09	1.0E+07	9.1E+07	5.7E+06	0.0E+00
5	2050	Container	Mediterranean Sea	0.0E+00	1.2E+10	2.3E+07	2.3E+08	1.3E+07	0.0E+00

5	2050	Non-cargo	Mediterranean Sea	0.0E+00	9.9E+09	2.1E+07	1.5E+08	1.1E+07	0.0E+00
5	2050	Tank	Mediterranean Sea	0.0E+00	3.8E+09	6.8E+06	7.0E+07	3.7E+06	0.0E+00
5	2050	Gas	Mediterranean Sea	0.0E+00	5.0E+09	7.1E+06	7.1E+07	4.0E+06	0.0E+00
5	2050	Bulk	Baltic Sea	0.0E+00	5.6E+08	2.7E+05	2.3E+06	1.8E+05	0.0E+00
5	2050	Other-cargo	Baltic Sea	0.0E+00	1.7E+09	8.0E+05	4.7E+06	5.6E+05	0.0E+00
5	2050	Container	Baltic Sea	0.0E+00	1.1E+09	5.6E+05	4.1E+06	3.8E+05	0.0E+00
5	2050	Non-cargo	Baltic Sea	0.0E+00	4.0E+09	1.9E+06	1.1E+07	1.3E+06	0.0E+00
5	2050	Tank	Baltic Sea	0.0E+00	7.9E+08	3.8E+05	2.9E+06	2.6E+05	0.0E+00
5	2050	Gas	Baltic Sea	0.0E+00	3.9E+08	1.8E+05	1.5E+06	1.2E+05	0.0E+00
5	2050	Bulk	North Sea	0.0E+00	1.8E+09	8.7E+05	6.9E+06	5.8E+05	0.0E+00
5	2050	Other-cargo	North Sea	0.0E+00	3.8E+09	1.8E+06	1.2E+07	1.2E+06	0.0E+00
5	2050	Container	North Sea	0.0E+00	6.3E+09	3.1E+06	2.4E+07	2.1E+06	0.0E+00
5	2050	Non-cargo	North Sea	0.0E+00	3.1E+09	1.3E+06	7.4E+06	9.4E+05	0.0E+00
5	2050	Tank	North Sea	0.0E+00	2.2E+09	1.1E+06	8.0E+06	7.3E+05	0.0E+00
5	2050	Gas	North Sea	0.0E+00	2.1E+09	7.1E+05	6.4E+06	5.1E+05	0.0E+00
6	2030	Bulk	Atlantic Ocean	6.3E+11	6.5E+09	1.6E+07	1.1E+08	8.2E+06	0.0E+00
6	2030	Other-cargo	Atlantic Ocean	7.8E+11	8.4E+09	2.0E+07	1.5E+08	1.0E+07	0.0E+00

6	2030	Container	Atlantic Ocean	1.5E+12	1.4E+10	3.7E+07	2.6E+08	1.9E+07	0.0E+00
6	2030	Non-cargo	Atlantic Ocean	4.1E+11	4.2E+09	1.0E+07	6.3E+07	5.3E+06	0.0E+00
6	2030	Tank	Atlantic Ocean	3.2E+11	3.3E+09	8.1E+06	6.1E+07	4.2E+06	0.0E+00
6	2030	Gas	Atlantic Ocean	1.4E+11	2.2E+09	3.4E+06	2.5E+07	1.9E+06	0.0E+00
6	2030	Bulk	Black Sea	1.1E+11	1.4E+09	2.9E+06	2.8E+07	1.5E+06	0.0E+00
6	2030	Other-cargo	Black Sea	1.1E+11	1.5E+09	2.9E+06	2.4E+07	1.5E+06	0.0E+00
6	2030	Container	Black Sea	5.1E+10	5.6E+08	1.3E+06	1.1E+07	6.8E+05	0.0E+00
6	2030	Non-cargo	Black Sea	1.5E+10	1.7E+08	3.8E+05	2.3E+06	2.0E+05	0.0E+00
6	2030	Tank	Black Sea	5.7E+10	7.8E+08	1.5E+06	1.4E+07	8.1E+05	0.0E+00
6	2030	Gas	Black Sea	6.8E+09	8.1E+07	1.8E+05	1.5E+06	9.3E+04	0.0E+00
6	2030	Bulk	Mediterranean Sea	9.6E+11	1.1E+10	2.5E+07	2.2E+08	1.3E+07	0.0E+00
6	2030	Other-cargo	Mediterranean Sea	1.2E+12	1.4E+10	3.1E+07	2.3E+08	1.6E+07	0.0E+00
6	2030	Container	Mediterranean Sea	2.9E+12	2.9E+10	7.3E+07	5.6E+08	3.8E+07	0.0E+00
6	2030	Non-cargo	Mediterranean Sea	1.5E+12	1.5E+10	3.7E+07	2.2E+08	1.9E+07	0.0E+00
6	2030	Tank	Mediterranean Sea	5.2E+11	6.3E+09	1.4E+07	1.2E+08	7.1E+06	0.0E+00
6	2030	Gas	Mediterranean Sea	2.3E+11	3.2E+09	6.0E+06	4.7E+07	3.2E+06	0.0E+00

6	2030	Bulk	Baltic Sea	1.3E+10	1.6E+09	8.5E+05	2.4E+07	6.1E+05	6.2E+04
6	2030	Other-cargo	Baltic Sea	1.5E+11	4.4E+09	2.3E+06	5.3E+07	2.6E+06	1.8E+05
6	2030	Container	Baltic Sea	6.1E+10	2.5E+09	1.3E+06	3.0E+07	1.3E+06	1.4E+05
6	2030	Non-cargo	Baltic Sea	3.0E+11	6.0E+09	3.2E+06	7.7E+07	4.3E+06	1.9E+05
6	2030	Tank	Baltic Sea	9.7E+09	1.3E+09	7.0E+05	1.8E+07	4.9E+05	6.0E+04
6	2030	Gas	Baltic Sea	2.2E+09	2.3E+08	1.2E+05	3.2E+06	8.9E+04	1.0E+04
6	2030	Bulk	North Sea	9.0E+10	4.8E+09	2.6E+06	8.4E+07	2.3E+06	1.2E+05
6	2030	Other-cargo	North Sea	1.6E+11	9.4E+09	5.0E+06	1.4E+08	4.3E+06	2.6E+05
6	2030	Container	North Sea	5.6E+11	1.5E+10	8.2E+06	2.7E+08	9.4E+06	3.0E+05
6	2030	Non-cargo	North Sea	2.1E+11	4.6E+09	2.3E+06	6.0E+07	3.1E+06	1.3E+05
6	2030	Tank	North Sea	4.5E+10	3.6E+09	2.0E+06	5.8E+07	1.5E+06	1.2E+05
6	2030	Gas	North Sea	1.4E+10	1.4E+09	5.4E+05	1.8E+07	4.7E+05	5.0E+04
6	2050	Bulk	Atlantic Ocean	2.1E+11	4.8E+09	6.4E+06	1.1E+08	4.1E+06	0.0E+00
6	2050	Other-cargo	Atlantic Ocean	1.8E+11	6.3E+09	7.9E+06	1.3E+08	5.1E+06	0.0E+00
6	2050	Container	Atlantic Ocean	4.7E+11	1.0E+10	1.4E+07	2.3E+08	8.7E+06	0.0E+00
6	2050	Non-cargo	Atlantic Ocean	1.1E+11	2.6E+09	3.3E+06	5.1E+07	2.2E+06	0.0E+00
6	2050	Tank	Atlantic Ocean	3.0E+10	8.4E+08	1.1E+06	1.8E+07	6.7E+05	0.0E+00
6	2050	Gas	Atlantic Ocean	-5.9E+10	8.7E+08	-1.2E+06	7.6E+06	-4.2E+05	0.0E+00

6	2050	Bulk	Black Sea	1.9E+10	9.8E+08	8.1E+05	2.1E+07	5.7E+05	0.0E+00
6	2050	Other-cargo	Black Sea	9.1E+09	1.4E+09	1.0E+06	2.4E+07	7.1E+05	0.0E+00
6	2050	Container	Black Sea	1.1E+10	4.9E+08	4.1E+05	1.1E+07	2.9E+05	0.0E+00
6	2050	Non-cargo	Black Sea	2.7E+09	1.3E+08	1.1E+05	2.5E+06	8.1E+04	0.0E+00
6	2050	Tank	Black Sea	3.0E+09	2.2E+08	1.7E+05	4.4E+06	1.1E+05	0.0E+00
6	2050	Gas	Black Sea	1.0E+09	5.5E+07	4.7E+04	1.2E+06	3.3E+04	0.0E+00
6	2050	Bulk	Mediterranean Sea	2.5E+11	7.3E+09	8.3E+06	1.6E+08	5.5E+06	0.0E+00
6	2050	Other-cargo	Mediterranean Sea	2.5E+11	1.0E+10	1.1E+07	2.1E+08	7.4E+06	0.0E+00
6	2050	Container	Mediterranean Sea	7.3E+11	2.1E+10	2.3E+07	4.6E+08	1.5E+07	0.0E+00
6	2050	Non-cargo	Mediterranean Sea	3.3E+11	9.0E+09	1.1E+07	1.8E+08	7.2E+06	0.0E+00
6	2050	Tank	Mediterranean Sea	4.3E+10	1.6E+09	1.7E+06	3.5E+07	1.1E+06	0.0E+00
6	2050	Gas	Mediterranean Sea	-1.8E+10	1.8E+09	1.1E+05	3.0E+07	3.9E+05	0.0E+00
6	2050	Bulk	Baltic Sea	5.8E+10	1.1E+09	4.5E+05	6.6E+06	8.9E+05	2.9E+05
6	2050	Other-cargo	Baltic Sea	9.8E+10	3.3E+09	1.2E+06	1.3E+07	2.0E+06	8.4E+05
6	2050	Container	Baltic Sea	1.1E+11	2.1E+09	8.6E+05	1.1E+07	1.7E+06	5.4E+05
6	2050	Non-cargo	Baltic Sea	2.0E+11	3.9E+09	1.5E+06	1.5E+07	3.1E+06	1.1E+06

6	2050	Tank	Baltic Sea	1.4E+10	3.4E+08	1.4E+05	1.8E+06	2.4E+05	8.7E+04
6	2050	Gas	Baltic Sea	5.8E+09	1.5E+08	5.5E+04	8.7E+05	1.0E+05	3.8E+04
6	2050	Bulk	North Sea	9.6E+10	3.4E+09	1.3E+06	2.0E+07	2.0E+06	8.9E+05
6	2050	Other-cargo	North Sea	1.4E+11	6.8E+09	2.6E+06	3.3E+07	3.7E+06	1.8E+06
6	2050	Container	North Sea	3.2E+11	1.1E+10	4.3E+06	6.2E+07	6.6E+06	2.8E+06
6	2050	Non-cargo	North Sea	3.9E+10	2.5E+09	6.5E+05	1.1E+07	1.2E+06	6.9E+05
6	2050	Tank	North Sea	2.0E+10	9.6E+08	4.0E+05	4.9E+06	5.1E+05	2.3E+05
6	2050	Gas	North Sea	-4.1E+10	6.8E+08	3.6E+04	3.7E+06	-1.8E+05	1.1E+05
7	2030	Bulk	Atlantic Ocean	6.3E+11	6.5E+09	1.6E+07	1.1E+08	8.2E+06	0.0E+00
7	2030	Other-cargo	Atlantic Ocean	7.8E+11	8.4E+09	2.0E+07	1.5E+08	1.0E+07	0.0E+00
7	2030	Container	Atlantic Ocean	1.5E+12	1.4E+10	3.7E+07	2.6E+08	1.9E+07	0.0E+00
7	2030	Non-cargo	Atlantic Ocean	4.1E+11	4.2E+09	1.0E+07	6.3E+07	5.3E+06	0.0E+00
7	2030	Tank	Atlantic Ocean	3.2E+11	3.3E+09	8.1E+06	6.1E+07	4.2E+06	0.0E+00
7	2030	Gas	Atlantic Ocean	1.4E+11	2.2E+09	3.4E+06	2.5E+07	1.9E+06	0.0E+00
7	2030	Bulk	Black Sea	1.1E+11	1.4E+09	2.9E+06	2.8E+07	1.5E+06	0.0E+00
7	2030	Other-cargo	Black Sea	1.1E+11	1.5E+09	2.9E+06	2.4E+07	1.5E+06	0.0E+00
7	2030	Container	Black Sea	5.1E+10	5.6E+08	1.3E+06	1.1E+07	6.8E+05	0.0E+00
7	2030	Non-cargo	Black Sea	1.5E+10	1.7E+08	3.8E+05	2.3E+06	2.0E+05	0.0E+00

7	2030	Tank	Black Sea	5.7E+10	7.8E+08	1.5E+06	1.4E+07	8.1E+05	0.0E+00
7	2030	Gas	Black Sea	6.8E+09	8.1E+07	1.8E+05	1.5E+06	9.3E+04	0.0E+00
7	2030	Bulk	Mediterranean Sea	9.6E+11	1.1E+10	2.5E+07	2.2E+08	1.3E+07	0.0E+00
7	2030	Other-cargo	Mediterranean Sea	1.2E+12	1.4E+10	3.1E+07	2.3E+08	1.6E+07	0.0E+00
7	2030	Container	Mediterranean Sea	2.9E+12	2.9E+10	7.3E+07	5.6E+08	3.8E+07	0.0E+00
7	2030	Non-cargo	Mediterranean Sea	1.5E+12	1.5E+10	3.7E+07	2.2E+08	1.9E+07	0.0E+00
7	2030	Tank	Mediterranean Sea	5.2E+11	6.3E+09	1.4E+07	1.2E+08	7.1E+06	0.0E+00
7	2030	Gas	Mediterranean Sea	2.3E+11	3.2E+09	6.0E+06	4.7E+07	3.2E+06	0.0E+00
7	2030	Bulk	Baltic Sea	1.3E+10	1.6E+09	8.5E+05	2.4E+07	6.1E+05	0.0E+00
7	2030	Other-cargo	Baltic Sea	1.5E+11	4.4E+09	2.3E+06	5.3E+07	2.6E+06	0.0E+00
7	2030	Container	Baltic Sea	6.1E+10	2.5E+09	1.3E+06	3.0E+07	1.3E+06	0.0E+00
7	2030	Non-cargo	Baltic Sea	3.0E+11	6.0E+09	3.2E+06	7.7E+07	4.3E+06	0.0E+00
7	2030	Tank	Baltic Sea	9.7E+09	1.3E+09	7.0E+05	1.8E+07	4.9E+05	0.0E+00
7	2030	Gas	Baltic Sea	2.2E+09	2.3E+08	1.2E+05	3.2E+06	8.9E+04	0.0E+00
7	2030	Bulk	North Sea	9.0E+10	4.8E+09	2.6E+06	8.4E+07	2.3E+06	0.0E+00
7	2030	Other-cargo	North Sea	1.6E+11	9.4E+09	5.0E+06	1.4E+08	4.3E+06	0.0E+00

7	2030	Container	North Sea	5.6E+11	1.5E+10	8.2E+06	2.7E+08	9.4E+06	0.0E+00
7	2030	Non-cargo	North Sea	2.1E+11	4.6E+09	2.3E+06	6.0E+07	3.1E+06	0.0E+00
7	2030	Tank	North Sea	4.5E+10	3.6E+09	2.0E+06	5.8E+07	1.5E+06	0.0E+00
7	2030	Gas	North Sea	1.4E+10	1.4E+09	5.4E+05	1.8E+07	4.7E+05	0.0E+00
7	2050	Bulk	Atlantic Ocean	1.3E+10	4.8E+09	6.4E+06	1.1E+08	4.1E+06	0.0E+00
7	2050	Other-cargo	Atlantic Ocean	2.9E+10	6.3E+09	7.9E+06	1.3E+08	5.1E+06	0.0E+00
7	2050	Container	Atlantic Ocean	1.4E+10	1.0E+10	1.4E+07	2.3E+08	8.7E+06	0.0E+00
7	2050	Non-cargo	Atlantic Ocean	1.6E+10	2.6E+09	3.3E+06	5.1E+07	2.2E+06	0.0E+00
7	2050	Tank	Atlantic Ocean	3.8E+09	8.4E+08	1.1E+06	1.8E+07	6.7E+05	0.0E+00
7	2050	Gas	Atlantic Ocean	2.0E+09	8.7E+08	-1.2E+06	7.6E+06	-4.2E+05	0.0E+00
7	2050	Bulk	Black Sea	1.2E+09	9.8E+08	8.1E+05	2.1E+07	5.7E+05	0.0E+00
7	2050	Other-cargo	Black Sea	4.8E+08	1.4E+09	1.0E+06	2.4E+07	7.1E+05	0.0E+00
7	2050	Container	Black Sea	3.2E+08	4.9E+08	4.1E+05	1.1E+07	2.9E+05	0.0E+00
7	2050	Non-cargo	Black Sea	5.4E+08	1.3E+08	1.1E+05	2.5E+06	8.1E+04	0.0E+00
7	2050	Tank	Black Sea	3.9E+08	2.2E+08	1.7E+05	4.4E+06	1.1E+05	0.0E+00
7	2050	Gas	Black Sea	1.4E+08	5.5E+07	4.7E+04	1.2E+06	3.3E+04	0.0E+00
7	2050	Bulk	Mediterranean Sea	1.6E+10	7.3E+09	8.3E+06	1.6E+08	5.5E+06	0.0E+00

7	2050	Other-cargo	Mediterranean Sea	4.2E+10	1.0E+10	1.1E+07	2.1E+08	7.4E+06	0.0E+00
7	2050	Container	Mediterranean Sea	2.2E+10	2.1E+10	2.3E+07	4.6E+08	1.5E+07	0.0E+00
7	2050	Non-cargo	Mediterranean Sea	5.7E+10	9.0E+09	1.1E+07	1.8E+08	7.2E+06	0.0E+00
7	2050	Tank	Mediterranean Sea	6.0E+09	1.6E+09	1.7E+06	3.5E+07	1.1E+06	0.0E+00
7	2050	Gas	Mediterranean Sea	3.7E+09	1.8E+09	1.1E+05	3.0E+07	3.9E+05	0.0E+00
7	2050	Bulk	Baltic Sea	3.7E+09	1.1E+09	4.4E+05	6.6E+06	4.4E+05	0.0E+00
7	2050	Other-cargo	Baltic Sea	1.5E+10	3.2E+09	1.2E+06	1.3E+07	1.3E+06	0.0E+00
7	2050	Container	Baltic Sea	3.4E+09	2.1E+09	8.3E+05	1.1E+07	7.9E+05	0.0E+00
7	2050	Non-cargo	Baltic Sea	3.6E+10	3.9E+09	1.4E+06	1.5E+07	1.7E+06	0.0E+00
7	2050	Tank	Baltic Sea	1.4E+09	3.4E+08	1.4E+05	1.8E+06	1.3E+05	0.0E+00
7	2050	Gas	Baltic Sea	6.9E+08	1.5E+08	5.4E+04	8.7E+05	5.9E+04	0.0E+00
7	2050	Bulk	North Sea	6.1E+09	3.4E+09	1.3E+06	2.0E+07	1.3E+06	0.0E+00
7	2050	Other-cargo	North Sea	2.4E+10	6.8E+09	2.6E+06	3.3E+07	2.7E+06	0.0E+00
7	2050	Container	North Sea	9.9E+09	1.1E+10	4.2E+06	6.2E+07	4.0E+06	0.0E+00
7	2050	Non-cargo	North Sea	4.9E+09	2.5E+09	6.4E+05	1.1E+07	9.0E+05	0.0E+00
7	2050	Tank	North Sea	2.2E+09	9.6E+08	4.0E+05	4.9E+06	3.6E+05	0.0E+00

7	2050	Gas	North Sea	1.4E+09	6.8E+08	4.7E+04	3.7E+06	1.7E+05	0.0E+00
8	2030	Bulk	Atlantic Ocean	6.3E+11	6.5E+09	1.6E+07	1.1E+08	8.2E+06	0.0E+00
8	2030	Other-cargo	Atlantic Ocean	7.8E+11	8.4E+09	2.0E+07	1.5E+08	1.0E+07	0.0E+00
8	2030	Container	Atlantic Ocean	1.5E+12	1.4E+10	3.7E+07	2.6E+08	1.9E+07	0.0E+00
8	2030	Non-cargo	Atlantic Ocean	4.1E+11	4.2E+09	1.0E+07	6.3E+07	5.3E+06	0.0E+00
8	2030	Tank	Atlantic Ocean	3.2E+11	3.3E+09	8.1E+06	6.1E+07	4.2E+06	0.0E+00
8	2030	Gas	Atlantic Ocean	1.4E+11	2.2E+09	3.4E+06	2.5E+07	1.9E+06	0.0E+00
8	2030	Bulk	Black Sea	1.1E+11	1.4E+09	2.9E+06	2.8E+07	1.5E+06	0.0E+00
8	2030	Other-cargo	Black Sea	1.1E+11	1.5E+09	2.9E+06	2.4E+07	1.5E+06	0.0E+00
8	2030	Container	Black Sea	5.1E+10	5.6E+08	1.3E+06	1.1E+07	6.8E+05	0.0E+00
8	2030	Non-cargo	Black Sea	1.5E+10	1.7E+08	3.8E+05	2.3E+06	2.0E+05	0.0E+00
8	2030	Tank	Black Sea	5.7E+10	7.8E+08	1.5E+06	1.4E+07	8.1E+05	0.0E+00
8	2030	Gas	Black Sea	6.8E+09	8.1E+07	1.8E+05	1.5E+06	9.3E+04	0.0E+00
8	2030	Bulk	Mediterranean Sea	9.6E+11	1.1E+10	2.5E+07	2.2E+08	1.3E+07	0.0E+00
8	2030	Other-cargo	Mediterranean Sea	1.2E+12	1.4E+10	3.1E+07	2.3E+08	1.6E+07	0.0E+00
8	2030	Container	Mediterranean Sea	2.9E+12	2.9E+10	7.3E+07	5.6E+08	3.8E+07	0.0E+00
8	2030	Non-cargo	Mediterranean Sea	1.5E+12	1.5E+10	3.7E+07	2.2E+08	1.9E+07	0.0E+00

8	2030	Tank	Mediterranean Sea	5.2E+11	6.3E+09	1.4E+07	1.2E+08	7.1E+06	0.0E+00
8	2030	Gas	Mediterranean Sea	2.3E+11	3.2E+09	6.0E+06	4.7E+07	3.2E+06	0.0E+00
8	2030	Bulk	Baltic Sea	1.3E+10	1.6E+09	8.5E+05	2.4E+07	6.1E+05	0.0E+00
8	2030	Other-cargo	Baltic Sea	1.5E+11	4.4E+09	2.3E+06	5.3E+07	2.6E+06	0.0E+00
8	2030	Container	Baltic Sea	6.1E+10	2.5E+09	1.3E+06	3.0E+07	1.3E+06	0.0E+00
8	2030	Non-cargo	Baltic Sea	3.0E+11	6.0E+09	3.2E+06	7.7E+07	4.3E+06	0.0E+00
8	2030	Tank	Baltic Sea	9.7E+09	1.3E+09	7.0E+05	1.8E+07	4.9E+05	0.0E+00
8	2030	Gas	Baltic Sea	2.2E+09	2.3E+08	1.2E+05	3.2E+06	8.9E+04	0.0E+00
8	2030	Bulk	North Sea	9.0E+10	4.8E+09	2.6E+06	8.4E+07	2.3E+06	0.0E+00
8	2030	Other-cargo	North Sea	1.6E+11	9.4E+09	5.0E+06	1.4E+08	4.3E+06	0.0E+00
8	2030	Container	North Sea	5.6E+11	1.5E+10	8.2E+06	2.7E+08	9.4E+06	0.0E+00
8	2030	Non-cargo	North Sea	2.1E+11	4.6E+09	2.3E+06	6.0E+07	3.1E+06	0.0E+00
8	2030	Tank	North Sea	4.5E+10	3.6E+09	2.0E+06	5.8E+07	1.5E+06	0.0E+00
8	2030	Gas	North Sea	1.4E+10	1.4E+09	5.4E+05	1.8E+07	4.7E+05	0.0E+00
8	2050	Bulk	Atlantic Ocean	0.0E+00	4.5E+09	7.6E+05	7.8E+07	1.4E+06	0.0E+00
8	2050	Other-cargo	Atlantic Ocean	0.0E+00	5.9E+09	1.1E+06	9.8E+07	1.8E+06	0.0E+00
8	2050	Container	Atlantic Ocean	0.0E+00	9.7E+09	1.6E+06	1.7E+08	2.9E+06	0.0E+00

8	2050	Non-cargo	Atlantic Ocean	0.0E+00	2.5E+09	4.1E+05	4.0E+07	7.4E+05	0.0E+00
8	2050	Tank	Atlantic Ocean	0.0E+00	7.9E+08	1.5E+05	1.3E+07	2.4E+05	0.0E+00
8	2050	Gas	Atlantic Ocean	0.0E+00	9.4E+08	1.2E+05	1.2E+07	2.3E+05	0.0E+00
8	2050	Bulk	Black Sea	0.0E+00	9.5E+08	2.9E+05	1.9E+07	3.2E+05	0.0E+00
8	2050	Other-cargo	Black Sea	0.0E+00	1.3E+09	4.8E+05	2.2E+07	4.4E+05	0.0E+00
8	2050	Container	Black Sea	0.0E+00	4.8E+08	1.4E+05	9.3E+06	1.6E+05	0.0E+00
8	2050	Non-cargo	Black Sea	0.0E+00	1.3E+08	3.6E+04	2.2E+06	4.3E+04	0.0E+00
8	2050	Tank	Black Sea	0.0E+00	2.2E+08	7.8E+04	4.0E+06	7.1E+04	0.0E+00
8	2050	Gas	Black Sea	0.0E+00	5.4E+07	1.6E+04	1.0E+06	1.8E+04	0.0E+00
8	2050	Bulk	Mediterranean Sea	0.0E+00	6.9E+09	1.5E+06	1.3E+08	2.2E+06	0.0E+00
8	2050	Other-cargo	Mediterranean Sea	0.0E+00	9.9E+09	2.4E+06	1.7E+08	3.1E+06	0.0E+00
8	2050	Container	Mediterranean Sea	0.0E+00	2.0E+10	4.5E+06	3.6E+08	6.2E+06	0.0E+00
8	2050	Non-cargo	Mediterranean Sea	0.0E+00	8.5E+09	1.5E+06	1.4E+08	2.6E+06	0.0E+00
8	2050	Tank	Mediterranean Sea	0.0E+00	1.6E+09	4.3E+05	2.8E+07	4.9E+05	0.0E+00
8	2050	Gas	Mediterranean Sea	0.0E+00	1.8E+09	3.8E+05	2.9E+07	5.2E+05	0.0E+00
8	2050	Bulk	Baltic Sea	0.0E+00	1.1E+09	1.9E+05	6.6E+06	3.1E+05	0.0E+00

8	2050	Other-cargo	Baltic Sea	0.0E+00	3.1E+09	4.9E+05	1.3E+07	8.8E+05	0.0E+00
8	2050	Container	Baltic Sea	0.0E+00	2.0E+09	3.9E+05	1.1E+07	5.8E+05	0.0E+00
8	2050	Non-cargo	Baltic Sea	0.0E+00	3.7E+09	5.4E+05	1.5E+07	1.1E+06	0.0E+00
8	2050	Tank	Baltic Sea	0.0E+00	3.2E+08	6.7E+04	1.8E+06	9.5E+04	0.0E+00
8	2050	Gas	Baltic Sea	0.0E+00	1.5E+08	2.7E+04	8.7E+05	4.2E+04	0.0E+00
8	2050	Bulk	North Sea	0.0E+00	3.3E+09	9.1E+05	2.0E+07	1.1E+06	0.0E+00
8	2050	Other-cargo	North Sea	0.0E+00	6.6E+09	1.7E+06	3.3E+07	2.2E+06	0.0E+00
8	2050	Container	North Sea	0.0E+00	1.0E+10	2.9E+06	6.2E+07	3.4E+06	0.0E+00
8	2050	Non-cargo	North Sea	0.0E+00	2.5E+09	4.8E+05	1.1E+07	7.9E+05	0.0E+00
8	2050	Tank	North Sea	0.0E+00	9.4E+08	3.0E+05	4.9E+06	3.0E+05	0.0E+00
8	2050	Gas	North Sea	0.0E+00	7.2E+08	1.9E+05	3.7E+06	2.2E+05	0.0E+00

Table A- 5. a) Annual mean total deposition (wet + dry, in mg/m2/year) of nitrogen (oxidised + reduced), sulfur, ash particles, lead and cadmium on Mediterranean and Black Sea: Total atmospheric deposition and shipping contribution, absolute and relative, to the deposition. b) Annual total deposition (in kt/year) of nitrogen and sulfur, total and the shipping contribution, along with input of N from discharge of EGCS effluent to the Mediterranean Sea. c) Annual shipping contribution to the deposition of metals on the Mediterranean Sea (in t/year), along with input of metals from discharge of EGCS effluent. Where available, model means for SILAM and EMEP models are presented. Simulations of deposition of lead and cadmium from all anthropogenic sources are only available from the SILAM model (*), simulations of ash and metals are available only from the SILAM and EMEP models (**), simulations of scenario deposition from all sources in year 2050 are available only from the EMEP model (***).

a)

	Total deposition (mg m^{-2} $year^{-1}$)			**Shipping contribution (mg m^{-2} $year^{-1}$)**			**Relative shipping contribution**		
	2018	**2050 S3*** **	**2050 S8*** **	**2018**	**S3**	**S8**	**2018**	**2050 S3*** **	**2050 S8*** **
N deposition									
Mediterranean Sea	258	185	221	61.0	23.1	52.9	24%	13%	27%
Black Sea	298	273	270	23.8	15.8	23.2	8%	7%	6%
S deposition									
Mediterranean Sea	251	112	106	84.2	6.1	1.7	34%	6%	1%
Black Sea	326	100	94	27.9	7.3	1.4	9%	7%	1%
Ash deposition**									
Mediterranean Sea				0.68	0.16	0.02			

Black Sea				0.79	0.18	0.02			
Lead deposition**									
Mediterranean Sea	0.13*			1.2E-04	2.6E-05	2.7E-06	1.7E-04		
Black Sea	0.14*			4.9E-05	1.5E-05	2.0E-06	9.8E-05		
Cadmium deposition**									
Mediterranean Sea	0.004*			6.6E-06	1.4E-06	1.4E-07	3.0E-04		
Black Sea	0.009*			2.6E-06	7.9E-07	1.0E-07	7.9E-05		

b)

	Total deposition (kt/year)			**Shipping contribution to deposition (kt/year)**			**EGCS effluent discharge (kt/year)**		
	2018	**2050 S3****	**2050 S8****	**2018**	**S3**	**S8**	**2018**	**2050 S3****	**2050 S8****
Nitrogen									
Mediterranean Sea	652	466	559	154	58	134	0.12	15	0
Black Sea	126	115	114	10	6.7	9.8			
Sulfur									
Mediterranean Sea	633	282	268	213	15	4.2			
Black Sea	137	42	40	12	3.1	0.6			

c) Mediterranean Sea

Metal	Shipping atmospheric deposition (t/year)			EGCS effluent discharge (t/year)			Shipping deposition / (shipping deposition + SW discharge)		
	2018	2050 S3	2050 S8	2018	2050 S3	2050 S8	2018	2050 S3	2050 S8
Arsenic	0.22	0.045	0.0047	0.72	55	0.0	23%	0.08%	100%
Cadmium	0.017	0.00	0.0004	0.09	6.7	0.0	16%	0.05%	100%
Chromium	0.56	0.12	0.012	1.50	114	0.0	27%	0.10%	100%
Copper	0.67	0.14	0.015	4.0	305	0.0	14%	0.05%	100%
Iron	67	14	1.5	25	1891	0.0	73%	0.73%	100%
Mercury	0.017	0.0035	0.0004	0.008	0.63	0.0	67%	0.55%	100%
Nickel	109	23	2.4	4.8	369	0.0	96%	5.79%	100%
Lead	0.31	0.064	0.007	0.95	72	0.0	25%	0.09%	100%
Vanadium	221	46	4.8	18	1392	0.0	92%	3.20%	100%
Zinc	6.4	1.3	0.14	11	873	0.0	36%	0.15%	100%